



Republic of Iraq
Ministry of Higher Education and Scientific Research
University of Misan/College of Engineering
Civil Engineering Department



POST FIRE DYNAMIC ANALYSIS OF STEEL BUILDINGS SUBJECTED TO WIND LOADINGS IN SOUTHERN IRAQ

**A THESIS
SUBMITTED TO THE COLLEGE OF ENGINEERING OF
MISAN UNIVERSITY IN PARTIAL FULFILLMENT OF
THE REQUIREMENTS FOR THE DEGREE OF MASTER OF
SCIENCE IN CIVIL ENGINEERING
(STRUCTURES)**

**BY
AMEEN ISMAEL ATYA
B.Sc. in Civil Engineering, 2016**

**Supervised by
Assist. Prof. Dr. Abbas Oda Dawood**

March 2019

Rbye al'awal 1440



I dedicate this work to...

My Parents

*for their help, moral,
encouragement, and
material support*

My brother

*for his help him

in my research*

My Friends

for their encouragement

My Colleagues

for their help practical

Acknowledgements

*Before everything, praise and thanks to
Allah who reconciles me to complete this study.*

*I would like to express my thanks and regard to Dean
of the College of Engineering Prof. Dr. **Ahmad Khadim Al-Shara.***

*And also to my supervisor, Assist Prof. Dr. **Abbas Oda Dawood** for his time
and help during all stages of this work.*

*Their Precious notes and advices gave me the light to go
forward with my study.*

*Tanks are due to Assist Prof. Dr. **Saad Fahad**, for providing
The facilities to complete this work.*

*Thanks to all the staff of Civil Engineering
Department /College of Engineering /University
of Misan for their appreciable support.*

*Special Thanks also go to Dr. **Fareed H. M. Al- Mosawi**
for his effort in helping me in SAPV2000 program
and introducing advices.*

*Finally I wish to express my cordial thanks and
deepest gratitude to my father, mother, brothers, sister, wife
and friends for their sustenance which allows me
to complete my study.*

*Thanks a lot to everybody pray
and wish success for me.*

Certification of the supervisor

I certify that this thesis entitled “Post Fire Dynamic Analysis of Steel Buildings Subjected to Wind Loadings in Southern Iraq”, which is being submitted by Ameen Ismael Atya, was made under my supervision at University of Misan/College of Engineering, in partial fulfillment of the requirements for the Degree of Master of Philosophy in Civil Engineering (Structures).

Signature:

Name: Assist. Prof. Dr. Abbas O. Dawood

(Supervisor)

Date: / / 2019

In view of the available recommendations, I forward this thesis for debate by the examining committee.

Signature:

Name: Assist. Prof. Dr. Abbas O. Dawood

Head of the Civil Engineering Department /University of Misan

Date: / / 2019

Certificate of Examination Committee

We certify that we have read this thesis entitled “Post Fire Dynamic Analysis of Steel Buildings Subjected to Wind Loadings in Southern Iraq” and as an Examining Committee, we examined the student (Ameen Ismael Atya) in its content and in what is connected with it and that in our opinion it meets standard of a thesis for the degree of Master of Philosophy in Civil Engineering (Structures).

Signature :

Name: Assist. Prof. Dr. David A. M. jawad

(Chairman)

Date : / /2019

Signature :

Name: Assist. Prof .Dr. Abdulkhaliq A. Jaafer

(Member)

Date : / /2019

Signature :

Name: Assist. Prof. Dr. Mohmmmed S. Abd-Ali

(Member)

Date : / /2019

Signature :

Name: Assist. Prof. Dr. Abbas O. Dawood

(Supervisor)

Date : / /2019

Approved by the Dean of the College of Engineering

Signature :

Name : Prof. Dr. Ahmad Khadim Al-Shara.

Acting Dean, College of Engineering / University of Misan

Date : / /2019

ABSTRACT

Post-fire analysis of a six-story square steel building under the action of static and dynamic wind forces in the south of Iraq is presented. The nonlinear time-history analysis using direct integration method is accomplished by SAP 2000 V16 program while geometric nonlinear parameters are included via P-delta effect.

The post fire deformations values and their configurations along building are based on available literature that related to post fire deformations of steel buildings at 550°C, in which maximum beam deflection is L/60 and maximum column lateral displacement is L/40. With reducing of yield stress and modulus of elasticity) by 10% due to fire than its value before fire. In this study two post fire scenarios are considered, i.e., CaseF1 and CaseF2.

The static wind load on steel building is calculated by ASCE7-02 procedure in which different coefficients and parameters that are suitable for southern Iraq conditions are selected. The deterministic time-domain dynamic approach is used to estimate the dynamic wind loads on the building in which the wind velocity time history records are obtained from the literature and then scaled via design wind speed for south of Iraq. Two wind speeds are used for scaling the time histories of wind velocities, strong and moderate winds in which the wind speeds are 42 m/s and 21 m/s respectively. The objective of this study is to investigate the post-fire dynamic behavior of a multi storey steel moment-resisting building subjected to along wind loads and compare the different responses of the building and members before and after fire for different fire scenarios according to standards limitations for these responses.

It is concluded that, the similarity in natural frequencies and mode shapes in the free vibrations after and before the fire, as well as there is no resonance phenomenon because $\omega_n \neq \omega$ for all modes. And found that base shear, base moment, from post-fire states (Case F1 and Case F2) are larger than before fire state (CaseF0) by 12% and 15% respectively, under the effect of strong wind load while the drift ratio and displacement from post-fire states (Case F1 and Case F2) are large than before fire state (CaseF0) by 20% and 5% respectively,

under the same conditions due to fire deformations and their configurations, but there are considerable differences at stories affected by temperature. The bending stress, shear stress, bending moment and shear force from post-fire state Case F2 are larger than before fire state by 33%, 70%, 30% and 0% respectively, under the effect strong wind load while due to moderate wind load 26%, 70%, 23% and 0% respectively, but there is large differences at first, second and third stories which are affected by fire. While it can be seen that there is a similarity between CaseF0 and Case 0.25ΔF1, this means that if the maximum deflection in beams does not exceed $L/160$ and the columns drift is not exceeding $L/240$, the fire deformations may be neglected or the maximum deflection in beams is equal to $L/120$ and the columns drift is equal to $L/80$, the fire deformations may be critical and the structural decision for the building safety should be done structural analysis of the building taking into consideration different issues related to post fire effects.

CONTENTS

Title		Page No.
Acknowledgments		I
Certification		II
Committee's Report		III
Abstract		IV
Contents		VI
List of Figures		XII
List of Tables		XVIII
List of Symbols		XXI
Section No.	Title	Page No.
Chapter One: Introduction		
1.1	General	1
1.2	Structural Collapse and Distort in Fire	3
1.3	The Fundamental Stages of A Fire	4
1.4	Steel Behavior at Elevated Temperature	5
1.5	The wind	5
1.6	Types of wind	6
1.7	Nature of wind	7
1.8	Wind turbulence	8
1.9	Effects of Static and Dynamic Winds on Structures	9
1.10	Forms of steel buildings resistance	10
1.10.1	Moment-resisting frames (rigid frames)	10
1.10.2	Framed tube structures	11
1.10.3	Staggered truss system	12

Section No.	Title	Page No.
1.10.4	Concentrically braced frames	13
1.10.5	Eccentrically braced frames	13
1.10.6	Hybrid structural systems	14
1.11	Objective of research	14
1.12	Thesis layout	15
Chapter Two: Literature Review		
2.1	General	16
2.2	Literature of post-fire structure	17
2.3	Literature of wind loadings	20
2.4	Concluding remark	24
Chapter Three: Post Fire Investigation		
3.1	Introduction	25
3.2	Types of imperfections	26
3.2.1	Geometrical imperfections	26
3.2.2	Material imperfections	26
3.2.3	Structural imperfections	27
3.3	Residual stresses	28
3.4	Buckling and other visible deformation due to fire	29
3.5	Categories of post-fire steel damages	32
3.6	Connection	37
3.7	Steel behavior with temperature increasing	38
3.8	Post-fire tolerances	39
3.8.1	Tolerances for beam	39
3.8.2	Tolerances for column	40

Section No.	Title	Page No.
3.9	Post-Fire Reduction of Yield Stress of Steel	40
3.10	Post-Fire Configurations	40
Chapter Four: Wind Analysis		
4.1	Introduction	47
4.2	Variation of wind velocity with height	48
4.3	Wind loadings	50
4.4	Design wind speed	52
4.5	Methods of analysis	54
4.5.1	Dynamic analysis	54
4.5.2	Equivalent static analysis	55
4.6	Wind loading simulation	55
4.6.1	Dynamic approach	55
4.6.1.1	Wind pressure coefficients	56
4.6.1.2	Time-history of wind loading	57
4.6.2	Static approach	60
4.6.2.1	Validation of south of Iraq conditions for ASCE7-05 parameters	61
4.6.2.2	Determination of wind design loads by analytical procedure of ASCE7-05 (method 2)	62
4.6.2.3	Wind pressure, p	66
4.6.2.4	Wind force(F) on structural frames	67
4.6.2.5	Summarized steps of analysis wind loads procedure	67
4.7	Dynamic wind load calculations	68
4.8	Static wind load calculations	70
4.9	Structural tolerances for wind load	71

Section No.	Title	Page No.
Chapter Five: Applications, Results and Discussion		
5.1	Introduction	72
5.2	Verification strategy	73
5.3	Structural modeling	75
5.3.1	Structural configuration	75
5.3.2	Applied loads	77
5.3.3	Material properties	79
5.3.4	Post-fire buildings configuration	80
5.3.5	Measurements	82
5.4	Analysis metrology	82
5.5	Analysis cases	83
5.5.1	Case1 free vibrations analysis	83
5.5.2	Case2 static versus dynamic analysis	88
5.5.2.1	Base shear in x-dir. for Case F0	88
5.5.2.2	Base moment in y-dir. for Case F0	89
5.5.2.3	Max. drift ratio in x-dir. for Case F0	90
5.5.2.4	Max. stresses (S ₁₁ , S ₁₂ and S ₁₃) for Case F0	91
5.5.2.5	Max. bending moment, M ₃₃ for Case F0	94
5.5.2.6	Max. axial force and shear force for Case F0	95
5.5.2.7	Max. displacements in x-dir. for Case F0	96
5.5.3	Case3 wind speed effect on dynamic response strong versus moderate	98
5.5.3.1	Base shear in x-dir. for Case F2	99
5.5.3.2	Base moment in y-dir. for Case F2	99
5.5.3.3	Max. drift ratio in x-dir. for Case F2	100

Section No.	Title	Page No.
5.5.3.4	Max. stresses (S_{11} , S_{12} and S_{13}) for Case F2	101
5.5.3.5	Max. bending moment, M_{33} for Case F2	103
5.5.3.6	Max. axial force and shear force for Case F2	104
5.5.3.7	Max. displacements in x-dir. for Case F2	106
5.5.4	Case4 linear and nonlinear dynamic analysis effect	107
5.5.4.1	Base shear in x-dir. for Case F1	108
5.5.4.2	Base moment in y-dir. for Case F1	109
5.5.4.3	Max. drift ratio in x-dir. for Case F1	110
5.5.4.4	Max. stresses (S_{11} , S_{12} and S_{13}) for Case F1	111
5.5.4.5	Max. bending moment, M_{33} for Case F1	114
5.5.4.6	Max. axial forces and shear force for Case F1	115
5.5.4.7	Max. displacements in x-dir. for Case F1	117
5.5.5	Case5 post-fire analysis, fully deformation (Δ)	118
5.5.5.1	Base shear in x-dir. for Case F0 and Case F2	119
5.5.5.2	Base moment in y-dir. for Case F0 and Case F2	121
5.5.5.3	Max. drift ratio in x-dir. for Case F0 and Case F2	123
5.5.5.4	Max. stresses (S_{11} , S_{12} and S_{13}) for Case F0 and Case F2	124
5.5.5.5	Max. bending moment, M_{33} for Case F0 and Case F2	127
5.5.5.6	Max. axial force and shear force for Case F0 and Case F2	128
5.5.5.7	Max. displacements in x-dir. for Case F0 and Case F2	131
5.5.6	Case 6 post-fire analysis fully deformations (Δ) versus quarter of deformities (0.25Δ), Case F1	133
5.5.6.1	Base shear in x-dir. for Case 6	133
5.5.6.2	Base moment in y-dir. for Case 6	134
5.5.6.3	Max. drift ratio in x-dir. for Case 6	134
5.5.6.4	Max. stresses (S_{11} , S_{12} and S_{13}) for Case 6	135

Section No.	Title	Page No.
5.5.6.5	Max. bending moment, M_{33} for Case 6	138
5.5.6.6	Max. axial force and shear force for Case 6	140
5.5.6.7	Max. displacements in x-dir. for Case 6	142
5.5.7	Case 7 post-fire analysis fully deformations (Δ) versus half of deformities (0.5Δ), Case F1	143
5.5.7.1	Base shear in x-dir. for Case 7	144
5.5.7.2	Base moment in y-dir. for Case 7	144
5.5.7.3	Max. drift ratio in x-dir. for Case 7	145
5.5.7.4	Max stresses (S_{11}, S_{12} and S_{13}) for Case 7	146
5.5.7.5	Max. bending moment, M_{33} for Case 7	148
5.5.7.6	Max. axial force and shear force for Case 7	150
5.5.7.7	Max. displacements in x-dir. for Case 7	152
5.6	Summary of state of building after analysis with limitations	153
Chapter Sex: Conclusions and Recommendations		
6.1	Introduction	154
6.2	Recommendations	157
References		159

LIST OF FIGURES

Figures No.	Title	Page No.
1-1	Deformation shape (mill of Misan) after fire	2
1-2	Steel Structural Failure Due To Fire	3
1-3	Stages of Fire Development (Buchanan, 2001)	4
1-4	Variation of wind velocity with time	6
1-5	Building collapse due to wind load	10
1-6	Moment-resisting frame	11
1-7	Framed tube	12
1-8	Staggered truss system	13
1-9	Concentrically and eccentrically braced frames	14
2-1	Procedure of applying time history along-wind load along the height on exterior side of tall building	21
2-2	Wind time-history loading typical point load	23
3-1	Variance of dimensions	26
3-2	Out-of-plumbness and straightness	26
3-3	Variance of material properties	27
3-4	Residual stresses	27
3-5	Eccentricities in joints	27
3-6	UL steel roof assembly after successful ASTM E119 fire test (courtesy of underwriters laboratories, Inc.)	31
3-7	One meridian plaza in Philadelphia after Feb. 23-24, 1991 fire	31
3-8	Considerable thermally induced beam	34
3-9	Severe local buckle in beam	35
3-10	Severe local buckle in column	36

Figures No.	Title	Page No.
3-11	Connection failure at end of buckled beam	37
3-12	Geometry and section of the eight-storey plane frame	42
3-13	Deformation shape at 650°C during the heating phase	42
3-14	Deformation shape at 800°C during the heating phase	43
3-15	Deformation shape at 20°C after the cooling phase	43
3-16	Geometry and section of the five-storey plane frame	44
3-17	Deformed of steel frame under different temperatures in the fire	45
4-1	Influence of exposure terrain on variation of wind velocity with height	49
4-2	Variation of wind velocity with height	50
4-3	Contour map for basic wind speeds m/s of Iraq	53
4-4	Digitized strong wind velocity data	58
4-5	Digitized moderate wind velocity data	59
4-6	Equivalent time history for strong wind velocity at 10m in south of Iraq	59
4-7	Equivalent time history for moderate wind velocity at 10m in south of Iraq	60
4-8	Variation of wind velocity with height	70
4-9	Dynamic strong wind loads for third floor	70
4-10	Dynamic moderate wind loads for third floor	71
4-11	Static wind pressures data	72
5-1	Structural details of the three-story (SAC3) steel building	75
5-2	X-Y plan diagram of steel framed building	77
5-3	X-Z plan diagram of steel framed building	78
5-4	Stress-strain curve after fire reduced 10% from original	80
5-5	Fire in Case F1	82

Figures No.	Title	Page No.
5-6	Fire in Case F2	82
5-7	First mode shapes \emptyset n Case F0	85
5-8	First mode shapes \emptyset n Case F2 and Case F1 respectively	86
5-9	Second mode shapes \emptyset n Case F0	86
5-10	Second mode shapes \emptyset n Case F2 and Case F1 respectively	87
5-11	Sine wave properties	88
5-12	Base shear x-dir. strong wind for case F0	89
5-13	Base moment y strong wind for case F0	90
5-14	Drift ratio % vs. story no. for Case F0	91
5-16	Bending stress vs. story no. for Case F0	93
5-17	Shear stress vs. story no. for Case F0	94
5-18	Bending moment vs. story no. for Case F0	95
5-19	Axial force vs. story no. for Case F0	97
5-20	Shear force vs. story no. for Case F0	97
5-21	Max. displacement vs. story no. for Case F0	99
5-22	Max. base shear strong wind for Case F2	100
5-23	Max. base shear due to moderate wind for case F2	100
5-24	Max. base moment due to strong wind for case F2	101
5-25	Max. base moment due to moderate wind for Case F2	102
5-26	Max. drift ratio due to strong and moderate wind for Case F2	103
5-27	Max. axial stress due to strong and moderate wind for Case F2	105
5-28	Max. bending stress by strong and moderate wind for Case F2	105
5-29	Max. shear stress due to strong and moderate wind for Case F2	106

Figures No.	Title	Page No.
5-30	Bending moment due to strong and moderate wind for Case F2	107
5-28	Max. bending stress by strong and moderate wind for Case F2	105
5-29	Max. shear stress due to strong and moderate wind for Case F2	106
5-30	Bending moment due to strong and moderate wind for Case F2	107
5-31	Axial forces due to strong and moderate wind for Case F2	109
5-32	Shear forces due to strong and moderate wind for Case F2	109
5-33	Displacement per by story strong and moderate wind for Case F2	111
5-34	Base shear x-dir. strong wind for Case F1 by linear analysis	112
5-35	Base shear x-dir. strong wind for Case F1 by nonlinear analysis	112
5-36	Base moment y-dir. strong wind for Case F1 by linear analysis	113
5-37	Base moment y-dir. strong wind for Case F1 by nonlinear analysis	114
5-38	Drift ratio for linear and nonlinear analysis due to strong wind for Case F1.	115
5-39	Axial stresses for linear and nonlinear analysis for strong wind, Case F1.	117
5-40	Bending stresses for linear and nonlinear analysis for strong wind, Case F1.	117
5-41	Shear stresses for linear and nonlinear analysis for strong wind, Case F1	118
5-42	Bending moment for linear and nonlinear analysis for strong wind, Case F1	119
5-43	Axial forces for linear and nonlinear by strong wind, Case F1	121
5-44	Shear forces for linear and nonlinear by strong wind, Case F1	121
5-45	Max. drift story for linear and nonlinear analysis for strong wind, Case F1	123
5-46	Base shear in x-dir. due to strong wind, Case F0	124

Figures No.	Title	Page No.
5-47	Base shear in x-dir. due to strong wind, Case F2	125
5-48	Base shear in x-dir. due to moderate wind, Case F0	125
5-49	Base shear in x-dir. due to moderate wind, Case F2	125
5-50	Base moment in y-dir. due to strong wind, Case F0	126
5-51	Base moment in y-dir. due to strong wind, Case F2	127
5-52	Base moment in y-dir. due to moderate wind, Case F0	127
5-53	Base moment in y-dir. due to moderate wind, Case F2	127
5-54	Drift ratio % vs. story no. for Case F0 and Case F2	128
5-55	Axial stress vs. story no. for Case F0 and case F2	131
5-56	Bending stress vs. story no. for Case F0 and case F2	131
5-57	Shear stress vs. story no. for Case F0 and case F2	132
5-58	Bending moment vs. story no. for Case F0 and case F2	133
5-59	Axial force vs. story no. for Case F0 and case F2	135
5-60	Shear force vs. story no. for Case F0 and case F2	136
5-61	Max. displacements vs. story no. for Case F0 and case F2	137
5-62	Max. drift ratio due to strong wind	140
5-63	Max. axial stress S_{11} under strong dynamic wind loa	142
5-64	Max. bending stress S_{12} under strong dynamic wind load	143
5-65	Max. shear stress S_{13} under strong dynamic wind load	143
5-66	Max. bending moment due to strong wind load	144
5-67	Max. axial forces due to strong wind load	146
5-68	Max. shear forces due to strong wind load	146
5-69	Max. displacements due to strong wind load	148
5-70	Max. drift ratio due to strong wind	151
5-71	Max. axial stress S_{11} under strong dynamic wind load	153

Figures No.	Title	Page No.
5-72	Max. bending stress S_{12} under strong dynamic wind load	154
5-73	Max. shear stress S_{13} under strong dynamic wind load	154
5-74	Max. bending moment due to strong wind load	155
5-75	Max. axial forces due to strong wind load	157
5-76	Max. shear forces due to strong wind load	157
5-77	Max. displacements due to strong wind load	159

LIST OF TABLES

Tables No.	Title	Page No.
4-1	The beaufort scale of wind force	52
4-2	Moderate wind speeds m/s Iraqi meteorological organization and seismology	53
4-3	Exposure categories and their applicability for south of Iraq	61
4-4	Importance factor, I (Table 6-1 Of ASCE7-05)	64
4-5	Values of z_g and α for each exposure category	65
5-1	Cross section properties of building members	77
5-2	Static wind load on building per elevation	79
5-3	Steel properties before fire	80
5-4	Steel properties after fire	81
5-5	Deformations after fire	81
5-6	Natural frequency for first 10 modes before and after fire	85
5-7	Base shear x-dir. for Case F0	89
5-8	Base moment y-dir. for Case F0	90
5-9	Max. stresses for Case F0	92
5-10	Bending moment per story no. for Case F0	95
5-11	Max. axial force and shear force for Case F0	96
5-12	Max. Displacement in x-dir. for Case F0	98
5-13	Max. base shear in x-dir. for Case F2	100
5-14	Max. base moment in y-dir. for Case F2	101
5-15	Max. stresses for Case F2	104
5-16	Max. bending moment for Case F2	107

Tables No.	Title	Page
5-17	Max. Axial and shear force for Case F2	108
5-18	Max. Displacement in x-dir. for Case F2	110
5-19	Base shear x-dir. for Case F1	112
5-20	Base moment y-dir. for Case F1	113
5-21	Max. stresses for Case F1	116
5-22	Max. bending moment for Case F1	119
5-23	Max. axial and shear force for Case F1	120
5-24	Max. displacement in x-dir. for Case F1	122
5-25	Base shear x-dir. before and after fire	124
5-26	Base moment y-dir. before and after fire	126
5-27	Stresses before and after fire	130
5-28	Bending moment before and after fire	133
5-29	Axial force and shear force before and after fire	135
5-30	Max. Displacement before and after fire	137
5-31	Case 6 deformations for Case F1 configuration	138
5-32	Max. base shear in x-dir.	139
5-33	Max. base moment in y-dir.	139
5-34	Max. stresses under strong wind load	142
5-35	Bending moment due to strong wind load	144
5-36	Axial and shear force due to strong wind load	145
5-37	Max. displacement due to strong wind load	147
5-38	Case 7 deformations for Case F1 configuration	149
5-39	Max. base shear in x-dir.	149
5-40	Max. base Moment y-dir.	150
5-41	Max. stresses under strong wind load	153

Tables No.	Title	Page
5-42	Bending moment due to strong wind load	155
5-43	Axial and shear force due to strong wind load	156
5-44	Max. displacement due to strong wind load	158
5-45	State of building after analysis	160

LIST OF SYMBOLS

Item	Description
$\bar{\rho}$	Density of air (kg/m ³).
\bar{T}	The force time period.
°C	Degrees Celsius.
0.5 Δ	Half of deformations.
0.25 Δ	Quarter of deformations.
A	Area upon which wind acts (m ²).
A _g	The gross area of that wall in which a _o is identified.
A _{gi}	The sum of gross surface areas of the exterior walls and roof (building envelope) not included A _g .
AISC	American Institute of Steel Construction
A _o	Total area of openings in a wall receiving positive external pressure.
A _{oi}	The sum of areas of openings in the exterior walls and roof (Building envelope) not included A _o .
AS	Australian Standards
AS/NZS	Australian Standards/ New Zealand Standard
ASCE	American Society of Civil Engineers
ASTM	American society for testing and materials.
BS	British standards (BSI: British standards institute)
BS	British Standard
C	The damping.
Case F0	The building before being exposed to fire.
Case F1,F2	The building after fire.
CBF	Concentrically braced frames.

Item	Description
C_d	Drag force coefficient.
C_p	External pressure coefficient.
EBF	Eccentrically braced frames.
EI	Stiffness of structure.
E_s	Elastic modulus of steel.
et al.	And others.
F	Force.
FE	Finite element.
FEM	Finite element method.
Fig.	Figure.
F_u	Ultimate steel tensile stress.
F_y	Minimum steel yield stress.
G	Shear modulus.
G	Gust effect factor.
g	Gravitational acceleration.
GC_{pi}	Internal pressure coefficient.
GLF	Gust loading factor.
h	Hour.
HSS	High strength steel.
I	Importance factor.
IQS	Iraqi Specification.
K_{zt}	Topographic factor.
M	The global mass (lumped).
M ₃₃	Bending moment.
Max.	Maximum.

Item	Description
Min.	Minimum.
MPa	Mega Pascal (MN/m ²) (equal to N/mm ²).
MRF	Moment-resisting frame.
NBC	National Building Code
No.	Number.
Ø _n	Mode shapes.
P	Wind pressure.
q	Wind pressure.
RCC	Reinforced Cement Concrete
RLB	Recommendations for Loads on Buildings
S ₁₁	Axial stress.
S ₁₂	Bending stress.
S ₁₃	Shear stress.
Sap	Systems applications and products.
t	Time.
T _n	Natural time period.
U _x	Displacements x-dir.
V	Wind speed.
V _(x, t)	Velocity of the wind at any level (x), at any time (t).
V _{10(t)}	Reference velocity, at 10 m above the base in m/sec.
V ₂	Shear force.
V _g	Gradient wind speed assumed constant above the boundary layer.
V _{ol}	Volume of element.
V _z	Mean wind speed at height z above ground.
X,Y,Z	Global coordinate system (denoting cartesian coordinate).

Item	Description
Z	Height above ground.
Z_g	Nominal height of boundary layer.
A	Power law coefficient.
γ	Steel density.
Δ	Deformations.
ζ	The structural damping ratio of building.
ν_s	Poison's ratio of steel.
ω	The natural force frequency.
ω_i and ω_j	Natural frequencies for the i and j modes of vibration (rad/sec).
ω_n	The natural frequency in free vibrations.

A vertical scroll of aged, yellowish paper is unrolled, held by four dark grey circular fasteners at the corners. The scroll is slightly wrinkled and has a soft shadow cast to its right. In the center of the unrolled portion, the text "Chapter One Introduction" is written in a bold, black, italicized serif font. To the right of the scroll, a quill pen with a dark nib and a light-colored, textured shaft is positioned diagonally, pointing towards the bottom right corner of the scroll.

Chapter One
Introduction

CHAPTER 1

INTRODUCTION

1.1 General

Steel and concrete are the two main materials used for building in high rise structures. Structural steel is generally used to build larger buildings due to the cost of material and labor, steel has been used for the framework of buildings since almost 200 years. Fire can attack all buildings, hence the engineer may encounter a variety of materials in fire damaged frameworks which are in a suitable condition for reinstatement. The occurrence of a fire in a steel structure would, lead to a significant deterioration in material strength and stiffness as shown in Fig. (1-1) . Consequently the fire cause large losses both in lives and property because the physical properties of steel are temperature dependent [1].

When steel is heated the material softens and undergoes thermal expansion, which in the case of a beam leads to bending and extension. Both of these phenomena are however resisted by the adjacent cooler structure, leading to permanent deformations, often including shortening of the heated members. When the steel members then cool down, they regain their strength and contract, resulting in residual forces. After a fire event, the member exposure to extreme temperature variations could have reduced the section and their load bearing capacities. The main reason for this is the reduction in post-fire mechanical properties (yield strength, elastic modulus) of steels.

Fire has always been a very destructive natural phenomenon. Its severe damaging effects on structures, which could range from a building being functionally disabled up to its collapse, have been known for centuries [3].



Figure (1-1): Deformation shape after fire [1].

Naturally, people tried to protect their construction either by transitioning to more fire-resistant materials, such as stone, or by improving their fire suppression mechanisms or protection the structures.

However, recent appraisals of the cost of steel construction carried out in the UK in 1982 showed that fire protection of a steel structure accounts for around 30% of the total cost of the structure [2].

Nowadays fire still poses a great threat to structures. If not dealt with properly, it can lead to loss of property and most importantly to loss of human lives. Modern construction very often uses steel structural framing to carry the structural loading, making, therefore, the study of its response to fire effects a necessity [3].

1.2 Structural Collapse and Distort in Fire

All structural materials can suffer from damage as a result of a severe fire, because they all lose strength and expand when heated to elevated temperatures. When steel structures are exposed to fire, strength and stiffness are decreased with increasing temperature. The structure is then deformed and the deformation depends upon the applied load and support conditions. Unprotected steel members show large deformation due to fire as shown in Fig. (1-2). Whereas well protected members can be reused without further investigation if they do not show any deflection after cooling members usually exhibit no damage [1]. In many situations structural steelwork remains undistorted the building has involved in fire frequently engineers are concerned that the steel may have suffered permanent metallurgical damage as a result of the fire. Very little information has been published to advise engineers when deciding which members can be safely used again or require replacement [1]. Often only small areas of the building are involved in the fire, required to decide on the basis of a visual inspection, which parts be reinhabited so that the original use may be continued after suitable refurbishing of fire damaged materials. It is frequently very convenient to reuse the structural members to avoid consequential losses and the inevitable inconvenience which is when parts of an otherwise sound structure are replaced [1].



Figure (1-2): Steel structural failure due to fire [1].

1.3 The Fundamental Stages of A Fire

There are four fundamental stages in a natural fire. These stages are schematically illustrated in Fig. (1-3). The first stage is the incipient ignition phase, wherein heating of the potential fuel source takes place. The second stage is the growth stage, which involves ignition with visible flaming combustion. As the fire grows and reaches sufficiently high temperatures about 1,100 °F (600 °C), it may become fully developed within the compartment and reach the so-called flashover which is the abrupt transition from relatively light burning of a small number of combustibles in the room, or a small portion of the room, to full-room involvement in fire. Generally marks the beginning of the third stage called the burning period. The temperatures and heat flux are so great within the fire compartment that all exposed surfaces are burning and the available ventilation will govern the rate of heat release. This most severe stage of the fire causes has the greatest effects on the building elements. Eventually, the fuel for the fire in the given compartment becomes exhausted, and the fire will start to die out during the fourth stage called the decay period. The decay phase is generally begins when about 70 percent of the combustible materials in the compartment have burned [1].

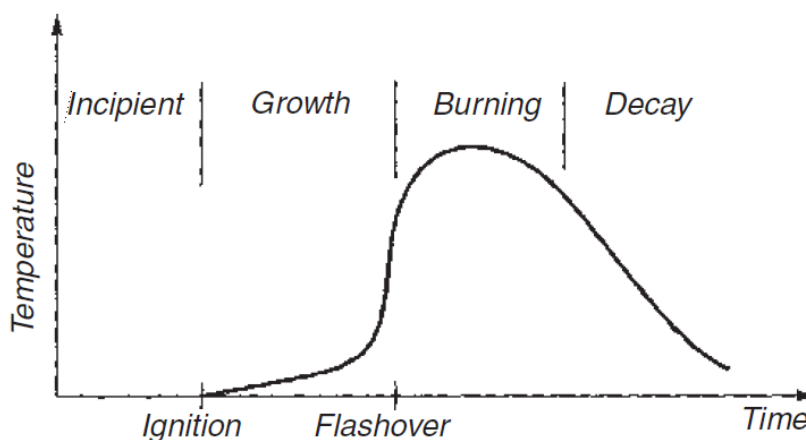


Figure (1-3): Stages of Fire Development (Buchanan, 2001) [1].

1.4 Steel Behavior at Elevated Temperature

Like all materials, steel weakens with an increase in temperature. Strength loss for steel is generally accepted to begin at about 300°C and increases rapidly after 400°C. By 550°C steel retains about 60% of its room temperature yield strength. However, at temperatures below about 600°C, if the steel is cooled it returns to its original strength, stiffness and ductility.

At temperatures above approximately 600°C, structural steel may suffer some deterioration in residual properties after cooling. For normal grade steel (yield strength 250MPa to 275 MPa), however, in no situation, whatever the fire temperature, will the room temperature yield stress or tensile strength fall further than 10% below their original values. Thus, where it can be assumed that the steel members will be utilized to less than 90% of their maximum load bearing capacity, replacement of the member should not be considered necessary, provided other performance characteristics, such as straightness, have not been compromised [4].

1.5 The Wind

Wind is essentially the large scale horizontal movement of free air or it means the motion of air in the atmosphere. It plays an important role in design of tall structures because it exerts loads on building .The response of structures to wind depends on the characteristics of the wind. Wind is caused by air flowing from high pressure to low pressure. Since the earth is rotating, however, the air does not flow directly from high to low pressure, but it is deflected to the right (in the northern hemisphere; to the left in the southern hemisphere), so that the wind flows mostly around the high and low pressure areas [5]. Tall buildings

are critically affected by wind loads. Wind exerts forces and moments on the structures. Hence, it has become of utmost importance to study the effect of wind and air flow on the building.

1.6 Types of wind

Winds that are of interest in the design of buildings can be classified into three major types: prevailing winds, seasonal winds, and local winds.

1. Prevailing winds. Surface air moving toward the low-pressure equatorial belt is called prevailing winds or trade winds. In the northern hemisphere, the northerly wind blowing toward the equator is deflected by the rotation of the earth to become northeasterly and is known as the northeast trade wind. The corresponding wind in the southern hemisphere is called the southeast trade wind.
2. Seasonal winds. The air over the land is warmer in summer and colder in winter than the air adjacent to oceans during the same seasons. During summer, the continents become seats of low pressure, with wind blowing in from the colder oceans. In winter, the continents experience high pressure with winds directed toward the warmer oceans. These movements of air caused by variations in pressure difference are called seasonal winds. The monsoons of the China Sea and the Indian Ocean are an examples.
3. Local winds. Local winds are those associated with the regional phenomena and include whirlwinds and thunderstorms. These are caused by daily changes in temperature and pressure, generating local effects in winds. The daily variations in temperature and pressure may occur over irregular terrain, causing valley and mountain breezes. All three types of wind are of equal importance in design. However, for the purpose of evaluating wind loads, the characteristics of the

prevailing and seasonal winds are analytically studied together, whereas those of local winds are studied separately. This grouping is to distinguish between the widely differing scale of fluctuations of the winds; prevailing and seasonal wind speeds fluctuate over a period of several months, whereas the local winds vary almost every minute, The variations in the speed of prevailing and seasonal winds are referred to as fluctuations in mean velocity. The variations in the local winds, are referred to as gusts [6].

Maysan province climate is warm to hot so there is no any snow may effect on structures. There are two main winds in south of Iraq, North and North-Western winds and South and south-Eastern winds. The North winds prevail in south of Iraq during all seasons of the year and its dry and hot at summer while dry and cool at winter. The East winds are relatively warm and with high humidity. In additional to above two common winds, Iraq as a whole be under the effect of 120 weak cyclones per year, these cyclones disturb the flow air and lead to winds with variation directions. There are no good understand whether these weak winds in different directions have any effects on structures, thus for very dynamic sensitive structures or the structures that may suffer from resonance phenomenon these weak cyclones may need to be checked [7].

1.7 Nature of Wind

Wind is the term used for air in motion and is usually applied to the natural horizontal motion of the atmosphere. Motion in a vertical or nearly vertical direction is called a current. Movement of air near the surface of the earth is three-dimensional, with horizontal motion much greater than the vertical motion. Vertical air motion is of importance in meteorology but is of less importance near the ground surface. On the other hand, the horizontal

motion of air, particularly the gradual retardation of wind speed and the high turbulence that occurs near the ground surface, are of importance in building engineering. In urban areas, this zone of turbulence extends to a height of approximately one-quarter of a mile aboveground, and is called the surface boundary layer. Above this layer, the horizontal airflow is no longer influenced by the ground effect. The wind speed at this height is called the gradient wind speed, and it is precisely in this boundary layer where most human activity is conducted. Therefore, how wind effects are felt within this zone is of great concern. Structures no doubt experience the constant flow of wind, but intermittently it will experience sudden gusts of rushing air. This sudden variation in wind speed, called gustiness or turbulence, plays an important part in determining building oscillations [5].

1.8 Wind Turbulence

Motion of wind is turbulent. A concise mathematical definition of turbulence is difficult to give, except to state that it occurs in wind flow because air has a very low viscosity about one-sixteenth that of water. Any movement of air at speeds greater than 2 to 3 mph (0.9 to 1.3 m/s) is turbulent, causing particles of air to move randomly in all directions. This is in contrast to the laminar flow of particles of heavy fluids, which move predominantly parallel to the direction of flow.

For structural engineering purposes, velocity of wind can be considered as having two components: a mean velocity component that increases with height, and a turbulent velocity that remains the same over height. Similarly, the wind pressures, which are proportional to the square of the velocities as shown in Fig. (1.4). [5]

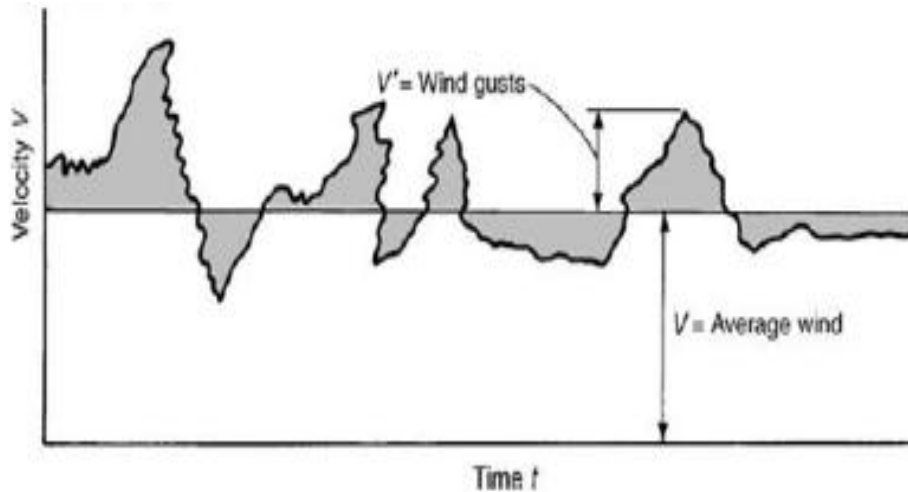


Figure (1-4): Variation of wind velocity with time [5].

1.9 Effects of Static and Dynamic Winds on Structures

Effects of wind on structures can be classified as ‘static’ and ‘dynamic:

1. Static wind effect primarily causes bending and twisting of structure(mean velocity).
2. Dynamic For tall, long span and slender structures a dynamic analysis of the structure is essential .Wind gusts cause fluctuating forces on the structure which induce large dynamic motions, including oscillations change with time_(Turbulence velocity).

The wind is the most powerful and unpredictable force affecting tall buildings causing movement, known as wind drift, which should be kept within acceptable limits. Wind on buildings increases considerably with the increase in building heights. Furthermore, the speed of wind increases with height, and the wind pressures increase as the square of the wind speed. Thus, wind effects on a building is compounded as its height increases. Despite all the engineering sophistication performed with computers, wind is still a complex phenomenon. Unlike dead loads and live loads, wind loads change rapidly and even abruptly,

and if creating effects much larger than when the same loads were applied gradually. If the wind loads are greater than the structural capacitance, the collapse of the building will occur, as shown in Fig. (1-5) [8].



Figure (1-5): Building collapse due to wind load [8].

1.10 Forms of Steel Buildings Resistance

The main structural forms suitable for earthquake and wind resistance are [8]:

- (1) Moment-resisting frames.
- (2) Framed tube structures.
- (3) Staggered truss system.
- (4) Concentrically braced frames.
- (5) Eccentrically braced frames.
- (6) Hybrid structural systems.

1.10.1 Moment-Resisting Frames (Rigid Frames)

A frame is considered rigid when its beam to column connections have sufficient rigidity to hold virtually unchanged the original angles between

intersecting members. In this system, as shown in Fig. (1-6), lateral loads are resisted primarily by the rigid frame action; that is, by the development of shear forces and bending moments in the frame members and joints. The continuity at both ends of beams also assists in resisting gravity loads more efficiently by reducing positive moments in beam spans [5].

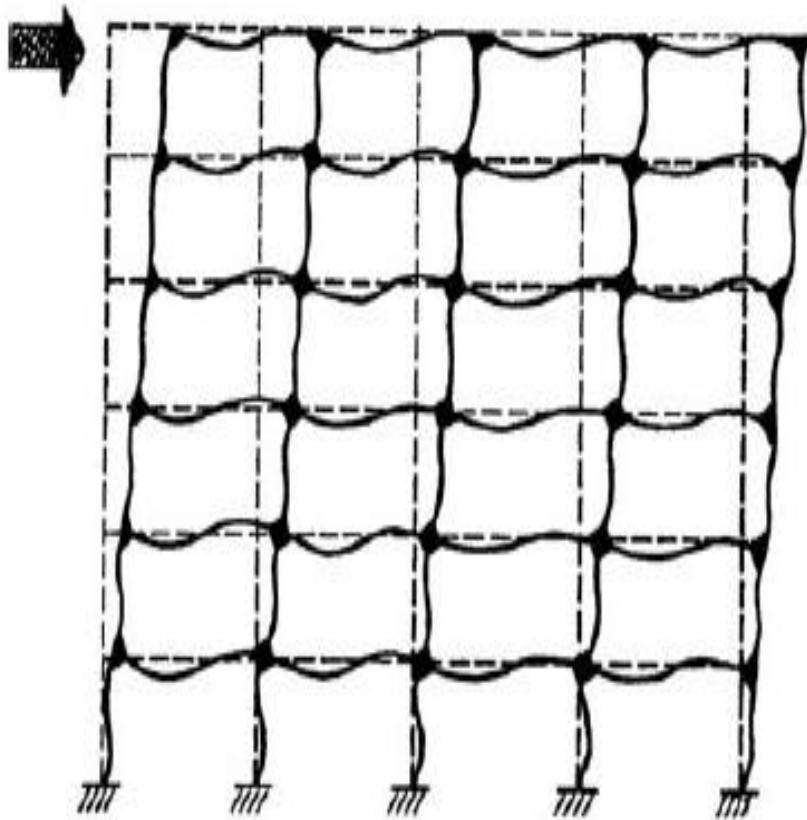


Figure (1-6): Moment-resisting frame [5].

1.10.2 Framed Tube Structures

The framed tube system is a special case of the moment resisting frame, which usually consists of closely spaced wide steel columns combined with relatively deep beams. These frames are usually, but not only located on the perimeter of the structure, and introduce more stiffness to overcome the problems of excessive horizontal deflection of the common moment-resisting frames, shown in Fig. (1-7) [6].

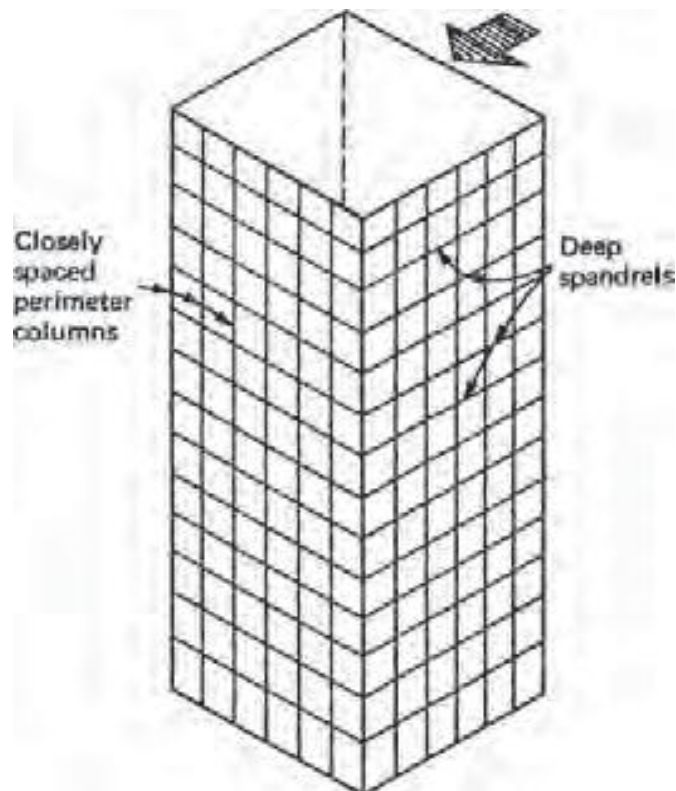


Figure (1-7): Framed tube [6].

1.10.3 Staggered Truss System

Acts as a diaphragm transferring lateral loads in the short direction to the trusses. Lateral loads are thereby resisted by truss diagonals and are transferred into direct loads in the columns. The columns therefore receive no bending moments. The truss diagonals are eliminated at the corridor locations to allow for openings. Since the diagonal is eliminated, the shear is carried by the bending action of the top and bottom chord members at these locations. Because the staggered truss system resists a majority of gravity and lateral loads in direct stresses, it is quite stiff. In general, additional steel tonnage required for controlling drift is quite small. Therefore, high-strength steels may be used throughout the entire frame. The system has been used for buildings in the 35- to 40-story range. Transverse spans must be long enough to make the trusses efficient, with 45ft (13.72 m) considered the minimum practical limit [5], as shown in Fig. (1-8).

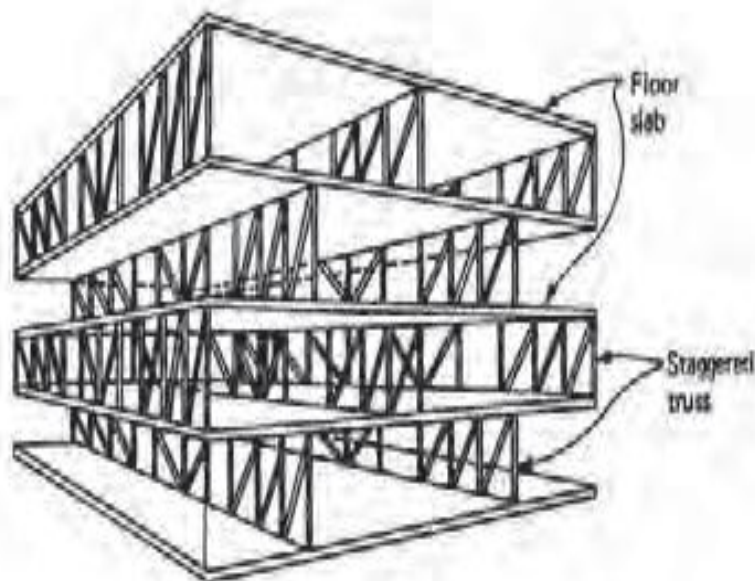


Figure (1-8): Staggered truss system [5].

1.10.4 Concentrically Braced Frames

Concentrically braced frames (CBF) are those where the centre-lines of all intersecting members meet at a point, Fig. (1-9a). This traditional form of bracing is, of course, widely used for all kinds of construction such as towers, bridges, and buildings, creating stiffness with great economy of materials in two-dimensional trusses or three-dimensional space frames. Traditional design of trussed structures lays great importance on keeping the forces in the structure to axial only, avoiding moments by ensuring that the centre-lines of all intersecting members meet at a point [6].

1.10.5 Eccentrically Braced Frames

An eccentrically braced frame (EBF) is a brace frame system in which one end of the brace is connected to the beam instead of a frame node, Fig. (1-9b). In eccentrically braced frames the axial forces in the braces are transmitted

to the columns through bending and shear in the beams, and if designed correctly, the system of bracing possesses more ductility than concentrically braced frames [6,9].

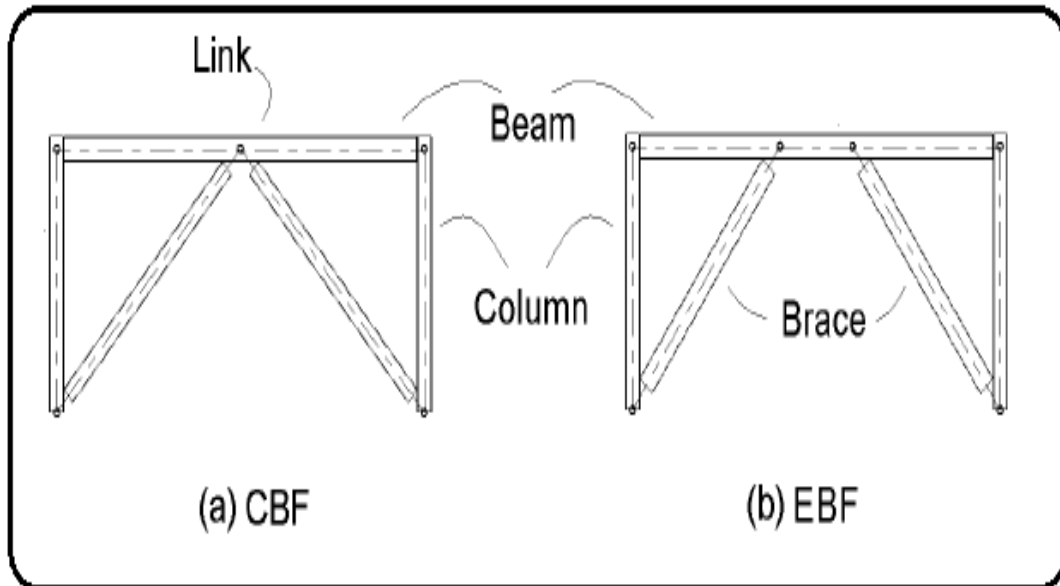


Figure (1-9): Concentrically and eccentrically braced frames [10].

1.10.6 Hybrid Structural Systems

Structures are often built in which the lateral resistance is provided by more than one of the above methods [6].

1.11 Objective of Research

The objective of this research is to study the post-fire dynamic analysis of a multi-storey steel moment-resisting building subjected to along wind loads and determination of static and dynamic wind loads on building and estimate the parameters that are suitable for southern Iraq conditions and show if the building is safe after effect the fire according to limitations in codes and effects of measurements on the building after fire with winds influence. These objectives are studied by following items.

1. Investigating the mechanical properties after fire, namely reduction in yield stress and the modulus of elasticity (F_y , E) after fire.
2. Investigating the deformation scenario or configuration of steel building due to fire.
3. Investigating difference imperfection in steel building due to fire.
4. Estimating the suitable values for design wind speed in southern Iraq, namely design wind speed according to Iraq codes and prevailing wind speed for the past 30year.
5. Performing the nonlinear dynamic analysis for post-fire building by using finite element method via SAP v2000 software.
6. Studying the difference ranges of post-fire deformations to reflect the difference degree of temperature or fire duration.
7. Specifying if the building is safe or not according to standards limitations.

1.12 Thesis Layout

After this introductory chapter, review of the main research papers concerned with the subject are discussed in chapter two. Chapter three investigates the steel building via effect of fire. Chapter four deals with the effects of wind load on building and mathematical formulation of the nonlinear finite element analysis due to wind load. Chapter five presents the applications, results and discussions. Chapter six gives the main conclusions and recommendations for future work.

A scroll of parchment is unrolled, showing the title. The scroll is held by four black circular fasteners at the corners. A quill pen is tucked under the right side of the scroll. The parchment is yellowed and has some irregular edges.

Chapter Two
Literature
Review

CHAPTER 2

LITERATURE REVIEW

2.1 General

The present study deals with two topics; they are fire and wind engineering.

In the past decades, the post-fire performance of structural steel elements had attracted many researchers. Although the fire safety of a structure is of paramount importance, the reinstatement of fire damaged structures is the center of interest nowadays. Since 1960s, the research is focused on the mechanical properties of the material. Exposure to fire will subject structural steel to thermally induced environmental conditions that may alter its properties. Assessing these altered properties requires a combined knowledge of metallurgical and structural behavior as the fire raises the steel temperature and the steel later cools. Knowledge of steel properties and behavior developed from basic steel production, thermal cutting, thermal or mechanical straightening (or curving), heat-treating and welding provides the requisite information.

Fire represents a transfer of energy from a stable condition to a transient condition as combustion occurs; examples are the burning of warehouse contents, office furniture, books, filing cabinet contents, or other material. During this process, the steel temporarily absorbs a significant amount of thermal energy. Subsequently, the steel structure returns either to a stable or unstable condition after cooling to ambient temperatures. During this cycle, individual members may become badly bent or damaged without affecting the stability of the whole structure. It is possible to predict the range of temperatures that a particular steel member of a building experienced during a fire using

current heat transfer theories. Damaged members are indicative of energy redistribution within the member itself and possibly the whole structure. Assessing overall structural stability can proceed after the condition of the individual members has been established. And through the study of research has been found some studies that are close to this research and benefit from them as follows.

2.2 Literature of Post-Fire Structure

Smith et al. 1981 [11], studied the factors which can cause steelwork to distort and collapse during fires. Laboratory based experiments were described in which the strengths of various grades of steel were determined at elevated temperatures. The effects on mechanical properties of heating steelwork to temperatures in the range 100 - 1000 °C and cooling back to ambient temperature have been assessed.

They concluded that relatively small changes in mechanical strength occur to steelwork after heating in a fire. The building codes used in the design of steel frame buildings incorporate large safety factors which permit the framework of buildings was heated to around 550 °C before the flow stress falls to the design stress. If steelwork was heated above that temperature then some expansion effects and distortion will normally be visible. The laboratory simulations have indicated that little change in room temperature strength occurs after cooling until fire temperatures in excess of 650 °C were achieved, and in this situation the structure was liable to have collapsed.

Kirby et al. 1986 [1], studied the possibilities of reinstatement of fire damaged steel and iron framed structures. Two mild steels were tested. The tests were carried out by heating the material in a furnace at temperatures between

100 °C and 1000 °C for 1 h and 4 h periods. After the heat treatment, the material was cooled in air and tested according to BS18 Part 2. Two Grade 43A, which largely corresponds to S275, mild steels were studied; one with a high room temperature yield (335 N/mm²), and one with low strength (238 N/mm²). The tests showed that exposure to temperatures up to 600 °C had virtually no effect on the strength of the steel, regardless of exposure time. With higher temperatures the strength started to decrease and also the exposure time had an effect on the strength; the longer the exposure, the more the strength decreased. The high strength mild steel was also more affected than the low strength mild steel. They concluded that regardless of exposure temperature and time, the strength properties were unlikely to fall more than 10 % of the specified value.

Outinen et al. 2004[12], studied the mechanical properties of structural steel member that exposure to the rise of temperature, namely: (a) the yield stress F_y and (b) Young's modulus of elasticity E which obtained after a specific number of fire tests. The procedure of these tests was to test at least one specimen for each temperature gradient starting from 20 °C and using an increment of 100 °C or 50°C, up to 1000°C. From the obtained stress-strain curve the properties of interest (E , F_y) were measured. They concluded that the values of the yield stress and the modulus of elasticity decreases gradually up to about 400°C and then drops rapidly to zero at approximately 1000°C. At approximately 1000°C. The modulus of elasticity and yielding strength were both zero at temperature 1000 °C .

Iua,et al. 2005[13], studied an eight-storey composite frame that was designed as a three bay-deep and five-bay-wide structure at the Cardington fire test in the UK. All of the out-of-plane degrees of freedom of this frame were restrained and all connections were designed as rigid in the computer modelling. A distributed load of 5.48kN/m², corresponding to the mean dead and imposed

loading of the test, was applied. The maximum temperature was approximately 800°C and the frame cools to ambient temperature. They concluded that the structure after cooling to ambient temperature, the lateral displacement increases inward to 155.28mm in column and 220.17 mm in mid beam while 192.01mm in edge beam, this fire analysis due to the thermal contraction force of the beam member under cooling.

Maraveas, 2014 [14], studied the mechanical properties of structural steel exposed to fire and cooled down. He presented the lack of satisfactory recommendations concerning the post-fire properties of steel or the post-fire performance of a steel member, which shows the need for further research on the topic.

He investigated a total of 128 test results from six studies, the initial yield strength (F_y) at ambient temperature while the values of (F_y) were in the range of 231 to 1045 MPa and 100 to 1000°C. The residual properties were obtained from tension tests on steel specimens after heating and cooling to room temperature via different cooling methods.

He noted that the post-fire behaviour of structural steel was hardly influenced hardly after exposure to temperatures up to 600°C. In addition, the residual ultimate strength of mild steel was found greater than 90% of the initial one, whereas none of the properties of hot-rolled steel was reduced more than 75%.

The distinguish between mild steel and high strength steel (HSS) in which his conclusions were agreed with British Standard 5950-8 in Appendix(B) recommended the reuse of S235 and S275 reduced by 10% of the initial strength, whereas for S355 at least 75% of the strength was regained on cooling from temperatures above 600 °C.

2.3 Literature of Wind Loadings

The wind action on building is studied by many researchers and they deal with different topics of this subject, in this section only previous works related to the present study were reviewed.

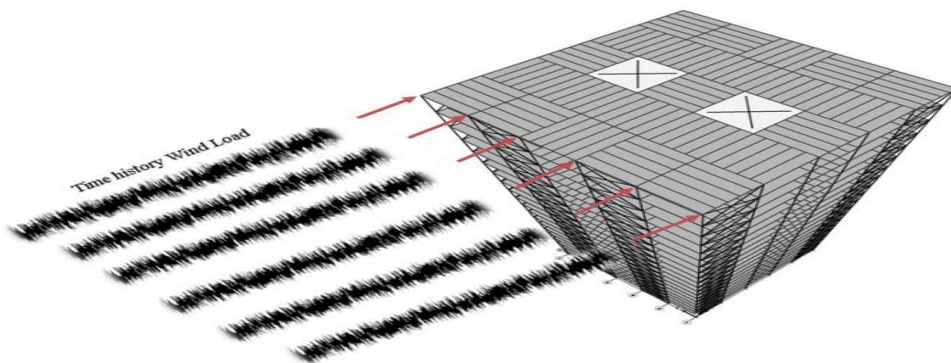
Zhou et al. 2002[15], presented a comprehensive assessment of the source of the scatter that exists among the wind effects predicted by the various codes and standards under similar flow conditions, through a comparison of the along-wind loads and their effects on tall buildings recommended by major international ASCE 7-98, AS1170.2-89, NBC-1995, RLB-AIJ-1993, and Eurocode-1993. They noted that the scatter in the predicted wind loads and their effects arises primarily from the variations in the definition of wind field characteristics in the respective codes and standards.

Holmes et al. 2009 [16], described a comparison of wind load calculations on buildings using fifteen different wind loading codes. Three buildings were studied the low rise building (steel portal-framed industrial warehouse building), the medium-height building (a 48-metre high office building) and the high-rise building (183 meters high). The comparisons showed varying degrees of agreement between codes, in which ASCE7-05 procedure gave reasonable results in comparison with the other codes.

Kumar and Swami, 2010 [17], studied the differences of heights buildings analysis wind loads static pressure and gust pressure along wind load on tall buildings, multistory frames ranging from 20 to 100 storeys were considered. He concluded that the gust pressures method increase with the height of building and they were more critical than static pressures and the difference in the values of gust pressures computed for single and two bays was small, however for

exact determination of internal stresses, the size effect given by number of bays is to be considered.

Bakhshi and Nikbakht, 2011 [18], studied the distribution of dynamic wind and earthquake load, to investigate the height beyond which the wind load would be dominant over the seismic loading condition. In this study, 5 tall steel frames buildings with various lateral resisting systems were investigated via three-dimensional models. The effect of dynamic time history wind load was considered and when it's applied along the height of tall buildings, the fluctuating wind speed was simulated as multivariate stochastic process, and the fast Fourier transform was needed to estimate the fluctuating wind speed components acting on the structure. For two basic wind speed (47 m/s and 76 m/s) according to ASCE7-05, mean wind speed along the height was calculated and with accumulating this component with fluctuation wind speed component, wind speed along the height at each level can be computed Fig. (2-1), for the nonlinear dynamic analysis. They concluded that peak drift and displacement were two important parameters for comfort criteria that affect human perception to motion in the low frequency range of 0-1 Hz encountered in tall buildings and peak displacements derived from dynamic wind and seismic load, separately, the structures with bracing system were more flexible than ones with shear wall system.



Figure(2-1): Procedure of applying time history along-wind load along the height on exterior side of tall building [18].

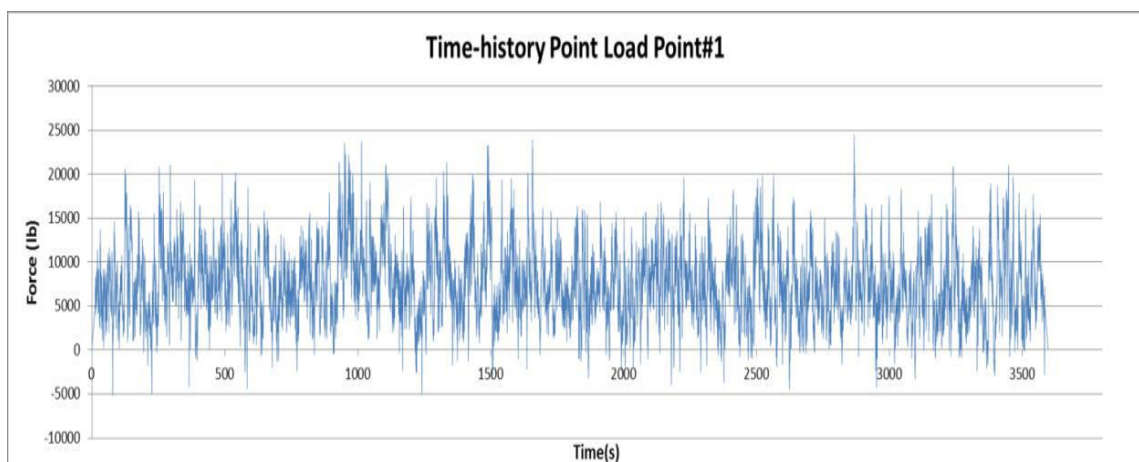
Ambadkar and Bawner, 2012 [19], presented the analysis of (G+11) multi story building for different terrain category in significant relation of moment, forces and displacement. The modelling and analysis was done by using STAAD Pro. software. For the analysis basic wind speed were taken 44 m/s, 47m/s, and 50m/s. They concluded that wind speed increases bending moment values also increases according to category.

Suresh et al. 2012 [20], studied rigid and flexible structures. His investigation deals with the calculation of wind loads using static and gust factor method for a sixteen storey high rise building and results were compared with respect to drift. Structure was analyzed in STAAD Pro. With wind loads calculated by gust factor as per IS 875-Part III with and without X- bracings at all the four corners from bottom to top. They concluded that axial loads in the external frame exterior columns in braced structure were high when compared with unbraced structure, reduced gradually and at top floor both were almost same.

Prajapati, 2013 [21], discussed the analysis and design procedure that may be adopted for the evaluation of symmetric multi-storey building under effect of wind and earthquake forces. Structures were designed to resist moderate and frequently occurring earthquakes and wind and must have sufficient stiffness and strength to control displacement and to prevent any possible damage. It was found that it was inappropriate to design a structure to remain in the elastic region, under severe earthquakes and wind lateral forces, because of the economic constraints. The inherent damping of yielding structural elements can advantageously be utilized to lower the strength requirement, leading to a more economical design. This yielding usually provides the ductility or toughness of the structure against the sudden brittle type structural failure.

Rehan and Mahure, 2014 [22], Presented the analysis and design of (G+15) Storeys under the effect of earthquake and wind for Composite, Steel and RCC structure. The modelling and analysis was done by using STAAD Pro. They compare the result of Composite, RCC and steel building such as story displacement, story drift and maximum bending moment and shear forces. They suggest that composite structure was better option compare to RCC and Steel.

Mohammadi, 2016 [23], studied three height of buildings (47, 40 and 30story) steel moment frame high-rise buildings. In this study, using time-history method for analysis as shown in Fig. (2-2).The nonlinear dynamic responses of the buildings to different wind hazard levels were evaluated by developing 3D nonlinear finite element models and utilizing a wind incremental dynamic analysis (IDA) approach.. He concluded that minor building shape details may locally affect on the local wind pressure of interest for cladding design. But they did not affect the overall wind loads very significantly and the 47-story building's shape details did not significantly affect the mean and fluctuating components of the wind force.



Figure(2-2):Wind time-history loading typical point load [23].

2.4 Concluding Remark

The pervious literature review reveals the following points:

1. Dynamic wind load data significantly influence the behavior of the structures.
2. Most studies considered the base shear, roof displacement, natural frequency, mode shapes, story drift ratio, axial forces and moments in members as main parameters to compare the performance of buildings.
3. The mechanical properties (yield strength F_y , elastic modulus E) of steels after fire is about 90% of that before fire.
4. The time history method along-wind load will be imposed at the location of perimeter beam-column joints (major joint of each floor).

Consequently, in this research work different types of wind loads (static and dynamic(strong, moderate) are used including after fire deformation for six story moment resistant building, taking into consideration reduction in steel strength due to fire. The time history analysis method is used with SAP2000 program. The present study used available deformed steel building due to fire as start point including deformation quantities, deflected shape reduction in material properties, and then apply static and dynamic wind loads for southern Iraq conditions.

A scroll of aged, yellowish paper is unrolled, held by four dark circular fasteners at the corners. The scroll is slightly wrinkled and has a small tear on the left side. A quill pen is tucked under the bottom right corner of the scroll. The text is centered on the scroll in a bold, italicized serif font.

Chapter Three
Post Fire
Investigation

CHAPTER 3

POST FIRE INVESTIGATION

3.1 Introduction

Post-fire performance of a structural element has gained considerable attention recently, apart from the fire safety of a structure, the reinstatement of fire damaged structures is at the centre of interest nowadays. The present study is focused on whether, it is possible to reuse (reinstatement) the structural element after fire when subjected to wind dynamic loads based on deformation limitations, and taking into consideration after fire process effect like, reduction in steels strength (the yield stress and the modulus of elasticity (F_y , E)) the imperfection in structure elements.

Despite the significance of fire design of steel structures, no specific guidelines have been established by the current design codes for the determination of the remaining capacity of steel members after fire, with the exception of some recommendations by the British standard, which is no longer in use. It is founded that contributes to the assessment of fire damaged steel and its subsequent reuse .

The steel is subjected to several effects after fire to cooling process where the yield stress and modulus of elasticity values are reduced in member due to fire in the steel building, then the deformities begin to appear in the building the result of these effects are displacements in column and deflection on beam also some of buckling occurred on beam and column and elongation of member due to fire all these deformations are called the imperfections.

3.2 Types of Imperfections

3.2.1 Geometrical Imperfections

Meaning the variance of dimensions of a structure or a member ($b \pm \Delta$) or lack of verticality of a structure and straightness [24] (erection out-of-plumbness, member out-of-straightness) as shown in Figs. (3-1) and (3-2).

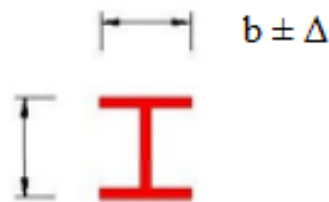


Figure (3-1): Variance of dimensions [24].

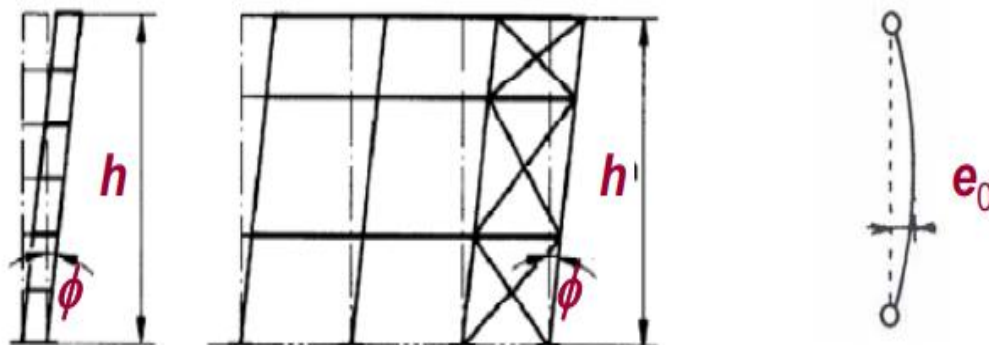


Figure (3-2): Out-of-plumbness and straightness [24].

3.2.2 Material Imperfections

The variance of material properties or residual stresses (distribution in a cross section usually considered uniform along the member) is called material imperfections, as shown in Figs. (3-3) and (3-4).

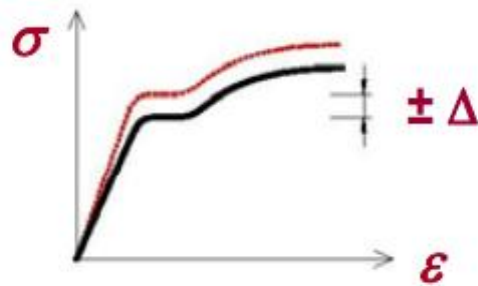


Figure (3-3): Variance of material properties [24].

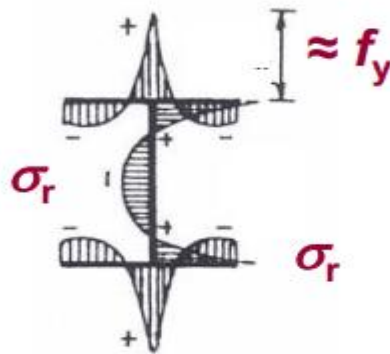


Figure (3-4): Typical residual stress pattern for I-shaped steel member [24].

3.2.3 Structural Imperfections

It is Mean the variance of boundary conditions, eccentricities in joints as shown in Figs. (3-5).



Figure (3-5): Eccentricities in joints [24].

When steel structures are exposed to fire, strength and stiffness are decreased with increasing temperature. The structure then deteriorates and the deformations that happen after the cooling process will be composed as imperfections, appropriate allowances shall be incorporated in the structural analysis to cover the effects of imperfections. This study takes into consideration material imperfections which include residual stresses by changed stiffness (EI) meaning reducing E to 90% and material mechanical properties such as (F_y , E) reducing same value [25] while geometrical imperfections such as lack of verticality (erection out-of-plumbness) and elongation are represented as displacement deformation value in story after fire while out of straightness and buckling (local buckling ,lateral-torsional buckling) are not considered in this study because SAP V2000 software is unable to represent these cases and also minor eccentricities presented in joints of the structure are not considered here.

3.3 Residual Stresses

Residual stress evaluation is measured by removing instrumented areas or coupon samples from the fire exposed steel member. Prior to coupon removal, either mechanical or electrical strain gages are attached and calibrated with an initial reading taken. The coupon is then carefully removed from the member and the strain is measured until the recorded strain data stabilizes. The difference between initial and final readings indicates the internal member strain at the gage location. Placing gages at carefully chosen locations permits a reasonable prediction of the resultant stress distribution in the member [26].

Although residual stresses influence on the steel member capacity, Tide [26], plastic design research summarized by Lehigh [27] and ASCE [28] indicates design specifications accurately predict steel member behavior. The

combination of externally applied forces and internal residual stresses are accommodated by redistribution when plastic hinges form. Residual stresses will increase deflections above those theoretically predicted for residual stress free members. The deflections can become significant as the applied load approaches the member's ultimate capacity. However, the deviation from theoretical behavior is not significant at or below service loads, and usually cannot be detected. In the present study the residual stresses after fire are included by changed stiffness (EI) [25], for this study reducing to 90% from the modulus of elasticity before fire in order to take into consideration effect of residual stresses.

3.4 Buckling and Other Visible Deformation Due to Fire

Due to the thermal elongations coupled with reductions in steel strength and stiffness that occur at elevated temperatures, even minor member end restraint, imperfections, crookedness, or force eccentricity can initiate visible local flange and/or web buckling, or overall member buckling, above about 600 °F (315 °C). With complete restraint from thermal expansion, these may occur at temperatures as low as 250 °F (120 °C). Buckling is very likely to occur at temperatures in the range 1,200 to 1,400 °F (650 to 760 °C), when the strength and stiffness are less than 50 percent of their nominal ambient values. Past experience from flame curving and straightening indicates that local buckling often can occur quite suddenly at, and above, this temperature range [26, 29].

In addition to these buckling distortions of the member, the steel will experience increasing end rotation and vertical deflections during the fire from the existing dead and live loads. Under fire conditions, both for uncontrolled natural exposures and in standard tests, the temperature-induced deflections of

fire-resistive steel beam/concrete floor systems can be large. Actual fires have produced deflections ranging from several inches up to, in extreme cases, 0.9 to 1.2 m, which are an order of magnitude greater than the normal serviceability limits that are anticipated for buildings.

In this sense, it must be remembered that the intended structural outcome of fire safety design is to maintain building integrity and prevent (or delay) catastrophic collapse, Fig.(3.6) shows a UL(Underwriters Laboratories) test of a roof assembly in the furnace after a successful fire test. Steel deck sag and beam buckling are visible as shown in Fig.(3-7) [29].

It should be noted again that visible deformations are not by themselves indicators that the steel had been heated to temperatures beyond 1,300 °F (700 °C), given the possibility of steel buckling even at lower temperatures, depending on the magnitudes of the actual applied loads.

However, and very importantly, the converse is also true - steel that is not grossly deformed and is deemed to be repairable probably did not experience temperatures beyond 1,300 °F (700 °C). When heated to high levels, steel is also likely to change its external appearance and color.

If the steel temperatures have not exceeded about 1,300 °F (700 °C), tightly adherent mill scale will remain, and the color will look normal. At steel temperatures hotter than 1,300 °F (700 °C) for more than about 20 minutes, the steel surface will become noticeably oxidized and possibly pitted, with some accompanying erosion and loss of cross-sectional thickness.

The appearance of significantly “burned” steel is ordinarily light gray or white, but it also could assume the color of the fuel contents in the room, such as black from the combustible residues[29].



Figure (3-6): UL steel roof assembly after successful ASTM E119 fire test (courtesy of underwriters laboratories, Inc.) [29].



Figure (3-7): One meridian plaza in Philadelphia after Feb. 23-24, 1991 fire [29].

3.5 Categories of Post-Fire Steel Damages

The steel must be heated above the lower phase transformation temperature of 1330 °F (721°C) before any temperature induced residual stress increase can occur. At lower temperatures, stress relieving may occur, especially if the steel is protected. Restraint induced forces are more likely to cause yielding resulting in a change and rearrangement of residual stresses. For the usual loading conditions associated with steel-framed buildings, the effect of residual stresses at service loads is innocuous. Shakedown theory and testing, Eyre (1970) [49], indicated after a few cycles of loading that causes yielding, the effect of the residual stresses is essentially eliminated. The deflection behavior of the structure during any subsequent loading is based on elastic behavior.

Steel members having noticeable distortions are categorized separately in terms of their metallurgical and structural properties. Test data reported by Kirby (1986) [1], Saul [31], Dill [32], Smith [33], and Wright [34] indicate that severely distorted steel may remain metallurgically unchanged because buckling and large deflections probably occurred at temperatures well below 1200°F (650°C). Experience gained from heat straightening Saul [31], Stitt [35], Pattee [36], Holt [37], Stewart [38], and Avent [39] reinforces the following statement made by Dill [32]: "Steel which has been through a fire but which can be made dimensionally re-usable by straightening with the methods that are available may be continued in use with full expectance of performance in accordance with its specified mechanical properties."

Wright [34], Avent [39], confirms that this statement is as true and suggested that the criteria for evaluating fire exposed and damaged steel is a function of reparability, rather than inconsequential metallurgical changes .

A recent and more detailed discussion of these issues is provided by Tide [26]. He recommended that a fire damaged structure be assessed in one of three categories:

- A. Category 1: Straight members that appear to be unaffected by the fire, including those that have slight distortions that are not easily visually observable, (Within 4 or 5 times ASTM A6 rolling tolerances).
- B. Category 2: Members that are noticeably deformed but that could be heat straightened, if economically justified.
- C. Category 3: Members that are so severely deformed that repair would be economically unfeasible when compared to the cost of replacement.

Category 1 and 2 members are unlikely to have exceeded 1,300 °F (700 °C) for any appreciable length of time during the fire. Hence, it can be reasoned that they did not suffer any permanent changes in their properties after cooling back to ambient temperatures. Smith et al [33], gave further information on steel properties after heating and cooling.

The relative economies of straightening versus replacement are particularly relevant for Category 2 since, from a structural performance perspective, these members can be repaired by straightening and remain in service.

The severe fire damage representative of the category 3 designation usually favors replacement of the member, both due to the higher repair cost and possible adverse residual properties. Such members have probably experienced temperatures in excess of 1,300 °F (700 °C) for a prolonged time, and consequently, may have suffered noticeable, adverse, and permanent external and internal changes during the fire. Once the condition of each

individual member is determined, the safety of the whole structure can be established. A member inventory should be performed before an assessment of repair or replacement can begin. The biggest challenge often encountered with this evaluation is convincing the interested parties that the basic steel properties of category 1 and 2 members were unaffected by the fire. Camber and sweep of each fire exposed, structural steel member should be determined using appropriate measurement techniques (plumb bob, string line, laser or theodolite). A category 1, 2 or 3 designation should then be assigned to each member. Most often, the category 2 or 3 designations can be assigned without measuring because of severe local buckles or excessive deflections. Illustrative examples of member categorization are presented in Figs. (3-8) to (3-10). In Fig.(3-8), the two twisted steel beams would be classified as category 2. Members like this would usually be discarded for economical reasons even though heat straightening is possible. Similarly, the buckled beam shown in Fig.(3-9) would probably be replaced for economical reasons [26].



Figure (3-8): Considerable thermally induced beam [26].

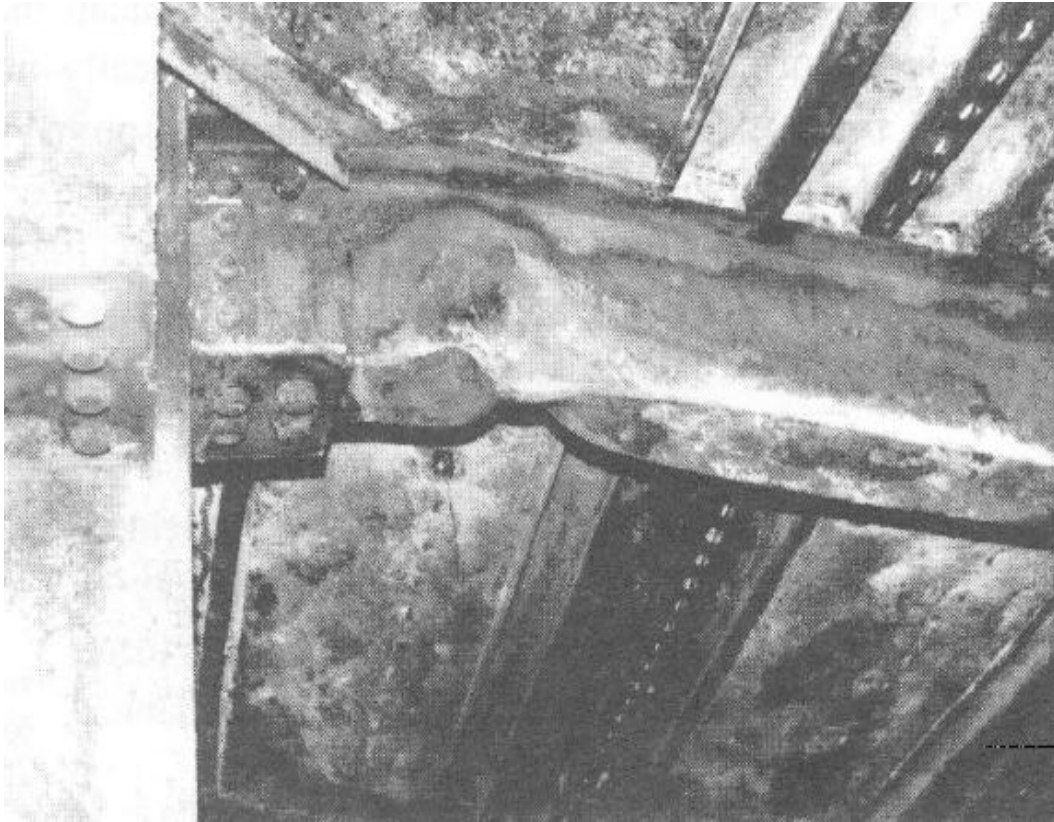


Figure (3-9): Severe local buckle in beam [26].

In comparison, the severe local buckling in the column shown in Fig.(3-10) would normally be repaired under loaded conditions. Because of supported load above and the location, the cost to replace the column justifies in-place repair by either reinforcing plates, heat straightening, or both. However, for this particular case there was unacceptable vertical displacement, and therefore the column was replaced after jacking up the column shaft so that the floor grade could be reestablished.

Earlier studies demonstrate that category 1 straight members require only minimal consideration, Kirby [1], Dill [32], Smith [33], Avent [39] and others. Metallurgical or structural degradation does not occur with a category 1 appearance. For any significant metallurgical degradation to occur, temperatures would have to exceed 1330 degrees F (721°C). Prior to reaching this elevated temperature level, buckling or large deflections would certainly

occur. Slightly deformed category 1 members, with deformations greater than rolling tolerances, must be analyzed to determine the repair level. Depending on individual circumstances, the analysis will determine if these members can be accepted unconditionally, heat straightened, stabilized with supplemental braces, or reinforced with plates and shapes.

Category 2 members require additional attention because the decision to repair or replace is often a function of the nearby members' condition. A beam is easy to replace when compared to a column supporting several floors (see Fig.(3.10). If a category 2 member is heat straightened, the change in metallurgical and structural properties will be inconsequential. Rehabilitation or replacement of category 2 members is usually dependent on expediency, economics or overcoming the human psychological rejection of what appears to be damaged steel. In the present study the members are considered exceeded category 1 that have slight distortions and category 2 that are noticeably deformed but could be heat straightened thus the categories 1 and 2 can be re-used again while category 3 can't be reused because a better solution is to replace members which yield less expensive and more resistant than its repair.

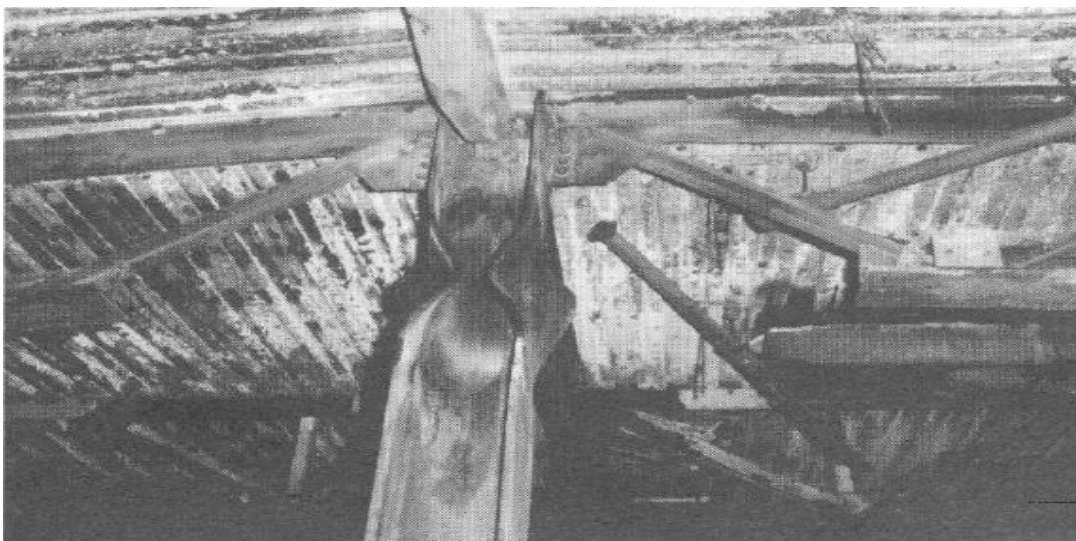


Figure (3-10): Severe local buckle in column [26].

3.6 Connection

Connection behavior is different than main member behavior when the temperature increases because of their relative compactness. The axial force developed by a restrained member will impose large forces on the end connections. Generally, the beam will buckle or deform to accommodate the axial force. Under these conditions, connection distress is easy to identify when a category 1 steel beam cools, if the connection has fractured, the steel beam will pull away from the adjacent member revealing the damage.

It is common to see fractured connections at the ends of buckled beams. As the buckled beam cools and shortens, the connection material, bolts or welds, will be torn apart similar to the connection of Fig.(3-11) this type of bracket failure behavior occurs because the AISC specifications contain a higher safety factor or reliability for bolts and welds than plain steel. Bolts heated to the tempering temperature and held there for several hours will generally have a reduced pretension force once they return to ambient temperatures[26].

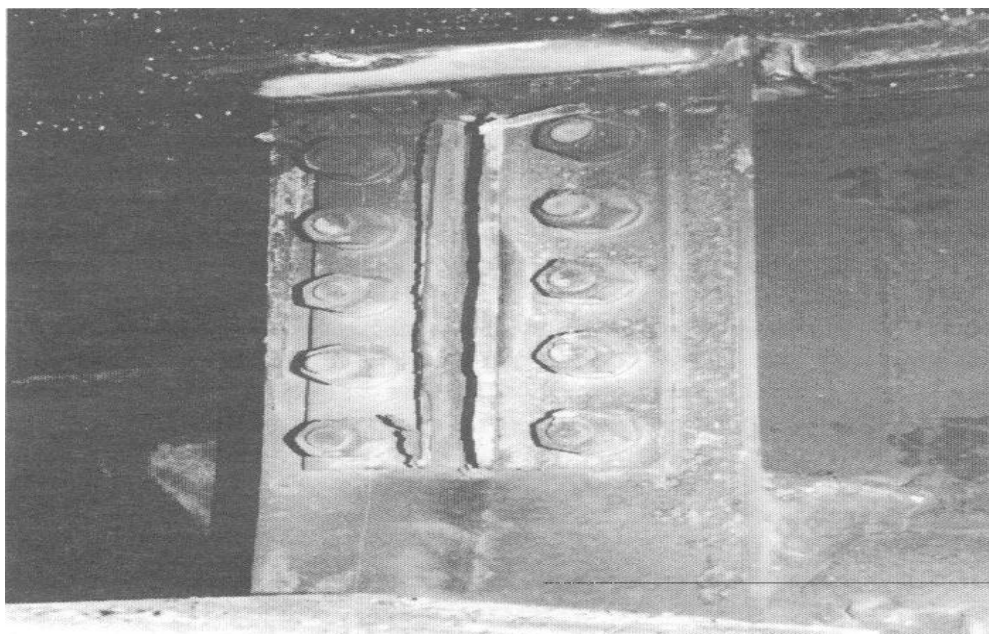


Figure (3-11): Connection failure at end of buckled beam [26].

because of the variability of bolt installation procedures and quality control, it is impossible for a visual inspection to determine temperature effects on high strength bolts. Changes in metallurgical properties of high strength bolts can only be determined by non-destructive or destructive testing. Destructive bolt tests by Kirby [1], provide guidance on testing procedures that can be considered.

In the present study post-fire investigations of connection is not considered because its representation needs complex operations.

3.7 Steel Behavior with Temperature Increasing

For most hot rolled shape production, final rolling occurs when the steel is at about 1,600 °F (870 °C) or higher. Intentionally reheating steel to higher temperatures is also well known for special material treatments, with stress relieving done at temperature range of 1,100 °F to 1,200 °F (590 °C to 650 °C), and annealing and normalizing temperatures reaching 1,500 °F to 1,600 °F (820 °C to 870 °C). Likewise, the traditional and successful heat straightening and curving practices for fabrication of steel members are done at temperatures up to 1,200 °F (650 °C). ASTM E119 fire test standard specifies a limiting average temperature of 1,100 °F (593 °C) and a limiting maximum temperature of 1,300 °F (704 °C) for unrestrained ratings for steel beams and steel framed floors [26].

Therefore, if the temperatures in the steel do not exceed the transformation temperature of 1,300 °F (700 °C) for a measurable amount of time, the steel can be expected to have acceptable metallurgical properties upon cooling back to ambient conditions.

Its residual properties will be the same, or perhaps better, than in the original pre-fire condition. Smith et al [33] provides further confirmation data on steel properties after heating and cooling. The mechanical properties of the

steel continue to degrade with increasing temperatures, until near total strength and stiffness depletion occurs around 2,000 °F (1,100 °C). The actual melting point of steel is in the range of 2,500 °F to 2,700 °F (1,370 °C to 1,480 °C), which can vary with the particular chemistry and accompanying phase changes. However, for practical purposes, relatively little strength and stiffness of steel are retained beyond about 1,300 °F (700 °C), less than 20 percent of the ambient values. Beyond 1,600 °F (870 °C), steel's metallurgical microstructure undergoes a permanent transformation relative to its original chemical composition that will result in grain coarsening and hardening, which, with the subsequent cooling, will adversely affect its residual mechanical properties [26].

Steel contracts as it cools. When inelastic deformations occur during a significant fire due to applied service loads and existing thermal restraint, the steel will experience permanent set and will not return to its original shape upon cooling. These geometric changes from fire and subsequent cooling have caused several instances of steel beam connections that were reported to have failed in tension [26].

3.8 Post-Fire Tolerances

3.8.1 Tolerance for Beam

The permissible limits for beam deflection based on American specifications, is $(L/360)$ (for beams that have not been subjected to other or deflection distortions such as twisting and no change in steel properties).

For any deflection less than or equal to that ratio is considered to be acceptable, but if the deflection exceeds this percentage, it is considered to have been subject to major deformities not acceptable constructively.

However, if it is exposed to other deformation other than deflection such as twisting, the limits have been adopted deviation in ASTM A6, which does not exceed the difference between the flange ends of 3 mm where the element is safe if the deformation caused by the fire is (4 to 5) of the deviation limits permitted in ASTM A6 [26].

3.8.2 Tolerance for Column

The deviation limits are in ASTM A6 and AISC which do not exceed the displacement between up and down the shaft ($L / 500$) where the element is safe if the deformation caused by the fire is (4 to 5) the permissible deviation limits in ASTM A6 and AISC [26], the straightness tolerance permitted is 1mm/m of the length [1].

3.9 Post-Fire Reduction of Yield Stress of Steel

The idea of reducing the mechanical properties of steel was based on the researcher Maraveas, 2014 [14] which investigated the mechanical properties of structural steel exposed to fire and cooled down where mechanical properties were reduced by 10% of The initial strength before the fire for normal strength steel under the temperature of 600 °C. While if the temperature greater than 600 °C the steel will lose more than 10% , so this ratio depended on types of steel strength and also value of temperature that building arrived to it. In the present study the yield stresses after fire is reduced about 10% from before fire.

3.10 Post-Fire Configurations

The concept of post-fire investigation in the present study is based on scenarios or configuration of steel frames deformation due to fire after cooling

phase which are available in literature. Thus the present procedure for post fire analysis of steel frame is applicable to any damage scenario due to fire.

In this study two scenarios are considered namely, Iua et al. and Lien et al.

1- Iua et al. 2005 [13], studied an eight-storey composite frame was designed as a three bay-deep and five-bay-wide structure at the Cardington fire test in the UK. The geometry and member section of a typical plane frame and fire place are also displayed in Fig.(3-12).

The results and the deformation shapes of the plane frame for the heating sequence of 650°C , 800° , and 20°C are displayed in Figs. (3-13) to (3-15).

They were found that after the structure cooling to ambient temperature, the lateral displacement increases inward to 155mm in column and 220mm in mid beam while 192mm in edge beam, the values of displacement in column and deflection in beam after cooling back are 155mm, 220mm respectively, these values of deformations through 800°C and cooling back to 20°C ambient temperature.

In the present study the maximum deformation considered for this scenario are $L/40$, $L/60$ for column and beam respectively, which reflect steel building subjected to a temperature of 550°C .

After the cooling phase, the deformation shape is shown in Fig.(3-15). It is clearly noticed that the columns displaced to inside and the beams sag downward, and assuming these values are reduced from bottom in place of fire to top of building

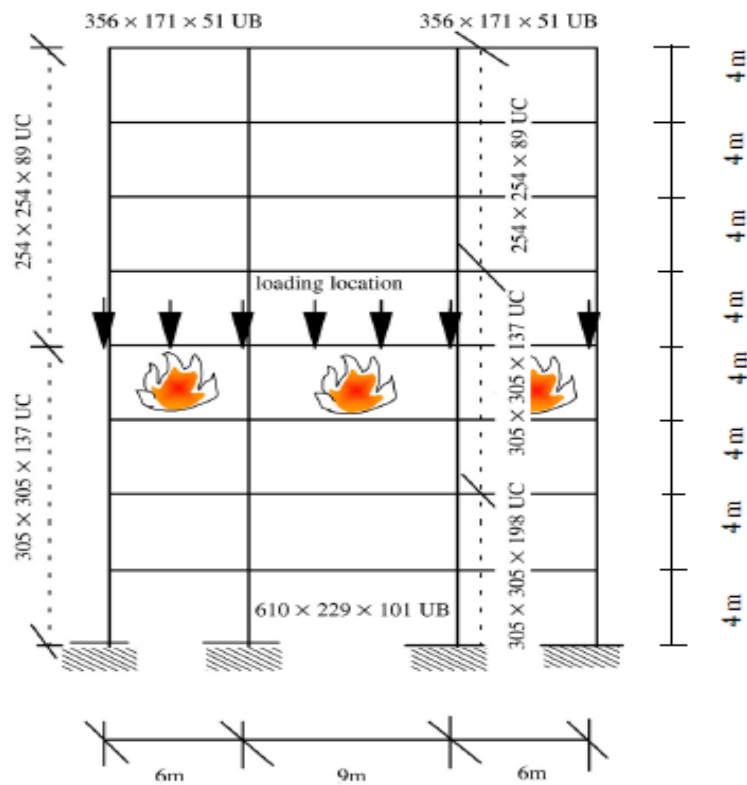


Figure (3-12): Geometry and section of the eight-storey plane frame [13].

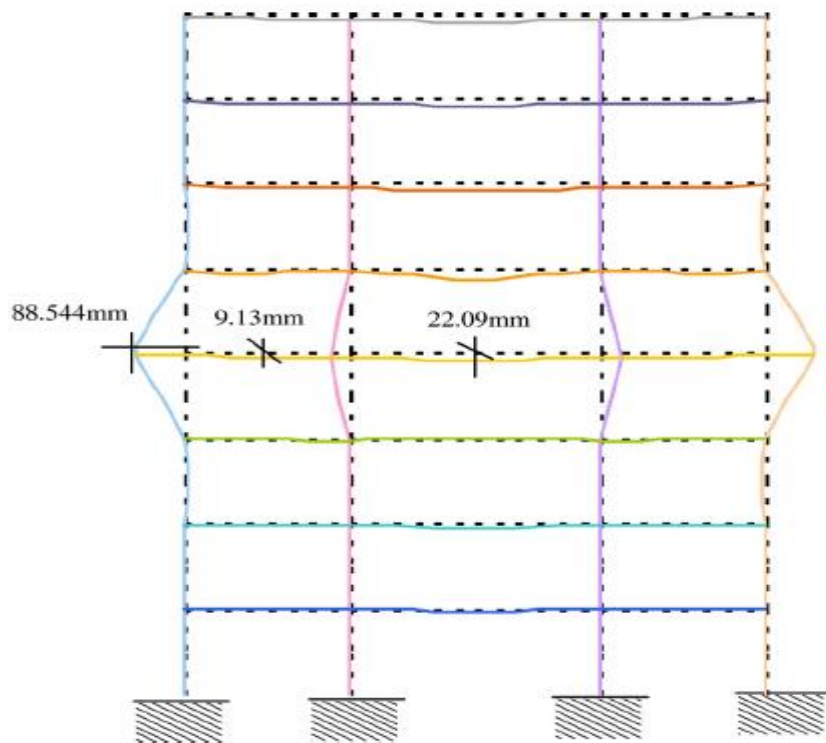


Figure (3-13): Deformation shape at 650°C during the heating phase [13].

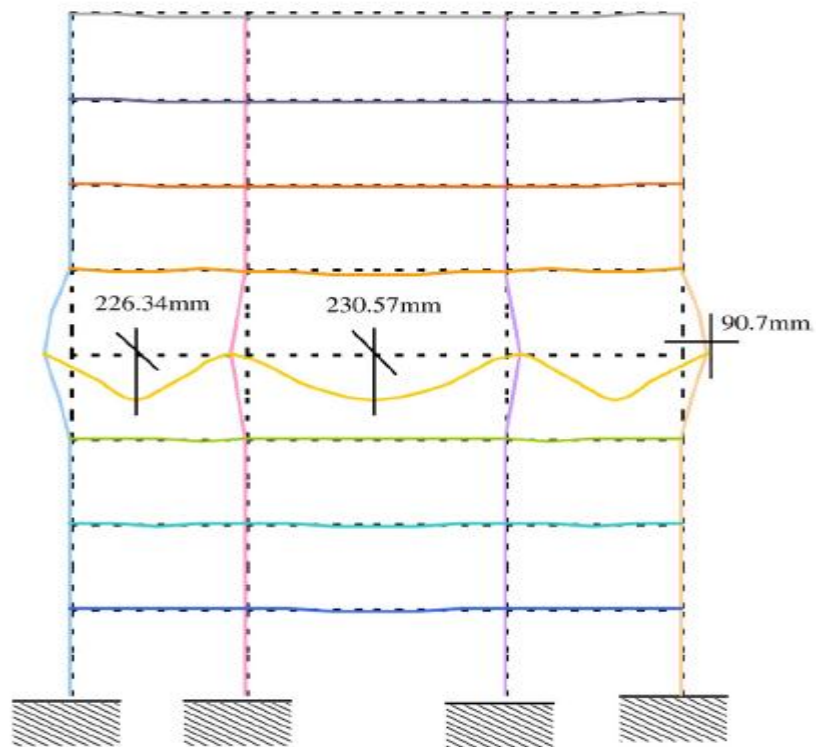


Figure (3-14): Deformation shape at 800°C during the heating phase [13].

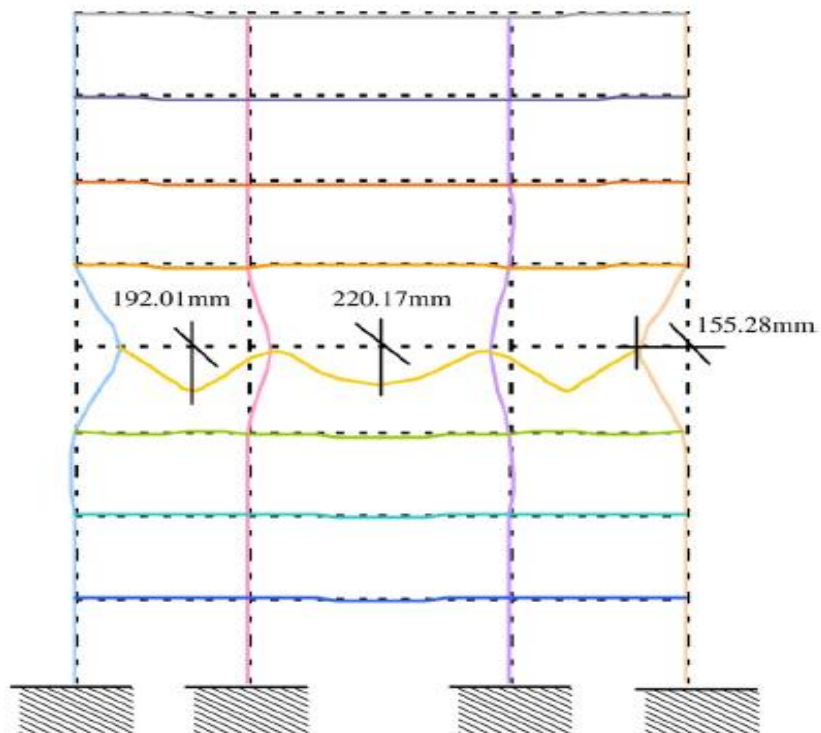


Figure (3-15): Deformation shape at 20°C after the cooling phase[13].

2- Lien et al. 2009 [40], studied the nonlinear structural behavior of steel structures during the cooling as well as the heating phases of fire. The geometry and member section of a typical plane frame and fire place are also displayed in Fig.(3-16). the column become out of plain during the process of fire and during an increase in temperature due to the expansion of the beam to the outside, which leads the column to outside either during the process of cooling back was shrink beam to pulls up with the column to inside.

From this study, the benefit is knowing the deformed shape after fire, the columns displayed to inside and the beams sag down. As shown in Fig.(3-17).

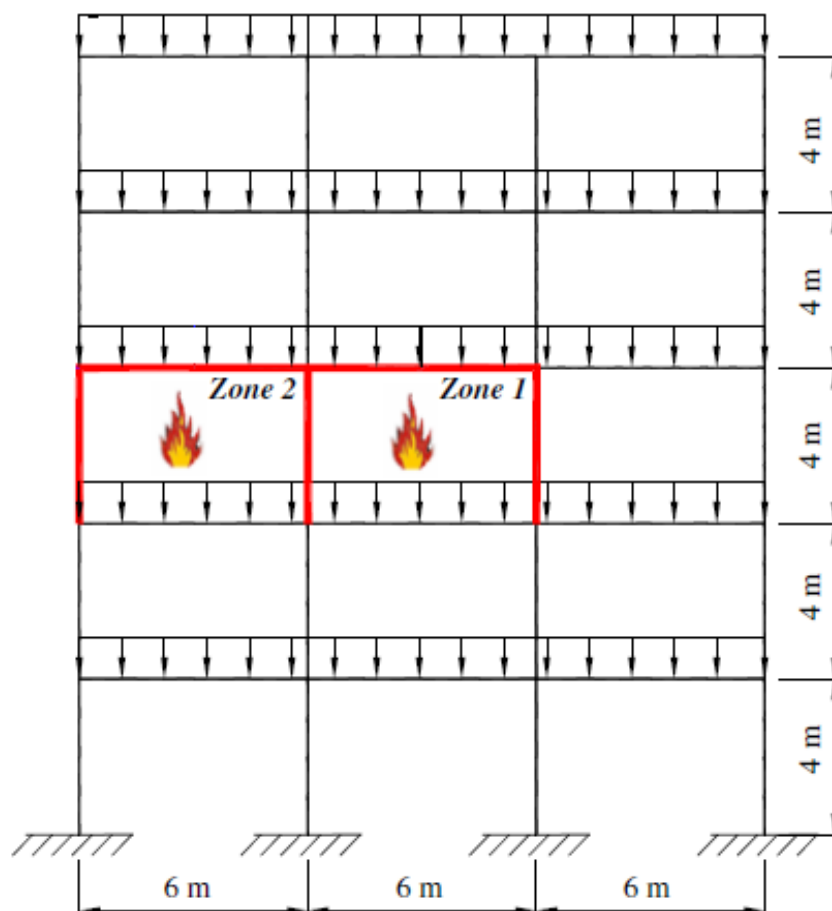


Figure (3-16): Geometry and section of the five-storey plane frame [40].

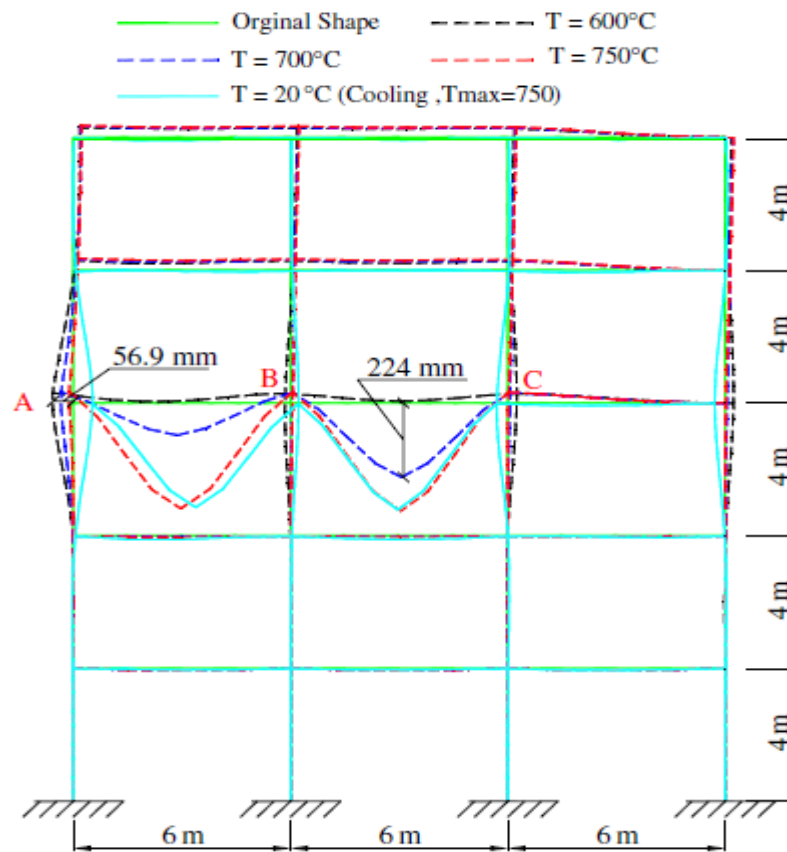


Figure (3-17): Deformation of steel frame under different temperatures in the fire [40].

A vertical scroll of aged, yellowish paper is unrolled, held by four dark grey circular fasteners at the top and bottom. The scroll is slightly wrinkled and has a soft shadow cast to its right. A quill pen, also made of aged paper, lies diagonally across the bottom right corner of the scroll. The text is centered on the scroll in a bold, italicized serif font.

Chapter Four
Wind Analysis

CHAPTER 4

WIND ANALYSIS

4.1 Introduction

The lateral loadings due to wind and earthquakes are the major factor that causes the design of high-rise buildings to differ from those of low-rise buildings. For many countries, the action of wind forces on structures has been classified as one of the important forces that cause structural failures. Two methods have been made to measure wind action, first the speeds of winds, and second the wind forces on structures. The development of modern materials and construction techniques has resulted in the emergence of a new generation of structures. Such structures generally, display an increased susceptibility to the action of wind. The dynamic wind problems arise from periodic variations in the pressure distribution on the shell of the building.

For purpose of analysis, it is common to split the response into static and dynamic approaches. The calculations of the wind load acting on a structure and the response of the structure to this load have numerous shapes. These include the description of the wind field, the dynamic characteristics of the structure and the wind structure interaction. Due to the inadequacy of information on one shape or the other and also in order to simplify the analysis, suitable assumptions have to be made for the analysis of structures under the wind[58].

There are no universally accepted definitions for these terms, proposes the classification of buildings by number of storeys (low-rise = 1-5 stories, mid-rise = 6-12 stories and high-rise = 13 stories and above) these definitions are useful for explain the effect of wind [7].

4.2 Variation of Wind Velocity with Height

The viscosity of air reduces its velocity adjacent to the earth's surface to almost zero, as shown in Fig. (4-1). A retarding effect occurs in the wind layers near the ground, and these inner layers in turn successively slow the outer layers. The slowing down is reduced at each layer as the height increases, and eventually becomes negligibly small. The height at which velocity ceases to increase is called the gradient height, and the corresponding velocity, the gradient velocity. This characteristic of variation of wind velocity with height is a well-understood phenomenon, as evidenced by higher design pressures specified [4].

Near the earth's surface, the motion is opposed, and the wind speed reduced, by the surface friction. At the surface, the wind speed reduces to zero and then begins to increase with height, the motion may be considered to be free of the earth's frictional influence, and the important characteristic of wind is the variation of its speed with height. The wind speed increase follows a curved line varying from zero at the ground surface to a maximum at some distance above the ground [4].

For example a heights of approximately (366 m) aboveground, the wind speed is virtually unaffected by surface friction, and its movement is solely dependent on prevailing seasonal and local wind effects [4].

The height through which the wind speed is affected by topography is called the atmospheric boundary layer. The wind speed profile within this layer is given by

$$V_z = V_g \times \left(\frac{Z}{Z_g}\right)^{\frac{1}{\alpha}} \quad (4.1)$$

Where ;

V_z = mean wind speed at height Z aboveground

V_g = gradient wind speed assumed constant above the boundary layer

Z = height aboveground

Z_g = nominal height of boundary layer, which depends on the exposure (values for Z_g are given in Fig. (4-1).

α = power law coefficient

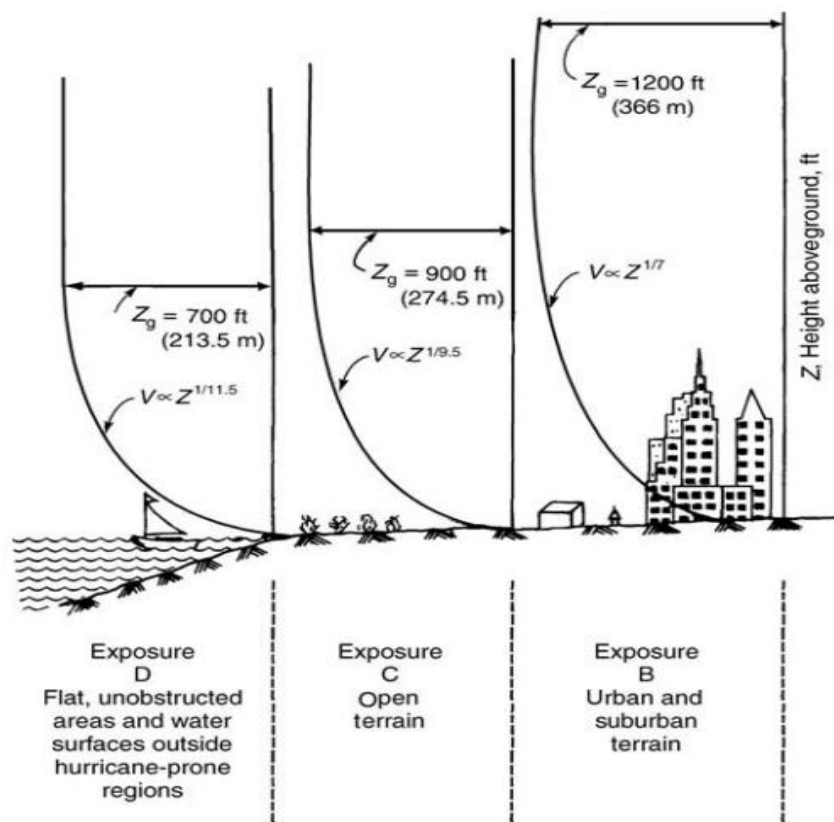


Figure (4-1): Influence of exposure terrain on variation of wind velocity with height [°].

with known values of mean wind speed at gradient height and exponent α , wind speeds at height Z are calculated by using Eq. (4.1). The exponent $1/\alpha$ and the depth of boundary layer Z_g vary with terrain roughness and the averaging time used in calculating wind speed. The factor α ranges from a low of 0.087 for open country and of 0.20 for built-up urban areas, signifying that

wind speed reaches its maximum value over a greater height in an urban terrain than in the open country [1].

An instantaneous picture of the along-wind variation of the wind field with the height z is shown in Fig. (4-2). Where $v(z)$ is the mean wind velocity and $U_x(x, y, z, t)$ is the turbulence of the wind field considered as weakly stationary stochastic processes [1].

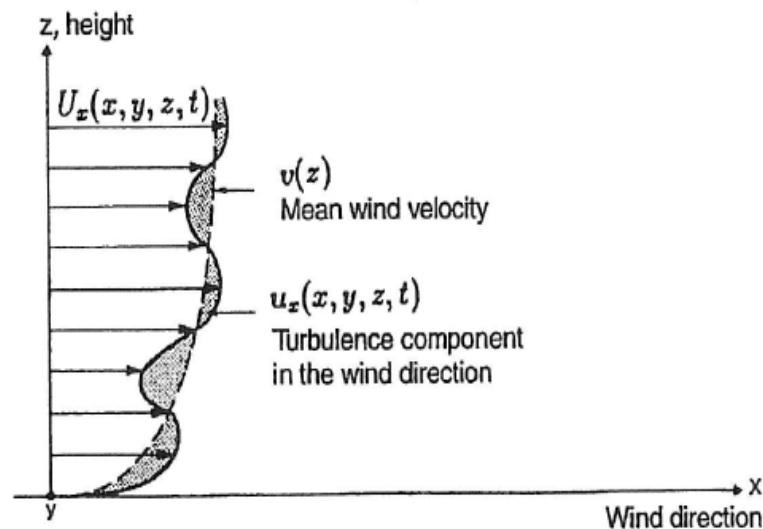


Figure (4-2): Variation of wind velocity with height [1].

4.3 Wind Loadings

The wind movement is free air caused, on a large scale, by thermal currents from areas of high pressure to areas of low pressure. As the air mass moves over the ground there is a boundary layer several hundred meters thick, near the bottom of which the wind speeds are measured [42]. When dealing with high rise building, an important consideration is the variation of wind speed with height. It is well known that roughness of the terrain retards the wind near the ground. The lower layers of air then retard those above them, resulting in different wind speeds from the ground level until the retarding

forces are diminished to zero. Therefore, several approximate equations have been developed to provide a better understanding of the wind gradient. One such equation is the power law wind formula [43, 44]. This equation is frequently used to calculate the wind speed at a height other than that at which the wind is measured:

$$\frac{V_1}{V_2} = \left(\frac{Z_1}{Z_2}\right)^\alpha \quad (4-2)$$

Where:

Z_1, Z_2 : heights (m)

V_1, V_2 : wind velocities (m/sec)

α : power law coefficient

The force on a structure is proportional to the square of wind speed; therefore, the design wind speed used for analysis is very important to determine the values of wind forces. These forces can be defined by the use of the general force function:

$$F = 0.5 \bar{\rho} V^2 CA \quad (4-3)$$

Where

F: Wind force (N)

$\bar{\rho}$: Density of air (kg/m^3)

V: wind speed (m/sec)

C: shape factor or force coefficient (C_d)

C_d : is drag force coefficient

A: area upon which wind acts (m^2)

The wind velocity can be determined using the Beaufort Wind Scale presented in Table (4-1), which estimates wind velocity by observing the wind's

effects on its surrounding environment; this is also a qualitative scale of wind forces [42, 44].

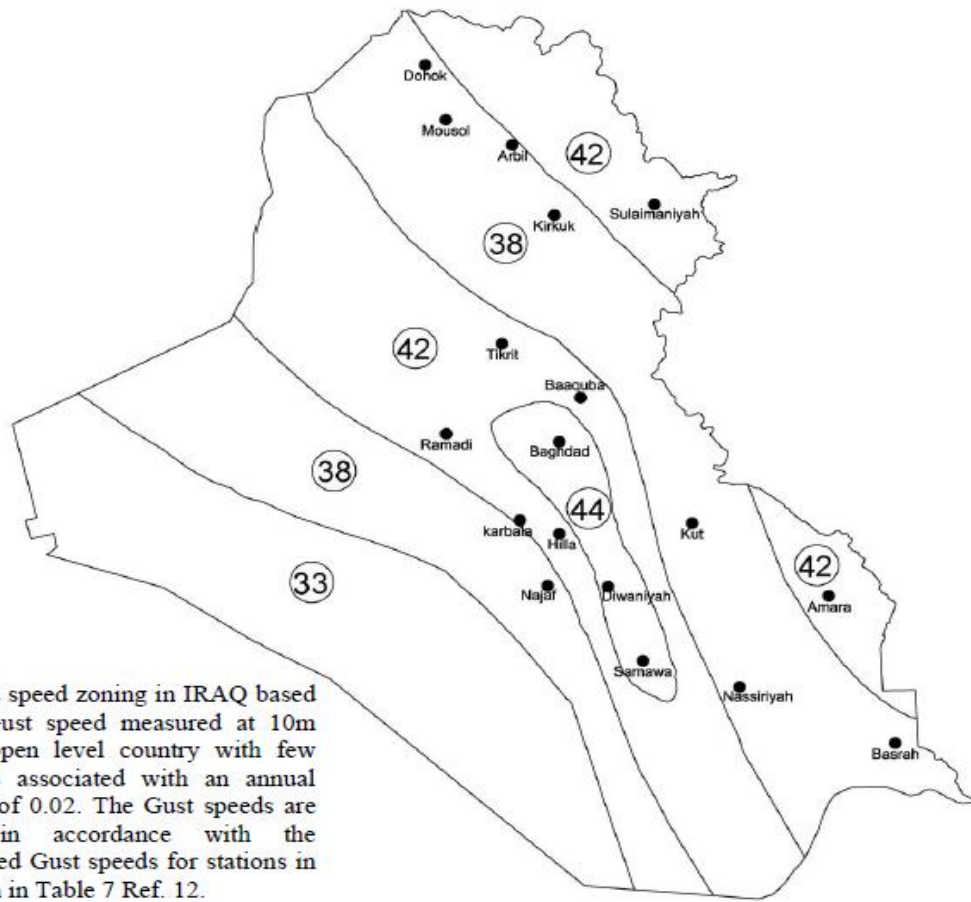
Table (4-1): Beaufort scale of wind force [42].

Beaufort force	Wind speed m/s in 10 m above ground	Type of wind
0	Less than 0.277	Calm
1	0.277 - 1.666	Light air
2	1,666 - 3.333	Light breeze
3	3.333 - 5.555	Gentle breeze
4	5.555 - 8.055	Moderate breeze
5	8.055 - 11.111	Fresh breeze
6	11.111 - 14.166	Strong Breeze
7	14.166 - 17.222	Near gale
8	17.222 - 20.833	Gale
9	20.833 - 24.722	Strong gale
10	24.722 - 28.611	Storm
11	28.611 - 43.000	Violent storm
12	more than 43.000	Hurricane

4.4 Design Wind Speed

In this study, along wind component is considered in the analysis. In the along wind direction, the wind speeds are obtained from Iraqi Code IQS.301 (Iraqi Code for forces and loadings) [45], which corresponds to the 3 second-Gust speed at 10 m above ground in open terrain. The basic design wind speeds for Iraq is shown in Fig. (4-3) from which it's clear that basic wind speed for example (Misan Province) is 42 m/sec.

The data for wind speed in Misan province for period from 1986 to 2016 is obtained from (Iraqi meteorological organization and seismology) and shown the Table (4-2). The maximum wind speed for 30 years period is 5.70 m/s which is much smaller than design wind speed presented by IQS.301. Thus using IQS.301 values for calculate wind loading on structures



Note: Wind speed zoning in IRAQ based on 3-sec Gust speed measured at 10m height in open level country with few obstructions associated with an annual probability of 0.02. The Gust speeds are modified in accordance with the recommended Gust speeds for stations in IRAQ given in Table 7 Ref. 12.

Figure (4-3): Contour map for basic wind speeds m/s of Iraq [٤٥].

Table (4-2): Moderate wind speeds m/s Iraqi meteorological organization and seismology.

South Of Iraq / Months	By Iraqi meteorological organization and seismology at 10 m above ground (2016-1986)											
	January	February	March	April	May	June	July	August	September	October	November	December
Al-Hayy	3.50	4.00	4.10	4.60	4.40	4.90	5.50	4.80	4.20	3.70	3.50	3.50
Qadisiyah	2.30	2.40	3.20	3.50	3.30	3.80	4.20	3.60	3.20	1.80	1.09	1.90
Nasiriyah	3.30	3.80	4.40	4.60	4.80	5.70	5.30	5.00	4.30	3.00	3.00	3.00
Salman	2.90	3.20	3.60	3.50	3.60	4.50	5.10	4.10	3.00	2.90	2.70	2.70
Basra	3.20	3.60	3.90	3.90	3.80	5.10	5.40	4.60	3.70	2.70	2.90	2.90

Can be observed there is clear difference between recorded wind speeds and recommended speed by IQS 301. so the most effect was used in speed and speed was 42 m /s.

In present study two wind speeds are considered.

1. Strong wind speed: which use the values of wind speeds presented by IQS 301. Namely for Misan province strong wind speed equal to 42m/s.
2. Moderate wind speed: which represent the commonly faced wind speed according to actual readings and it value assuming considered half of IQS 301 values to take into account fluctuations of wind as in section 4.2, namely for Misan province moderate wind speed is 21 m/s.

4.5 Methods of Analysis

Under the action of the wind flow, structures experience dynamic forces that include the drag (along-wind) force acting in the direction of the mean wind [6]. The wind load is presented either by using a dynamic approach or an equivalent static approach. The methods for determining the response of structures to wind loading can be classified into two kinds:

4.5.1 Dynamic Analysis

For the dynamic analysis there are four main techniques [7], which are:

- 1-Direct integration of the equation of motion, which is based on a Step-by-step procedure.
- 2-Normal mode analysis.
- 3-Response spectrum technique (Frequency domain analysis).
- 4-Time history, In this study, the Time history analysis is used.

4.5.2 Equivalent Static Analysis

The equivalent static analysis converts the dynamic wind pressure into an equivalent static pressure for the sake of analysis. The procedure of this technique commonly presented in Standard codes and specifications like ASCE, UBC, EURO CODE...etc.

4.6 Wind Loading Simulation

4.6.1 Dynamic Approach

Because the wind forces are time-dependent, the methods of structural dynamics may have to be employed to determine the response. In some cases the dynamic force may be small compared to the static force, however, it can be potentially more dangerous depending on the dynamic characteristics of the structure, particularly if resonance conditions are approached.

The velocity at any height can be estimated by using equation (4-1) depending on the measured velocity at 10 m above the ground as:

$$v_x(t) = v_{10}(t) \times \left(\frac{x}{10}\right)^{\frac{1}{\alpha}} \quad (4-3)$$

where ;

x : distance from ground level in a meter.

$v_{10}(t)$: reference velocity, at 10 m above the base in m/sec.

$v_x(t)$: the wind velocity at any height (x) in m/sec.

α : power-law coefficient commonly 0.143 [ξ^v].

In the present study along wind component is used. Estimation of the magnitude of the wind-induced loading (drag force) on buildings provides information vital for the design.

4.6.1.1 Wind Pressure Coefficients

The pressure coefficient is used to transform the stagnation pressure to a pressure which accounts for site exposure and building geometry. Pressure coefficients are dimensionless quantities that define pressure or suction acting normal to the surface of a building.

A positive value indicates that the wind pressure acts inward, and a negative value indicates that the wind pressure acts outward, the latter is referred to as suction. Pressure coefficients are dependent on shape and size of the building, location on the building surface and angle of attack of the wind. For rectangular buildings, they depend on the ratio of the two plan dimensions and on the ratio of the height to each plan dimension. It is not possible to obtain pressure coefficients using theoretical procedures. In general, the pressure coefficients increase with increase in relative height of the structure.

To calculate wind load acting on a building frame, the total wind pressure per unit area will be the sum of pressures acting on the windward side and the leeward side. This is obtained by multiplying the stagnation pressure by a drag coefficient, C_d which can be considered as a cumulative pressure coefficient by taking proper signs of pressure coefficients into account. For instance, if the pressure coefficient value at a point on the windward face of a building is +0.8 (positive sign means pressure acting toward the surface) and the pressure coefficient value at an identical location on the leeward face is -0.5 (negative sign means pressure acting away from the surface), then the drag coefficient value will be $+0.8 - (-0.5) = 1.3$.

4.6.1.2 Time-History of Wind Loading

The time-histories of the wind loads acting on a shear building during the passage of a wind storm are obtained by summing the mean and the fluctuating wind loads, and by multiplying the wind pressures by the appropriate tributary areas. Wind-induced loads on a structure are a function of wind parameters as well as shape and size of the structure.

Although many studies have been carried out to evaluate turbulent wind-induced forces on buildings, it is common practice to assume that the wind-induced drag force increases linearly with increase in wind fluctuating speed, neglecting the higher order term of the force which is proportional to the square turbulent wind speed.

The net drag force consists of the resultant over a given body surface of all components of elemental forces that are aligned with the drag, or along the wind, direction. The time-varying drag on a body completely enveloped by a flow is conventionally given by the formula of the along-wind forcing function [42, 43 and 48].

$$F=0.5 \bar{\rho} (V(t))^2 C_d A \quad (4-4)$$

The wind loading on buildings or buildings at level (x):

$$F=0.5 \bar{\rho} (V(x,t))^2 C_d A \quad (4-5)$$

where ;

F: dynamic wind load(N)

A: area upon which wind acts (m²)

C_d: drag coefficient (equal to 1.3 [49])

V (x, t): velocity of the wind at any level (x), at any time (t) (m/sec)

Consider the difficulty of representing dynamic along wind load in the Stochastic and random analysis techniques. The best solution is to represent it in time history method where this method is considered an easy and simplified deterministic method.

Time history was taken from Krauthammer [43] to represent along wind speed for strong and moderate wind speed shown in Figs. (4-4) and (4-5), the velocity at any level can be found by using the power law wind formula equation (4-3). In the present study, part of a recorded strong wind velocity data (44 sec.) and moderate wind velocity data (47 sec.) are considered.

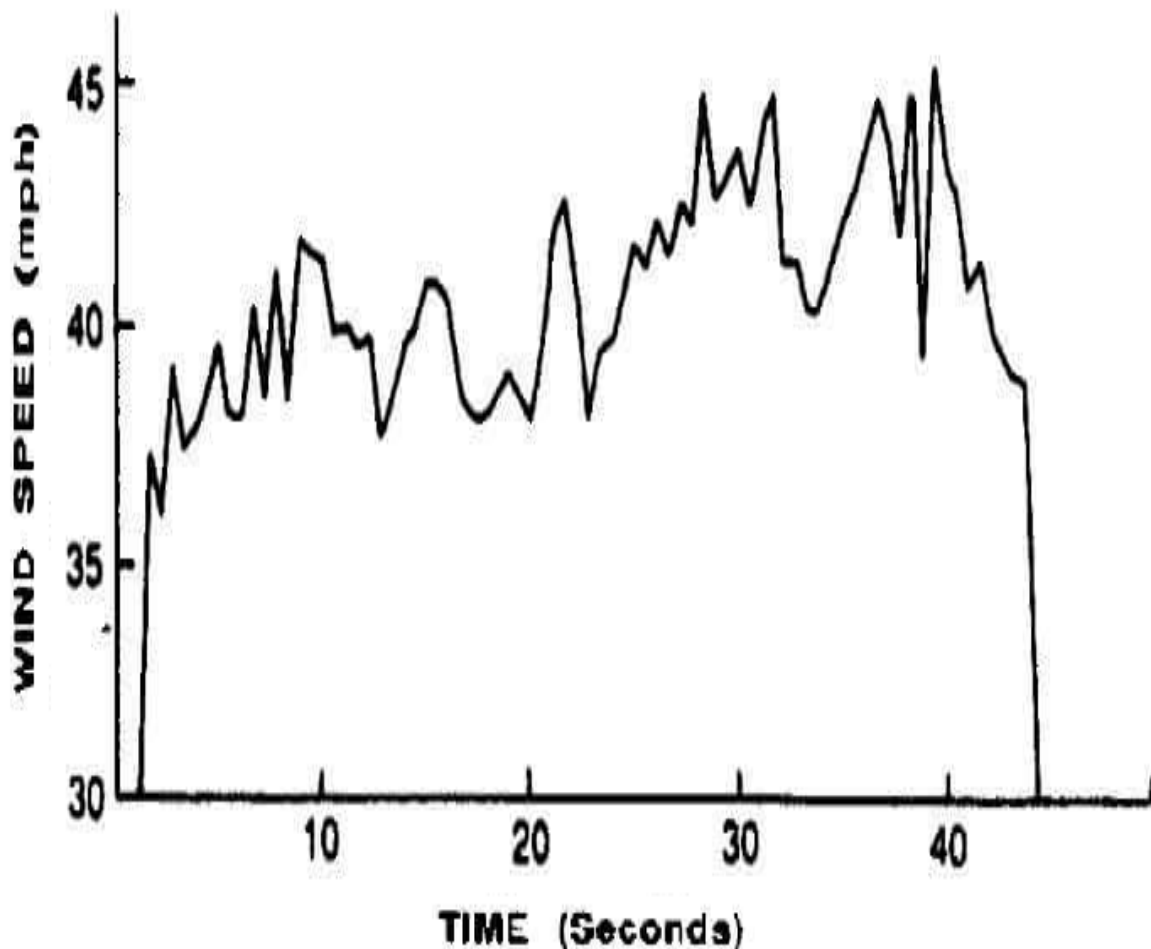


Figure (4-4): Digitized strong wind velocity data [43].

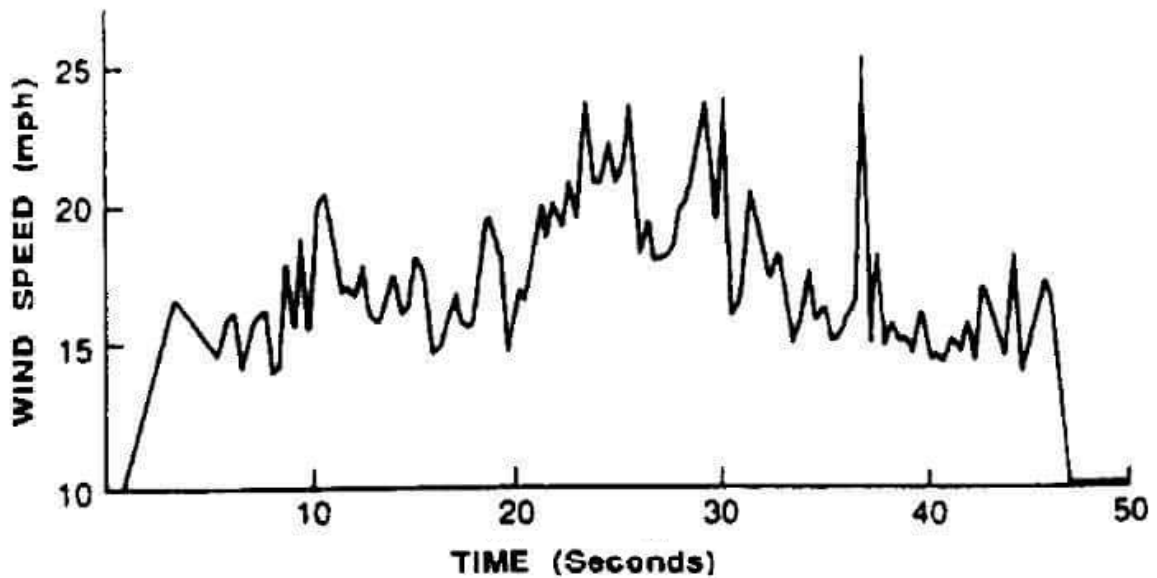


Figure (4-5): Digitized moderate wind velocity data [٤٣].

Then these data presented by Krauthammer [٤٣] are used to find equivalent wind time-history in south of Iraq for both strong and moderate wind speeds by scaling the maximum wind velocity as shown in Figs. (4-6) and (4-7).

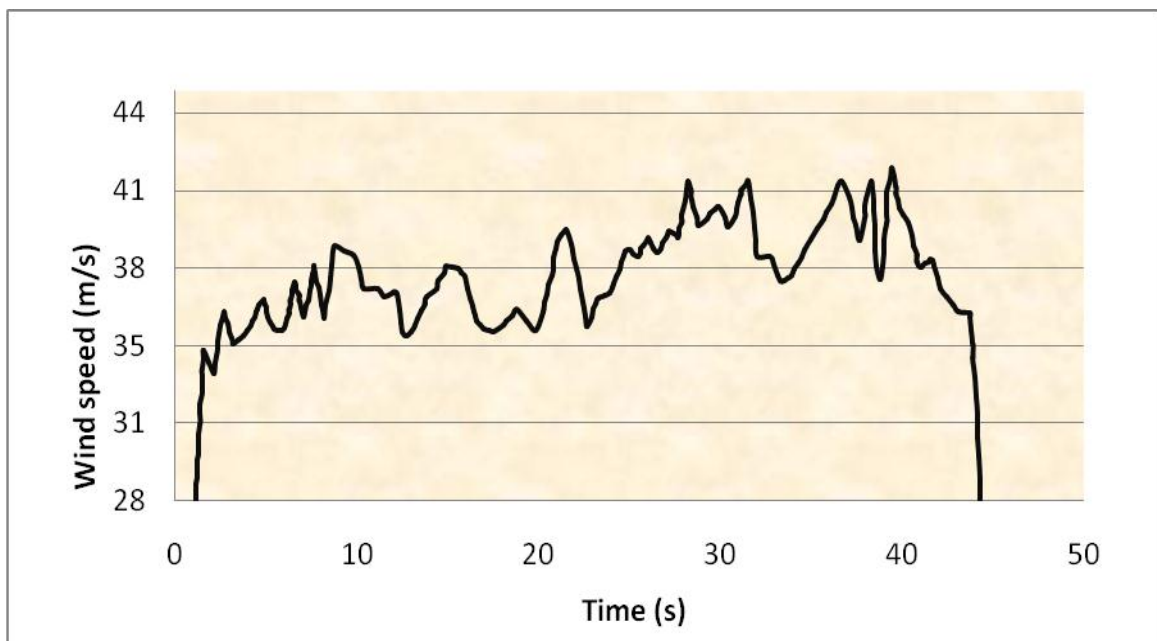


Figure (4-6): Equivalent time history for strong wind velocity at 10m in south of Iraq.

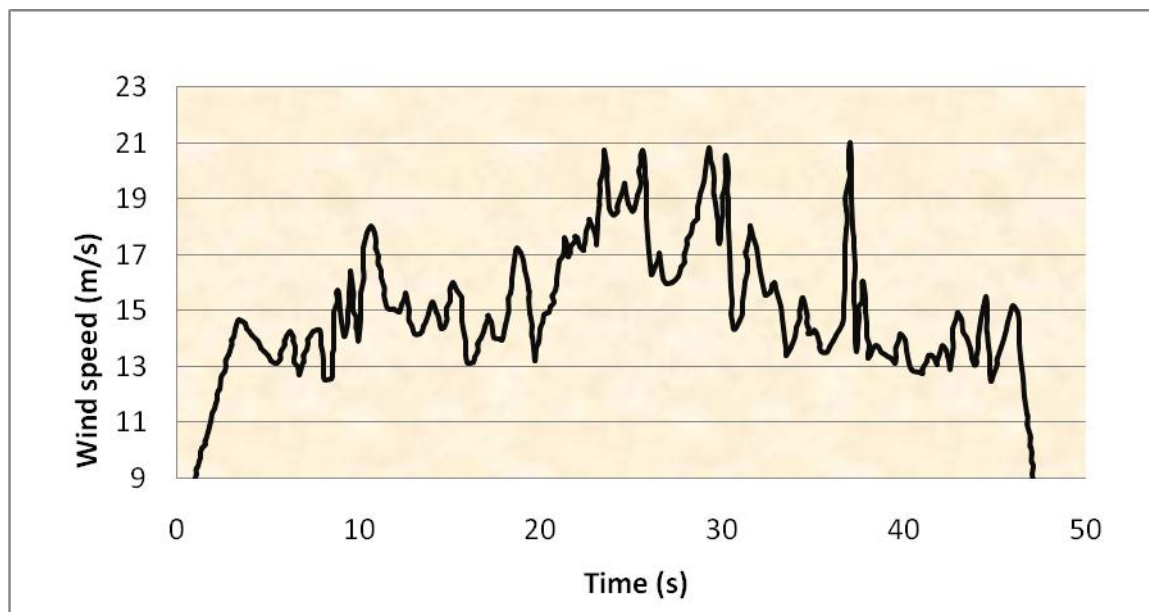


Figure (4-7): Equivalent time history for moderate wind velocity at 10m in south of Iraq.

4.6.2 Static Approach

In this approach wind force is replaced by equivalent static force, in which two methods could be used:

Method 1: Simplified Procedure (ASCE7-05 section 6.4)

Method 2: Analytical Procedure (ASCE7-05 section 6.5)

Choice of any one from above methods depends on the structural properties and surrounds environment characteristics. In general, static approaches are appropriate for all buildings and structures except for buildings or structures that have geometrically complex shapes, or slender or vibration-prone or subjected to severe environment conditions [50, ٥١ and ٥٢].

Here with common shapes steel buildings and with southern Iraq environment, the static approaches are adequate to determine design wind loads. In static approaches, the dynamic effect is accounted through the use of gust factor. Thus analytical approach (method 2) is the most suitable approach to determine the design wind loadings on high-rise buildings in the south of Iraq, as method 1 is limited to low rise buildings only.

4.6.2.1 Validation of South of Iraq Conditions for ASCE7-05 Parameters

A. Exposure categories

ASCE7-05 classifies the exposure into three categories B, C, and D depending on ground roughness and surrounding obstructions. These categories are summarized in Table (4-3), with their applicability for south of Iraq exposures.

Table (4-3): Exposure categories and their applicability for south of Iraq [7].

Exposure (ASCE7-05) definitions	Category	Applicability in Misan province
Urban , dense sub-urban and wooded areas, that satisfy : 792 m or $20 H$ continuous roughness H: height of building	B	Cities and towns only. Palm trees seldom satisfy the conditions of this category due to their distribution as narrow width lines parallel to rivers
Open terrain	C	Marshes lands, open country, villages, grassland and agriculture lands.

B. Buildings Categories

The buildings in south of Iraq can be classified directly into four categories I, II, III and IV according to the nature of occupancy as presented by ASCE7.

C. Enclosure Classifications

For the purpose of determining pressure of wind (internal pressure coefficients) all buildings should be classified as enclosed, partially enclosed or open as follows (ASCE7-05 section 6.5.9):

i. Open building: a building having each wall at least 80 % open, namely:

$$A_o \geq 0.8 \times A_g \quad (4-6)$$

Where

A_o : Total area of openings in a wall receiving positive external pressure

A_g : The gross area of that wall in which A_o is identified.

ii. Partially Enclosed Building: A building that compiles with the two following conditions:

$$A_o \geq 1.1 \times A_{oi} \text{ or } A_o > 0.37 \text{ m}^2 \quad \text{or} \quad A_o > 0.01 A_g \quad \text{smaller} \quad (4-7)$$

$$\text{And } (A_{oi}/A_{gi}) \leq 0.2 \quad (4-8)$$

Where ;

A_{oi} : The sum of areas of openings in the exterior walls and roof (Building Envelope) not included A_o .

A_{gi} : The sum of gross surface areas of the exterior walls and roof (building envelope) not included A_g .

iii. Enclosed Buildings: A building that does not comply with the requirements for open or partially enclosed buildings.

D. Height of Buildings

The buildings classified according to their heights to:

1- Low-rise Buildings: which satisfy the following two conditions.

a- Mean roof height, h is less than or equal to 18 m (60 ft)

b- Mean roof height, h does not exceed least horizontal dimension (width)

2- High-rise Buildings: all other buildings.

4.6.2.2 Determination of Wind Design Loads by Analytical Procedure of ASCE7-05 (Method 2)

The wind loads determined by equivalent static methods are based on the assumption that structural frames and components/cladding behave elastically in strong winds.

To use this method there are two limitations that should be satisfied:

i. Regular shape buildings

ii. No dynamic wind effects (like vortex shedding or across wind effects)

These conditions are applicable for common buildings and wind characteristics in the south of Iraq. In all codes, wind speed is used to calculate the pressure of wind on structures by using Bernoulli's equation [50, 51 and 52].

$$q = 0.5 \rho V^2 \quad (4-9)$$

Where q = wind pressure, ρ = mass density of air, v = velocity of air, thus with $\rho = 1.225 \text{ kg/m}^3$ which corresponds to a temperature of 15 C, Eq. (4-4) is rewritten as

$$q = 0.613 V^2 \quad (4-10)$$

The above pressure is called velocity pressure or dynamic pressure or stagnation pressure, in ASCE7 and here it will be called velocity pressure.

For design purposes, the velocity pressure at any height z is calculated by the following equation (ASCE7-05 section 6.5.10):

$$q_z = 0.613 K_z K_{zt} K_d V^2 I \quad (\text{N/m}^2) \quad (4-11)$$

where ;

K_z = Velocity pressure factor

K_{zt} = Topographic effect factor

K_d = Wind directionality factor

$K_d = 0.85$ for all buildings

I = Importance factor

These factors are determined as follow:

A. Importance Factor, I

This factor accounts for the degree of hazard to human life and damage to property. Importance factor is determined from Table (4-5) (Table 6-1 of ASCE7-05) which depends on building category that defined in Table (4-4)

Table (4-4): Importance factor, I (Table 6-1 of ASCE7-05).

Category	Non-Hurricane Prone Regions and Hurricane Prone Regions with V = 85-100 mph	Hurricane Prone Regions with V > 100 mph
I	0.87	0.77
II	1.00	1.00
III	1.15	1.15
IV	1.15	1.15

B. Topographic Factor, K_{zt}

This factor accounts for greater wind speed if the structure is located on a hill (elevated site). It's computed by the following equation:

$$K_{zt} = (1 + K_1 + K_2 + K_3)^2 \quad (4-12)$$

Where K_1 , K_2 and K_3 are determined from Fig. (6-4) of ASCE7-05

$$K_{zt} = 1.0 \text{ for structures located on level ground.} \quad (4-13)$$

As the south of Iraq mostly flat terrain, thus always $K_{zt} = 1.0$, except for elevated ground or hills at the east (Humreen Hills) parallel to Iraq-Iran borders, which may have oil or industries activities in future.

C. Velocity Pressure Factor, K_z

This factor depends on building height and exposure category as in Table (4-2), which reflects the variation of wind speed with elevation and with a roughness of site ground. K_z factor could determine using Table 6.3 of ASCE7-05 or use the following equations:

$$\text{For } 4.6 \text{ m} \leq Z \leq Z_g \quad \longrightarrow \quad K_z = 2.01 (Z/Z_g)^{2/\alpha} \quad (4-14)$$

$$\text{For } Z < 4.6 \text{ m} \quad \longrightarrow \quad K_z = 2.01(4.6/Z_g)^{2/\alpha} \quad (4-15)$$

$K_h = K_z$ at $z = h$, where h is mean roof height. Where z_g and α are determined from Table (4-5) depending on exposure category. z_g is called

gradient height and represent the height after which the wind speed does not affect by distance (height) from the ground.

Table (4-5): Values of z_g and α for each exposure category [7].

Exposure Category	z_g , m	α
B	366	7
C	274	9.5
D	213	11.5

D. Gust Effect Factor, G

Gust factor accounts for the additional loading effects of wind turbulence over the basic wind speed and dynamic amplification of structures. As the basic wind speed is based on a 3-second gust, thus these gust adjustments (gust factor) reduce the effect of an assumed distributed load over a large surface.

The gust factor is applied to account the dynamic effects of winds, thus to compute this factor G it should be specified if the structure is rigid or flexible.

Flexible structures are dynamic sensitive structures with a fundamental natural frequency less than 1 Hz (or time period, $T > 1$ sec). This analytical procedure is applicable for regular shapes flexible structures, but irregular shapes flexible structures and severe wind conditions should be designed by wind tunnel procedure [52, 53]. Rigid structures are structures with a fundamental natural frequency greater than 1 Hz (or time period, $T < 1$ sec), which mean that rigid structures are away from resonance phenomenon, massive structures are a clear example.

For design calculations, the structure is assumed rigid if the ratio of height to least horizontal dimension (width) not exceeding 4 [7] i.e.

$$\text{If } \frac{H \text{ (Height)}}{B \text{ (Width)}} < 4 \quad \rightarrow \quad \text{Rigid Structure} \quad (4-16)$$

thus most multi story steel buildings in south Iraq could be considered as rigid structures. Thus for Rigid Structures gust factor is:

Gust Factor = $G = 0.85$ according to ASCE7-05.

4.6.2.3 Wind Pressure, P

For rigid buildings the wind pressure is determined from the following equations:

1- For Windward Side:

$$P = q_z \times G \times C_p - q_h \times G C_{pi} \quad (4-17)$$

2- For Leeward Side:

$$P = q_h \times G \times C_p - q_h \times G C_{pi} \quad (4-18)$$

For all cases

$$p \geq p_{\min}, p_{\min} = 0.48 \text{ KN/m} \quad (4-19)$$

Where

q_z = Velocity pressure height (z)

q_h = Velocity pressure height (h)

$$q_h = q_z \text{ evaluated at } z = h. \quad (4-20)$$

G: Gust effect factor.

C_p : External Pressure Coefficient.

$G C_{pi}$: Internal pressure Coefficient.

The above coefficients are determined as follows:

A. Internal Pressure coefficient ($G C_{pi}$)

This factor is determined from Table 6-5 of ASCE7-05, $G C_{pi} = \pm 18$ for enclosed buildings.

B. External pressure coefficients (Cp)

This factor is determined from Fig. (6-6) of ASCE7-05, in which five values for Cp are presented: Cp for Windward walls, Cp for Leeward walls.

4.6.2.4 Wind Force (F) on Structural Frames

For analysis purposes the wind pressures assumed to be applied to the gross area of the vertical projection of walls, in general the wind pressures are assumed to be applied to projected area of building perpendicular to the wind direction. Thus wind force is calculated from the following equation:

$$F = P \times A \longrightarrow \quad (4-21)$$

Where

A: is the projected area perpendicular to the wind direction.

The analysis of multi-Story building is accomplished by computer structural programs, we use software (SAP), this software is commonly based on finite element method to idealize the structure in which all forces should be subjected at nodes or members (or elements) by transformed to forces through multiplying by area upon which wind acts on the building.

4.6.2.5 Summarized Steps of Analysis Static Wind Loads Calculation

Procedure

The steps of calculation wind speed on steel building are listed below [V].

- 1- Determine the exposure category B, C or D according to Table (4-3).
- 2- Determine building classifications I, II, III or IV according to ASCE7-05.
- 3- Determine enclosure classification open, enclosed or partially enclosed Eqs. (4-6) to (4-8).
- 4- Determine the basic wind speed.
- 5- Determine the velocity pressure (q_z or q_h) from Eq. (4-11) in which the factors are determined from:

- a- Directionality factor, $K_d = 0.85$
- b- Importance factor I , from Table (4-4).
- c- Topography factor, $K_{zt} = 1.0$
- d- Velocity pressure coefficients K_z and K_h from Eq. (4-14) and Eq. (4-15)
- 6- Determine whether the building rigid or flexible, from Eq. (4-16)
- 7- Determine Gust effect factor G , for rigid building $G = 0.85$
- 8- Determine design wind pressure, p from Eqs. (4-17), (4-18) and (4-19), in which the pressure factors are determined as follow:
 - a- Internal pressure factor, $G C_{pi}$.
 - b- External pressure factor, C_p (for windward sides, leeward sides,) from Fig. (6-6) of ASCE7-05.
- 9- Determine the force, F on building, from Eq. (4-21).
- 10- Apply the wind forces on members and transformed to nodes of members or elements by using software (SAP).

4.7 Dynamic Wind Load Calculations

Based on scaled time-histories of wind velocities for both strong wind (42m/s) and moderate wind (21 m/s), The dynamic wind loads on building are calculated by equation (4-5) in which the time-histories amplitudes change with height on each level of storey via equation (4-3), namely for each story then is specified time history.

Thus according to equation (4-5) the wind velocities are converted to forces by multiplying by projected area for each story, then the calculated per story is divided equally along nodes of projected face and modeled it as joint. Time-history load in SAP V2000 software. The dynamic wind analysis is based on the following data: C_d : drag coefficient 1.3 [49], α : power-law coefficient, commonly 0.16 [47], time step for load application 0.01. The variation of static

strong wind speed with height of the building, 19m is shown in Fig. (4-8). While the time-history of wind forces due to strong and moderate speeds at third story showed Figs. (4-9) and (4-10) respectively. Which showed that the shape of time-histories of wind velocities and forces are slightly different due to nonlinear variation of velocity with height according to power law.

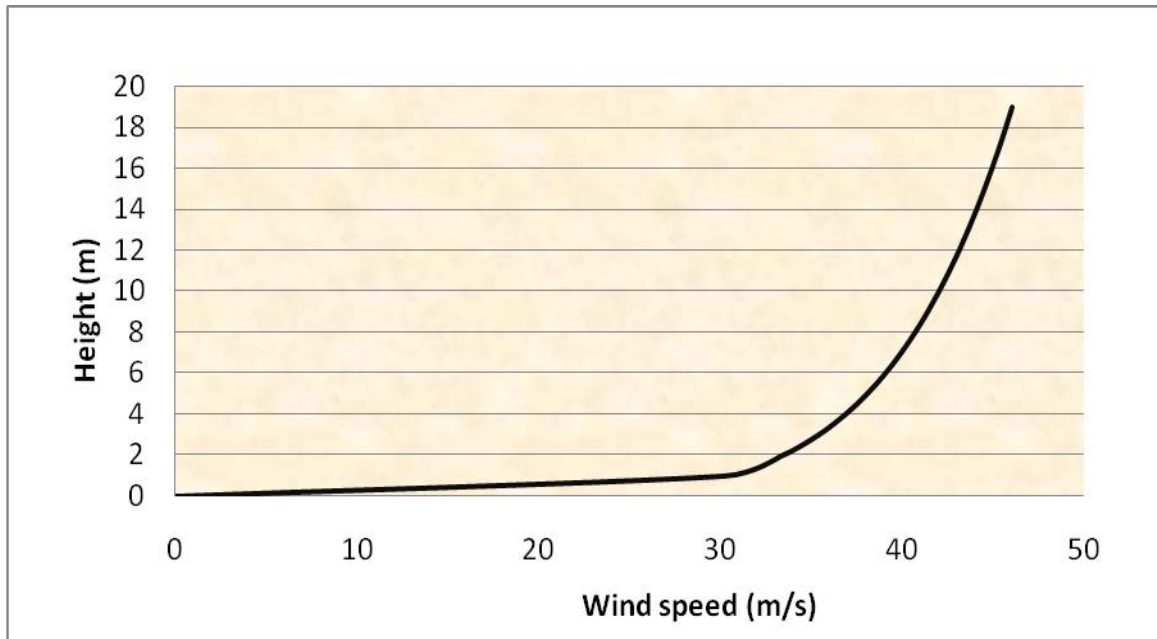


Figure (4-8): Variation of wind velocity with height.

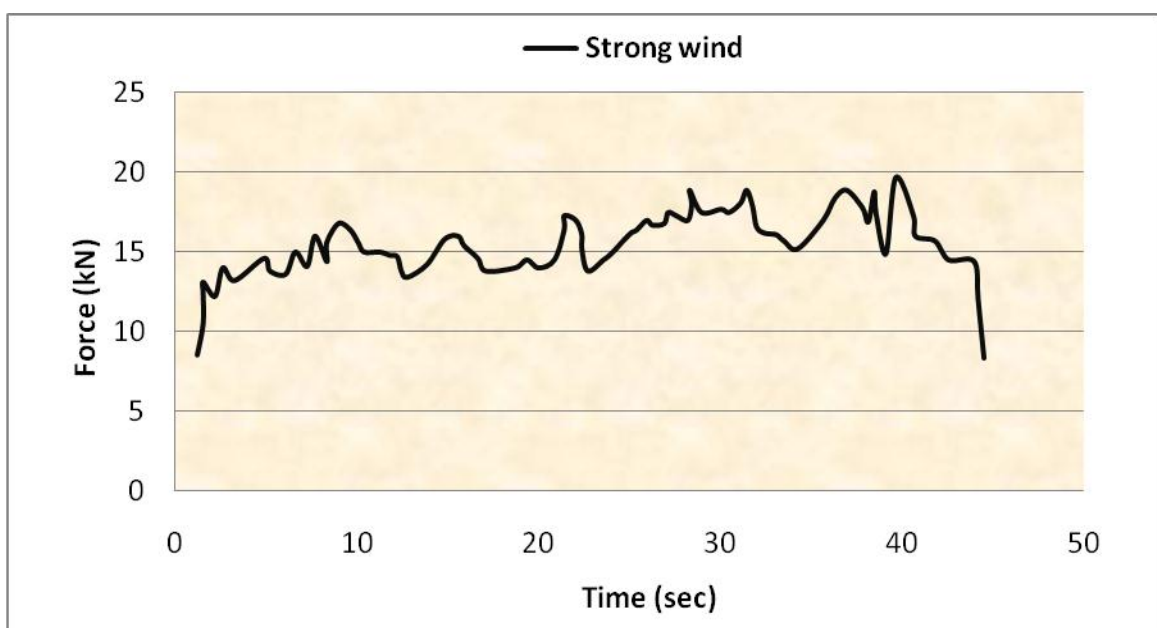


Figure (4-9): Dynamic strong wind loads for third floor.

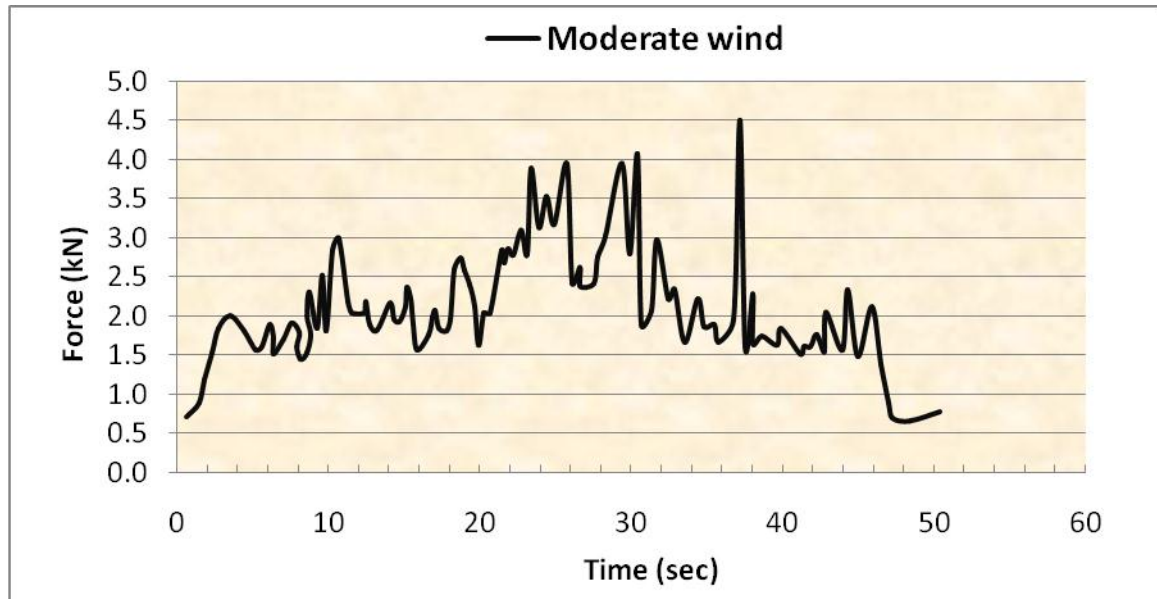


Figure (4-10): Dynamic moderate wind loads for third floor.

4.8 Static Wind Load Calculations

The results of the static wind pressure are obtained from Dawood [V]. Wind load along the building is summarized in Fig. (4-11) as pressure units for south of Iraq, which can be easily transformed to forces through multiplying by area upon which wind acts, then divided to numbers of nodes to become forces distribution on nodes. These pressures for 19m height (six stories), the static wind analysis pressures quantities is based on the following data:

- 1- Exposure: The building is located in Amarah City (Urban area) so Exposure B is used.
- 2-Importance factor, $I=1.0$
- 4- Basic wind speed, $V = 42 \text{ m/s}$
- 5- The buildings are considered rigid building, namely $H/B < 4$. Since the ratio of height to least horizontal dimension is less than 4, the fundamental natural is judged to be greater than 1Hz, $G = 0.85$
- 6-Topography factor, $K_{zt} = 1.0$
- 7- Directionality factor, $K_d = 0.85$

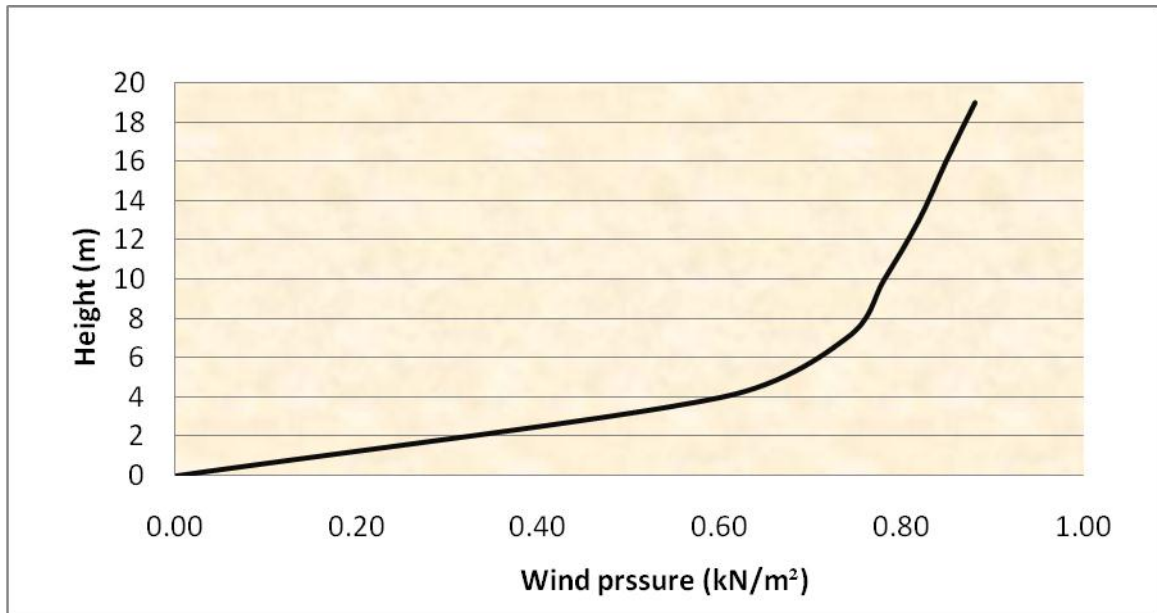
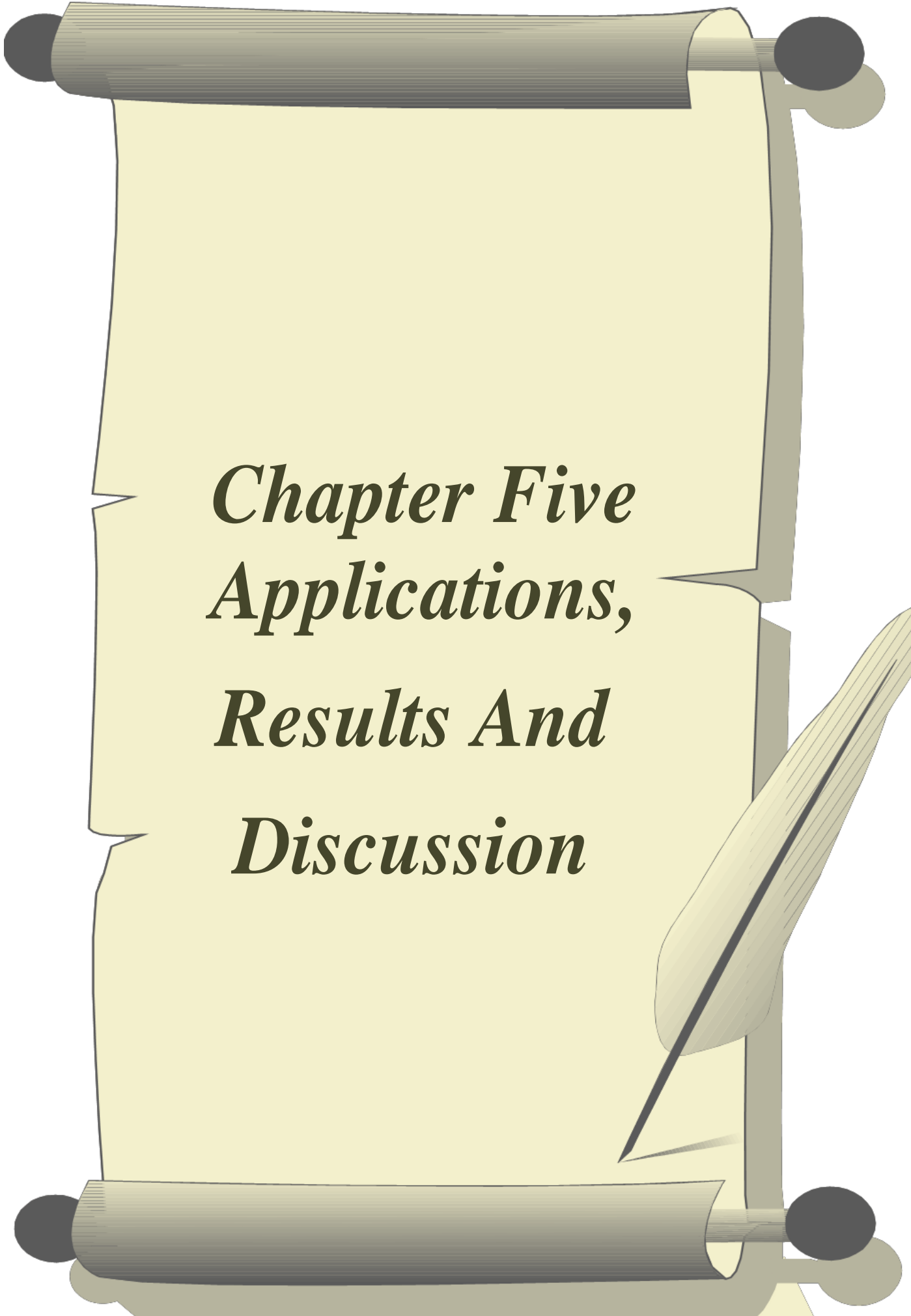


Figure (4-11): Static wind pressures data [v].

4.9 Structural Tolerances for Wind Load

According to BS 8110-Part 2: 1985 [54] the maximum allowable displacement is calculated as $h/500$, where h is the storey height for single story building. $h=19\text{m}$, $h/500=38\text{mm}$, should be the maximum top displacement (drift story) less than from this limitation, building is safe from wind load.

A scroll of parchment is unrolled, held by four black circular fasteners at the corners. The parchment is yellowed and has irregular, torn edges. A quill pen is positioned diagonally on the right side of the scroll. The text is centered on the scroll in a bold, italicized serif font.

*Chapter Five
Applications,
Results And
Discussion*

CHAPTER 5

APPLICATIONS, RESULTS AND DISCUSSION

5.1 Introduction

This chapter, modal, static and dynamic (time-history) analysis techniques are used to analyze the steel building models by using SAP2000 V16 software. In time-history analysis method, the numerical model is subjected to full range of loads patterns for the entire duration of wind by using wind dynamic records that represent the expected wind in south of Iraq.

The critical values of results are obtained by some operations between Sap and Microsoft Excel programs. As the loads are time-dependent which changes abruptly and the response of the structure is required at specific time, therefore, the solution is analyzed in multiple load steps.

SAP V2000 is high-quality structural analysis program which provides powerful analysis capabilities targeted at structural applications. SAP2000 is a general purpose finite element program which performs the static or dynamic, linear or nonlinear analysis of structural systems and design program for three dimensional structures.

The application has many features for solving a wide range of problems from simple 2-D trusses to complex 3-D structures. Creation and modification of the model, execution of the analysis, and checking and optimization of the design are all done through this single interface. Graphical displays of the results, including real-time animations of time-history displacements, are easily produced [55].

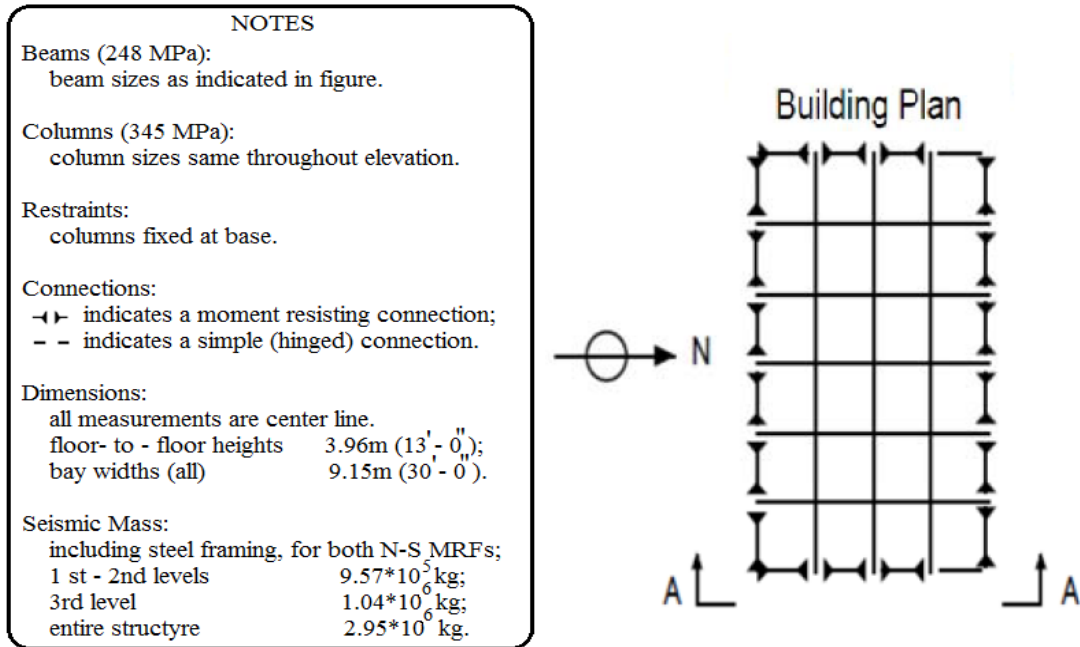
5.2 Verification Strategy

Three steel buildings of 3, 9 and 20-storey were designed by Brandow and Johnston Associates for SAC Phase II Project. Although not actually constructed, these structures meet seismic code and represent typical low-medium steel buildings designed for Los Angeles, California region Khalaf [96] and Ohtori [97]. The specifications for each of these buildings can be found in many references Luco [98] and Gupta [99]. The 3-storey benchmark steel structure is chosen for verification the performance of used analysis software and modeling validity for steel structures.

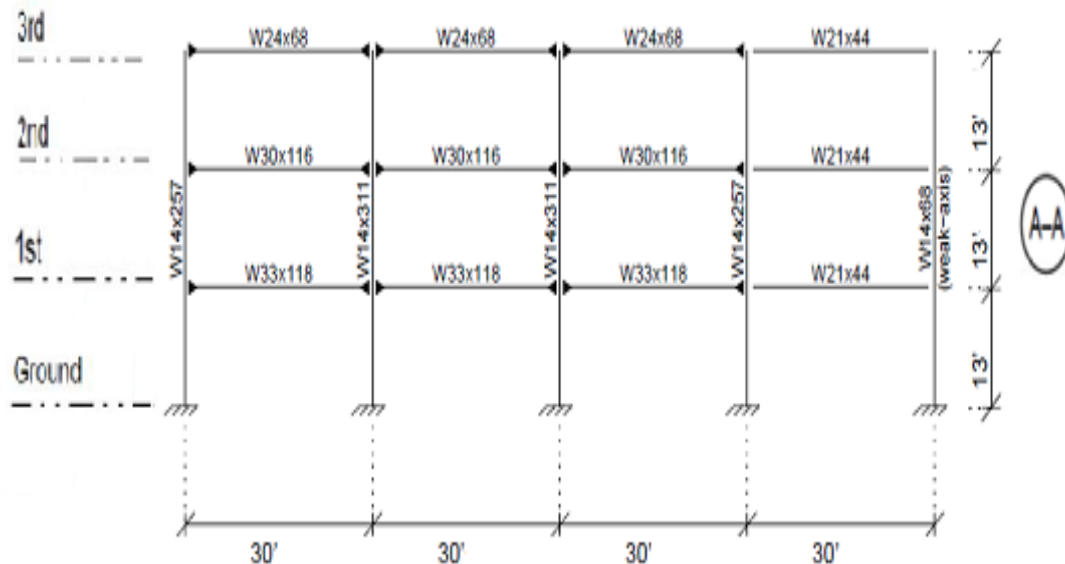
The three-storey benchmark steel building (SAC3) contains four bays in the N-S and six bays in E-W directions. The bays are 30 feet (9.15m) from center to center, in both directions, and then the total dimensions of the building are 36.58m by 54.87m in plan. Typical floor-to-floor heights measured from center of beams are 13 feet (3.96m), and then the total height of the building is 11.89m. The column bases are modeled as fixed at the ground level. The columns of the moment-resisting frame (MRF) are wide-flange of different sections. The seismic mass of the structure is due to various components of the structure, including the steel framing, floor slabs, ceiling/flooring, mechanical/electrical, partitions, roofing and a penthouse located on the roof. The seismic mass of the first and second levels is 9.57×10^5 kg and the third level is 1.04×10^6 kg. The structural details are summarized in Fig. (5-1).

The building is modeled and analyzed using SAP 2000 V16 program. The obtained result from analysis for fundamental natural time period is 0.97979 sec. This value is compared with the results of Ohtori [57] and Luco [58], which are 1.02 and 1.03 sec respectively. The ratio of result of worked study to result of Luco [58] (which is outmost value, i.e.1.03) is 0.95. The results show that

there is a good coincidence between the results of the considered references and the used program.



(a) Plan diagram



(b) N-S elevation.

Figure (5-1) Structural details of the three-storey (SAC3) steel building [56].

5.3 Structural Modeling

5.3.1 Structural Configuration

The structural frame model from Rackauskaite et al. [60] is used in this study. The AISC standard is considered in the design of the steel structure and ASCE/SEI 7–10 used to evaluate the applied live load.

The studied models are analyzed by linear and nonlinear time-history analysis using direct integration solution while geometric nonlinear parameters are included via P-delta effect.

In this study six storey steel building with 19m height is considered. Thus has similar plan dimensions in xy plane of 30x30m. The building has six bays in both x-direction and in y-direction each bay is (5 m x 5 m) center to center as shown in Fig. (5-2).

Assuming steel sheet deck with w-shape beam resting on the steel beams. Deck and beam structural system is supported on the steel columns. Typical floor to floor heights measured from centers of beams, is 4 m for the ground floor and 3m for the other storeys as shown in Fig. (5-3). The column bases are modeled as fixed at the ground level.

The mass of each element is assumed to be concentrated at the nodes. The distribution of element mass is equally divided between nodes. The mass of the structure includes the applied dead load, including the self-weight, and live load. The mass is equal to the weight defined by the dead and live load divided by the gravitational acceleration (g). Assuming all the dead load and only 50% of the live load are considered. All the beams and columns members in the studied buildings are W-shape shown in Table (5-1).

Table (5-1): Cross section properties of building members.

NO. level	Z(m)	beam section	column section
1	4	W 14x38	W 18x106
2	7	W 14x39	W 18x106
3	10	W 14x40	W 18x106
4	13	W 14x41	W 16x36
5	16	W 14x42	W 16x36
6	19	W 14x43	W 16x36

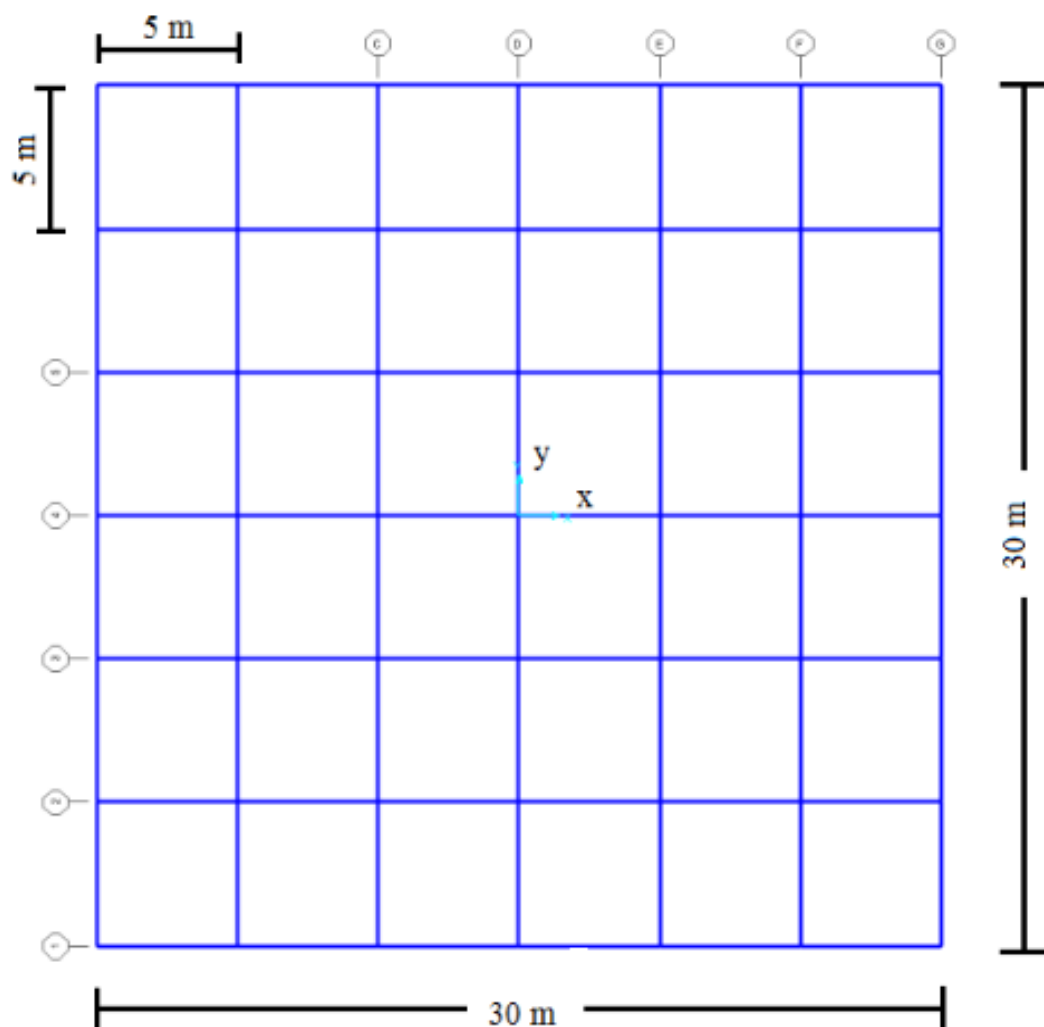


Figure (5-2): X-Y Plan diagram of steel framed building.

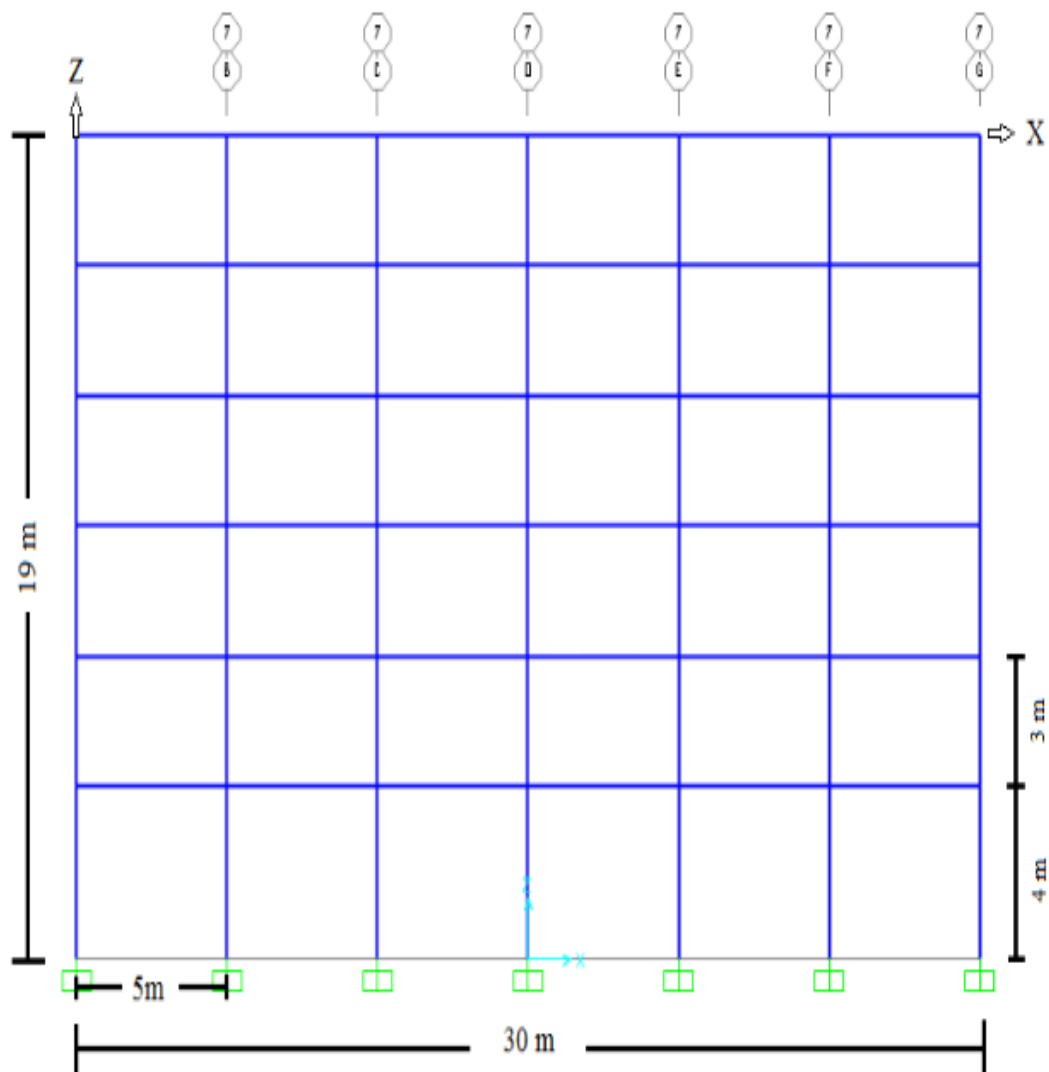


Figure (5-3): X-Z Plan diagram of steel framed building.

5.3.2 Applied Loads

The steel buildings are analyzed for dead, live, and static and dynamic wind load:

A. Dead load:

The dead load includes the weights of materials, equipments or components that remains constant throughout the structure's life. In addition to the self-weight, the roof dead load is taken as (4kN/m²). Assuming steel deck slab resist on W-shape beams.

B. Live load:

The live load includes any weight which is superimposed on, or temporarily attached to a structure (people, machinery and equipment, furniture, appliances, etc. From ASCE/SEI 7–10, live load is taken as (6kN/m²) for industrial building.

C. Static wind load:

The static wind loads on the building is obtained from Dawood [V], which presented in design table static wind pressures on buildings in south of Iraq. He calculated wind loads according to ACSE 7-10 standards and the present building static wind loads per elevation is shown in Table (5-2).

Table (5-2): Static wind load on building per elevation [V].

NO. level	Z(m)	Pressure (kN/m ²)	Area (m ²)	Force (kN)	Nodel Force (kN)
1	4	0.6	105	63	9
2	7	0.738	90	66.42	9.49
3	10	0.78	90	70.2	10.03
4	13	0.818	90	73.62	10.52
5	16	0.848	90	76.32	10.90
6	19	0.88	90	79.2	11.31

d. Dynamic wind load:

As mentioned in chapter 4, two dynamic wind records are used in the present study ,the strong wind of maximum wind speed 42m/s ,and the moderate wind speed 21m/s. These winds represented by time history method as applied loads on nodes for each storey in x- direction during 50 and 45sec for moderate and strong dynamic wind loads, respectively.

5.3.3 Material Properties

The properties of material of steel before fire used for both beams and columns is presented in Table (5-3) while the steel properties after fire presented in Table (5-4) in which there is reduction in yield stress and modulus of elasticity due to fire as mentioned in chapter 3 section 3.10. Constant damping ratio of ($\zeta = 0.02$)[4] is assumed α and β are coefficients representing mass and stiffness proportional damping 0.046 and 0.008 respectively [61]. The stress-strain curve for steel after fire is shown in Fig. (5-4).

Table (5-3): Steel properties before fire.

Item	Description	Unit	Value
Fy	Minimum yield stress	Ksi / Mpa	36 / 250
Es	Modulus of elasticity	GPa	210
ρ_s	Density	kN/m ³	77
ν_s	Poisson's ratio	—	0.3

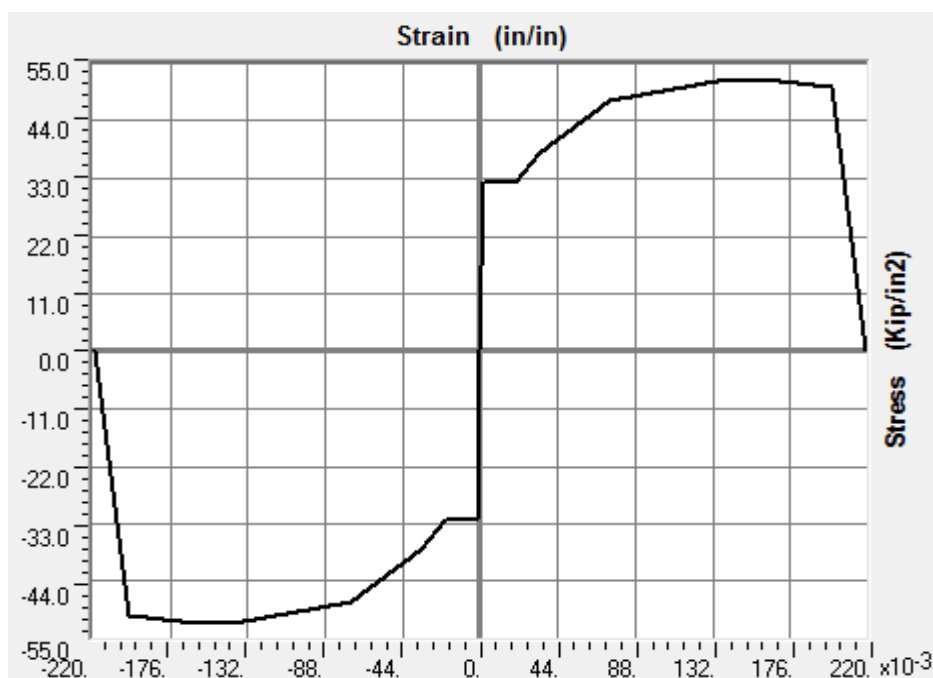


Figure (5-4): Stress-strain curve after fire reduced 10% from original.

Table (5-4): Steel properties after fire.

Item	Description	Unit	Value
Fy	Minimum yield stress	Ksi / Mpa	32.4 / 225
Es	Modulus of elasticity	GPa	189
ρ_s	Density	kN/m ³	77
ν_s	Poisson's ratio	—	0.3

5.3.4 Post-Fire Buildings Configurations

Three cases were studied, Case F0 is the state of the building before being exposed to fire but within the influence of gravity and wind loads. While the cases (Case F1 and Case F2) states of the building after fire occurred, namely cool back Case F1 the fire was on storeys third to sixth in the center four bays as shown in Fig. (5-5), while Case F2 a fire was from the first to the third in the corner of the building, as shown in Fig. (5-6). The data of the deformations were taken from Iua, et al. [13] which is for approximately 550°C temperature and these values are reduced from bottom in place of fire to top of building. In the present study a fully, half and quarter deformations is used to know the behavior of the building after a fire. The fire deformations divided into two

Table (5-5): Deformations after fire [13].

Member Types	Quantity	Deformation Types	Value
Column	Fully (Δ)	Displacement	L/60
Column	$\Delta/2$	Displacement	L/120
Column	$\Delta/4$	Displacement	L/240
Beam	Fully (Δ)	Deflection	L/240
Beam	$\Delta/2$	Deflection	L/80
Beam	$\Delta/4$	Deflection	L/160

component the first is deflection that is including the bent of beam after fire at the building on the fire area in the storeys that included fire while the second

component after fire is call a displacement of column under the effect of fire and they values of these deformations are presented in Table (5-5).

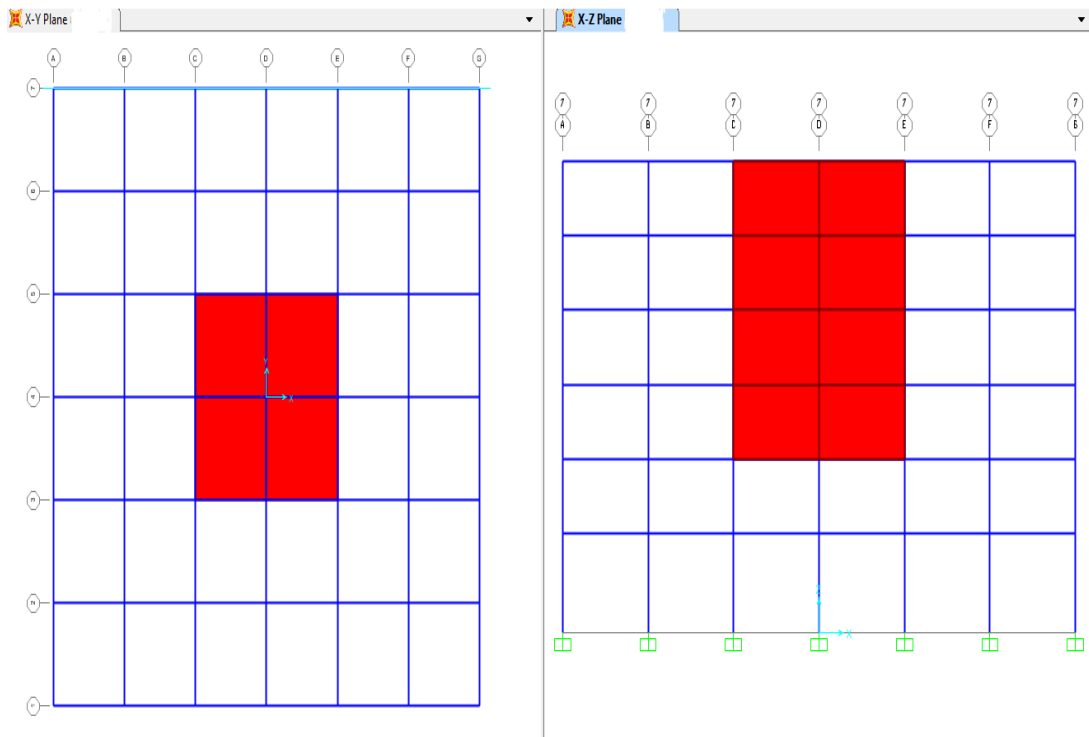


Figure (5-5): Fire in Case F1.

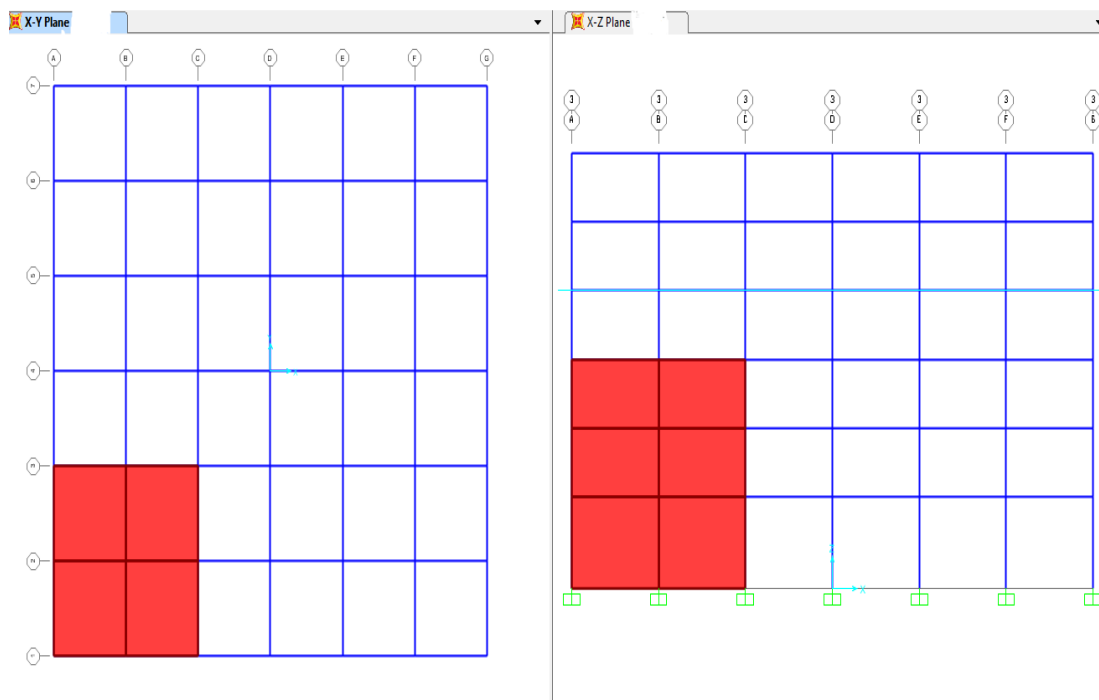


Figure (5-6): Fire in Case F2.

5.3.5 Measurements

In the present study the following quantities are used for the sake of the comparison between different cases in this study.

1. Maximum base shear x-direction.
2. Maximum base bending moment y-direction.
3. Maximum drift ratio x-direction: Relative difference of design displacement between the top and bottom of a storey, divided by the storey height.
4. Maximum stresses, axial stress (S_{11}), bending stress (S_{12}) and shear stress (S_{13}) (beam and column).
5. Maximum bending moment (M_{33}), Maximum axial force (P), shear force (V_2) and displacements x-direction (U_x).

5.4 Analysis Metrology

The Multi-storey steel buildings of 19m height under the action of wind static and dynamic forces are analyzed before and after fire for three cases (Case F1 and Case F2) with different bays and stories fire (Case F1 and Case F2).

The static wind load obtained from Dawood [7] which includes static wind pressures for each floor in south of Iraq, while the dynamic wind load using time-history analysis technique which includes two types of wind (strong and moderate wind load).

Analysis is adopted, using linear and nonlinear direction integration with p-delta effect using the finite element analysis of SAP v2000 16 software.

The response of buildings are investigated through several measurements such as the storey displacement, maximum joint displacement in x direction, storey drift, maximum base shear in x-direction and the fundamental natural frequency etc.

5.5 Analysis Cases

To investigate the behavior of steel building before and after fire and also to study the effect of wind on structure, the following cases are considered:

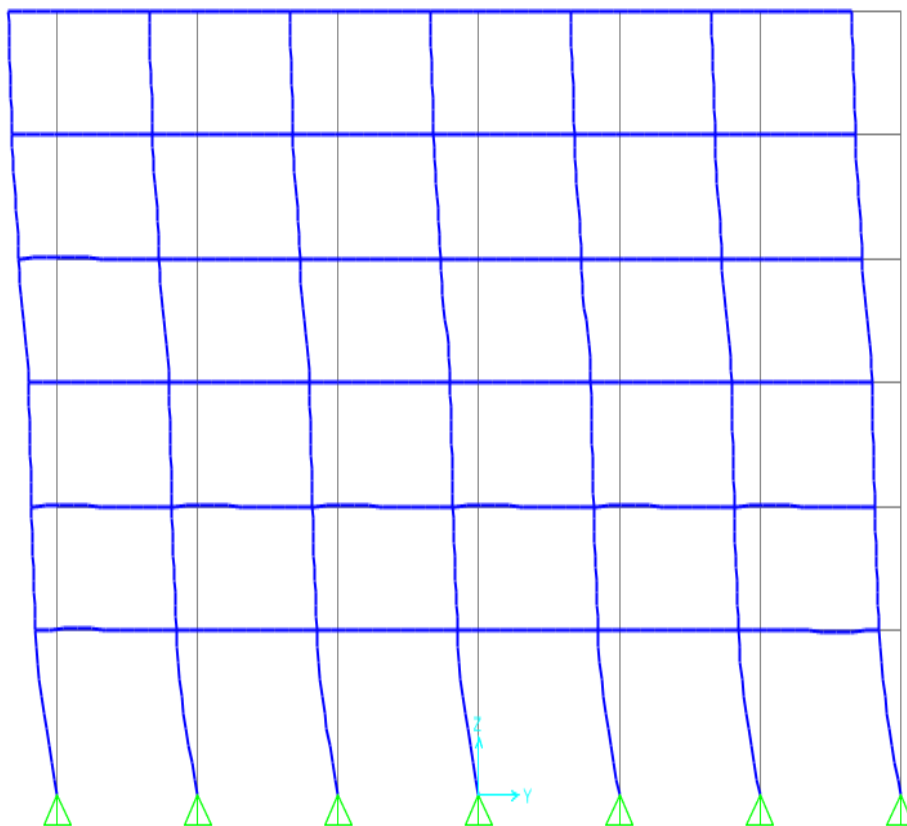
- 1: Case1 Free vibrations analysis.
- 2: Case2 Static versus dynamic analysis.
- 3: Case3 Wind speed effect on dynamic response strong versus moderate.
- 4: Case4 Linear and nonlinear dynamic analysis effect.
- 5: Case5 Post-fire analysis, fully deformation (Δ).
- 6: Case6 Post-fire analysis fully deformations (Δ) versus quarter of deformities (0.25Δ), Case F1.
- 7: Case7 Post-fire analysis fully deformations (Δ) versus half of deformities (0.5Δ), Case F1.

5.5.1 Case1 Free Vibrations Analysis

The free vibration analysis of any structure is very important to predict the natural frequencies and mode shapes of the structure. The free vibrations analysis is based on comparison the results of three cases (Case F0, Case F1 and Case F2). The results of natural frequencies are presented in Table (5-6) while the mode shapes of the first and second modes for the three cases are presented in Figs. (5-7) to (5-10). It's found that there is slightly difference between the natural frequency and mode shapes of the buildings, (ω_n, ϕ_n) for the three Cases (Case F0, Case F1 and Case F2). The natural vibrations properties ω_n and T_n depend only on mass and stiffness of structure. The mass consists of dead load and 50% live load before and after fire are the same, while the stiffness EI is slightly changed due to slight reduce in modulus of elasticity E after fire by 90% of that before fire which explain the slightly differences be natural frequency before and after fire.

Table (5-6): Natural frequency for first 10 modes before and after fire.

Analysis Type	StepNum	Case F0	Case F1	Case F2
OutputCase	Model	CircFreq	CircFreq	CircFreq
Text	Unitless	Hertz	Hertz	Hertz
Free vibrations model	1	0.272	0.289	0.269
Free vibrations model	2	0.318	0.313	0.329
Free vibrations model	3	0.403	0.399	0.397
Free vibrations model	4	0.506	0.461	0.473
Free vibrations model	5	0.511	0.500	0.490
Free vibrations model	6	0.553	0.518	0.517
Free vibrations model	7	0.620	0.586	0.580
Free vibrations model	8	0.622	0.608	0.600
Free vibrations model	9	0.675	0.663	0.650
Free vibrations model	10	0.699	0.679	0.661

Figure (5-7): First mode shapes \emptyset n Case F0.

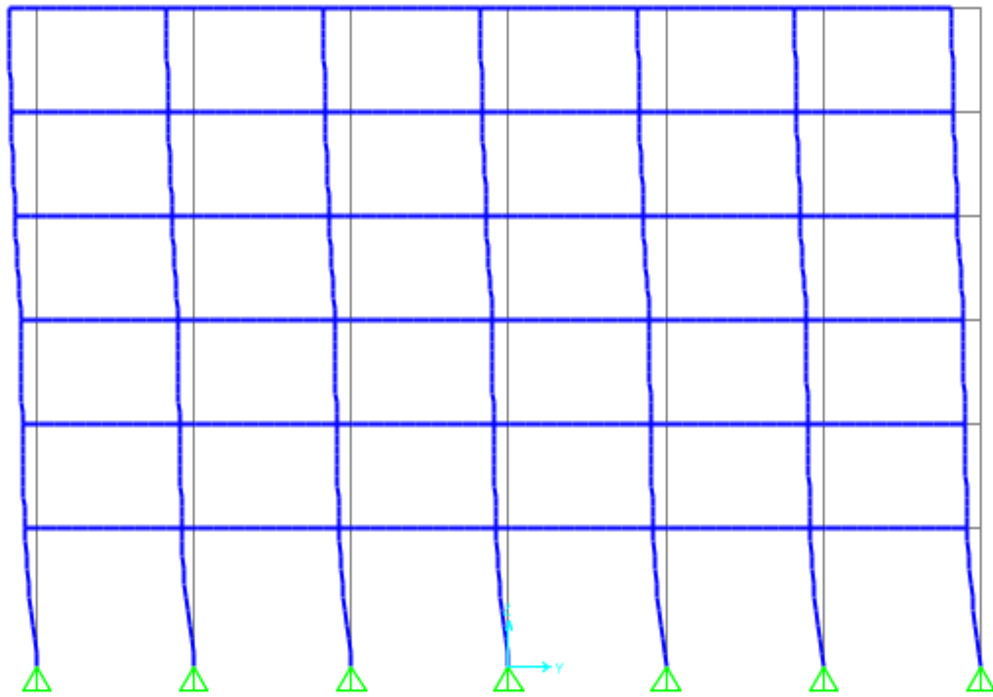


Figure (5-8): First mode shapes \emptyset n Case F1.

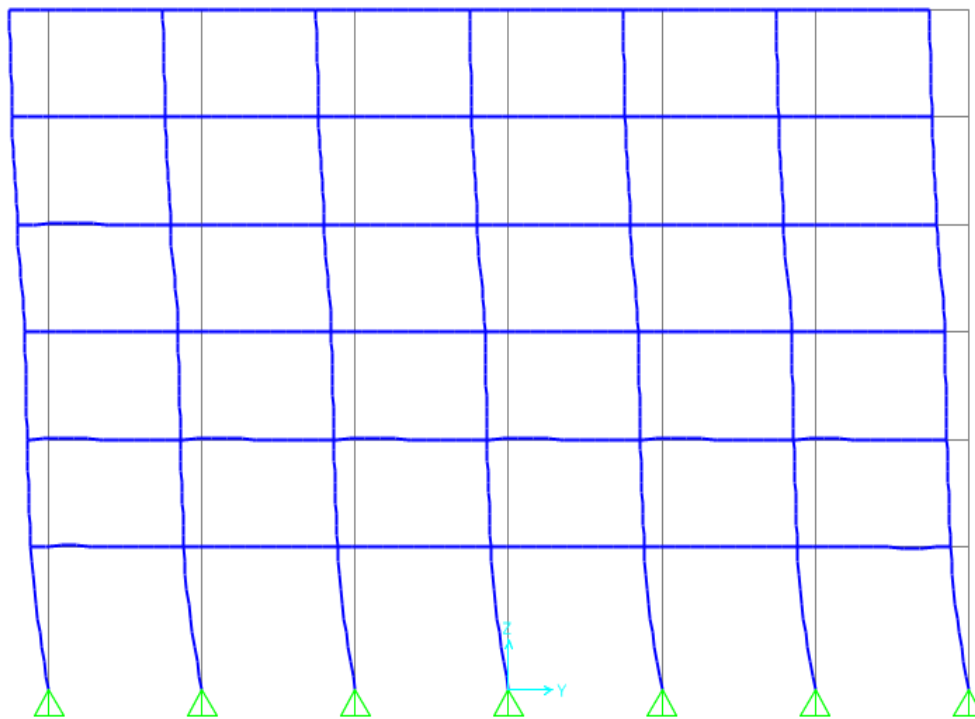


Figure (5-9): First mode shapes \emptyset n Case F2.

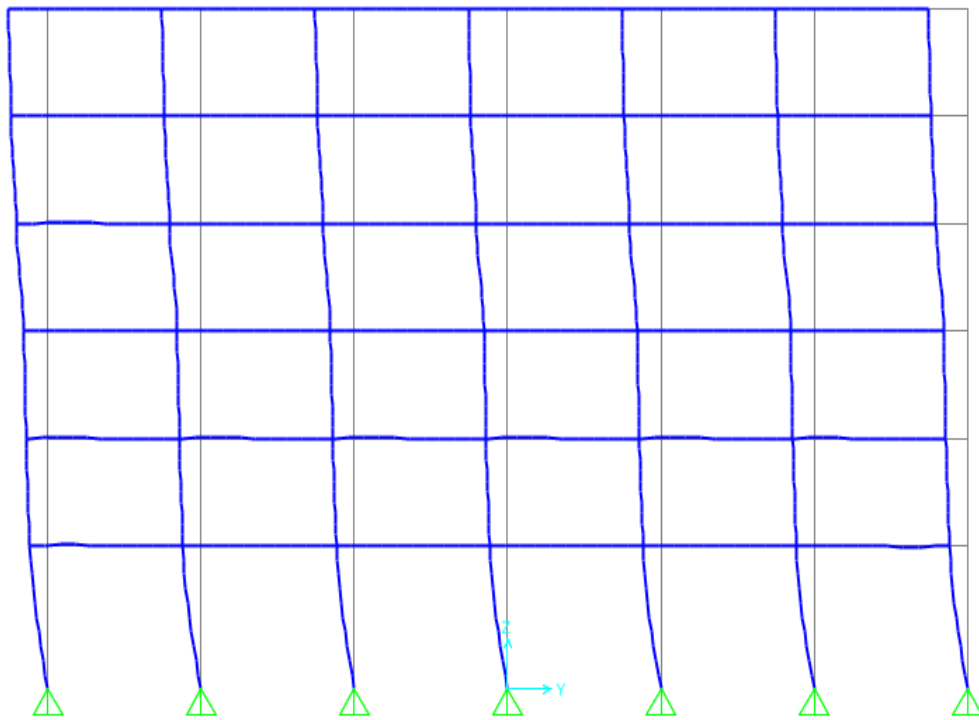


Figure (5-9): Second mode shapes \emptyset n Case F0.

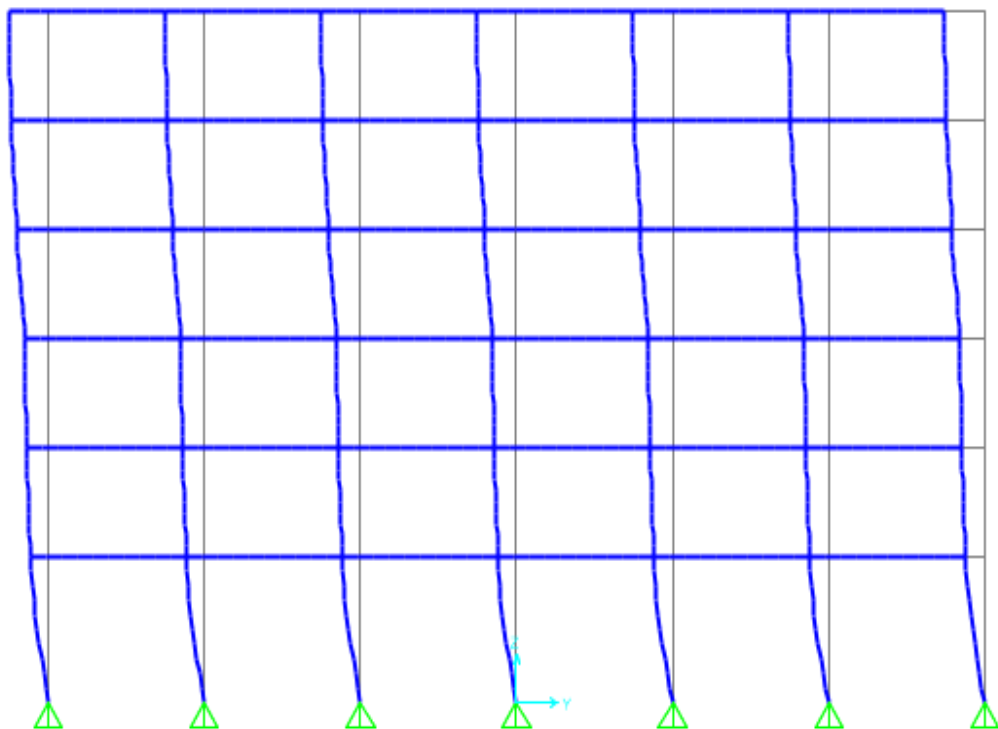


Figure (5-10): Second mode shapes \emptyset n Case F1.

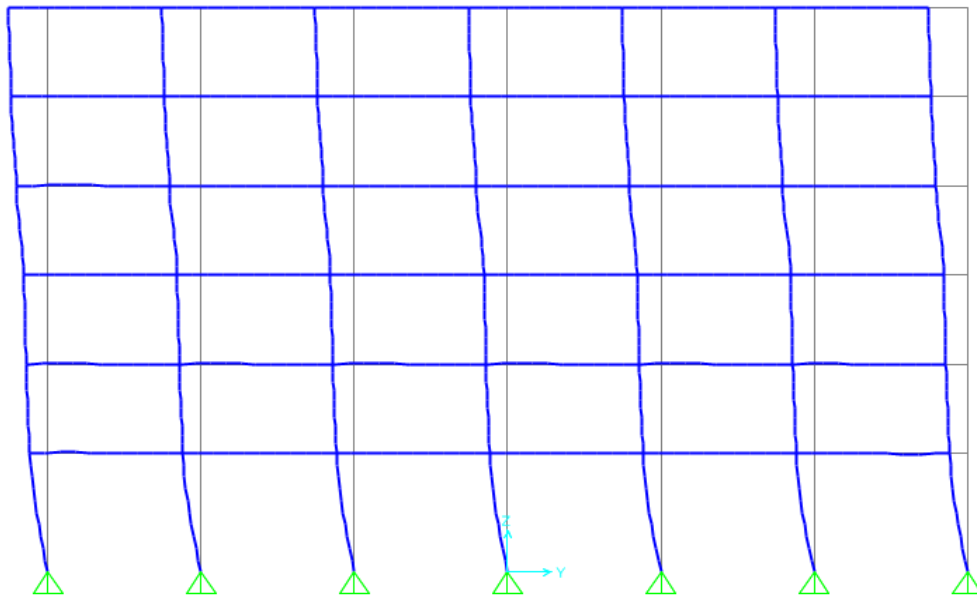


Figure (5-10): Second mode shapes on Case F2.

The wind force frequency could be approximately obtained from time-history of wind, similar to that shown in Fig. (5-11) using the following equation (5-1).

$$\omega = \frac{2\pi}{\bar{T}} \quad (5-1)$$

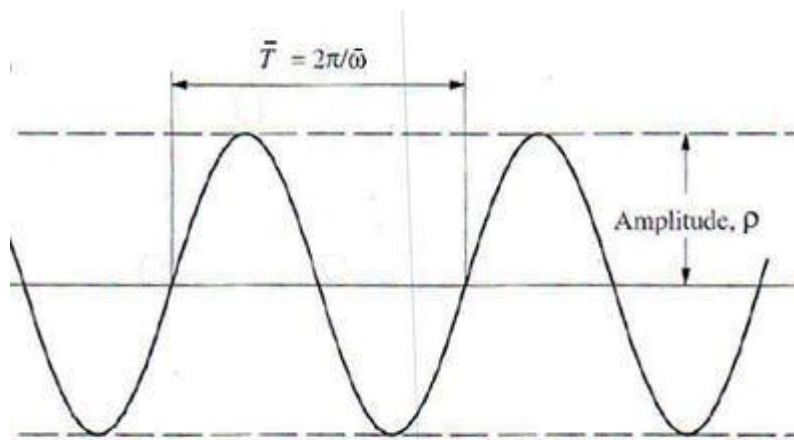


Figure (5-11): Sine wave properties.

The average natural Force frequency ω obtained is about 0.360 (Hertz) which lies between mode 2 and mode 3, so the building may face critical deformation that follow mode 2 or 3 especially in Case F2 which natural frequency is 0.329 Hz for mode 2 and 0.397 Hz for mode 3. But in all cases there is no resonance phenomenon because $\omega_n \neq \omega$ for all modes.

5.5.2 Case2 Static versus Dynamic Analysis

In this case, the effect of dynamic wind loads (strong) was studied and compared with the effect of static wind loads for Case F0 for nonlinear analysis with P-Delta effect. The similarity face of the comparison was dependent on both strong and static wind based on basic wind speed, $V = 42$ m/s at 10m above ground.

5.5.2.1 Base Shear in X-Direction for Case F0

From the Fig. (5-12) and Table (5-7) it can be seen clearly that the maximum base shear of Case F0 due to dynamic strong wind that equal to 763kN while the maximum under the effect of static wind is equal to 429kN from summation forces of wind in x direction, the difference between them is 44% because the strong wind loads in specific time greater than static wind loads.

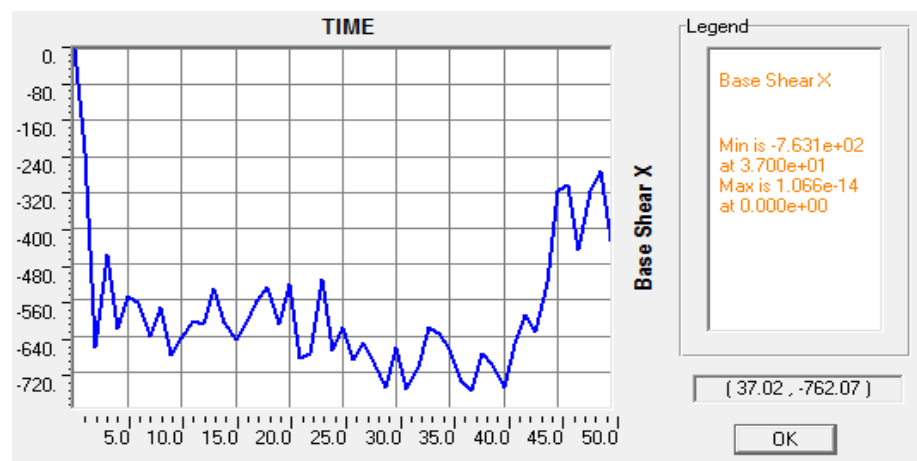


Figure (5-12): Base shear x-direction strong wind for Case F0.

Table (5-7): Base shear x-direction for Case F0.

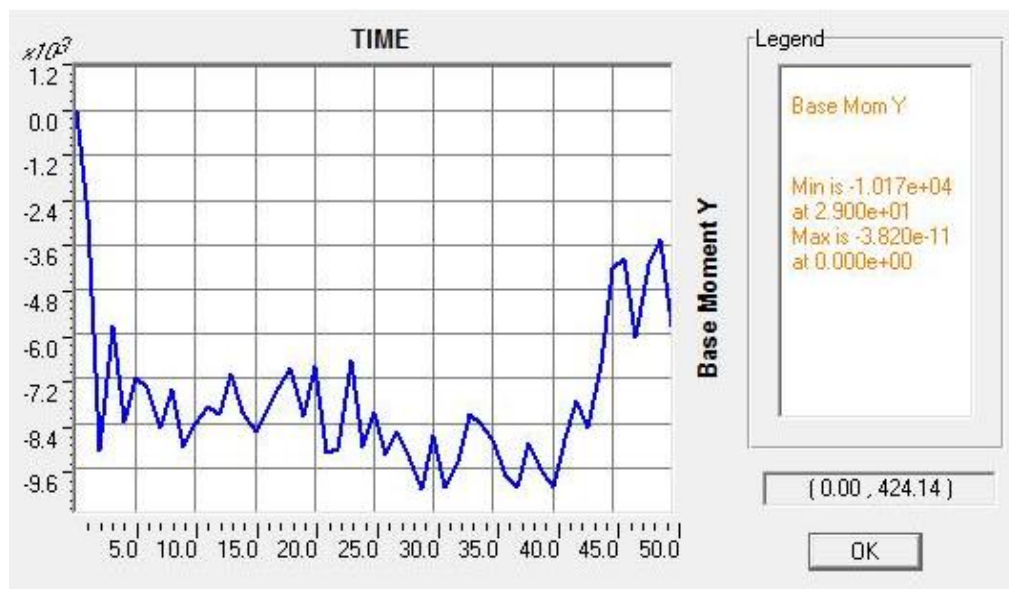
Output Case	Base shear x Case F0
Text	kN
Strong wind (dynamic)	763
Static wind	429

5.5.2.2 Base Moment in Y-Direction for Case F0

In Table (5-8) and Fig. (5-13) show the results of the base moment in y-direction, the maximum value under the effect of strong dynamic wind load is equal to 10170kN.m while the maximum value due to static wind load equal to 5598.4kN.m for Case F0, the difference between them is 44% because the dynamic characters of strong wind loads which same impulses its.

Table (5-8): Base moment y-direction for Case F0.

Output Case	Base moment y Case F0
Text	kN.m
Strong wind (dynamic)	10170
Static wind	5598

**Figure (5-13): Base moment y strong wind for Case F0.**

5.5.2.3 Maximum Drift Ratio in X-Direction for Case F0

The comparison between static wind load and dynamic strong, wind load for Case F0 in drift ratio x-direction for six storeys give the results shown in Fig. (5-14), these results showed that the maximum values due to strong dynamic wind load is 1.4% in last storey while the maximum value under the effect of static wind load equal to 0.57% in last storey, the difference between them is 56% because the dynamic characters of strong wind loads which same impulses its.

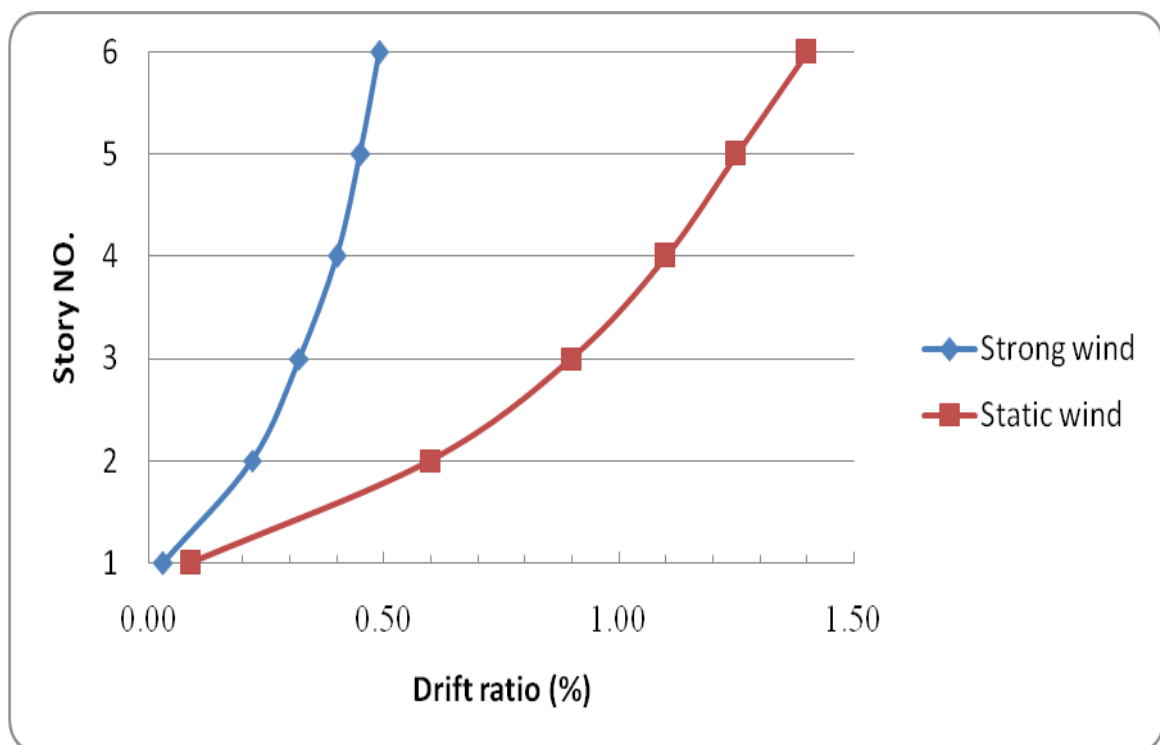


Figure (5-14): Drift ratio % vs. storey no. for Case F0.

5.5.2.4 Maximum Stresses (S₁₁, S₁₂ and S₁₃) for Case F0

The stresses results from this analysis shown in Table (5-9), The maximum axial stress (S₁₁) under the effect of dynamic strong wind occurred on the fourth storey equal to 231164kN/m² and the same storey for maximum static wind but the value is 218749.8kN/m². Namely the difference is 5% .The

maximum bending stress (S_{12}) of 56883kN/m^2 due to dynamic strong wind occurred on the last storey also approximately the same values and location for static wind. And the maximum shear stress (S_{13}) under the effect of strong wind happened on the last storey equal to 13515kN/m^2 same storey for maximum static wind but the value is 13446.8kN/m^2 , the difference between them is 0.5%. It's found that there is very little difference between dynamic and static in stresses.

Closed values for axial stresses (S_{11}) between static and dynamic is observed due to the axial stress depend on gravity load in column, as shown in Fig. (5-15) while the maximum distribution of bending and shear stresses (S_{12} and S_{13}) are similar between dynamic strong and static wind load in the fourth, fifth and sixth storeys but slightly difference on the first, second and third storeys as shown in Figs. (5-16) to (5-17).

The maximum (S_{11}) happened in column while maximum of (S_{12} and S_{13}) occurred in beam. When the stress becomes equal or greater than to the yield stress of the material F_y , yielding of the material will occur (failure) (i.e. $S \leq F_y$). According to Table (5-9), the maximum stresses is axial stress (S_{11}) for Case F0 equal to 231164kN/m^2 is less than yield stress (F_y) before fire, so building is safe.

Table (5-9): Maximum stresses for Case F0.

Strong Wind CaseF0			Static Wind CaseF0			
Story NO.	S13	S12	S11	S13	S12	S11
Text	kN/m^2	kN/m^2	kN/m^2	kN/m^2	kN/m^2	kN/m^2
1	12630	53643	149880	12350	52428	144267
2	12895	54749	133057	12593	53471	125043
3	12915	54890	134090	12629	53670	130634
4	13245	55923	231164	13211	56066	218749
5	13118	55283	221303	13062	55356	210521
6	13515	56882	202866	13447	56925	196129

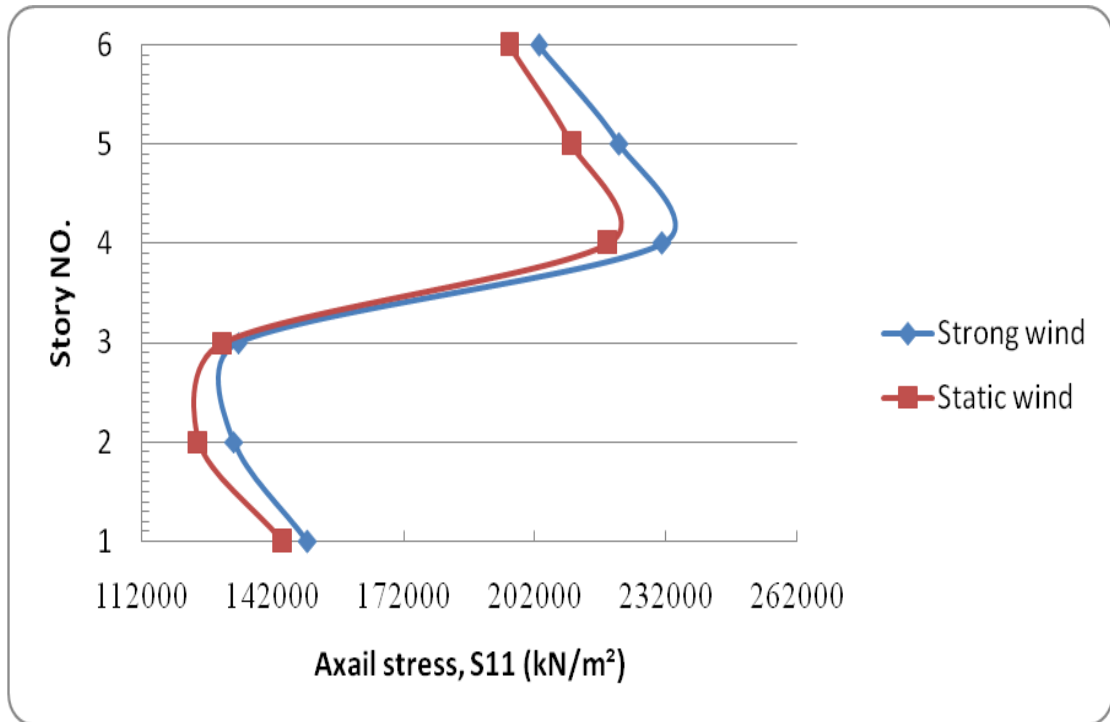


Figure (5-15): Axial stress vs. storey no. for Case F0.

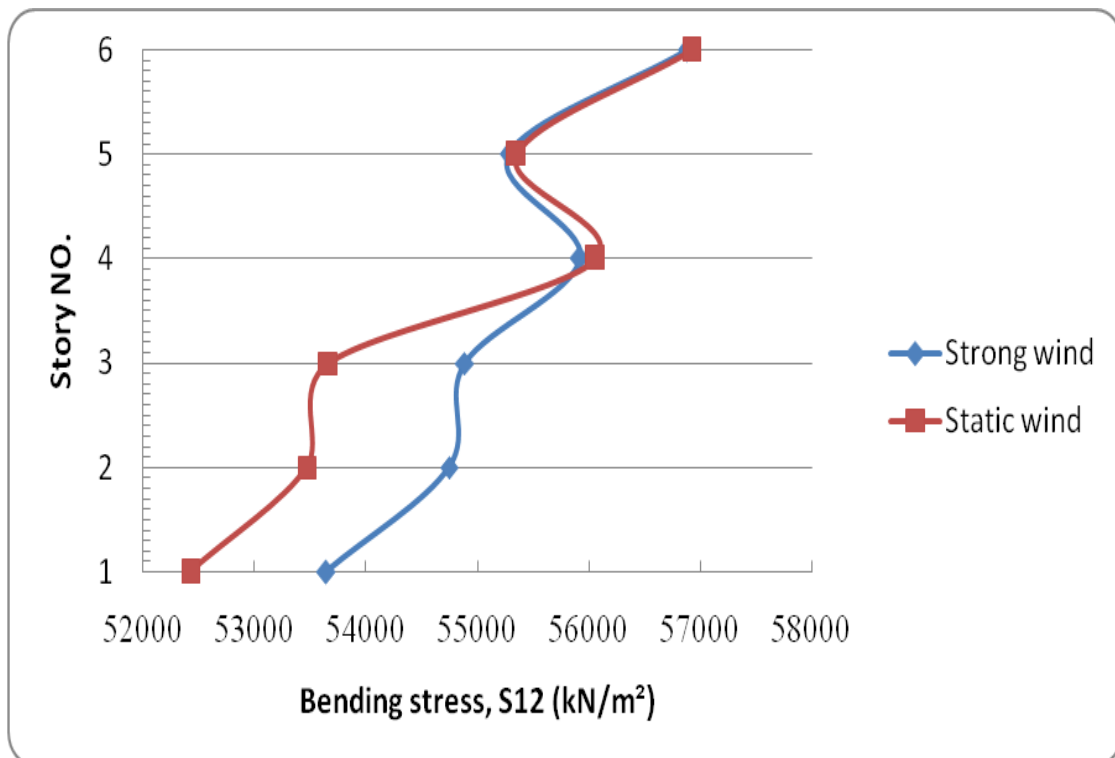


Figure (5-16): Bending stress vs. storey no. for Case F0.

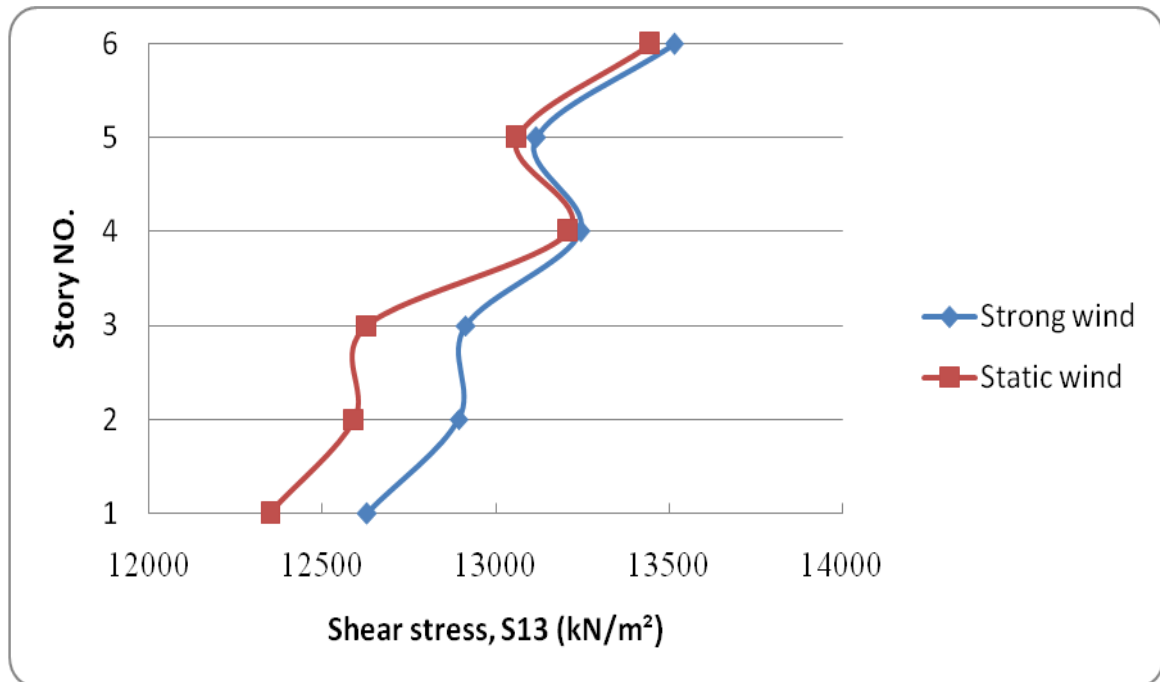


Figure (5-17): Shear stress vs. storey no. for Case F0.

5.5.2.5 Maximum Bending Moment, M33 for Case F0

It can be seen the results of bending moment in Table (5-10), the maximum bending moment under the effect of dynamic strong wind load in the third storey on beam equal to 136kN.m while the maximum bending moment due to static wind load in the same storey on beam equal to 128kN.m as shown in Fig. (5-18), the difference between them is 6% namely slightly differences.

Table (5-10): Bending moment per storey no. for Case F0.

Case F0	Strong	Static
Story No.	M33	M33
Text	kN.m	kN.m
1	129	121
2	136	127
3	136	128
4	130	123
5	132	128
6	112	112

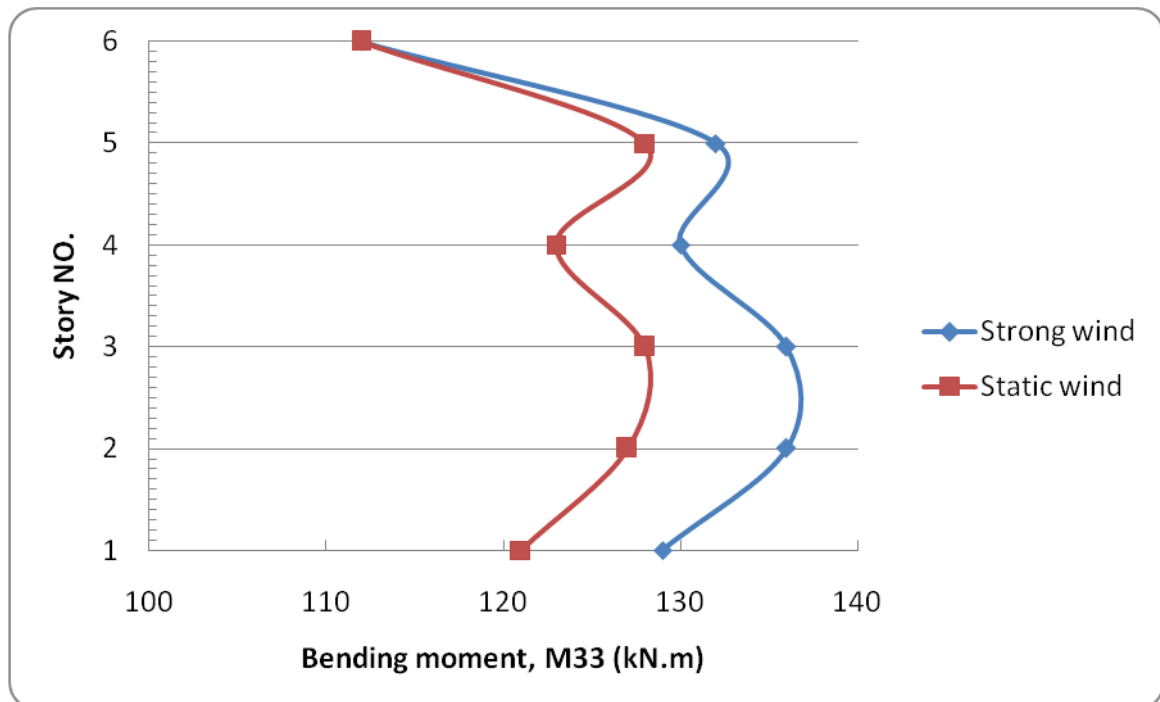


Figure (5-18): Bending moment vs. storey no. for Case F0.

5.5.2.6 Maximum Axial Force and Shear Force for Case F0

The maximum axial force and shear force results from this analysis are shown in Table (5-11), the maximum axial force (compression) in column under the effect of both dynamic strong wind loads and static wind loads is occurred in the first storey with value of 3120kN, namely there is no difference between them due to the axial forces depending on gravity load. It noted the axial forces decreasing with increasing number of storey because the axial force in specific storey is result from summation axial forces in all upper storeys, so the maximum happened in first storey as shown in Fig. (5-19).

The maximum shear force in beam under the effect of both dynamic strong wind loads and static wind loads in sixth storey equal to 144.5KN, namely there is no differences between them. But it is found that shear forces due to dynamic strong and static wind loads approximately are the same in the

fourth, fifth and sixth storeys but there is simple variation on the first, second and third storeys as shown in Figs. (5-20), because the similarity and difference of the forces of the dynamic strong wind at a specific time with a static wind when both types of wind are maximum.

Table (5-11): Maximum axial force and shear force for Case F0.

Case F0	Strong wind		Static wind	
Story No.	V2	P	V2	P
Text	KN	KN	KN	KN
1	136	3120	133	3121
2	139	2602	135	2603
3	139	2091	136	2092
4	142	1575	142	1576
5	140	1050	140	1051
6	144	528	144	528

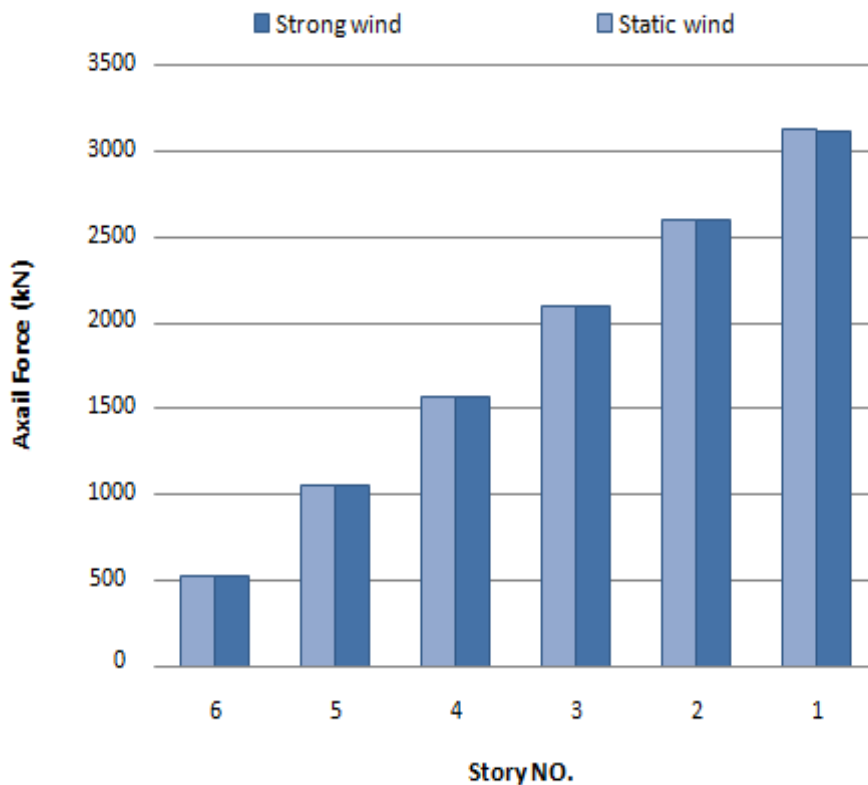


Figure (5-19): Axial force vs. storey no. for Case F0.

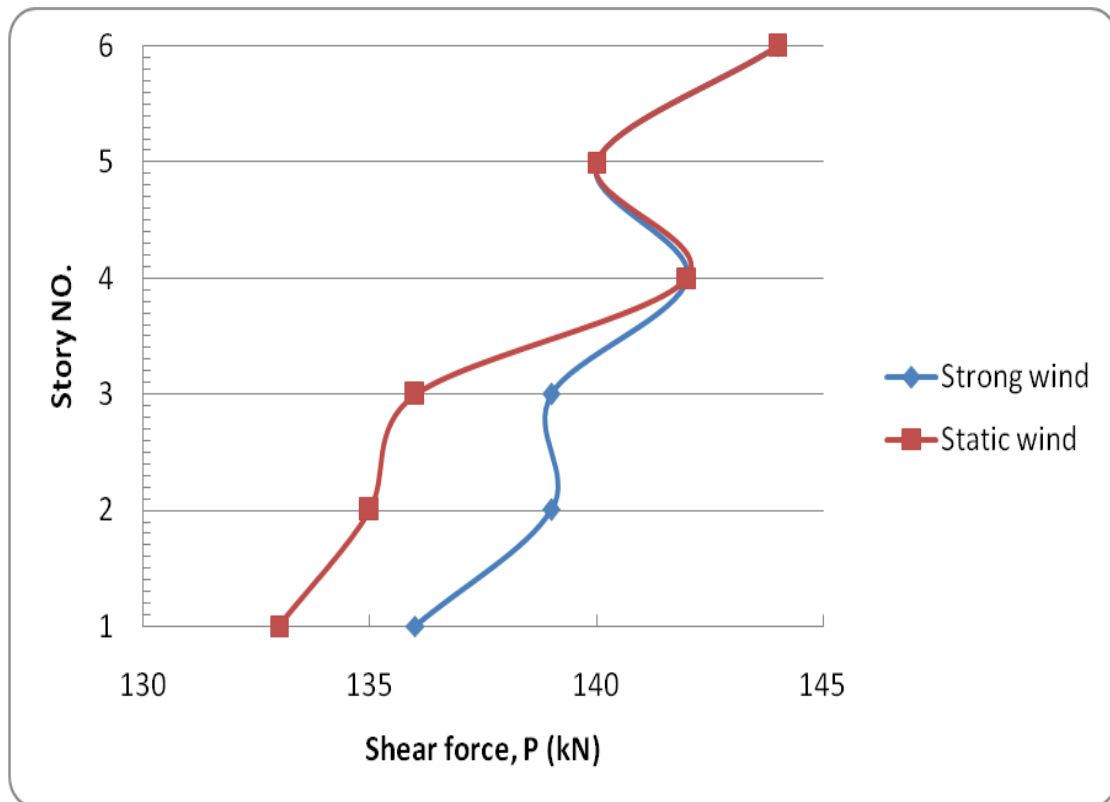


Figure (5-20): Shear force vs. storey no. for Case F0.

5.5.2.7 Maximum Displacements in X-Direction for Case F0

It's found that the displacement in x-direction is increasing with increasing height under the effects of wind loads. The maximum displacement under the effect of dynamic strong wind loads happened in last storey equal to 19.5mm while maximum displacement due to static wind loads for the same storey 7.9mm with 60% difference because the dynamic characters of strong wind loads which same impulses its as shown in Fig. (5-21). The results shown in Table (5-12).

According to BS 8110-Part 2:1985 the maximum allowable deflection is calculated as $h/500$, where h is the total height of building. Therefore, maximum allowable displacement value for building height of 19m is 38mm. The maximum value of displacement in serviceability limit condition obtained for

dynamic strong wind loads from the finite element 3-D model of SAP 2000.Pro is 19.5 mm is less than allowable (38 mm) for criteria failure, so the building is safe in both cases.

Table (5-12): Maximum displacement in x-direction for Case F0.

Case F0	Strong	Static
Story No.	U _x	U _x
Text	mm	mm
1	3.31	1.48
2	6.78	2.78
3	10.57	4.34
4	14.37	5.63
5	17.25	6.65
6	19.50	7.89

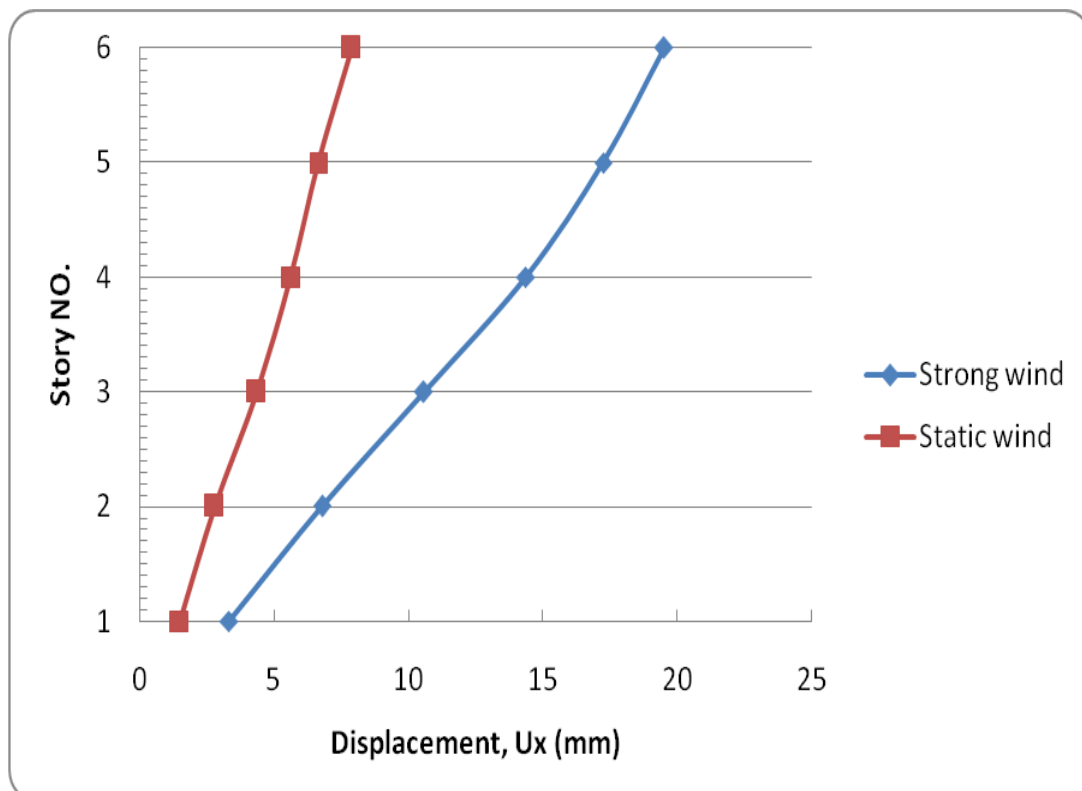


Figure (5-21): Maximum displacement vs. storey no. for Case F0.

5.5.3 Case3 Wind Speed Effect on Dynamic Response Strong versus Moderate

In this case, the effect of speed and its time history configurations on dynamic response of building is considered via strong and moderate wind effect on a building Case F2 using nonlinear analysis with P-Delta effect where strong and moderate wind based on basic wind speed of $V = 42$ m/s and $V = 21$ m/s respectively at 10m above ground.

5.5.3.1 Base Shear in X-Direction for Case F2

The maximum base shear due to strong wind loads arrived to 847.2kN while for moderate wind loads equal to 287.7kN as shown in Table (5-13), the difference between them is 65% because the greater strong value of speed, compared to moderate wind speed. It's found that the moderate wind time-history has a high oscillation and less time period in cycles also the top of the cycle is sharp and compared with strong wind time-history as shown in Figs.(5-22) and (5-23). This reflects the importance of estimation accurate dynamic wind speed.

Table (5-13): Maximum base shear in x-direction for Case F2.

Output Case	Base shear x
Text	kN
Strong wind	847
Moderate wind	288

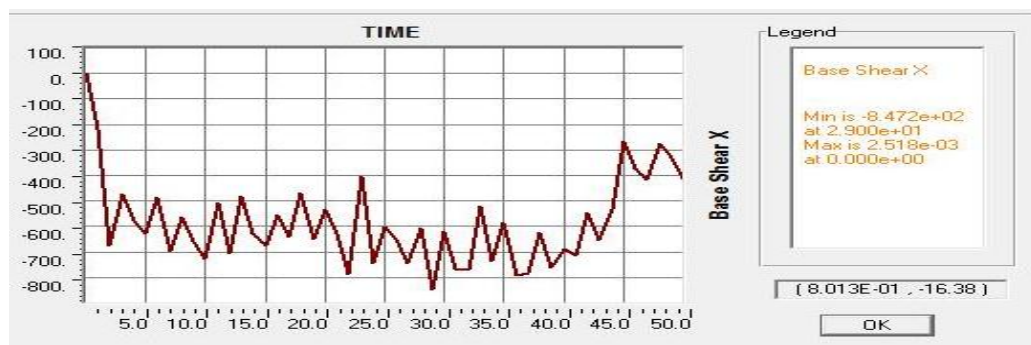


Figure (5-22): Maximum base shear due to strong wind for Case F2.

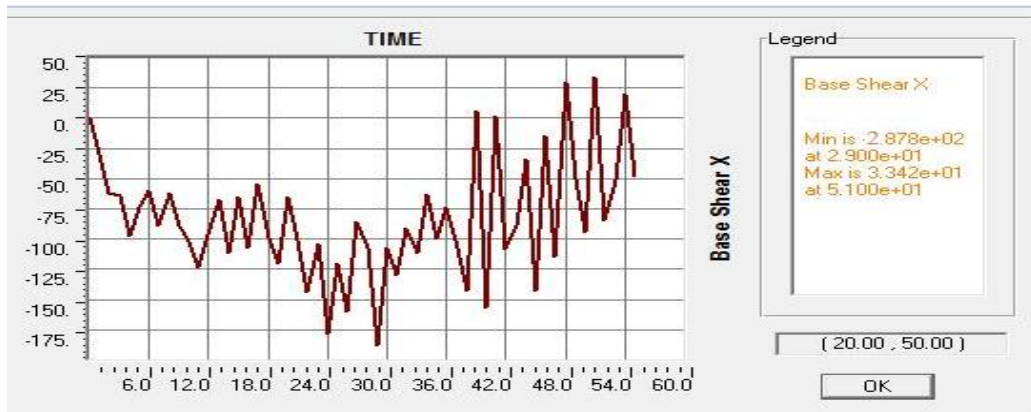


Figure (5-23): Maximum base shear due to moderate wind for Case F2.

5.5.3.2 Base Moment in Y-Direction for Case F2

Similar to base shear, the maximum base moment due to the strong wind is 12302kN.m while 3097.7kN.m under effect of moderate wind as shown in Table (5-14), the difference between them is 75% because the strong wind speeds greater than moderate wind speeds. So the differential between them a clearly in Figs. (5-24) and (5-25) below. This also reflects the importance of estimation accurate dynamic wind speed.

Table (5-14): Maximum base moment in y-direction for Case F2.

Output Case	Base moment y
Text	kN.m
Strong wind	12302
Moderate wind	3098

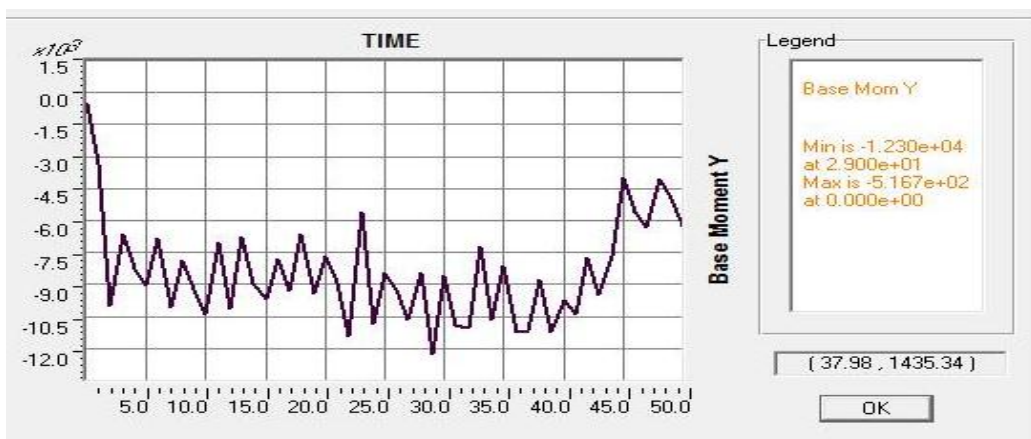


Figure (5-24): Maximum base moment due to strong wind for Case F2.

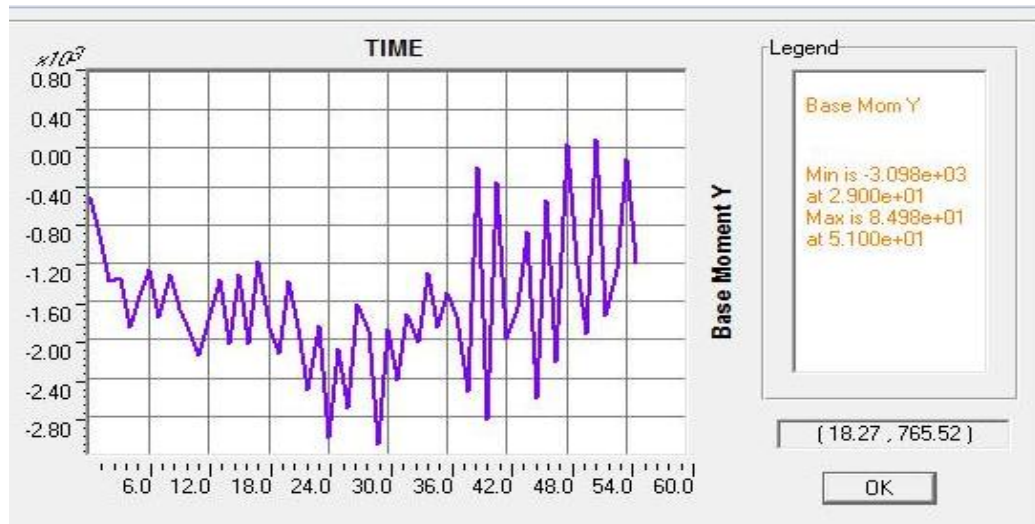


Figure (5-25): Maximum base moment due to moderate wind for Case F2.

5.5.3.3 Maximum Drift Ratio in X-Direction for Case F2

From Fig. (5-26) the drift ratio for Case F2 in x-direction after fire due to strong wind load is 1.41% in last storey while the maximum value of moderate wind load equal to 0.36% in the same storey, the difference between them is 70% because the strong wind speeds greater than moderate wind speeds. It can be seen that the drift ratio on the first and second storeys are increased as compared with upper storey due to the fire deformation.

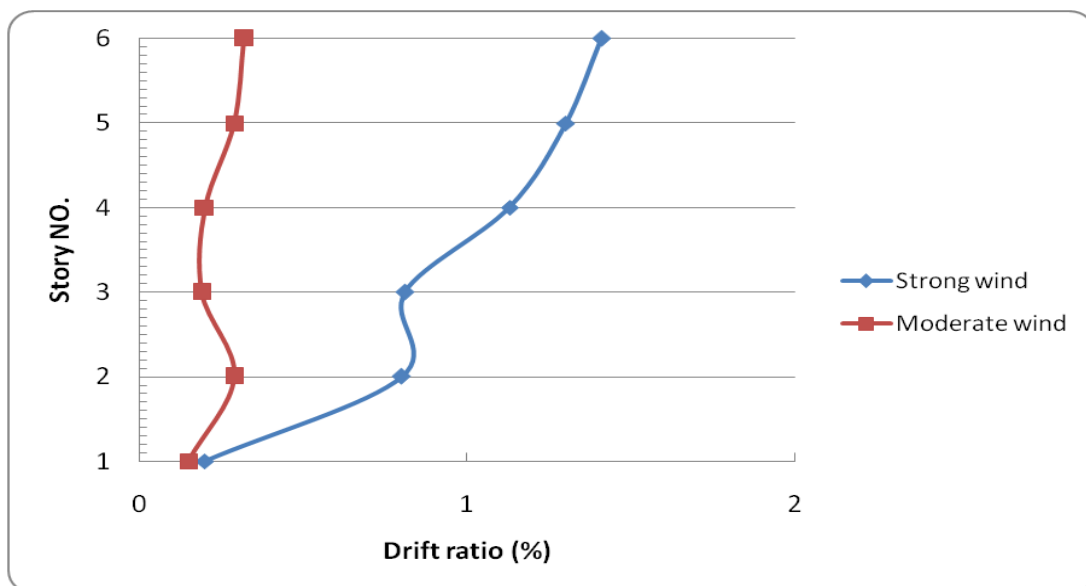


Figure (5-26): Maximum drift ratio due to strong and moderate wind for Case F2.

5.5.3.4 Maximum Stresses (S₁₁, S₁₂ and S₁₃) for Case F2

From stresses results shown in Table (5-15), The maximum axial stress (S₁₁) due to strong and moderate wind occurred on the fourth storey is equal to 266897, 252792.5kN/m² respectively, the difference between them is 5% while the maximum bending stress (S₁₂) for effect of strong and moderate wind occurred on the first storey with 75416.66, 71571kN/m² respectively, the difference between them is 5%. The maximum shear stress (S₁₃) due to strong and moderate wind occurred in the first storey equal to 46929, 44787kN/m² respectively, the difference between them is 5%.

It's found that there is slightly difference between strong and moderate wind after fire in all stresses as shown in Figs. (5-27), (5-28) and (5-29). But there is less agreement between results in first three storeys due to post-fire deformation in there storeys.

The maximum stresses are the axial stress (S₁₁) due to both strong and moderate wind loads obtained from the finite element 3-D model of Sapv2000 software namely 266897,252792kN/m² respectively, are more than yield stress(F_y) after fire, so building is not safe. Also It's found that the stresses for both of winds strong and moderate wind in the same direction of wind effect grater then fy in fourth, fifth and sixth storey on beam.

Table (5-15): Maximum stresses for Case F2.

Strong Wind CaseF2				Moderate Wind CaseF2		
Story NO.	S13	S12	S11	S13	S12	S11
Text	KN/m ²	KN/m ²	KN/m ²	KN/m ²	KN/m ²	KN/m ²
1	46929	75416	223839	44787	71571	199235
2	41862	70159	177228	41865	69841	172401
3	40310	69476	163327	39073	67138	149731
4	13287	56212	266897	13249	56067	252792
5	13166	55543	250315	13127	55494	237787
6	13528	56968	229953	13503	56952	222972

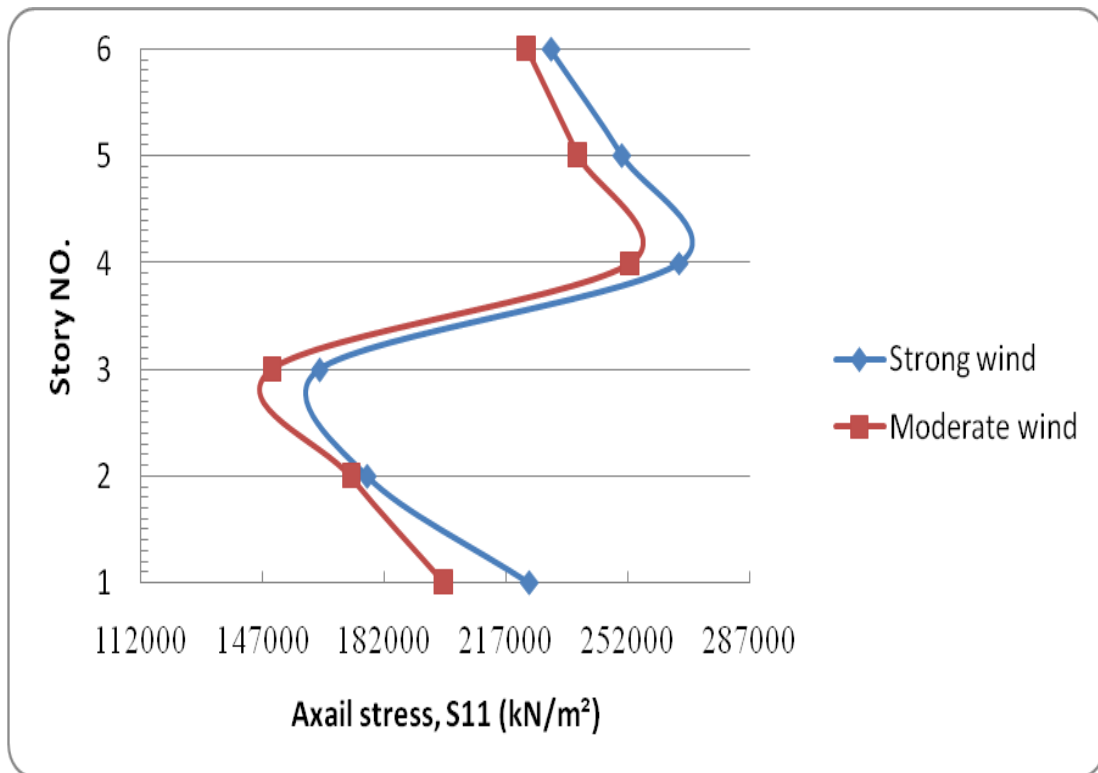


Figure (5-27): Maximum axial stress due to strong and moderate wind for Case F2.

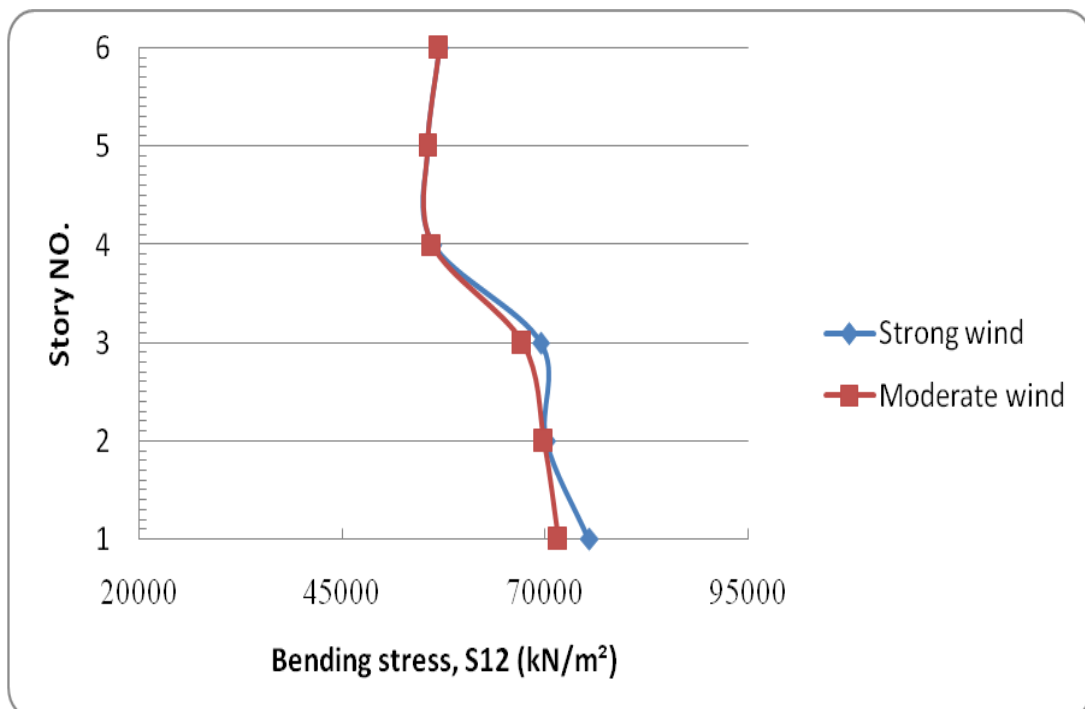


Figure (5-28): Maximum bending stress by strong and moderate wind for Case F2.

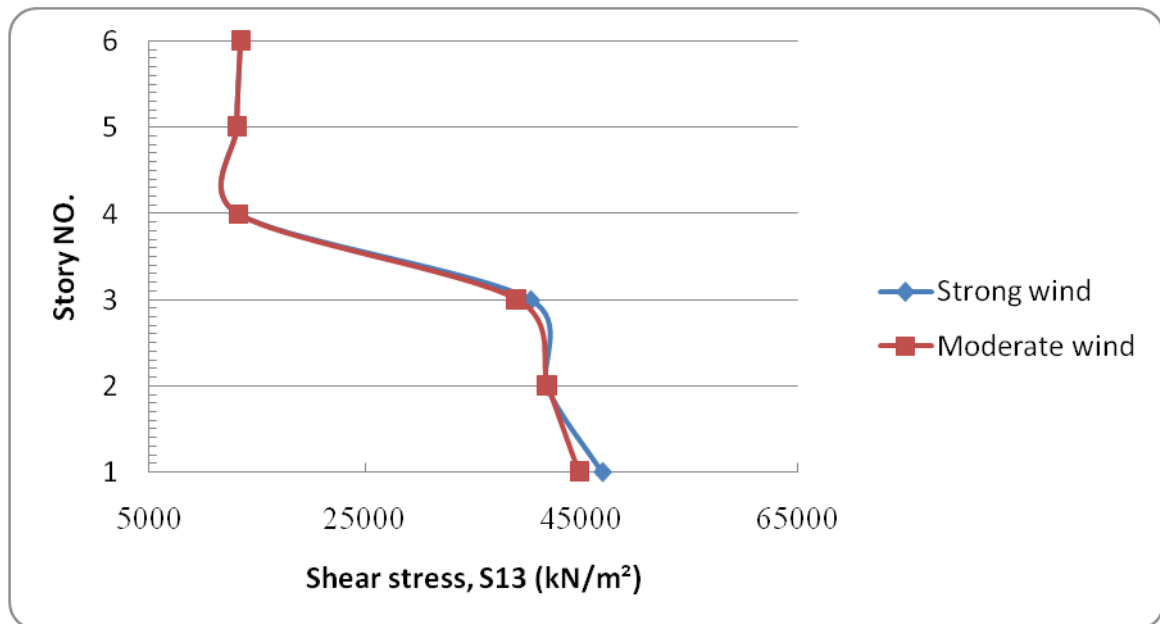


Figure (5-29): Maximum shear stress due to strong and moderate wind for Case F2.

5.5.3.5 Maximum Bending Moment, M33 for Case F2

The results of bending moments are listed in Table (5-16). The maximum bending moment under the effect of strong wind load is located in first storey on a beam equal to 174.5kN.m while the maximum bending moment negative due to moderate wind load is in the same location equal to 155kN.m as shown in Fig. (5-30), the difference between them is 11%. It's show slight difference between them due to the strong wind loads in specific time greater than static wind loads.

Table (5-16): Maximum bending moment for Case F2.

Case F2	Strong	Moderate
Story No.	M33	M33
Text	kN.m	kN.m
1	175	155
2	145	135
3	143	122
4	135	119
5	134	126
6	113	112

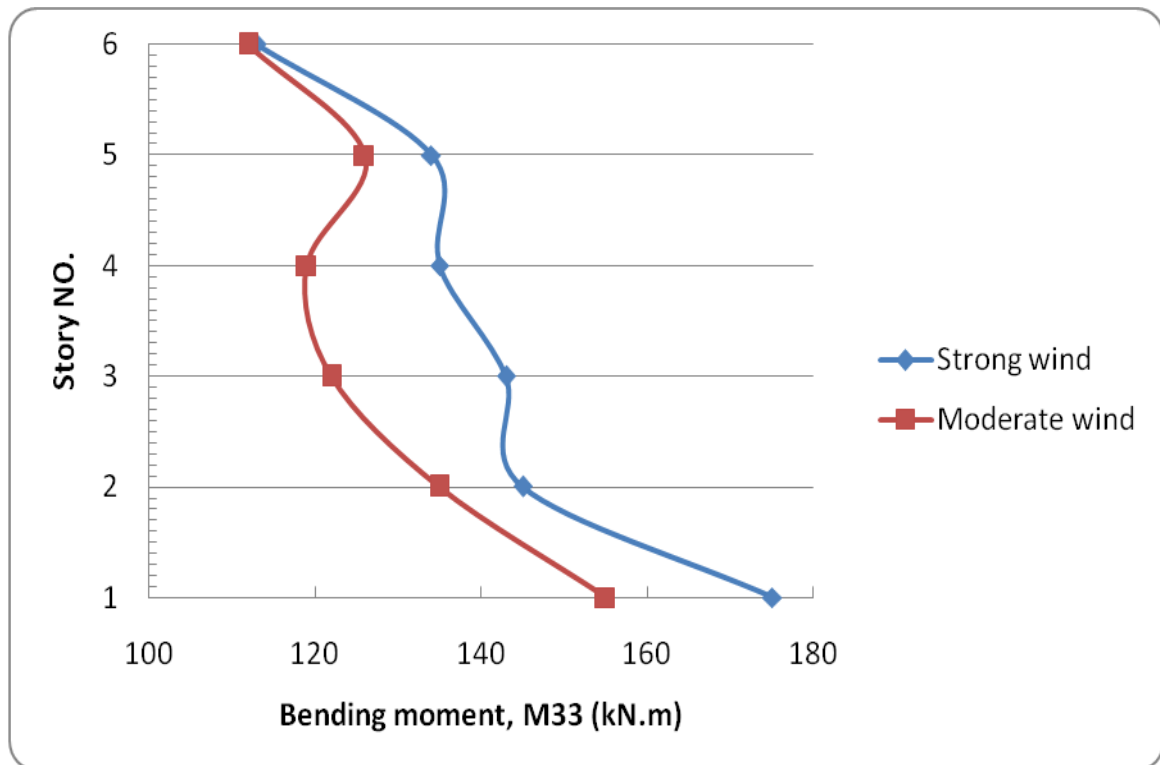


Figure (5-30): Bending moment due to strong and moderate wind for Case F2.

5.5.3.6 Maximum Axial Force and Shear Force for Case F2

The maximum axial force and shear force results from this case is shown in Table (5-17) the maximum axial force (compression) under the effect of strong wind loads is in column of the first storey with value of 3122.7kN while the maximum axial force (compression) for column in same storey due to moderate wind loads equal to 3123.4kN, the difference between them is negligible 0% as shown in Fig. (5-31). It's found that negligible difference between them due to the axial forces depending on gravity load.

The maximum of shear force under the effect of dynamic strong wind loads on beams of last storey equal to 144.7kN which equals 144.66kN due to moderate wind load in same location, so the difference is negligible. But the distribution along building much diverge in first three storeys due to fire

deformation at first three storeys while the fourth, fifth and sixth storeys not subjected to any fire deformation as shown in Fig. (5-32).

Table (5-17): Maximum axial and shear force for Case F2.

Case F2	Strong wind		Moderate wind	
Story No.	V2	P	V2	P
Text	KN	KN	KN	KN
1	142	3123	133	3123
2	143	2603	133	2603
3	142	2092	134	2093
4	143	1576	142	1576
5	141	1053	141	1053
6	145	529	145	529

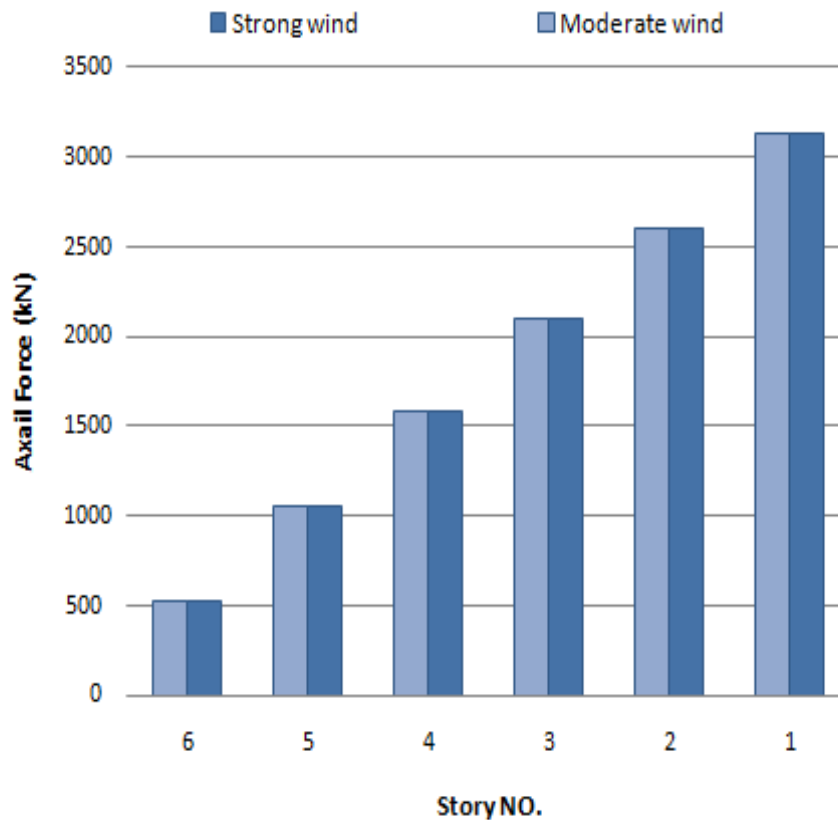


Figure (5-31): Axial forces due to strong and moderate wind for Case F2.

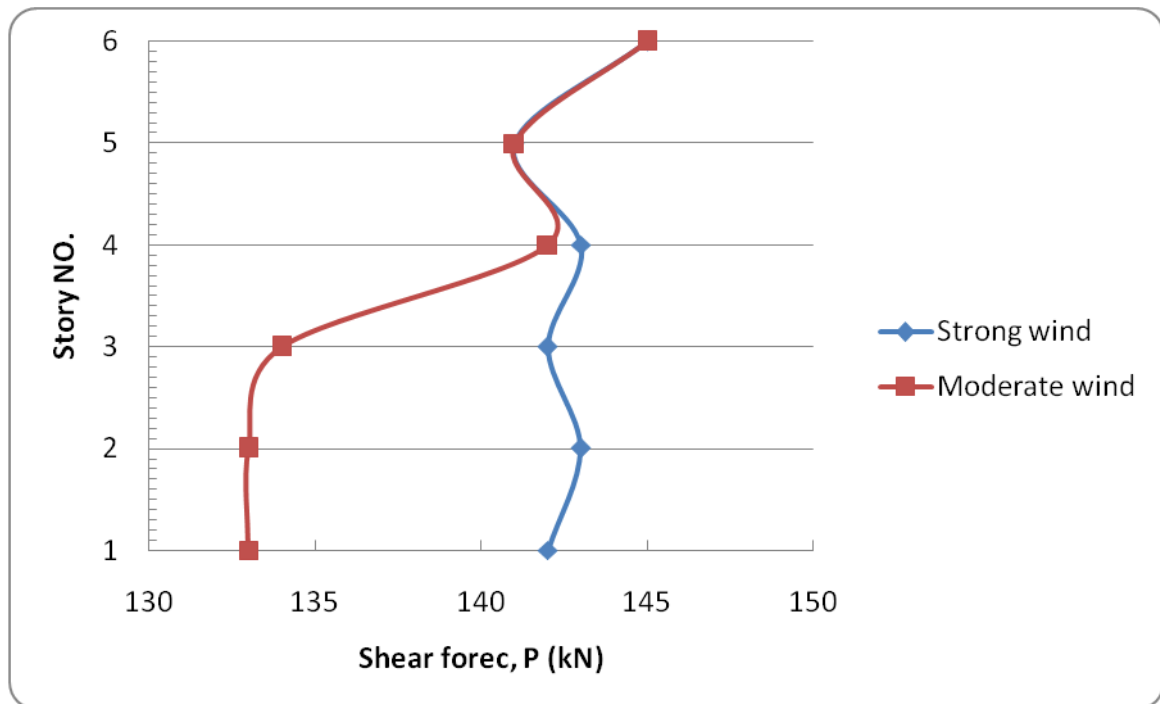


Figure (5-32): Shear forces due to strong and moderate wind for Case F2.

5.5.3.7 Maximum Displacements in X-Direction for Case F2

The displacement along building height due to strong and moderate winds are listed in Table (5-18). The maximum displacement under the effect of strong wind loads occurred in sixth storey and equals to 20mm while maximum displacement due to moderate wind loads for the same storey is 5mm as shown in Fig. (5-33). The difference between them is 75% because the strong wind speeds greater than moderate wind speeds. It's found that the displacement in x-direction in the first, second and third storeys due to moderate wind is large than the displacement in upper storeys due to the presence of deformations after the fire and reduced 10% of yield stress after fire.

According to BS 8110-Part 2: 1985 the maximum allowable displacement is calculated as $h/500$, where h is the total height of building. Therefore, maximum allowable displacement value for building height of 19m is 38mm. The maximum value of displacement in serviceability limit condition

obtained for dynamic strong wind loads from the finite element 3-D model of SAP 2000 software is 20 mm is less than allowable (38 mm) for criteria failure, so the building is safe in both cases.

Table (5-18): Maximum displacement in x-direction for Case F2.

Case F2	Strong	Moderate
Story No.	U _x	U _x
Text	mm	mm
1	8.56	5.92
2	10.83	4.80
3	11.75	2.90
4	15.10	3.26
5	17.17	3.91
6	20.05	5

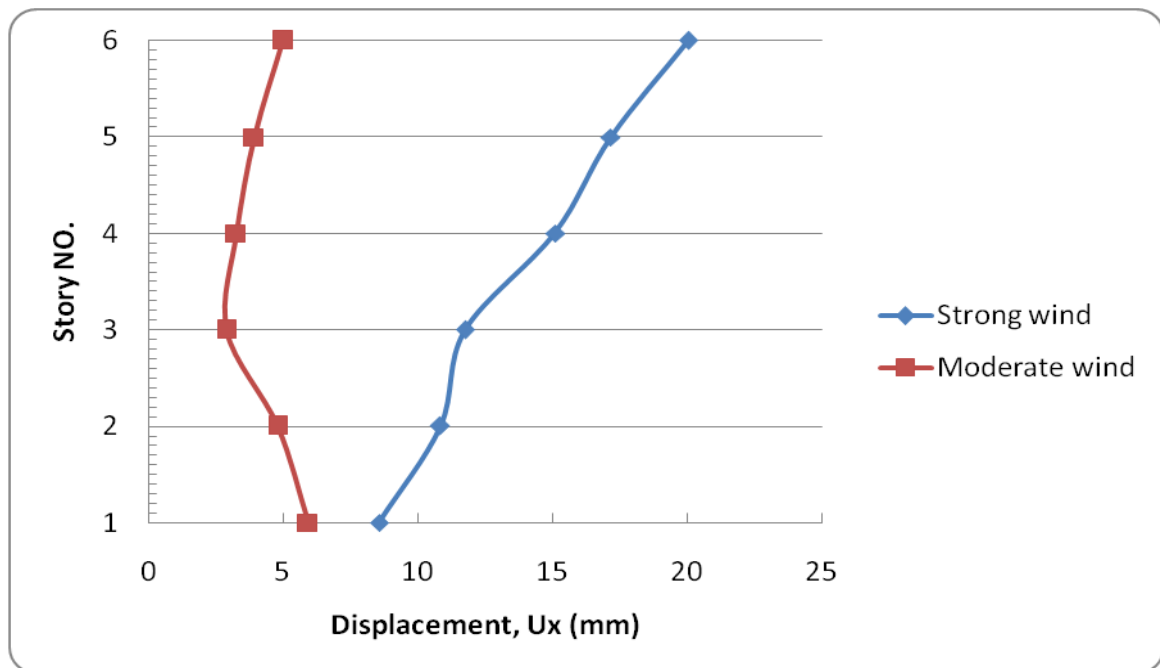


Figure (5-33): Displacement per storey strong and moderate wind, Case F2.

5.5.4 Case4 Linear and Nonlinear Dynamic Analysis Effect

In this case the study of the effect of linear behavior without P-Delta effect compared with nonlinear behavior with P-Delta effect for building Case

F1 under the effect of dynamic strong wind load that based on basic wind speed, $V = 42$ m/s at 10m above ground is presented.

5.5.4.1 Base Shear in X-Direction for Case F1

The maximum base shear of Case F1 under the effect of strong wind for linear analysis is equal to 814.3kN while due to nonlinear analysis is equal to 868.7kN, as shown in Table (5-19) the difference between them is 6% ,namely base shear less effected by P-Delta effect, and the material behavior is linear below yield stress. In addition there is slightly difference in time-history for linear and nonlinear behavior as shown in Figs. (5-34) and (5-35).

Table (5-19): Base shear x-direction for Case F1.

Output Case	Base moment y
Text	kN
Linear strong wind	814
Nonlinear static wind	868

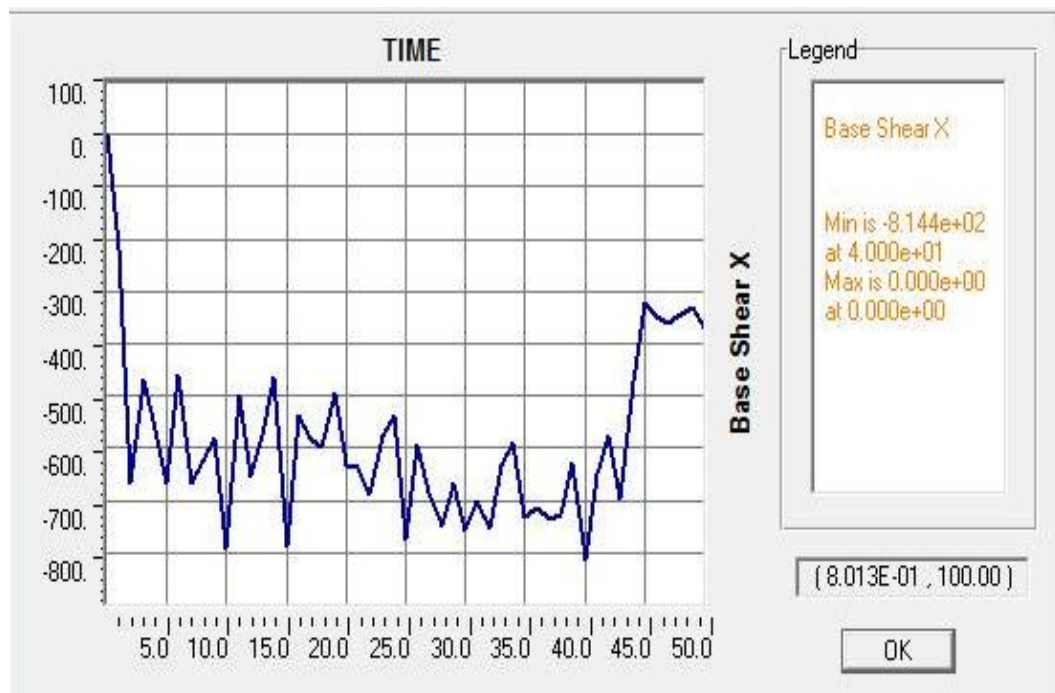


Figure (5-34): Base shear x-direction strong wind for Case F1 by linear analysis.

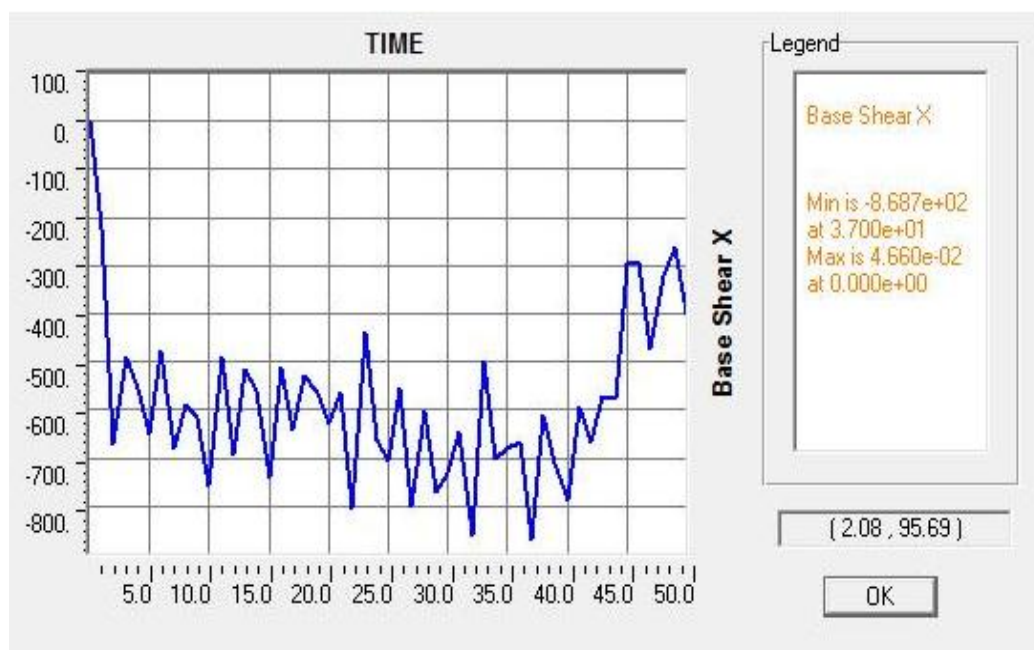


Figure (5-35): Base shear x-direction strong wind for Case F1 by nonlinear analysis.

5.5.4.2 Base Moment in Y-Direction for Case F1

Similar to base shear, the maximum base moment in y-direction due to the strong wind linear and nonlinear analysis is 10012, 12157.7kN.m respectively, under effect of strong wind analysis as shown in Table (5-20), the difference between them is 20% due to although linear elastic behavior of steel below yield stress, but geometric nonlinear effect is greater due to additional bending moment due to P-Delta effect, in addition there is identify in time-history for linear and nonlinear behavior as shown in Figs.(5-36) and (5-37). These reflect the importance of estimation accurate configuration of building after fire.

Table (5-20): Base moment y-direction for Case F1.

Output Case	Base moment y
Text	kN.m
Linear strong wind	10012
Nonlinear strong wind	12157

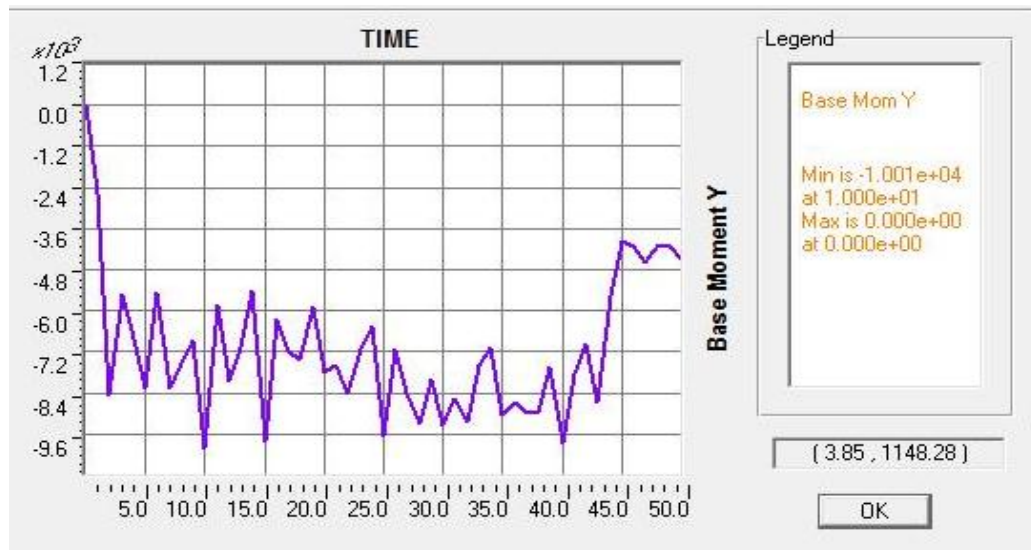


Figure (5-36): Base moment y-direction strong wind for Case F1 by linear analysis.

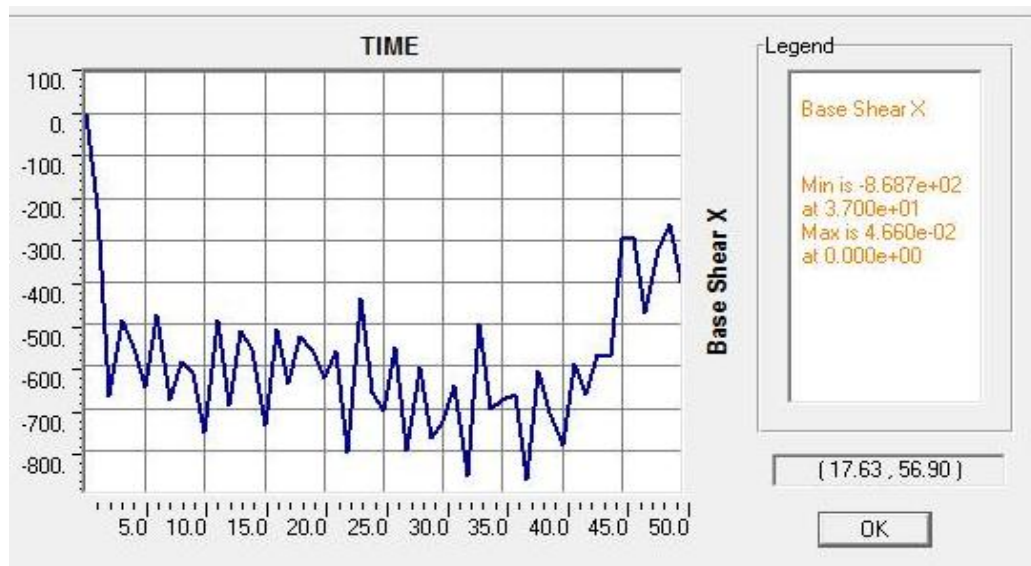


Figure (5-37): Base moment y-direction strong wind for Case F1 by nonlinear analysis.

5.5.4.3 Maximum Drift Ratio in X-Direction for Case F1

From results of drift ratio in x-Direction as shown in Fig. (5-38). These results show the maximum ratio in third storey for linear analysis and fourth storey nonlinear analysis are 0.19%, 0.20% respectively, the difference between them is 5% also it's found that slightly difference between them on the first,

second and third storeys but clear difference on the fourth, fifth and sixth storeys where fire occurred which reflect that post-fire behavior of steel building is nonlinear behavior and the linear analysis can not match the accurate behavior of the building especially for storey subjected to fire damage.

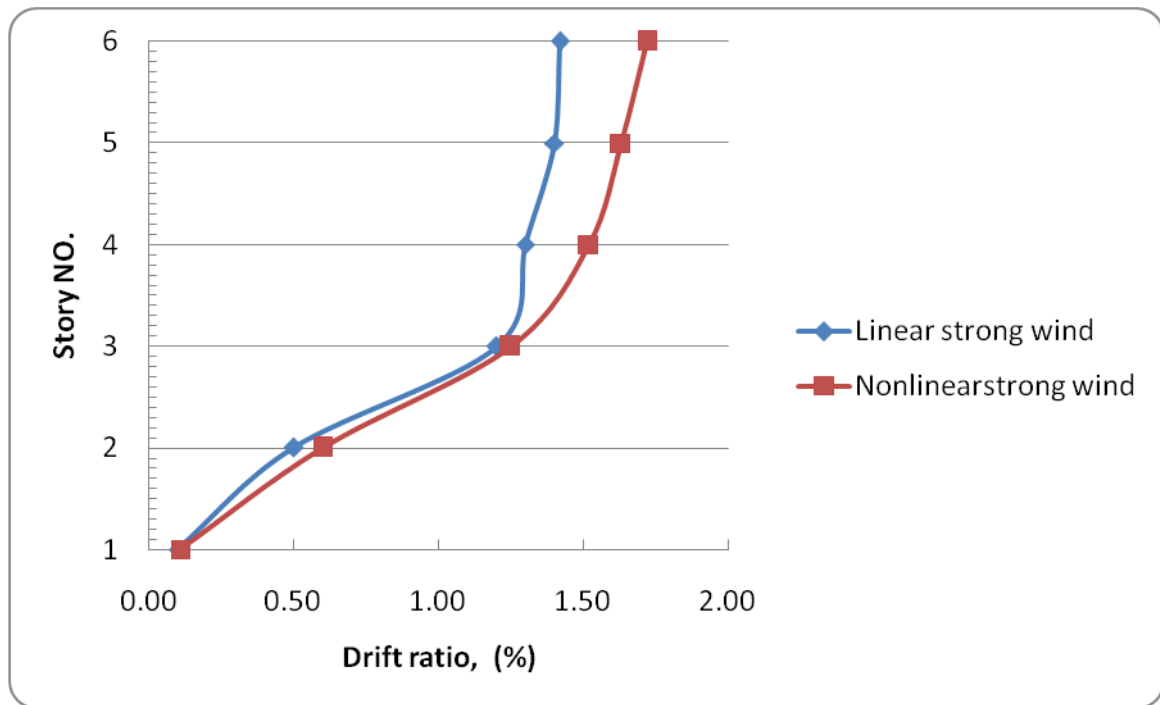


Figure (5-38): Drift ratio for linear and nonlinear analysis, strong wind for Case F1.

5.5.4.4 Maximum Stresses (S_{11} , S_{12} and S_{13}) for Case F1

The maximum stresses results obtained by both linear and nonlinear analysis are shown in Table (5-21), The maximum axial stress (S_{11}) under the effect of strong wind occurred on the fourth storey equal to 234198kN/m² for nonlinear and maximum strong wind linear but the value is 225450kN/m². The difference between them is 4%, namely negligible difference.

The maximum bending stress (S_{12}) due to strong wind occurred on the fourth storey are 66420kN/m² and 32181kN/m² for nonlinear and linear analysis, respectively. The difference between them is 50% which reflect sensitivity of

bending stress to nonlinear effects especially P-Delta effect. The maximum shear stress (S_{13}) under the effect of strong wind happened on the fourth storey is 37292kN/m^2 and 32181kN/m^2 for nonlinear and linear analysis respectively, the difference between them is 13% namely little difference between linear and nonlinear behavior in shear stresses.

The axial stress (S_{11}) is little effected by linear or nonlinear analysis due to the axial stress depend on gravity load, as shown in Fig. (5-39) while the shear stresses (S_{13}) is approximately similar between linear and nonlinear behavior on the first, second and third storeys but clear difference on the fourth, fifth and sixth storeys as shown in Fig. (5-41), because reducing of (F_y and E) 10% after fire making steel loses strength and stiffness.

Bending stress (S_{12}) is much effected to analysis type due to additional bending moment produced from P-Delta effect as shown in Fig. (5-40). All maximum types of stress occurred in beam.

The maximum stresses is axial stress (S_{11}) equal to 234198kN/m^2 in nonlinear behavior is more than yield stress (F_y) after fire, so building is not safe and 225060 kN/m^2 in linear behavior is approximately equal from yield stress (F_{ee}) after fire, so building is critical.

Table (5-21): Maximum stresses for Case F1.

Linear strong Wind CaseF1			Nonlinear moderate Wind CaseF1			
Story NO.	S13	S12	S11	S13	S12	S11
Text	KN/m ²	KN/m ²	KN/m ²	KN/m ²	KN/m ²	KN/m ²
1	11968	5395	140495	13015	55290	144175
2	12282	7888	128000	13393	56880	134761
3	11984	45829	132405	13517	57381	137549
4	32181	41539	225059	37292	66420	234198
5	25719	37377	204109	31262	61768	204418
6	21508	34899	189356	26780	58817	187458

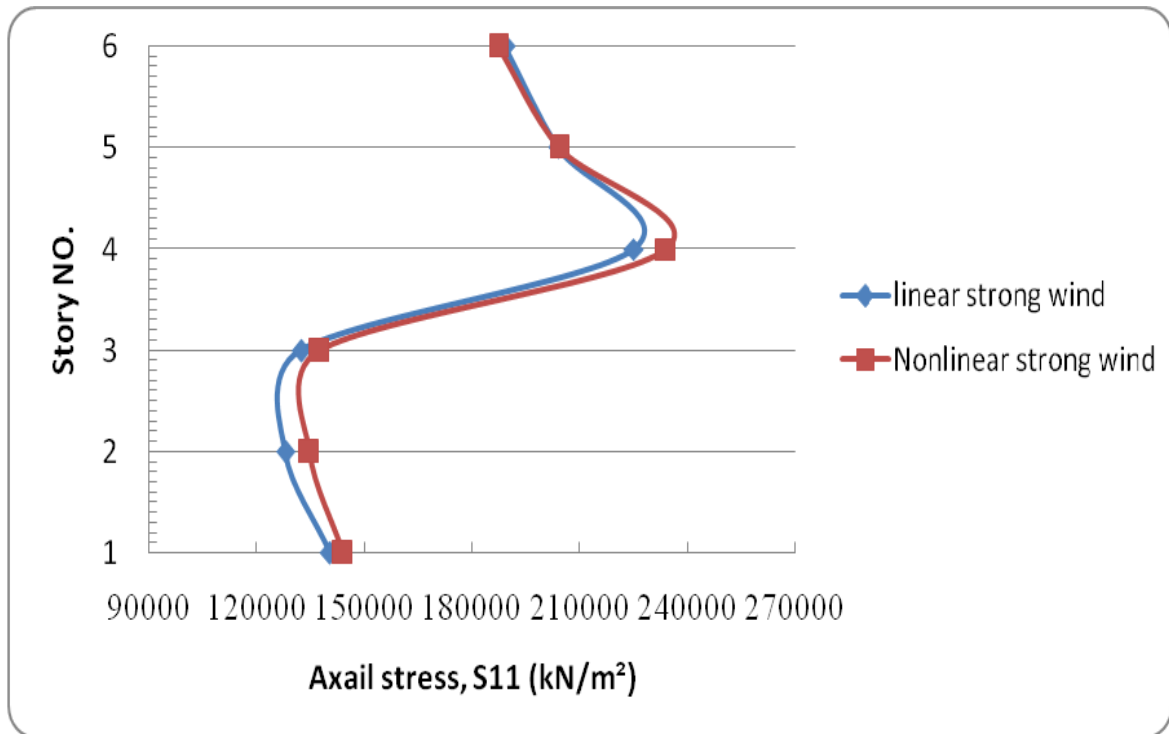


Figure (5-39): Axial stresses for linear and nonlinear analysis for strong wind, Case F1.

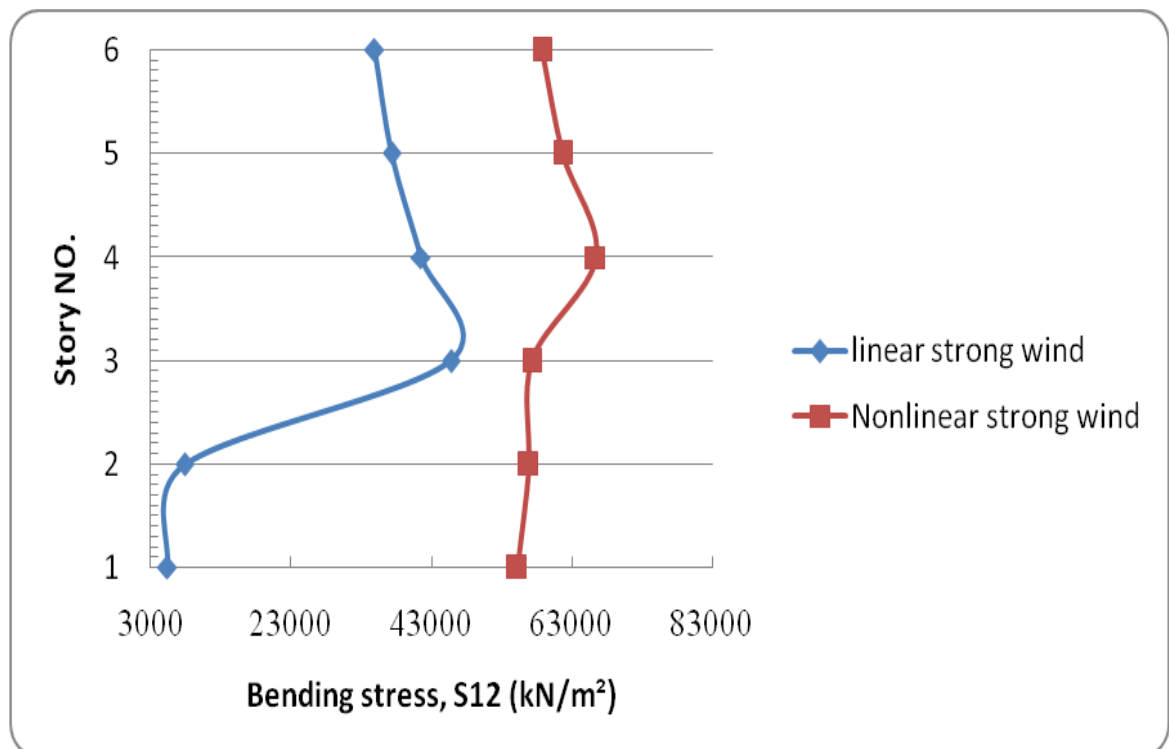


Figure (5-40): Bending stresses for linear & nonlinear analysis for strong wind, Case F1.

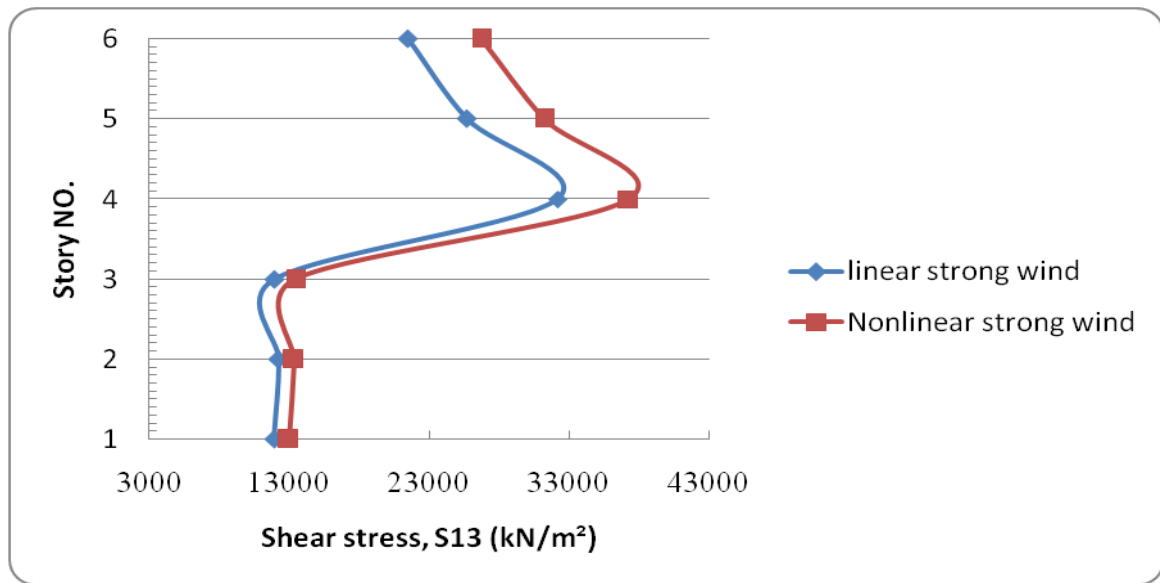


Figure (5-41): Shear stresses for linear and nonlinear analysis for strong wind, Case F1.

5.5.4.5 Maximum Bending Moment, M₃₃ for Case F1

From the Table (5-22) and Fig. (5-42) for Case F1, it can clearly be seen that the maximum bending moment occurred in beam of the third storey is equal to 152.2kN.m and 132kN.m for nonlinear and linear analysis respectively, the difference between them is 13% due to P-Delta effect on nonlinear behavior. Also it found that grater values in the third storey because of the solution techniques for linear analysis and start of effect fire in this story.

Table (5-22): Maximum bending moment for Case F1.

Strong	Linear	Nonlinear
Story No.	M ₃₃	M ₃₃
Text	kN.m	kN.m
1	84.69	139.24
2	80.45	149.80
3	131.81	152.22
4	105.25	144.51
5	92.84	139.84
6	102.80	112.96

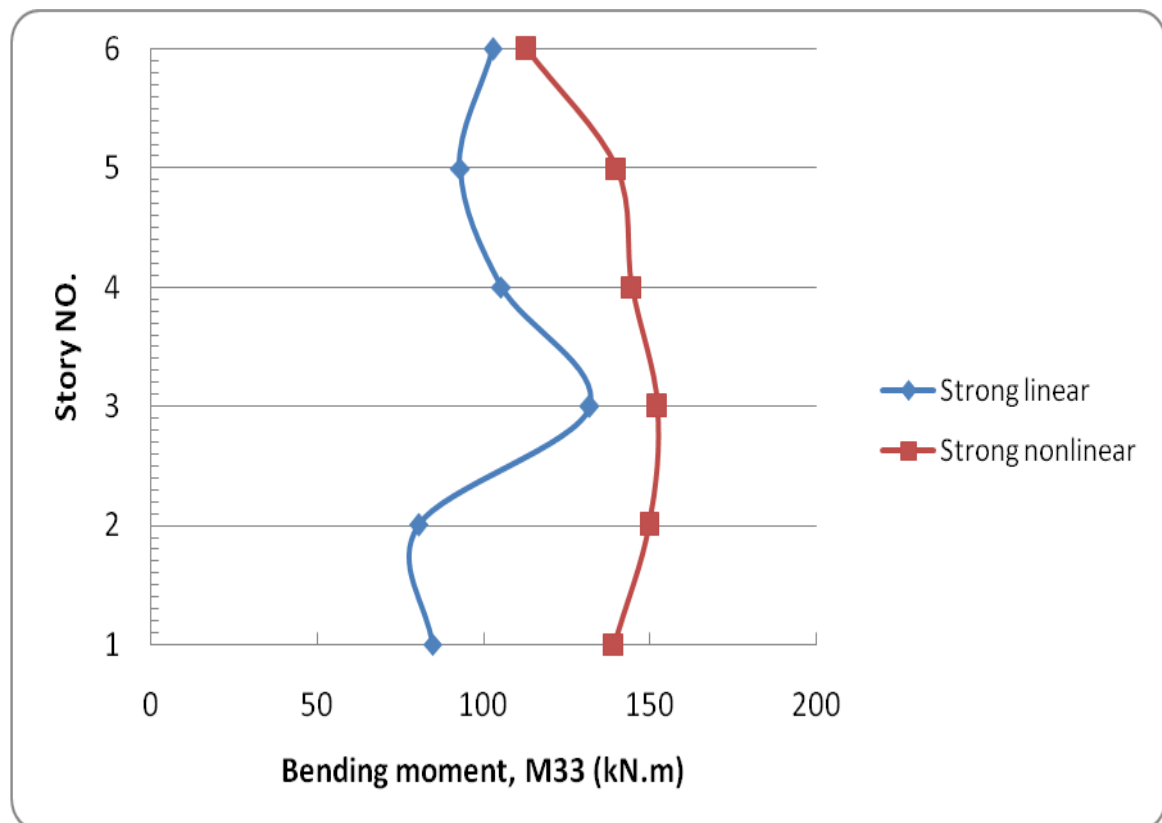


Figure (5-42): Bending moment for linear, nonlinear analysis for strong wind, Case F1.

5.5.4.6 Maximum Axial Force and Shear Force for Case F1

The maximum axial force and shear force results for this case is shown in Table (5-23), the maximum axial force (compression) under the effect of strong wind load is occurred in the first storey columns are 3131kN and for nonlinear and linear analysis respectively.

The difference between them is approximately 0.9% namely negligible difference as shown in Fig. (5-43).

The maximum shear force under the effect of strong wind load on the third storey beams is equal to 70.4kN for linear analysis and 144.9kN nonlinear on sixth storey beams, so the difference is equal to 51% due to reduced 10% of yield stress after nonlinearity effect fire as shown in Fig. (5-44).

Table (5-23): Maximum axial and shear force for Case F1.

Case F1	Linear strong wind		Nonlinear strong wind	
Story No.	V2	P	V2	P
Text	kN	kN	kN	kN
1	34	3158	137	3131
2	50	2640	140	2613
3	73	2126	141	2102
4	70	1604	144	1581
5	67	1070	143	1053
6	65	538	145	529

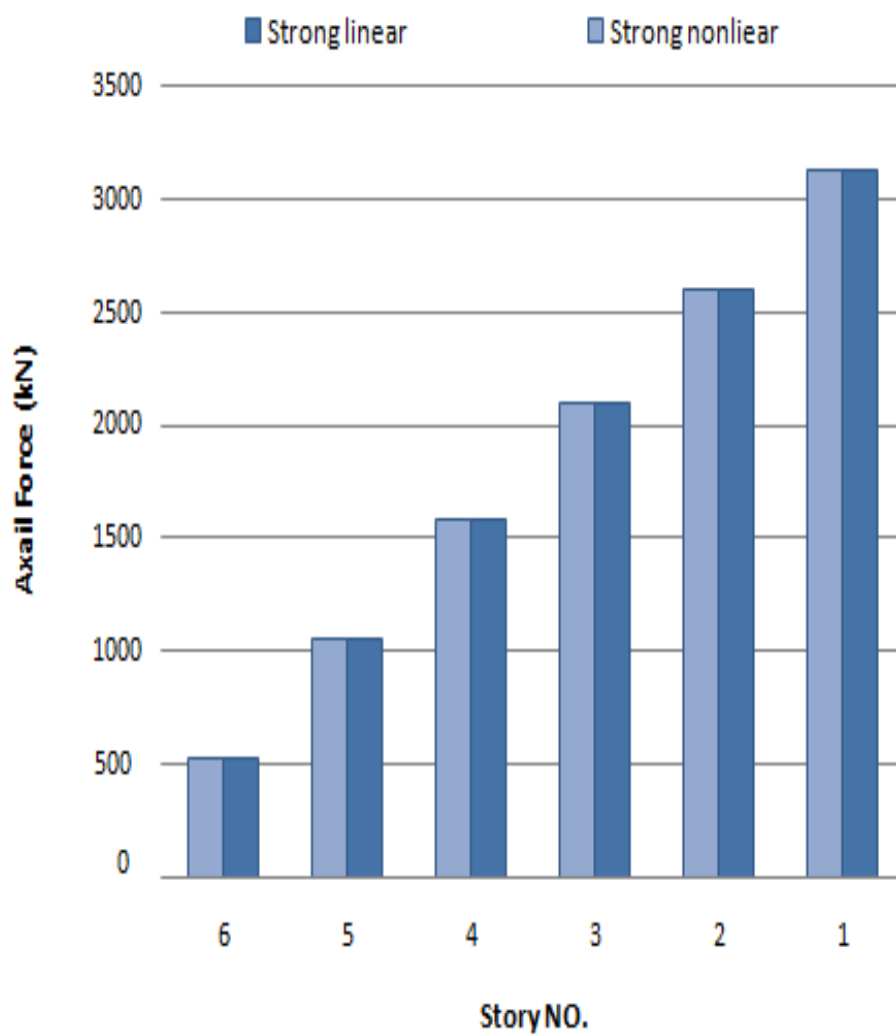


Figure (5-43): Axial forces for linear and nonlinear by strong wind, Case F1.

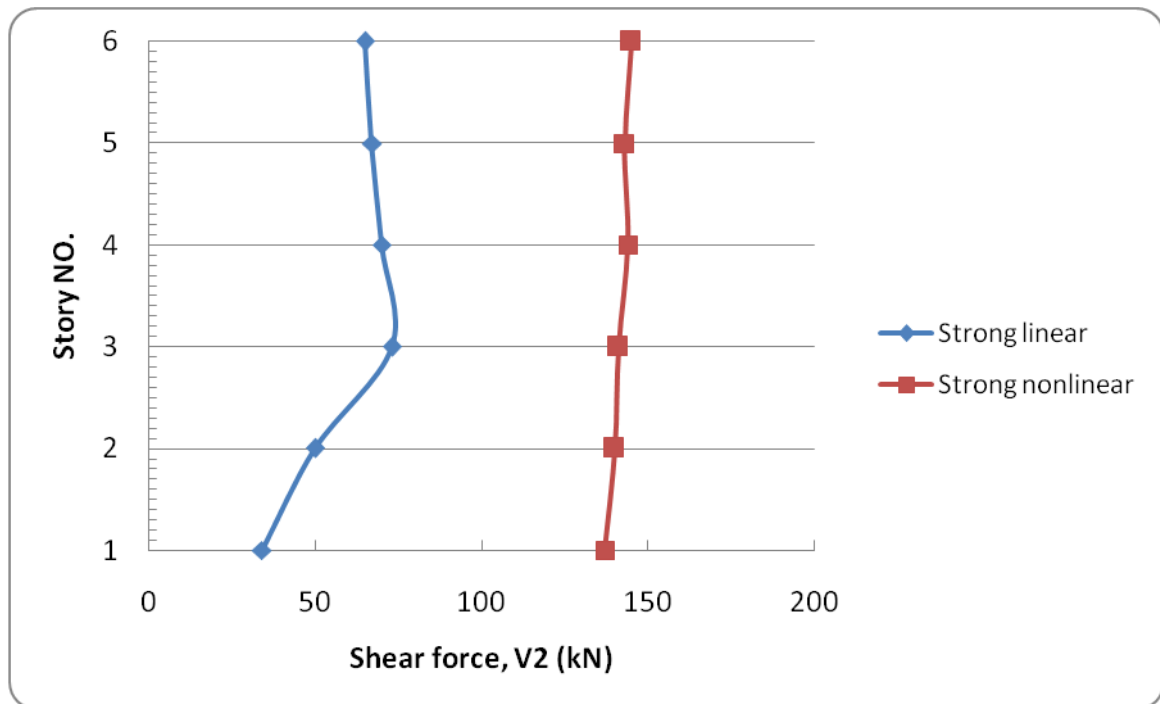


Figure (5-44): Shear forces for linear and nonlinear by strong wind, Case F1.

5.5.4.7 Maximum Displacements in X-Direction for Case F1

The displacement along building height due to strong wind loads in x-direction obtained by linear and nonlinear analysis is shown in Table (5-24), these results showed that the maximum displacement in last storey for linear and nonlinear behavior is 19, 25mm, respectively.

The difference between them is 25% because of the solution techniques of analysis for both behaviors and it's found that identify between them on the first, second and third storeys but clear difference on the fourth, fifth and sixth storeys where fire occurred, as shown in Fig. (5-45).

According to BS 8110-Part 2: 1985 the maximum allowable deflection is calculated as $h/500$, Therefore, maximum allowable displacement value for building height of 19m is 38mm. The maximum value of displacement in serviceability limit condition obtained for strong wind load nonlinear behavior

is 25 mm is less than allowable (38 mm) for criteria failure, so the building is safe in both cases.

Table (5-24): Maximum displacement in x-direction for Case F1.

Strong	Linear	Nonlinear
Story No.	U _x	U _x
Text	mm	mm
1	3.01	3.739
2	7.19	7.87
3	12.96	13.38
4	15.50	19.50
5	17.47	22.41
6	19.05	24.96

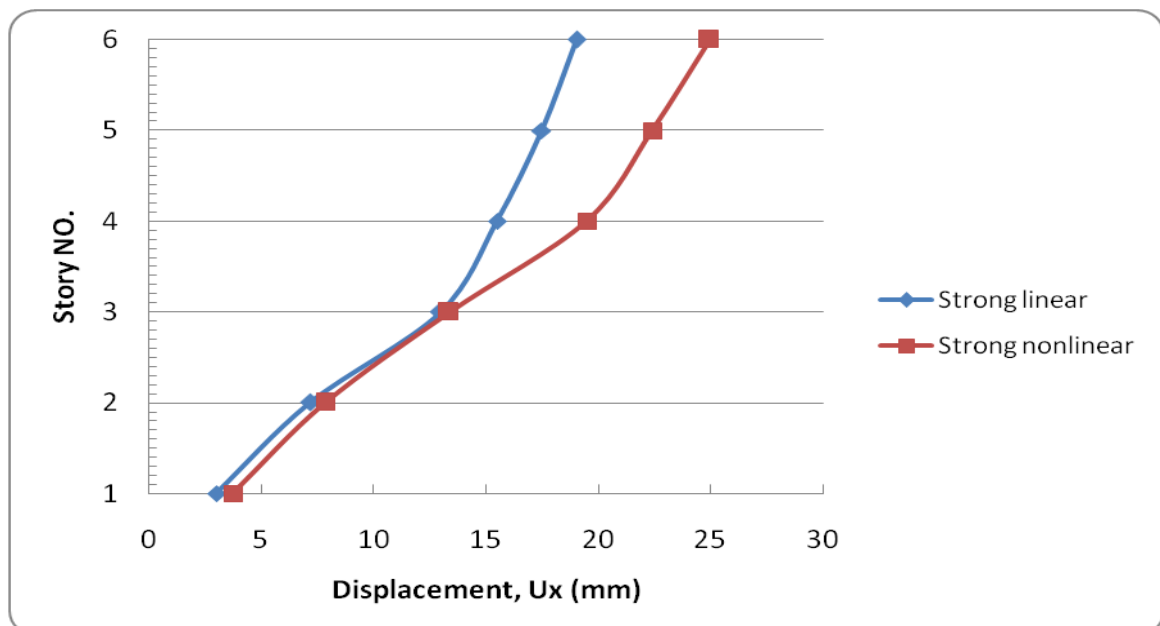


Figure (5-45): Maximum drift storey for linear and nonlinear analysis for strong wind, Case F1.

5.5.5 Case5 Post-Fire Analysis, Fully Deformation (Δ)

In this case, the post-fire behavior of steel building is studied via comparison the results with that before fire for building cases (Case F0 and Case F2) using nonlinear analysis with P-Delta effect, where both strong and

moderate winds based on basic wind speed, $V = 42 \text{ m/s}$ and $V = 21 \text{ m/s}$ respectively at 10m above ground are used.

5.5.5.1 Base Shear in X-Direction for Case F0 and Case F2

The maximum base shear before and after fire under the effect of strong wind loads equal to 763, 847kN respectively, the difference between them is 40% while the maximum before and after fire due to moderate wind loads equal to 203, 287kN respectively, the difference between them is 11% as shown in Table (5-25) there is slightly difference in time-history where there is sharply of oscillation in both of winds after fire as compared with before fire due to the fire that making reduced on yield stress and modulus of elasticity 10% from before fire as shown in Figs.(5-46) to (5-49).

Table (5-25): Base shear x-direction before and after fire.

Output Case	Base shear x Case F0	Base shear x Case F2
Text	kN	kN
Strong wind	763	847
Moderate wind	203	287

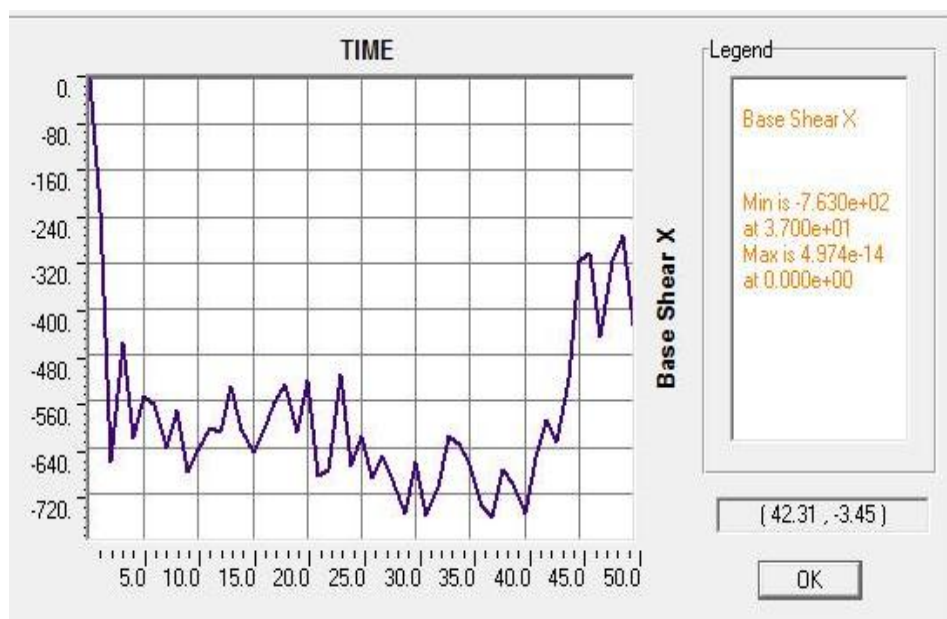


Figure (5-46): Base shear in x-direction due to strong wind, Case F0.

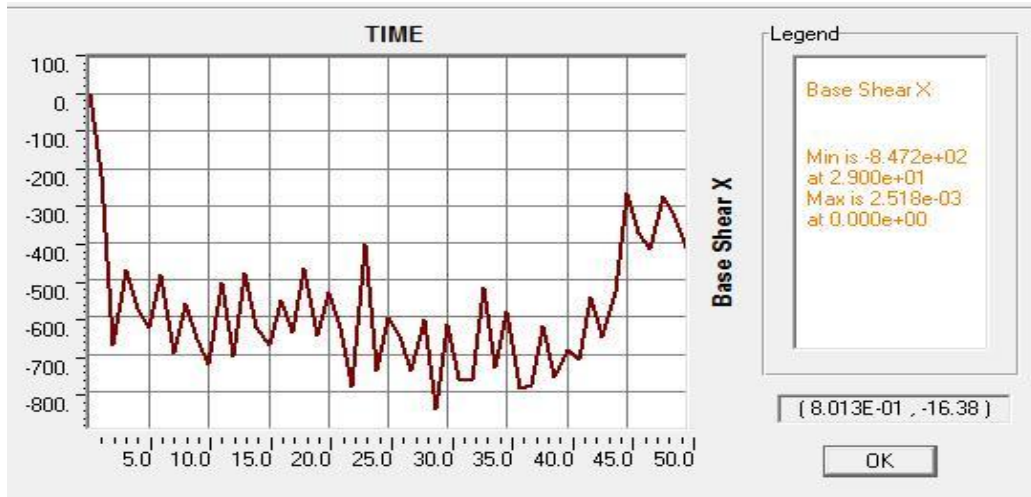


Figure (5-47): Base shear in x-direction due to strong wind, Case F2.

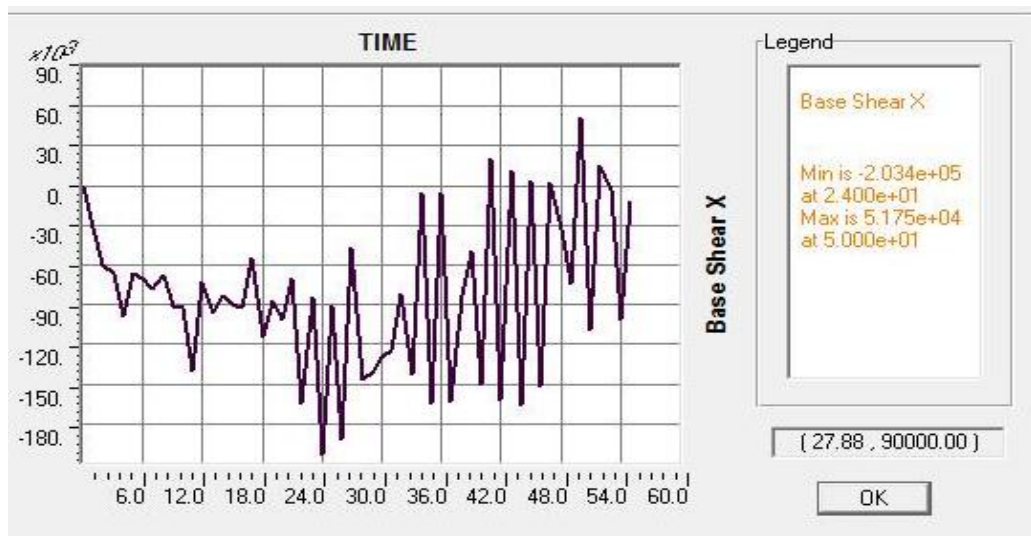


Figure (5-48): Base shear in x-direction due to moderate wind, Case F0.

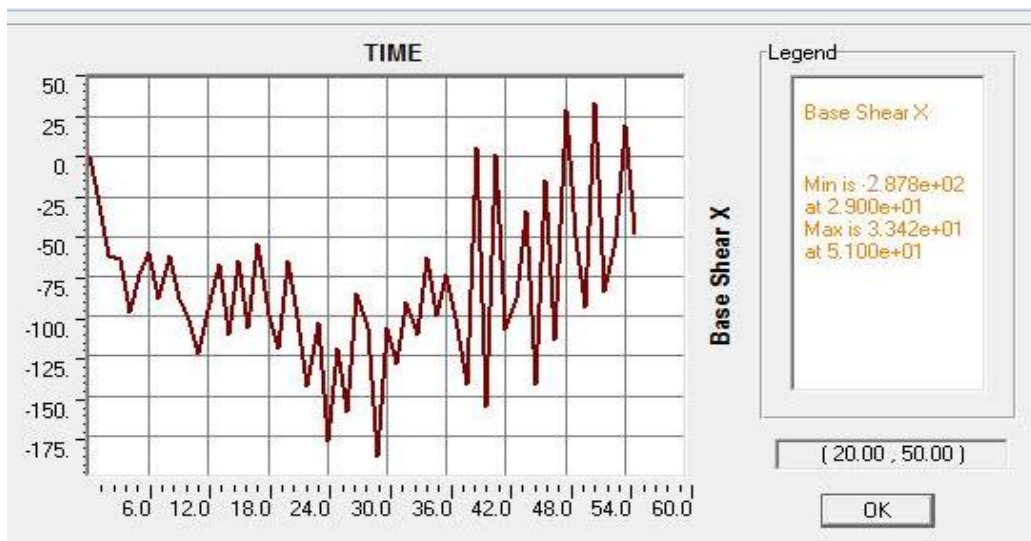


Figure (5-49): Base shear in x-direction due to moderate wind, Case F2.

5.5.5.2 Base Moment in Y-Direction for Case F0 and Case F2

The maximum base moment before and after fire under the effect of strong wind loads equal to 10170, 12302kN.m respectively, the difference between them is 20% while the maximum before and after fire due to moderate wind loads equal to 2865, 3097.7kN.m respectively.

The difference between them is 8% as shown in Table (5-26) and there is slightly difference between them same of effect of base shear as shown in Figs.(5-50) and (5-53).

Table (5-26): Base moment y-direction before and after fire.

Output Case	Base moment y Case F0	Base moment y Case F2
Text	kN.m	kN.m
Strong wind	10170	12302
Moderate wind	2865	3097

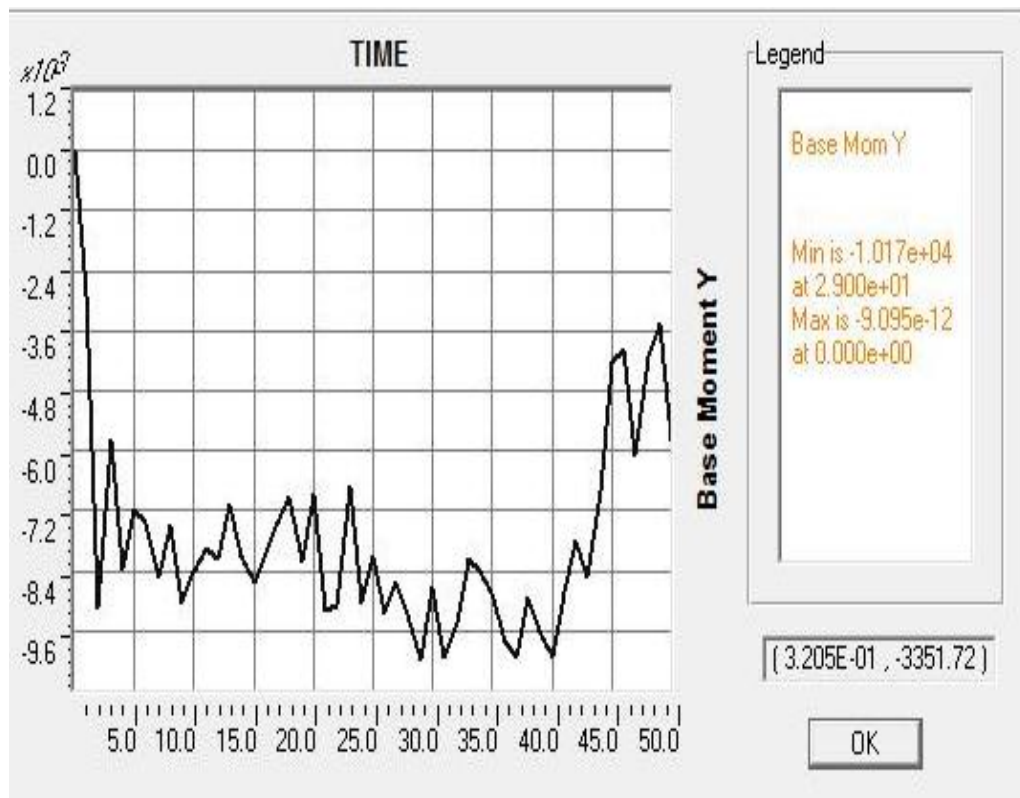


Figure (5-50): Base moment in y-direction due to strong wind, Case F0.

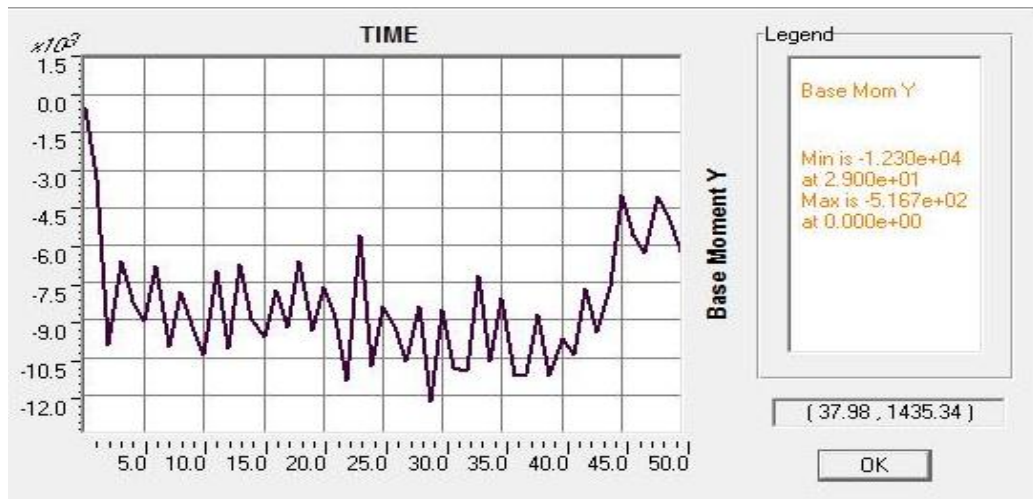


Figure (5-51): Base moment in y-direction due to strong wind, Case F2.

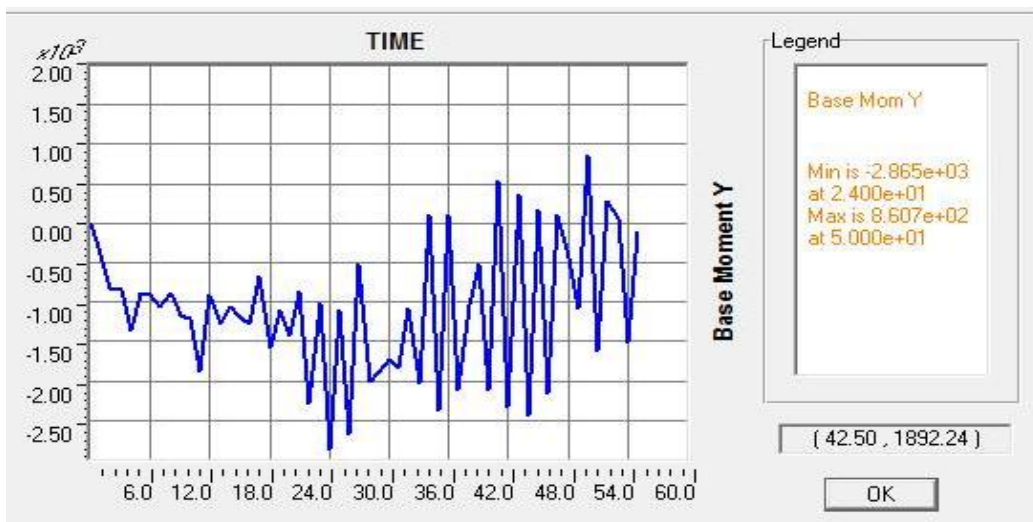


Figure (5-52): Base moment in y-direction due to moderate wind, Case F0.

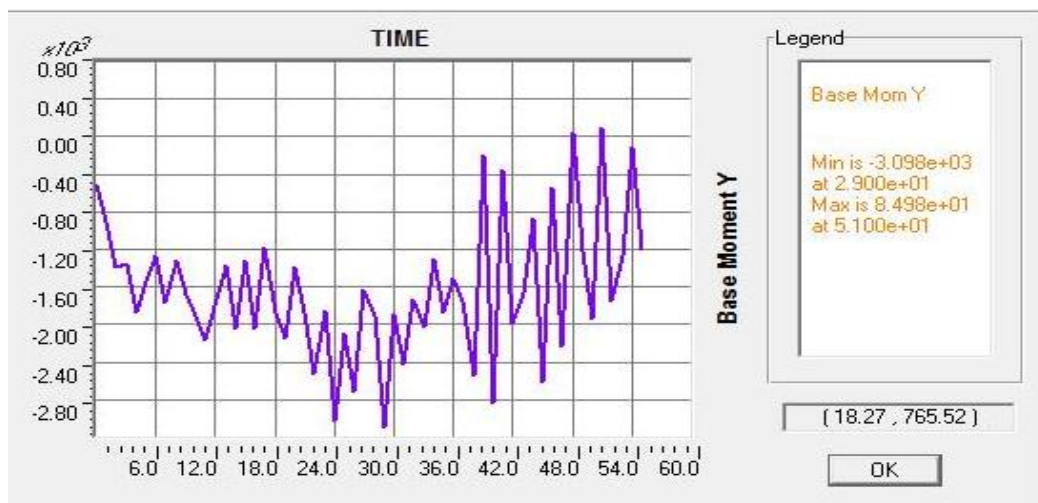


Figure (5-53): Base moment in y-direction due to moderate wind, Case F2.

5.5.5.3 Maximum Drift Ratio in X-Direction for Case F0 and Case F2

The drift ratio obtained from the numerical model for Case F0 compared with Case F2 results as shown in Fig. (5-54). The maximum drift ratio in last storey before and after fire under the effect of strong wind loads equal to 1.37%, 1.41% respectively, the difference between them is 3% ,

While the maximum drift ratio before and after fire due to moderate wind loads is equal to 0.41%, 0.42% respectively, the difference between them is 3%.

Although there is slightly difference in maximum drift ratio before and after fire in sixth storey for both strong and moderate wind, but there is clearly difference in the first and second storeys between cases Case F1 and Case F0 due to the fire damage in the first and second storeys which led to reduced 10% of F_y and E after fire.

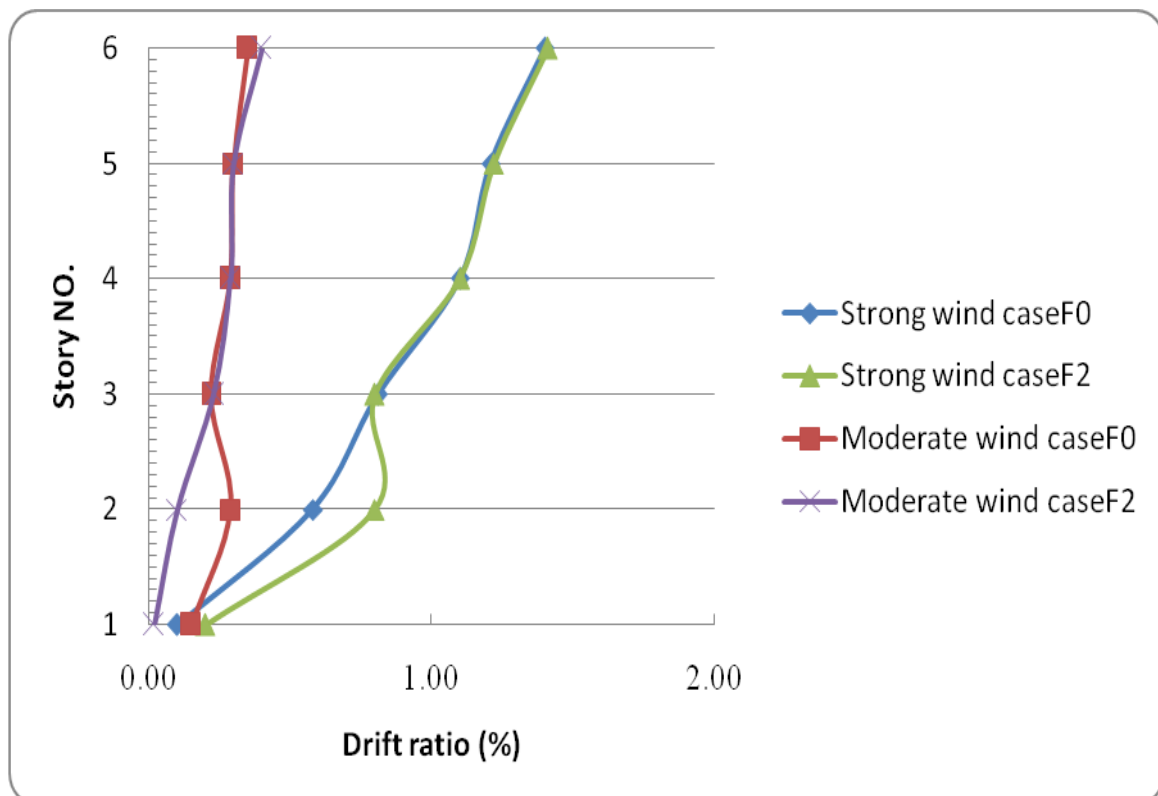


Figure (5-54): Drift ratio % vs. storey no. for Case F0 and Case F2.

5.5.5.4 Maximum Stresses (S_{11} , S_{12} and S_{13}) for Case F0 and Case F2

The maximum stresses results from this case are shown in Table (5-27). The maximum axial stress (S_{11}) on the fourth storey before and after fire under the effect of strong wind loads equal to 231164.2, 232200.5kN/m², respectively, the difference between them is 0.5% while the maximum before and after fire due to moderate wind loads for the same storey equal to 217760.7, 219929.5kN/m² respectively, the difference between them is 0.1%.

The maximum bending stress (S_{12}) on the last storey before fire and the first storey after fire under the effect of strong wind loads equal to 56883, 75417kN/m² respectively, the difference between them is 33% while the maximum before and after fire due to moderate wind loads for the same storey location is equal to 56880.63, 71571.35kN/m² respectively, the difference between them is 26%.

The maximum shear stress (S_{13}) on the last storey before fire and the first storey after fire under the effect of strong wind loads equal to 13515.38, 46929.45kN/m² respectively, the difference between them is 70% about strong wind after fire while the maximum before and after fire due to moderate wind loads for the same storey location is equal to 13464.37, 44787.12kN/m² respectively, the difference between them is 70%.

It's found that there is clearly difference between before and after fire for both strong and moderate wind in stresses. The axial stress (S_{11}) is little effected with more differences in the first and second storeys due to the fire deformations as shown in Figs. (5-55), due to depend on gravity loads .The bending and shear stresses (S_{12} and S_{13}) are considerable effected by fire damage under the action of strong and moderate wind loads it can be seen that the bending and shear stresses on the first and second and third storeys are

increased as compared with Case F0 due to reducing (F_y and E) 10% after cooling back. As shown in Figs. (5-65) and (5-66). The maximum (S_{11} , S_{12} and S_{13}) occurred in beam in Case F2.

When the stress becomes equal or less than to the yield stress of the material F_y , yielding of the material will occur (failure) (i.e. $S \leq F_y$). The maximum axial stresses (S_{11}) due to strong and moderate wind loads before fire are 231164, 217761 kN/m² respectively are less than yield stress (F_y) before fire so, Case F0 due to strong and moderate wind are safe. The maximum axial stresses (S_{11}) due to strong wind loads after fire is 232200 kN/m² more than yield stress (F_y) after fire, so Case F2 under effect of strong wind is not safe, but axial stress (S_{11}) due to moderate wind loads after fire is 219929 kN/m² less than yield stress (F_y) after fire, so the Case F2 under effect of moderate wind is safe.

Table (5-27): Stresses before and after fire.

Strong Wind CaseF0				Moderate Wind CaseF0		
Story NO.	S13	S12	S11	S13	S12	S11
Text	KN/m ²	KN/m ²	KN/m ²	KN/m ²	KN/m ²	KN/m ²
1	12629	53643	149880	12280	52133	139812
2	12894	54748	133057	12354	52522	122304
3	12914	54889	134090	12425	52822	128992
4	13245	55923	231164	13196	55916	217760
5	13118	55284	221303	13066	55279	211585
6	13515	56882	202866	13464	56880	197212
Strong Wind CaseF2				Moderate Wind CaseF2		
Story NO.	S13	S12	S11	S13	S12	S11
Text	KN/m ²	KN/m ²	KN/m ²	KN/m ²	KN/m ²	KN/m ²
1	46929	75416	194740	44787	71571	173335
2	41862	70159	154188	41864	69841	149989
3	40310	69478	142094	39073	67138	130266
4	13287	56212	232200	13249	56067	219929
5	13166	55543	217774	13127	55494	206875
6	13528	56969	200059	13503	56952	193986

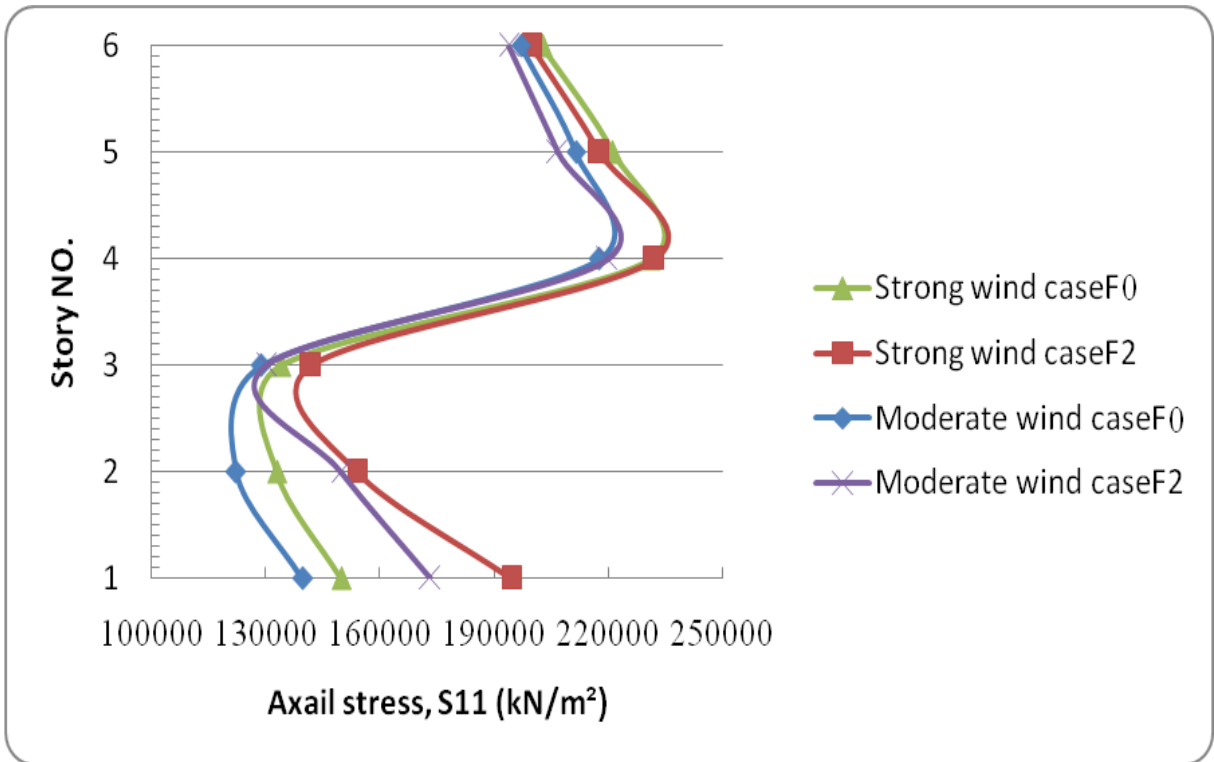


Figure (5-55): Axial stress vs. storey no. for Case F0 and Case F2.

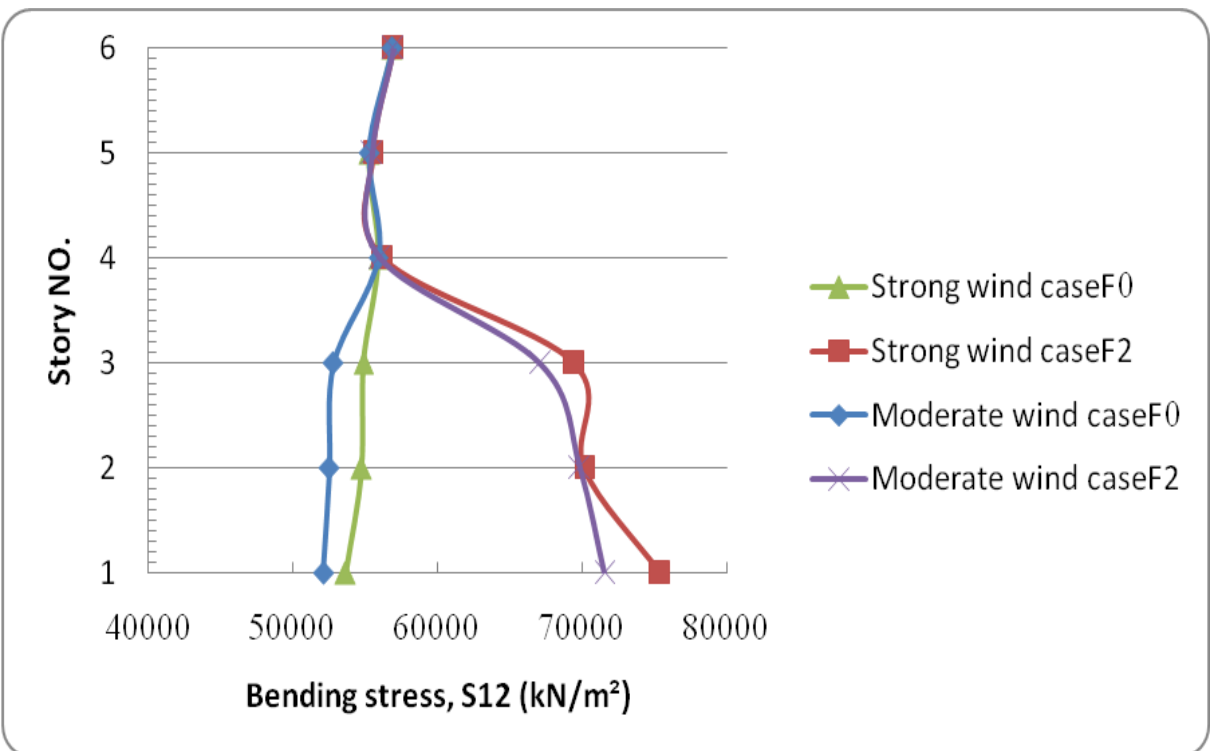


Figure (5-56): Bending stress vs. storey no. for Case F0 and Case F2.

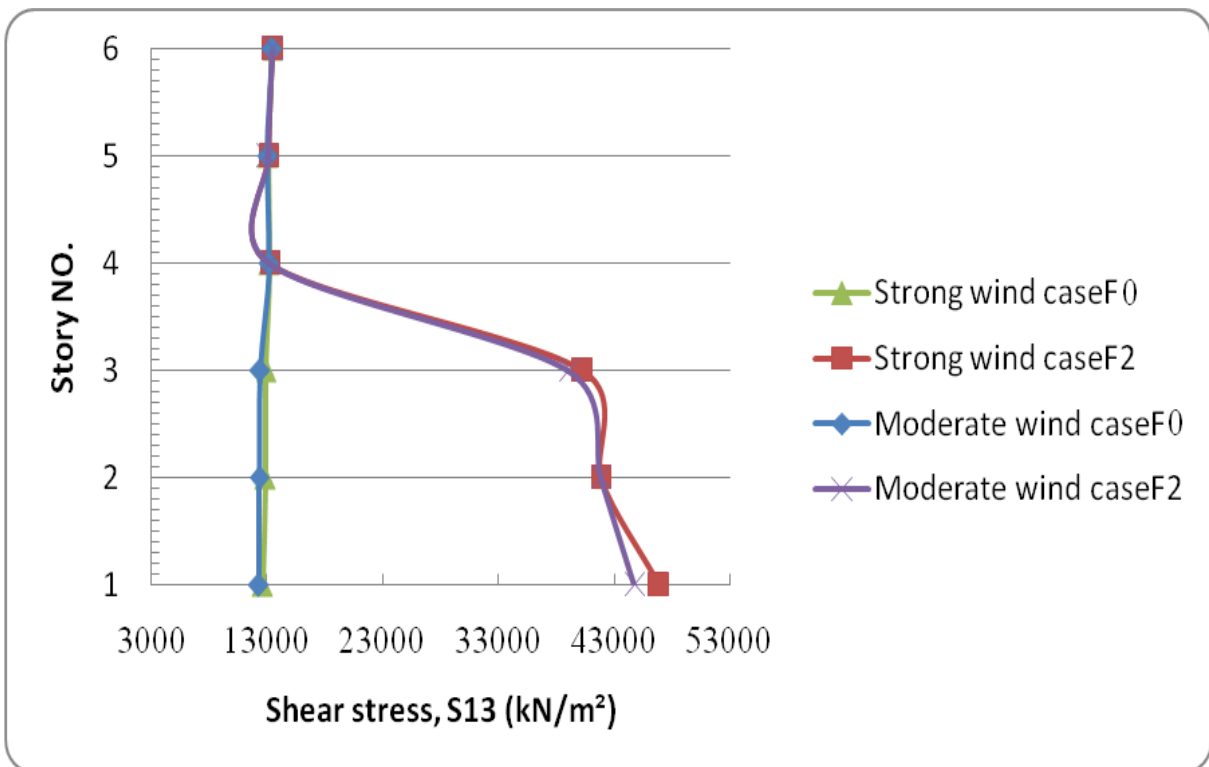


Figure (5-57): Shear stress vs. storey no. for Case F0 and Case F2.

5.5.5.5 Maximum Bending Moment, M_{33} for Case F0 and Case F2

From the Table (5-28), the maximum bending moment (M_{33}) in the third storey before fire and in the first after fire under the effect of strong wind loads equal to 136, 174.5kN.m, respectively.

the difference between them is 30% while the maximum before fire in the fifth storey and after fire in the first storey due to moderate wind loads equal to 125, 154kN.m, respectively.

The difference between them is 23%. All maximum bending moment occurred in beam. It found that the bending moment on the first and second and third storeys are increased as compared with Case F0 due to reducing (F_y and E) 10% after cooling back, as shown in Fig. (5-58).

Table (5-28): Bending moment before and after fire.

Case F0	Strong	Moderate
Story No.	M33	M33
Text	kN.m	kN.m
1	129	115
2	136	122
3	136	123
4	130	119
5	132	126
6	112	112
Case F2	Strong	Moderate
Story No.	M33	M33
Text	kN.m	kN.m
1	174	155
2	145	135
3	143	122
4	135	119
5	134	126
6	113	112

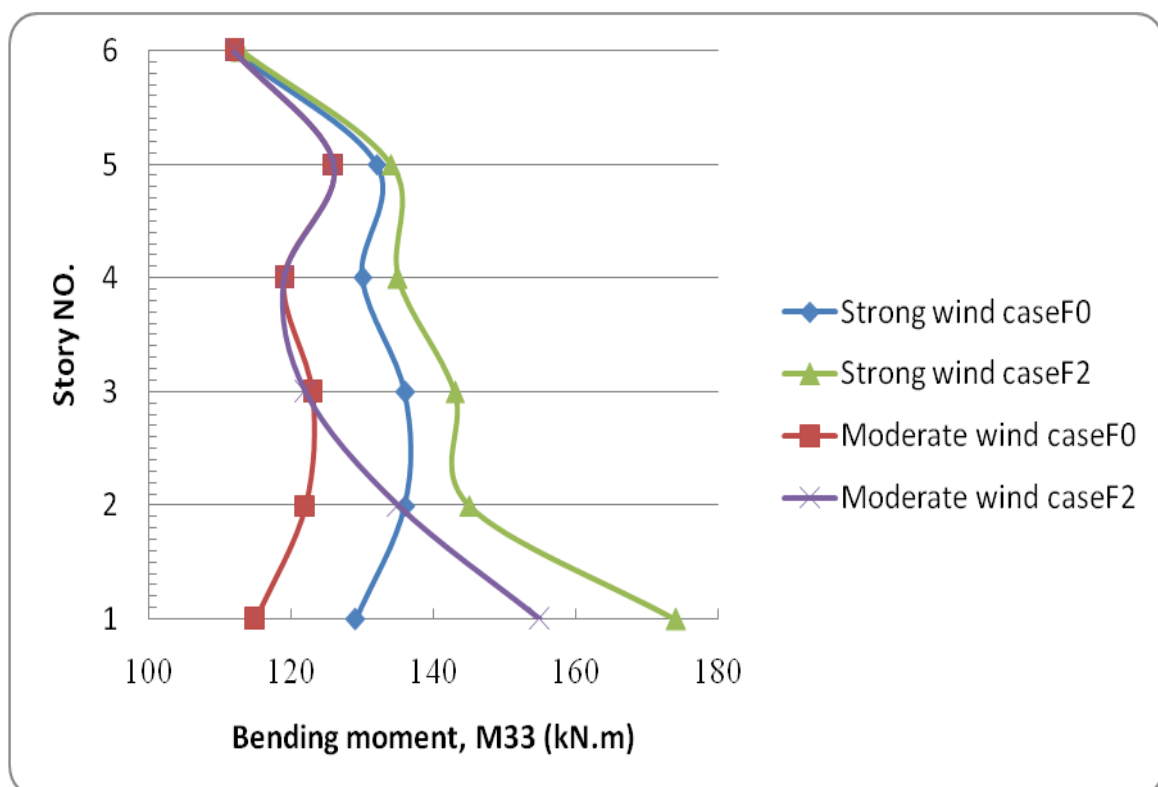


Figure (5-58): Bending moment vs. storey no. for Case F0 and Case F2.

5.5.5.6 Maximum Axial Force and Shear Force for Case F0 and Case F2

The maximum axial force and shear force results for this analysis shown in Table (5-29) and Table (5-30), the maximum axial force (compression) on the first storey before and after fire under the effect of strong wind loads equal to 3120, 3123kN respectively, the difference between is negligible while the maximum axial force before and after fire due to moderate wind loads in the same location equal to 3120, 3123kN respectively, as shown in Fig. (5-59), the difference between them is also negligible. The effect of the wind makes the axial force in the columns different where they are exposed to compression and others to tension as well as fire distortions, so there is a possibility formation the buckling in the columns.

The maximum shear force (V_2) on the last storey before and after fire under the effect of strong wind loads equal to 144, 144kN respectively, the difference between them is negligible .While the maximum before and after fire due to moderate wind loads in same location is equal to 144, 144kN respectively, the difference between them is also negligible. Although there is negligible difference in maximum values of shear forces at fourth ,fifth and sixth storeys , but there is large difference at first ,second and third storeys due to reduced 10% of yield stress after fire as shown in Fig. (5-60).

Table (5-29): Axial force and shear force before fire.

Case F0	Strong Wind Case F0		Moderate Wind Case F0	
Story No.	V2	P	V2	P
Text	kN	kN	kN	kN
1	138	3120	132	3120
2	139	2602	133	2602
3	139	2091	134	2091
4	142	1575	142	1575
5	140	1051	140	1051
6	144	528	144	528

Table (5-30): Axial force and shear force after fire.

Case F2	Strong Wind Case F2		Moderate Wind Case F2	
Story No.	V2	P	V2	P
Text	kN	kN	kN	kN
1	141	3123	135	3123
2	143	2603	136	2603
3	142	2092	137	202
4	142	1576	143	1576
5	141	1053	141	1053
6	145	529	145	529

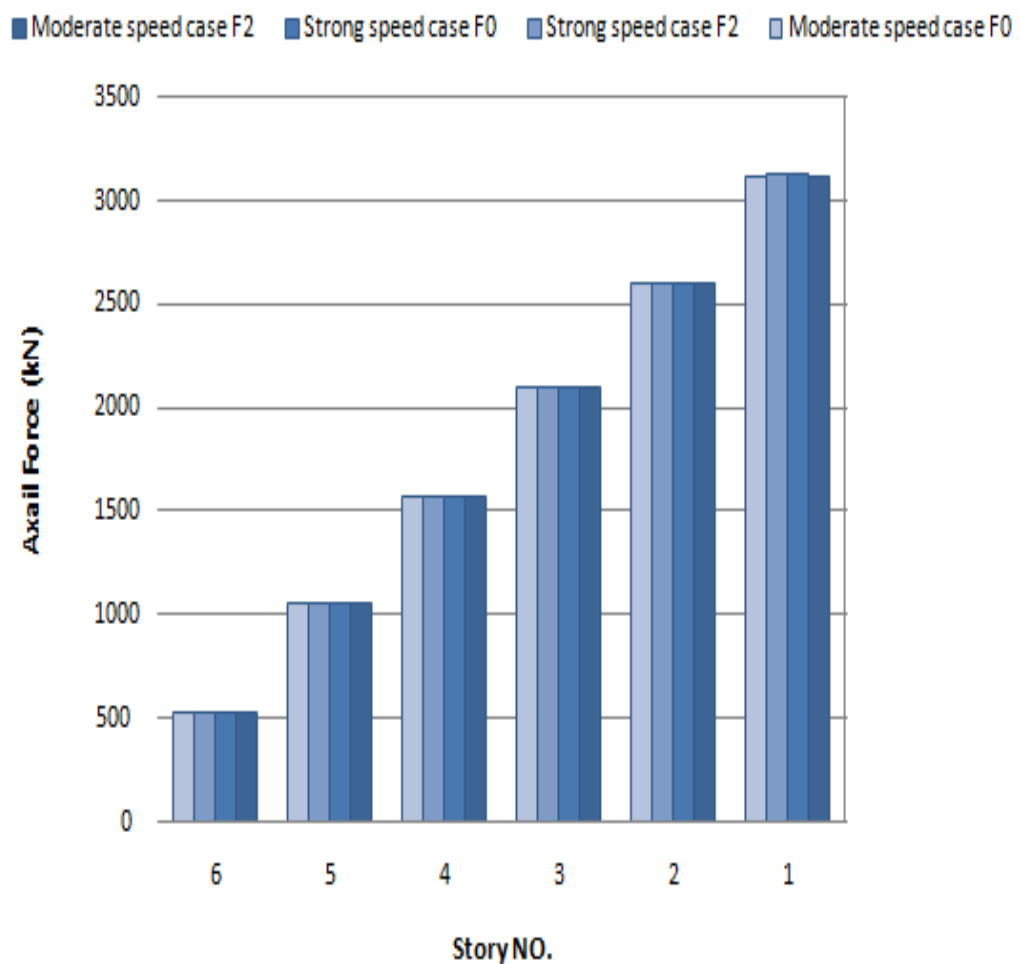


Figure (5-59): Axial force vs. storey no. for Case F0 and Case F2.

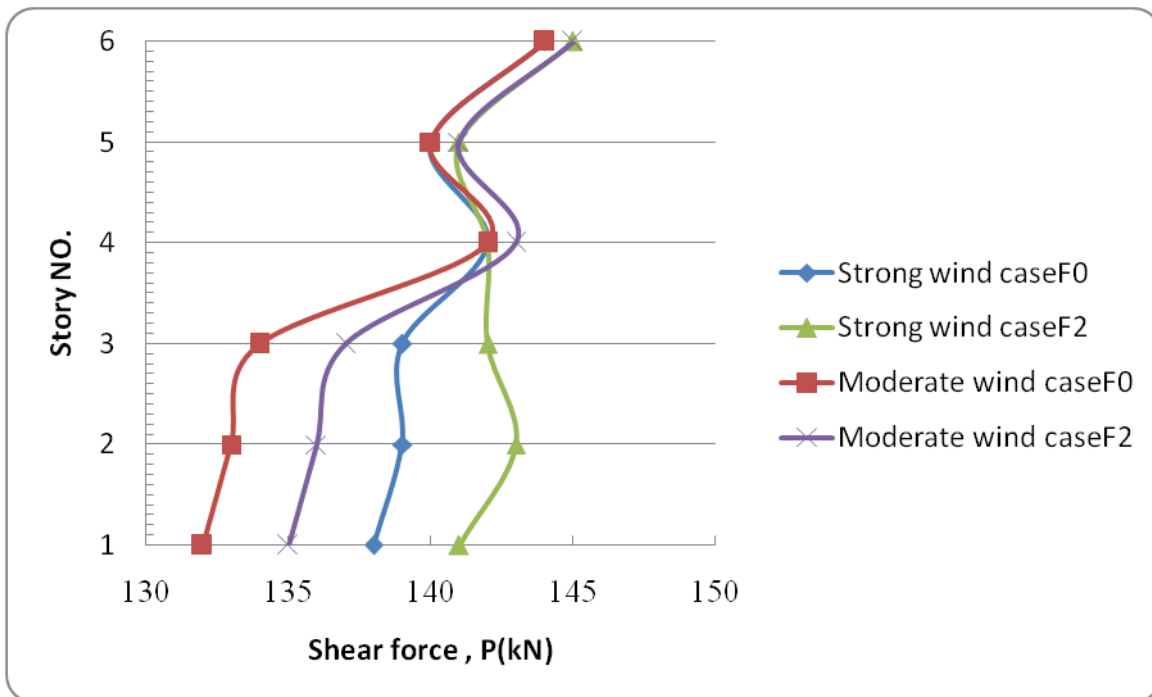


Figure (5-60): Shear force vs. storey no. for Case F0 and Case F2.

5.5.5.7 Maximum Displacements in X-Direction for Case F0 and Case F2

The maximum displacement on each level is listed in Table (5-30). The maximum displacement in last storey for displacement before and after fire under the effect of strong wind loads equal to 19.5, 20mm respectively, the difference between them is 8% while the maximum displacement before and after fire due to moderate wind loads equal to 5.6, 5.8mm respectively, the difference between them is 4%.

It's found that is slightly difference in maximum displacement due to the maximum occurred in last storey that is not included fire but there is clearly difference in the first and second storeys are increased as compared with Case F0 due to the fire which making to reduced 10% of F_y and E after fire as shown in Fig. (5-61). According to BS 8110-Part 2: 1985 the maximum allowable deflection is calculated as $h/500$, therefore, maximum allowable

displacement value for building height of 19m is 38mm. The maximum value of displacement in serviceability limit condition obtained for dynamic strong wind loads are less than allowable (38 mm) for criteria failure, so the building is safe in all cases.

Table (5-31): Maximum displacement before and after fire.

Case F0	Strong	Moderate
Story No.	U _x	U _x
Text	mm	mm
1	3.31	0.95
2	6.78	1.69
3	10.57	2.68
4	14.37	3.72
5	17.25	4.59
6	19.50	5.67
Case F2	Strong	Moderate
Story No.	U _x	U _x
Text	mm	mm
1	8.56	5.92
2	10.83	4.80
3	11.75	3.20
4	15.10	3.80
5	17.71	4.70
6	20.05	5.80

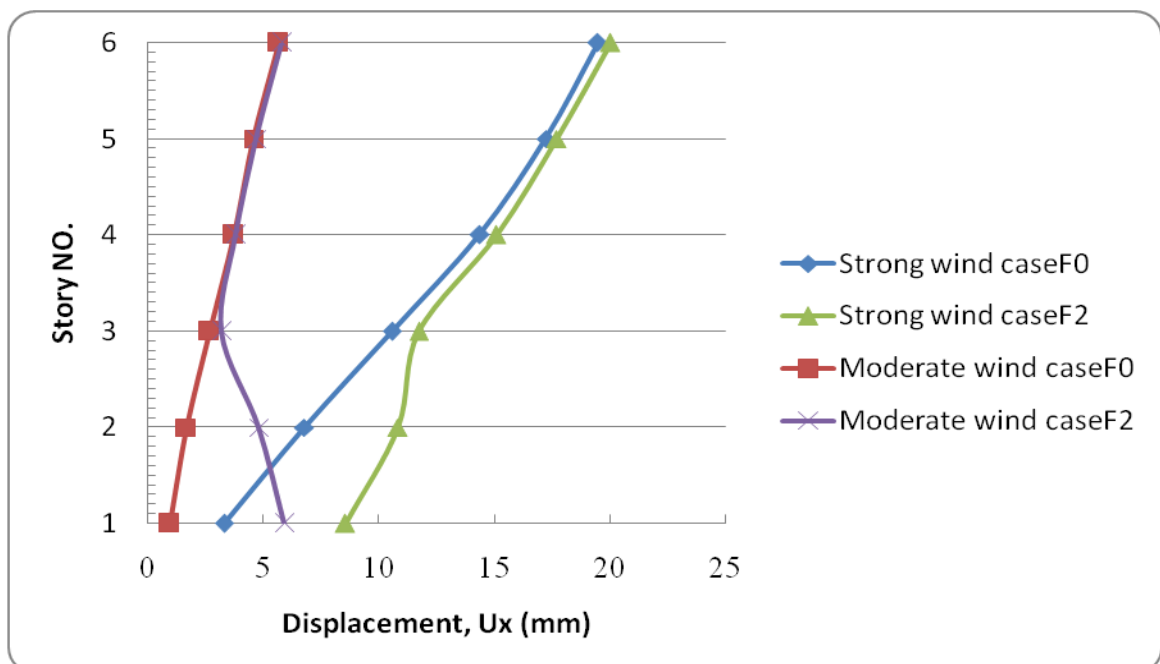


Figure (5-61): Maximum displacements vs. storey no. for Case F0 and Case F2.

5.5.6 Case6 Post-Fire Analysis Fully Deformations (Δ) versus Quarter of Deformities (0.25 Δ), Case F1

In this case, the same fire deformation configurations are used but with quantities divided by four (0.25 Δ), or quarter values which reflected that the building subjected to lower temperature or small fire duration considered as shown in Table (5.31). Thus quarter values of deformations of Case F1 are compared with before fire cases (Case F0) under the effect of dynamic strong wind in which nonlinear analysis included P-Delta effect is considered.

Table (5-32): Case 6 deformations for Case F1 configuration.

Member Types	Quantity	Deformation Types	Value
Column	Fully (Δ)	Displacement	L/60
Column	$\Delta/4$	Displacement	L/240
Beam	Fully (Δ)	Deflection	L/240
Beam	$\Delta/4$	Deflection	L/160

5.5.6.1 Base Shear in X-Direction for Case 6

From Table (5-32) it can clearly be seen that the maximum base shear of Case F0 under the effect of strong wind equal to 763kN while the maximum due to the same wind for Case 0.25 Δ and Case F1 are equal to 784.5, 868.7kN respectively, the difference between Case F0 and Case 0.25 Δ are 3%, the difference between Case F1 and Case 0.25 Δ are 10%. It's found that slightly difference for Case 0.25 Δ as compared with Case F0 while clear difference between fully and quarter of deformations, it's can be said clearly there is slightly difference between before fire and building's deformations of 0.25 Δ .

Table (5-33): Maximum base shear in x-direction.

Case Type	Case 0.25 F1	Case F1	Case F0
Output Case	Base shear x	Base shear x	Base shear x
Text	kN	kN	kN
Strong wind	784	869	763

5.5.6.2 Base Moment in Y-Direction for Case 6

The maximum base moment of Case F0 under the effect of strong wind is equal to 10170kN.m while the maximum due to the same wind for case 0.25 Δ and Case F1 are equal to 10665, 12157.7kN.m respectively as shown in Table (5-33), the difference between Case F0 and case 0.25 Δ are 5%, the difference between Case F1 and case 0.25 Δ are 12%.

It's found that slightly difference for case 0.25 Δ as compared with Case F0 while clear difference between fully and quarter of deformations, it's can said be clearly there is also similarity between before fire and after fire for building's deformations equal to quarter values.

Table (5-34): Maximum base Moment in Y-Direction.

Case Type	Case 0.25 F1	Case F1	Case F0
Output Case	Base moment y	Base moment y	Base moment y
Text	kN.m	kN.m	kN.m
Strong wind	10665	12158	10170

5.5.6.3 Maximum Drift Ratio in X-Direction for Case 6

The maximum drift ratio of Case F0 due to strong wind is equal to 1.37% while the maximum under the effect of the same wind for Case 0.25 Δ and Case F1 are equal to 1.54, 1.75% respectively, the difference between Case F0 and Case 0.25 Δ are 12%.

The difference between Case F1 and Case 0.25 Δ are 12%. It's found that the maximum of drift ratio for Case 0.25 Δ is lies between before and after fire, so clearly difference for case 0.25 Δ as compared with Case F0 due to fire effect. The results in Fig. (5-62).

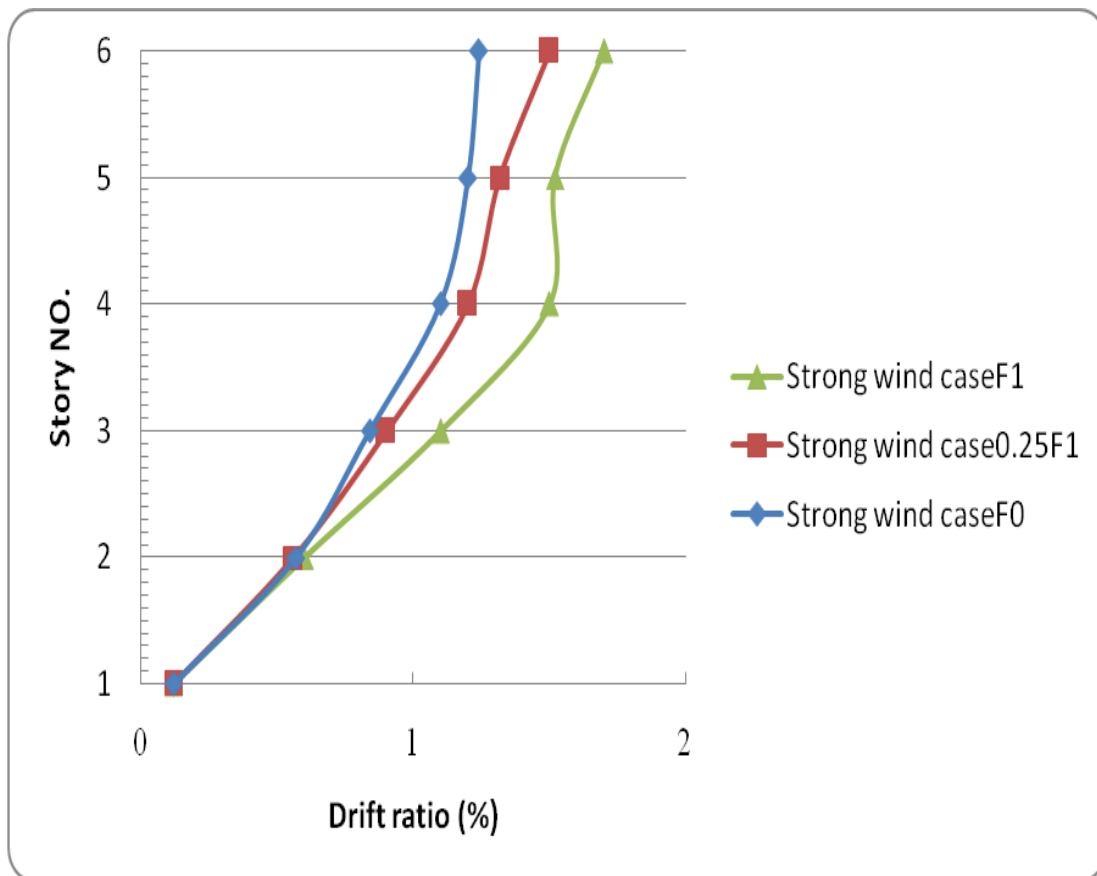


Figure (5-62): Maximum drift ratio due to strong wind.

5.5.6.4 Maximum Stresses (S_{11} , S_{12} and S_{13}) for Case 6

The stresses results from Case 6 shown in Table (5-34). The maximum axial stress (S_{11}) on column of the fourth storey of Case F0 due to strong wind equal to 231164 kN/m² while the same location for Case 0.25 Δ and Case F1 are equal to 230685, 234199kN/m² respectively, the difference between Case F0 and Case 0.25 Δ are 0.2%, the difference between Case F1 and Case 0.25 Δ are 1.5%. It's found that slightly difference between them due to (S_{11}) depend on gravity load. As shown in Fig. (5-63).

The maximum bending stress (S_{12}) on beam of the last storey for Case F0 due to strong wind is equal to 56883 kN/m² while for Case 0.25 Δ on the last

storey and Case F1 on the fourth storey are equal to 56946, 66420kN/m² respectively, the difference between Case F0 and Case 0.25Δ are 0.1% while the between Case F1 and Case 0.5Δ are 14%. It's clearly that maximum bending stresses are slightly difference for the three cases (Case F0 ,Case F1 and Case0.25Δ), but Case F1 considerably greater than Case F0 and Case 0.25Δ in fourth and fifth storeys due to fire deformation in these storeys, but Case F0 and Case 0.25Δ are closely for all storeys shown in Fig. (5-64).

The maximum shear stress (S₁₃) on beam of the last storey for Case F0 due to strong wind equal to 13515kN/m² while for Case 0.25Δ on the last storey and Case F1 on the fourth storey are equal to 13523, 37293kN/m² respectively for same conditions, the difference between Case F0 and Case 0.25Δ are negligible.

The difference between Case F1 and Case 0.25Δ are 64% similar to bending stresses there is considerable differences between Case F1 compared to Case F0 and Case 0.25Δ in fourth, fifth and sixth storeys due to fire deformations in three storeys, which cases Case F0 and Case 0.25Δ are closed for all storeys. As shown in Fig. (5-65).

It's found that slightly difference in all stresses for Case 0.25Δ as compared with Case F0 while clear difference between fully and quarter of deformations, it's can said be clearly there is also similarity between before fire and after fire for building's deformations equal to quarter values.

The maximum stresses is axial stress (S₁₁) due to strong wind loads for Case 0.25Δ and Case F1 are equal to 230685 and 234199kN/m² respectively are more than yield stress (F_y) after fire, So these cases are not safe. While Case F0 the maximum axial stress is 231164 kN/m² is less than yield stress (F_y) before fire, so this case is safe.

Table (5-35): Maximum stresses under strong wind load.

Strong	CaseF1			Case 0.25F1			CaseF0		
Story NO.	S13	S12	S11	S13	S12	S11	S13	S12	S11
Text	KN/m ²	KN/m ²	KN/m ²	KN/m ²	KN/m ²	KN/m ²	KN/m ²	KN/m ²	KN/m ²
1	13015	55290	144175	12751	54169	152855	12629	53643	149880
2	13393	56880	134762	13074	55558	138174	12894	54748	133057
3	13517	57381	137549	13174	56002	140691	12914	54889	134090
4	37292	66420	234198	13300	56227	230684	13245	55923	231164
5	31262	61768	204418	13143	55415	217802	13118	55283	221303
6	26780	58817	187458	13523	56946	200175	13515	56882	202866

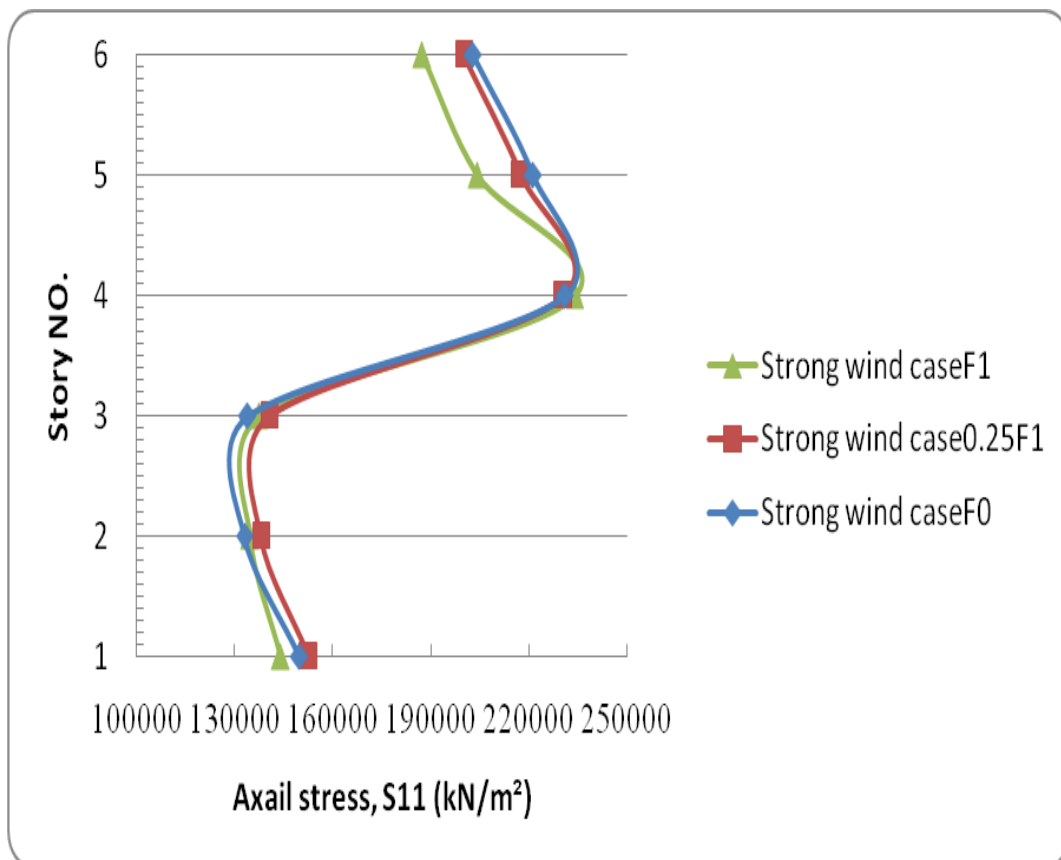


Figure (5-63): Maximum axial stress S11 under strong dynamic wind load.

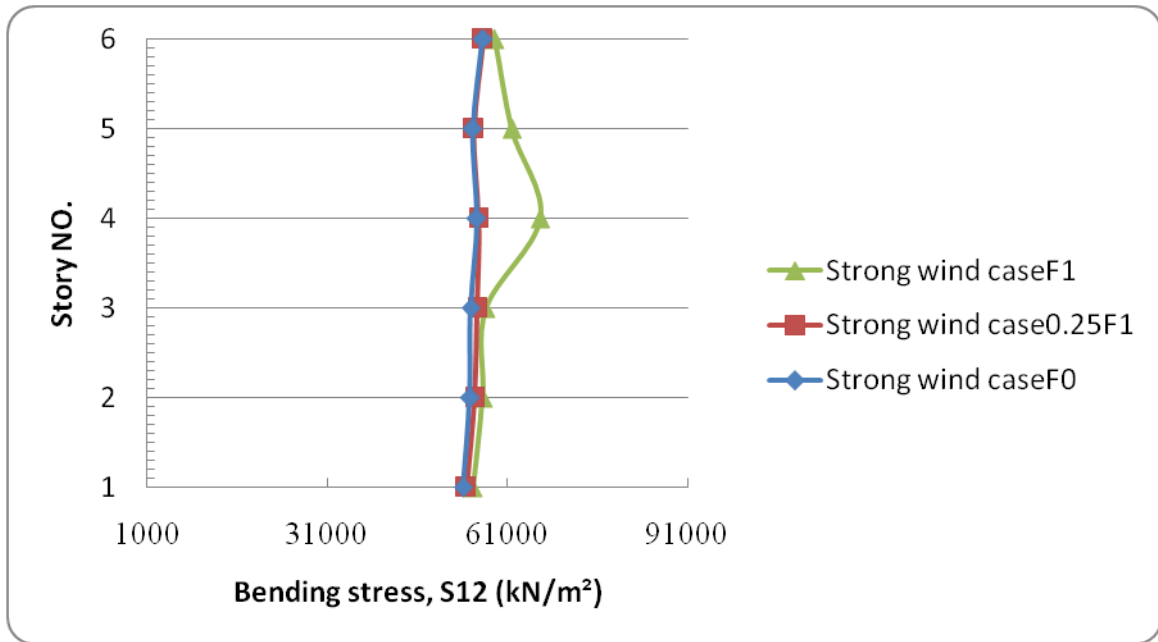


Figure (5-64): Maximum bending stress S12 under strong dynamic wind load.

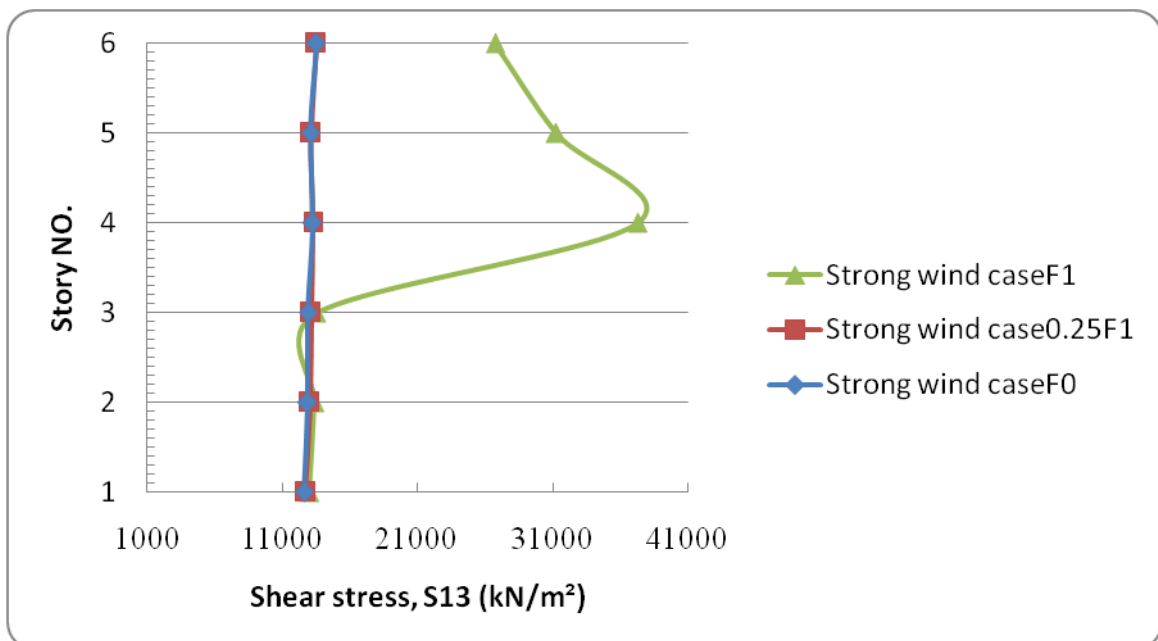


Figure (5-65): Maximum shear stress S13 under strong dynamic wind load.

5.5.6.5 Maximum Bending Moment, M33 for Case 6

From Table (5-35) it can clearly be seen that the maximum bending moment on beam of the third storey for Case F0 under the effect of strong wind

equal to 136.2kN.m while in same storey for Case 0.25 Δ and Case F1 are equal to 143,152kN.m on beam respectively, the difference between Case F0 and Case 0.25 Δ are 5%, the difference between Case F1 and Case 0.25 Δ are 6%, as shown in Fig. (5-66). It's found that the maximum bending moment for Case 0.25 Δ is lies between before and after fire, so clearly difference for Case 0.25 Δ as compared with Case F0 due to fire effect.

Table (5-36): Bending moment due to strong wind load.

Strong	Case F1	Case 0.25 F1	Case F0
Story NO.	M33	M33	M33
Text	kN.m	kN.m	kN.m
1	139	132	129
2	150	141	136
3	152	143	136
4	144	137	130
5	139	135	132
6	113	112	112

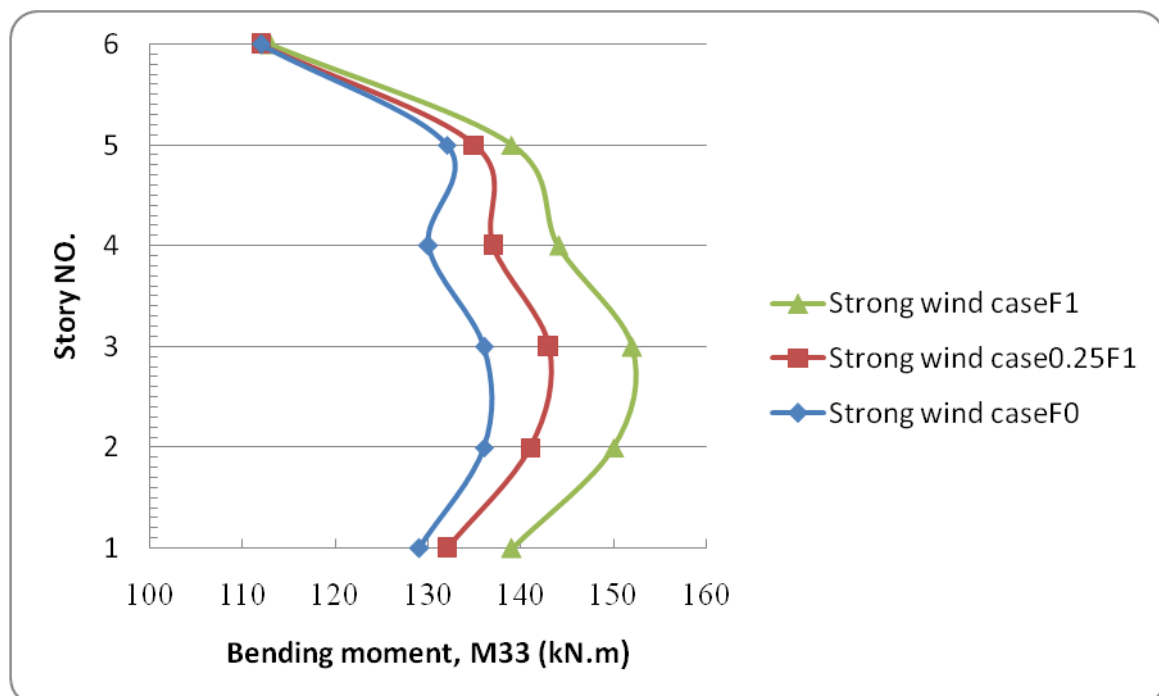


Figure (5-66): Maximum bending moment due to strong wind load.

5.5.6.6 Maximum Axial Force and Shear Force for Case 6

The results of axial and shear forces for Case 6 shown in Table (5-36). The maximum axial force (compression) on column of the first storey of Case F0 due to strong wind equal to 3120kN while for the same conditions for Case 0.25 Δ and Case F1 are equal to 3127, 3130kN respectively.

The difference between them approximately negligible. It's found that no difference between them due to the axial forces depending on gravity load on column , as shown in Fig.(5-67).

The maximum shear force on beam of the last storey for Case F0 due to strong wind is equal to 144.4kN/m² while for same conditions for Case 0.25 Δ and Case F1 are equal to 144.6, 144.9kN respectively

The difference between them are negligible, but there is clearly difference at third and fourth storeys due reduced 10% of yield stress after fire as shown in Fig. (5-68).

Table (5-37): Axial and shear force due to strong wind load.

Strong	Case F1		Case 0.25 F1		Case F0	
	V2	P	V2	P	V2	P
Story NO.	kN	kN	kN	kN	kN	kN
1	137	3131	137	3127	136	3120
2	140	2618	140	2609	139	2602
3	141	2101	140	2098	139	2091
4	144	1582	143	1579	142	1575
5	143	1053	141	1052	140	1051
6	145	528	145	528	144	528

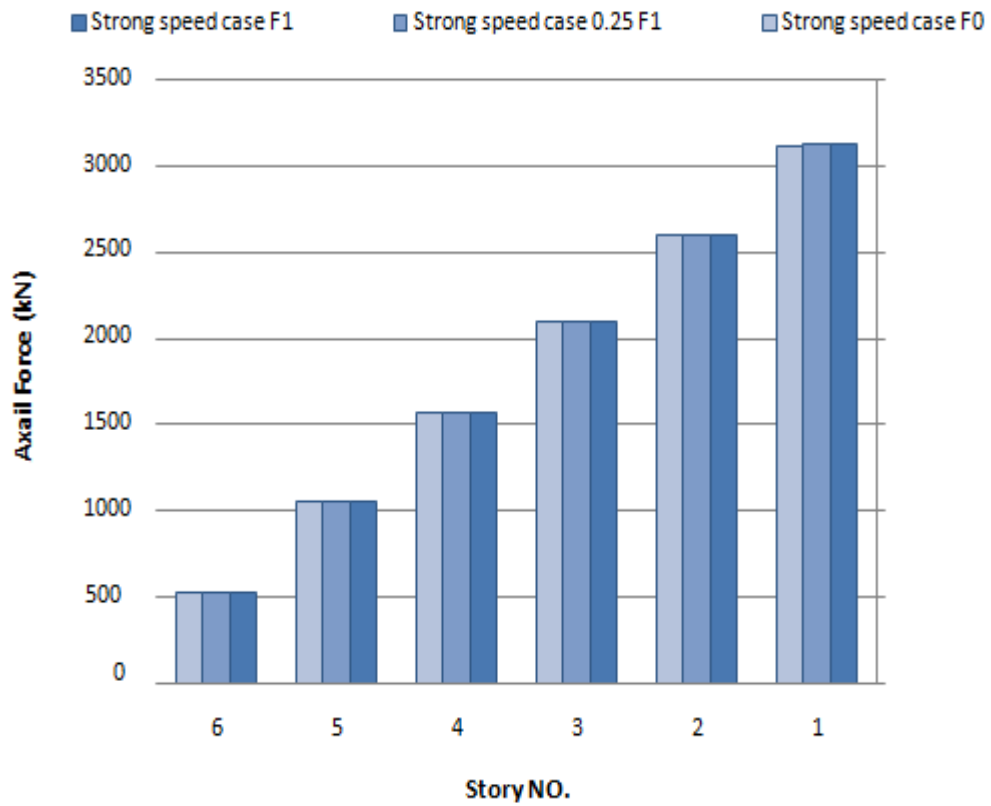


Figure (5-67): Maximum axial forces due to strong wind load.

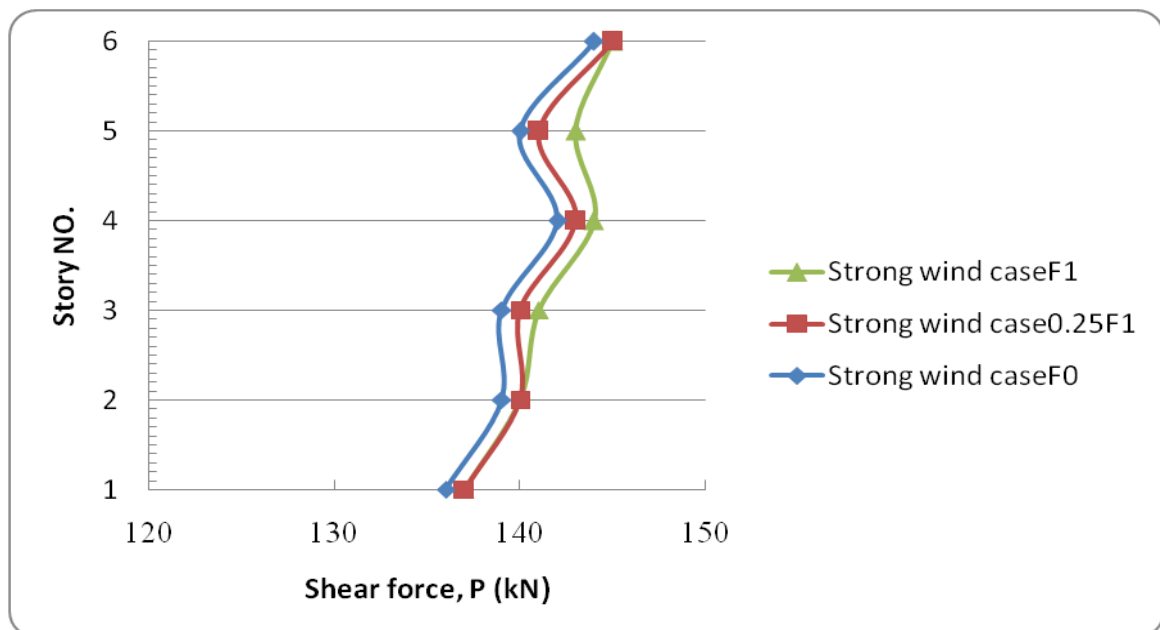


Figure (5-68): Maximum shear forces due to strong wind load.

5.5.6.7 Maximum Displacements in X-Direction for Case 6

The maximum displacement of Case F0 due to strong wind is equal to 19.5mm while for Case 0.25 Δ and Case F1 are equal to 21.6, 25mm respectively as shown in Table (5-37), the difference between Case F0 and Case 0.25 Δ is 12% but, the difference between Case F1 and Case 0.25 Δ is 12%. It's found that the maximum of displacement for Case 0.25 Δ is lies between that of before and after fire, so clearly difference for Case 0.25 Δ as compared with Case F0 due to fire effect as shown in Fig. (5-69).

According to BS 8110-Part 2: 1985 the maximum allowable deflection is calculated as $h/500$, therefore, maximum allowable displacement value for building height of 19m is 38mm. The maximum value of displacement in serviceability limit condition obtained for dynamic strong wind loads are less than allowable (38 mm) for criteria failure, so the building in safe in all cases.

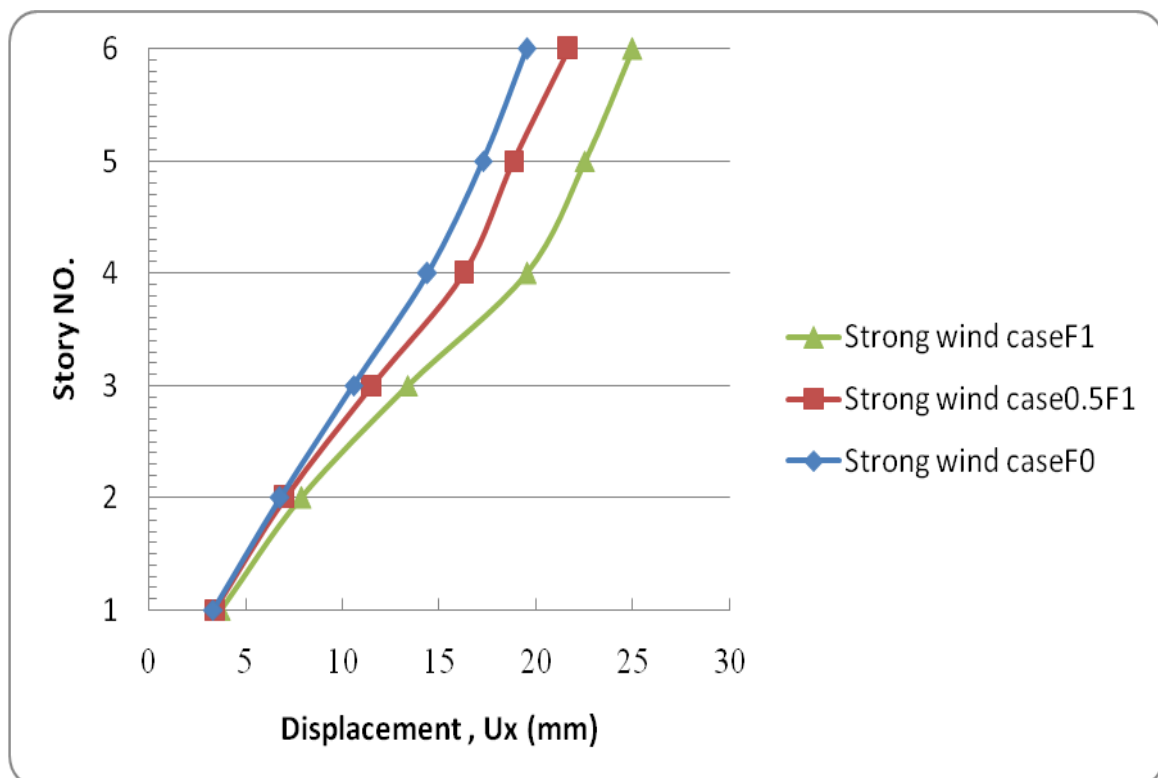


Figure (5-69): Maximum displacements due to strong wind load.

Table (5-38): Maximum displacement due to strong wind load.

Strong	Case F1	Case 0.25 F1	Case F0
Story NO.	U _x	U _x	U _x
Text	mm	mm	mm
1	3.73	3.44	3.31
2	7.87	7.04	6.78
3	13.38	11.53	10.57
4	19.50	16.27	14.37
5	22.51	18.83	17.25
6	24.96	21.67	19.50

5.5.7 Case7 Post-Fire Analysis Fully Deformations (Δ) versus Half of Deformities (0.5 Δ), Case F1

In this case, the same fire deformation configurations are used but with quantities divided by two (0.5 Δ), or half values which reflected that the building subjected to lower temperature or small fire duration then considered (see Table 5-38). Thus quarter values of deformations of Case F1 are compared with before fire cases (Case F0) under the effect of dynamic strong wind in which nonlinear analysis included P-Delta effect is considered.

Table (5-39): Case 7 deformations for Case F1 configuration.

Member Types	Quantity	Deformation Types	Value
Column	Fully (Δ)	Displacement	L/60
Column	$\Delta/2$	Displacement	L/120
Beam	Fully (Δ)	Deflection	L/240
Beam	$\Delta/2$	Deflection	L/80

5.5.7.1 Base Shear in X-Direction for Case 7

From Table (5-39) it can clearly be seen that the maximum base shear of Case F0 under the effect of strong wind equal to 763kN while the maximum due to the same wind for Case 0.5 Δ and Case F1 are equal to 789.2, 868.7kN respectively, the difference between Case F0 and Case 0.5 Δ are 4%, the difference between Case F1 and Case 0.5 Δ are 9%.

It's found that slightly difference for Case 0.5 Δ as compared with Case F0 while clear difference between fully and half of deformations, it's can be said clearly there is slightly difference between before fire and building's deformations of 0.5 Δ .

Table (5-40): Maximum base shear in x-direction.

Case Type	Case 0.5 F1	Case F1	Case F0
Output Case	Base shear x	Base shear x	Base shear x
Text	kN	kN	kN
Strong wind	789	869	763

5.5.7.2 Base Moment in Y-Direction for Case 7

The maximum base moment of Case F0 under the effect of strong wind is equal to 10170kN.m while the maximum due to the same wind for case 0.5 Δ and Case F1 are equal to 10816, 12157.7kN.m respectively as shown in Table (5-33), the difference between Case F0 and case 0.5 Δ are 6%.

The difference between Case F1 and case 0.5 Δ are 11%. It's found that slightly difference for case 0.5 Δ as compared with Case F0 while clear difference between fully and half of deformations, it's can said be clearly there is also similarity between before fire and after fire for building's deformations equal to half values.

Table (5-41): Maximum base Moment Y-Direction.

Case Type	Case 0.5 F1	Case F1	Case F0
Output Case	Base moment y	Base moment y	Base moment y
Text	kN.m	kN.m	kN.m
Strong wind	10816	12158	10170

5.5.7.3 Maximum Drift Ratio in X-Direction for Case 7

The maximum drift ratio of Case F0 due to strong wind is equal to 1.37% while the maximum under the effect of the same wind for Case 0.5 Δ and Case F1 are equal to 1.6, 1.75% respectively, the difference between Case F0 and Case 0.5 Δ are 17%, the difference between Case F1 and Case 0.5 Δ are 9%. It's found that the maximum of drift ratio for Case 0.5 Δ is lies between before and after fire, so clearly difference for case 0.5 Δ as compared with Case F0 due to fire effect. The results in Fig. (5-70).

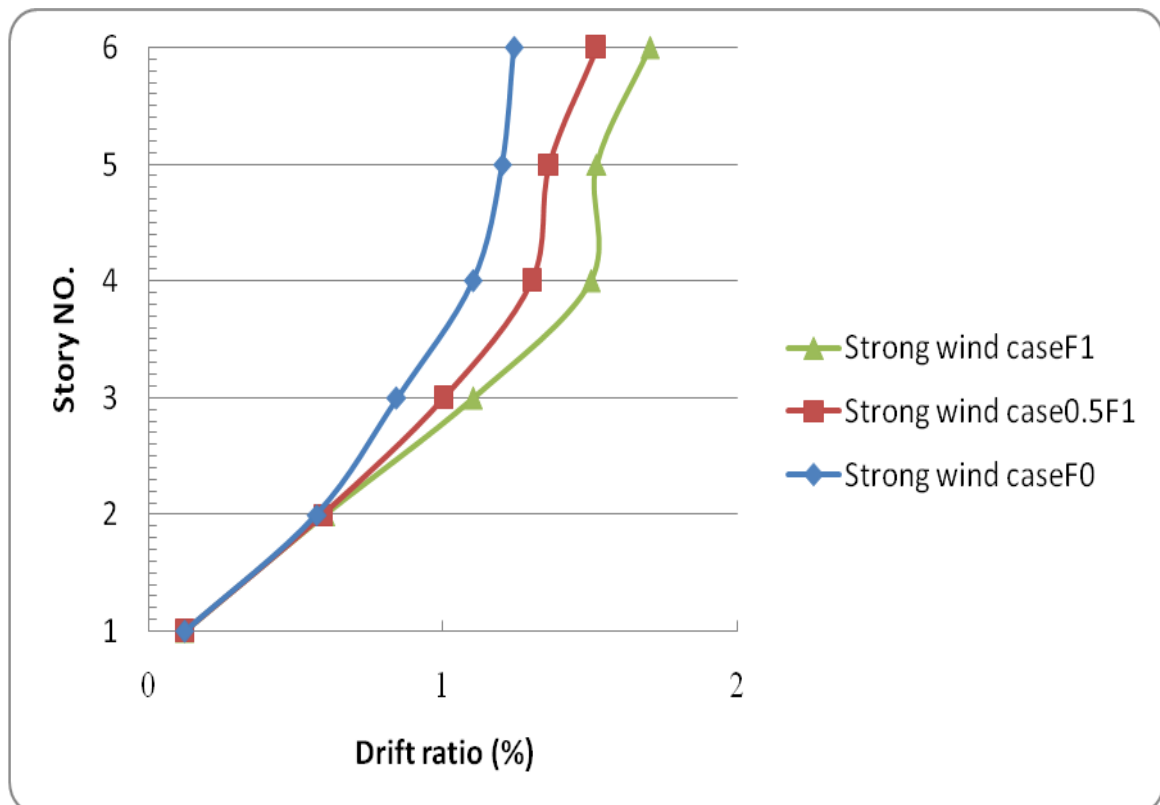


Figure (5-70): Maximum drift ratio due to strong wind.

5.5.7.4 Maximum Stresses (S_{11} , S_{12} and S_{13}) for Case 7

The stresses results from Case 6 shown in Table (5-41). The maximum axial stress (S_{11}) on column of the fourth storey of Case F0 due to strong wind equal to 231164 kN/m² while the same location for Case 0.5 Δ and Case F1 are equal to 232582, 234199kN/m² respectively, the difference between Case F0 and Case 0.5 Δ are 0.6%, the difference between Case F1 and Case 0.5 Δ are 0.7%. It's found that slightly difference between them as shown in Fig. (5-71).

The maximum bending stress (S_{12}) on beam of the last storey for Case F0 due to strong wind is equal to 56883 kN/m² while for Case 0.5 Δ on the last storey and Case F1 on the fourth storey are equal to 56956, 66420kN/m² respectively, the difference between Case F0 and Case 0.5 Δ are 0.1% while the between Case F1 and Case 0.5 Δ are 14%.

It's clearly that maximum bending stresses are slightly difference for the three cases (Case F0 ,Case F1 and Case0.25 Δ), but Case F1 considerably greater than Case F0 and Case 0.5 Δ in fourth and fifth storeys due to fire deformation in these storeys, but Case F0 and Case 0.5 Δ are closely for all storeys shown in Fig. (5-72).

The maximum shear stress (S_{13}) on beam of the last storey for Case F0 due to strong wind equal to 13515kN/m² while for Case 0.5 Δ on the last storey and Case F1 on the fourth storey are equal to 13540, 37293kN/m² respectively for same conditions, the difference between Case F0 and Case 0.5 Δ are negligible, but the difference between Case F1 and Case 0.5 Δ are 63% similar to bending stresses there is considerable differences between Case F1 compared to Case F0 and Case 0.5 Δ in fourth, fifth and sixth storeys due to fire deformations in three storeys, which cases Case F0 and Case 0.5 Δ are closed for all storeys as shown in Fig. (5-73).

It's found that slightly difference in all stresses for Case 0.5Δ as compared with Case F0 while clear difference between fully and half of deformations, it's can said be clearly there is also similarity between before fire and after fire for building's deformations equal to half values. The maximum stresses is axial stress (S11) due to strong wind loads for Case 0.5Δ and Case F1 are equal to 232582 and 234199kN/m² respectively are more than yield stress (Fy) after fire, So these cases are not safe. While Case F0 the maximum axial stress is 231164 kN/m² is less than yield stress (Fy) before fire, so this case is safe.

Table (5-42): Maximum stresses under strong wind load.

Strong	CaseF1			Case0.5F1			CaseF0		
Story NO.	S13	S12	S11	S13	S12	S11	S13	S12	S11
Text	KN/m ²	KN/m ²	KN/m ²	KN/m ²	KN/m ²	KN/m ²	KN/m ²	KN/m ²	KN/m ²
1	13015	55290	144175	12779	54307	153239	12629	53643	149880
2	13393	56880	134762	13117	55726	139400	12894	54748	133057
3	13517	57381	137549	13197	56091	141432	12914	54889	134090
4	37292	66420	234198	13304	56248	232581	13245	55923	231164
5	31262	61768	204418	13155	55442	218739	13118	55283	221303
6	26780	58817	187458	13539	56955	202448	13515	56882	202866

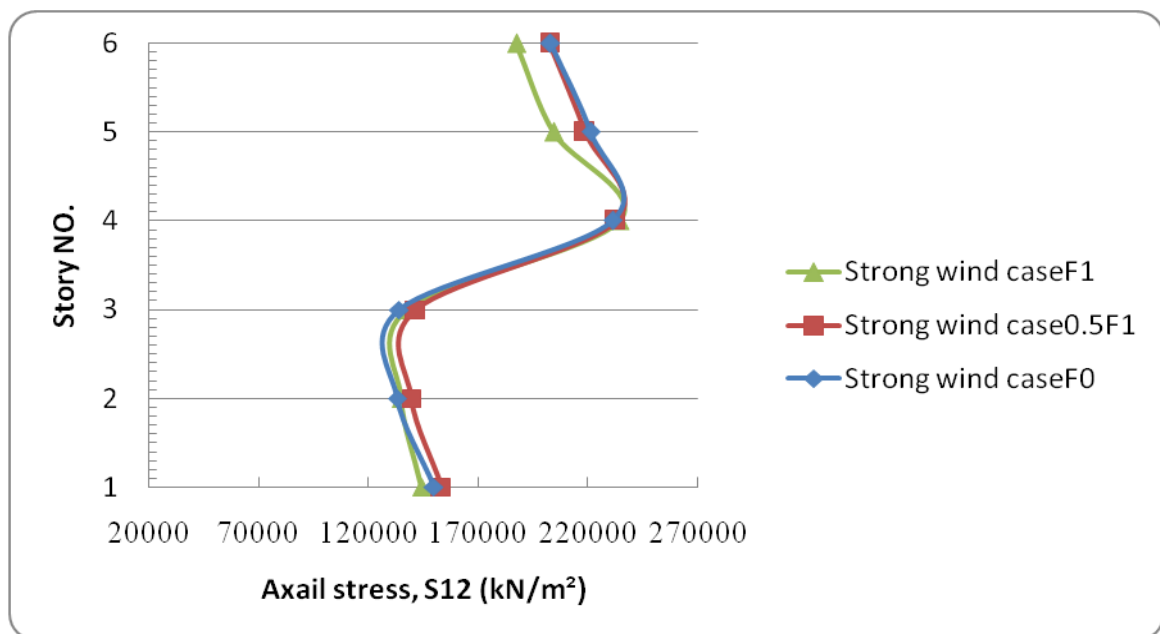


Figure (5-71): Maximum axial stress S11 under strong dynamic wind load.

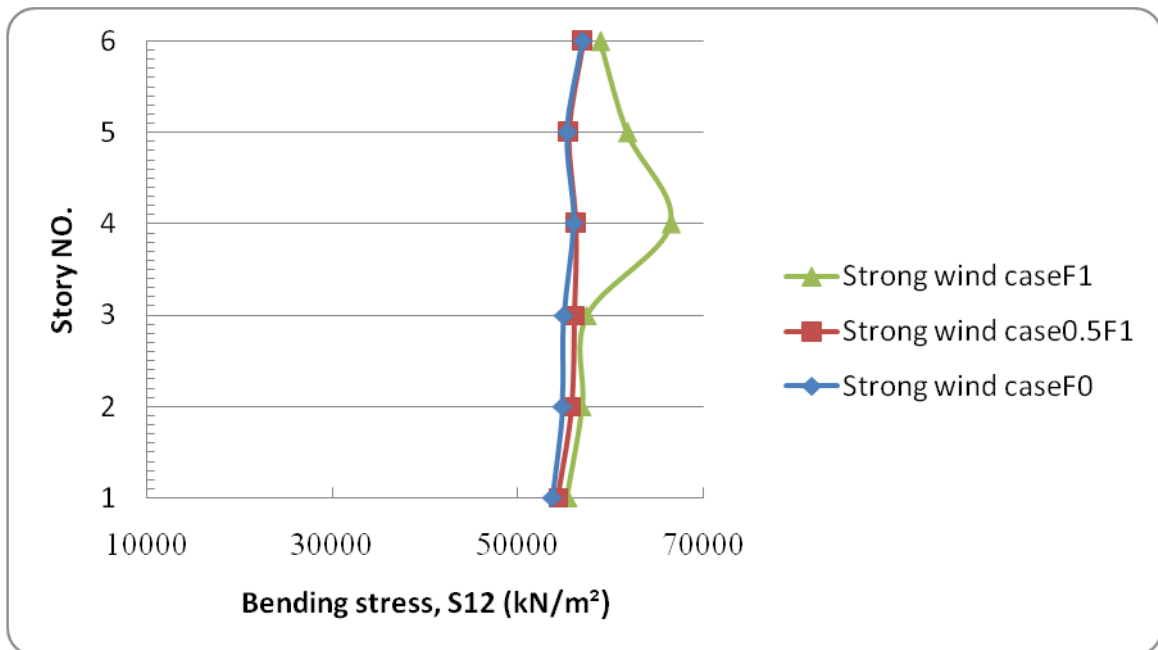


Figure (5-72): Maximum bending stress S12 under strong dynamic wind load.

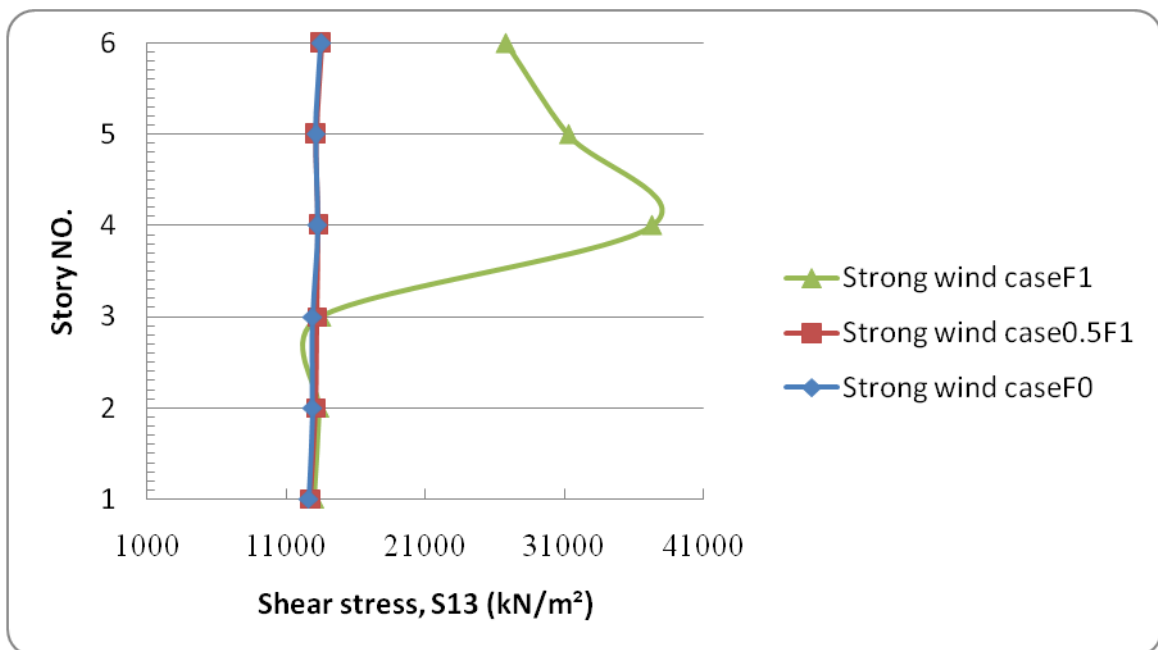


Figure (5-73): Maximum shear stress S13 under strong dynamic wind load.

5.5.7.5 Maximum Bending Moment, M33 for Case 7

From Table (5-42) it can clearly be seen that the maximum bending moment on beam of the third storey for Case F0 under the effect of strong wind

equal to 136.2kN.m while in same storey for Case 0.5 Δ and Case F1 are equal to 145,152kN.m on beam respectively, the difference between Case F0 and Case 0.5 Δ are 6%, the difference between Case F1 and Case 0.5 Δ are 5%, as shown in Fig. (5-74). It's found that the maximum bending moment for Case 0.5 Δ is lies between before and after fire, so clearly difference for Case 0.5 Δ as compared with Case F0 due to fire effect.

Table (5-43): Bending moment due to strong wind load.

Strong	Case F1	Case 0. 5 F1	Case F0
Story NO.	M33	M33	M33
Text	kN.m	kN.m	kN.m
1	139	134	129
2	150	143	136
3	152	145	136
4	144	138	130
5	139	137	132
6	113	113	112

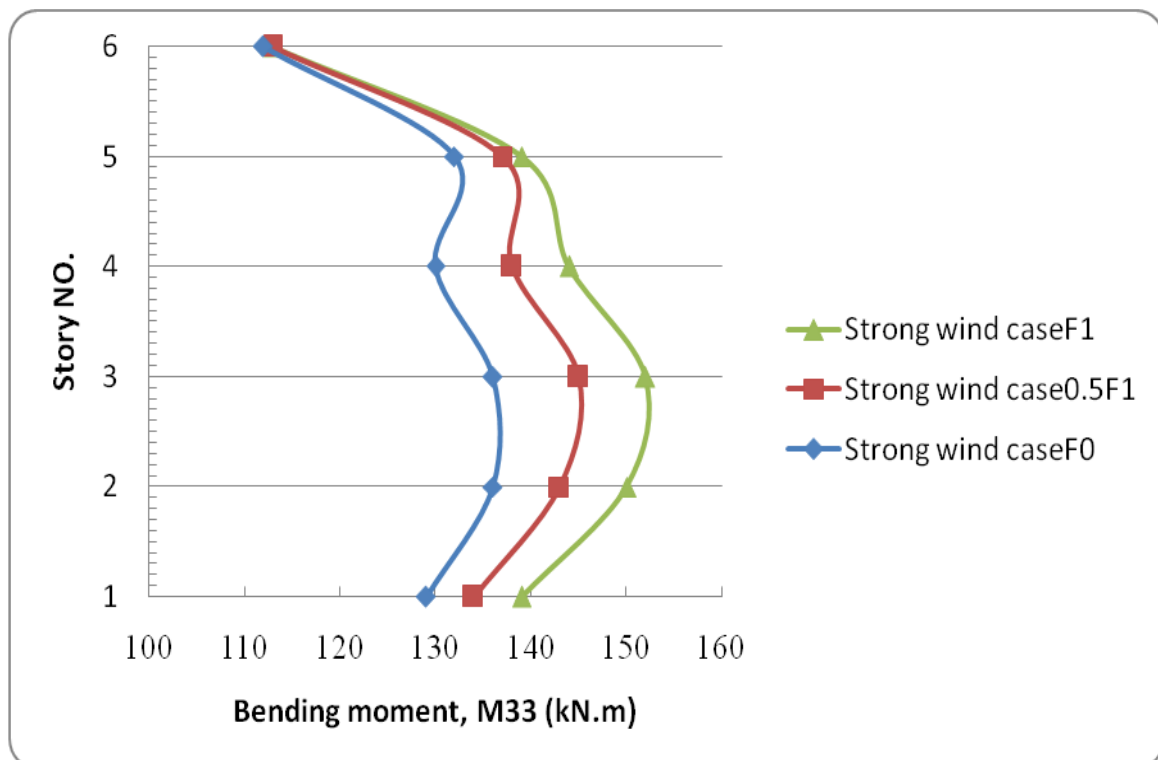


Figure (5-74): Maximum bending moment due to strong wind load.

5.5.7.6 Maximum Axial Force and Shear Force for Case 7

The results of axial and shear forces for Case 6 shown in Table (5-43). The maximum axial force (compression) on column of the first storey of Case F0 due to strong wind equal to 3120kN while for the same conditions for Case 0.5 Δ and Case F1 are equal to 3128, 3130kN respectively.

The difference between them approximately negligible. It's found that no difference between them due to the axial forces depending on gravity load on column , as shown in Fig.(5-75).

The maximum shear force on beam of the last storey for Case F0 due to strong wind is equal to 144.4kN/m² while for same conditions for Case 0.5 Δ and Case F1 are equal to 144.6, 144.9kN respectively.

The difference between them are negligible, but there is clearly difference at third and fourth storeys due reduced 10% of yield stress after fire as shown in Fig. (5-76).

Table (5-44): Axial and shear force due to strong wind load.

Strong	Case F1		Case 0.5 F1		Case F0	
	V2	P	V2	P	V2	P
Text	kN	kN	kN	kN	kN	kN
1	137	3131	137	3128	136	3120
2	140	2618	140	2610	139	2602
3	141	2101	140	2099	139	2091
4	144	1582	143	1580	142	1575
5	143	1053	142	1052	140	1051
6	145	528	145	528	144	528

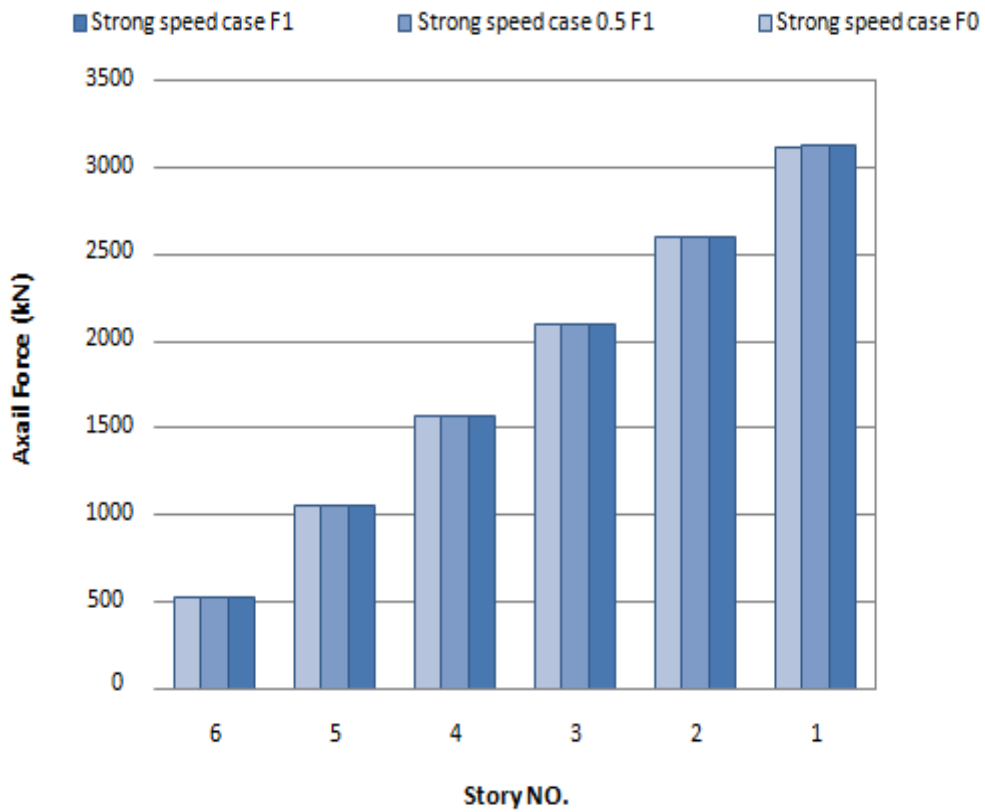


Figure (5-75): Maximum axial forces due to strong wind load.

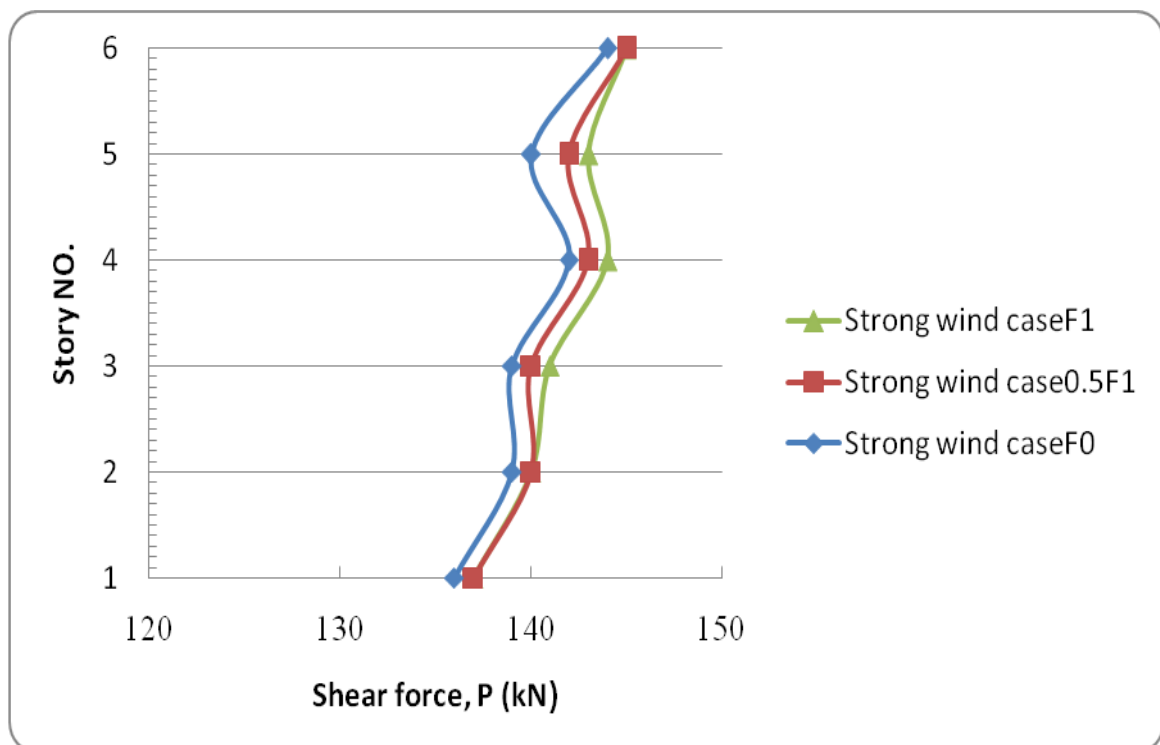


Figure (5-76): Maximum shear forces due to strong wind load.

5.5.7.7 Maximum Displacements in X-Direction for Case 7

The maximum displacement of Case F0 due to strong wind is equal to 19.5mm while for Case 0.5 Δ and Case F1 are equal to 23, 25mm respectively as shown in Table (5-44), the difference between Case F0 and Case 0.5 Δ is 18% but, the difference between Case F1 and Case 0.5 Δ is 8%. It's found that the maximum of displacement for Case 0.5 Δ is lies between that of before and after fire, so clearly difference for Case 0.5 Δ as compared with Case F0 due to fire effect as shown in Fig. (5-77).

According to BS 8110-Part 2: 1985 the maximum allowable deflection is calculated as $h/500$, therefore, maximum allowable displacement value for building height of 19m is 38mm. The maximum value of displacement in serviceability limit condition obtained for dynamic strong wind loads are less than allowable (38 mm) for criteria failure, so the building in safe in all cases.

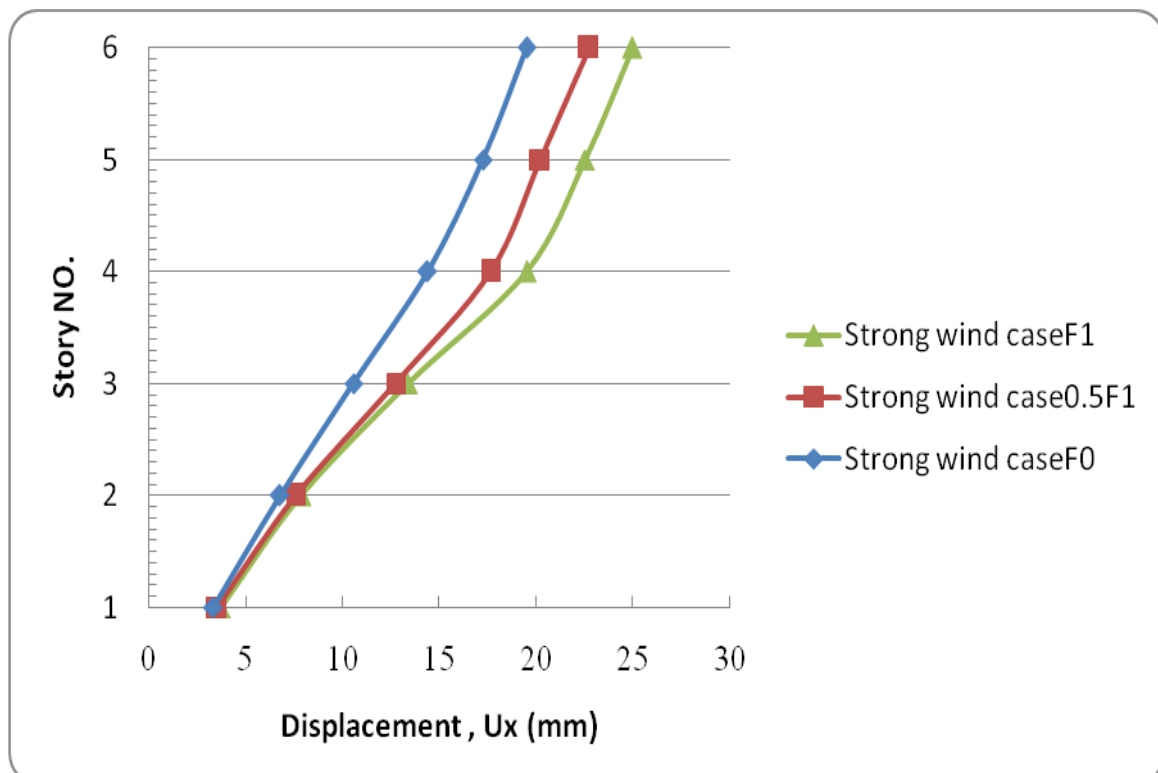


Figure (5-77): Maximum displacements due to strong wind load.

Table (5-45): Maximum displacement due to strong wind load.

Strong	Case F1	Case 0.5 F1	Case F0
Story NO.	U _x	U _x	U _x
Text	mm	mm	mm
1	3.73	3.51	3.31
2	7.87	7.60	6.78
3	13.38	12.75	10.57
4	19.50	17.66	14.37
5	22.51	20.19	17.25
6	24.96	22.73	19.50

5.6 Summary of state of building after analysis with limitations.

Through the analysis of the building by using the SAP program has been extracted values of the forces, moments, stresses and displacements where they were compared with limitations for drift storey according to BS 8110-Part 2: 1985, ($\Delta \leq L/500$) and yield stress according to ASCE/SEI 7-10 ($S \leq F_y$). So that we can know the building can be used again after fire or not, the Table (45-5) explain all cases according to codes standard.

Table (5-46): State of building after analysis.

No.	Type of wind	Type of analysis	State of building for drift story according to BS 8110-part 2: 1985, ($\Delta \leq L/500$)	Type of analysis	State of building for yielding stress according to ASCE EI 7-10 ($S \leq F_y$)	Place of failure	Story failure
1	CaseF0	Strong	Accepted	Nonlinear	Accepted	—	—
2	CaseF0	Moderate	Accepted	Nonlinear	Accepted	—	—
3	CaseF0	Static	Accepted	Nonlinear	Accepted	—	—
4	CaseF2	Strong	Accepted	Nonlinear	Failure	Beam	Fourth +Fifth
6	CaseF2	Moderate	Accepted	Nonlinear	Critical	Beam	Fifth
7	CaseF1	Strong	Accepted	Linear	Critical	Beam	Fourth
8	CaseF1	Strong	Accepted	Nonlinear	Failure	Beam	Fourth
9	Case0.25F1	Strong	Accepted	Nonlinear	Failure	Beam	Fourth
10	Case0.5F1	Strong	Accepted	Nonlinear	Failure	Beam	Fourth

A scroll of parchment is unrolled, held by four black circular fasteners at the corners. The parchment is yellowed and has irregular, torn edges. A quill pen is positioned diagonally on the right side of the scroll. The text is centered on the scroll in a bold, italicized serif font.

Chapter Six
Conclusions And
Recommendations

CHAPTER 6

CONCLUSIONS AND RECOMMENDATIONS

6.1 Introduction

Post-fire analysis of six stories steel buildings of 19m height subjected to fire of temperature equal to 550° C, under the action of wind static and dynamic wind forces are analyzed. The finite element modeling and analysis are accomplished by SAP 2000 V16 software. From the different cases studied the following conclusions can be drawn.

1. In free vibration analysis, the natural frequencies and mode shapes of the structure are almost identical in both cases before and after the fire, and there is no resonance phenomenon due to $\omega_n \neq \omega$ for all modes. Hence the free vibration characteristics of steel building are not affected by post fire deformation due to fire of 550° C temperature.
2. Base shear and base moment from post-fire states (Case F1 and Case F2) are large than before fire state (CaseF0) by 12% and 15% respectively, under the effect strong wind load due to fire deformations and their configurations. This yield the fact that base shear affected by both post fire deformation and also their configuration along building (post fire scenario).
3. Drift ratio and displacement from post-fire states Case F1 and Case F2 are large than before fire state (CaseF0) by 20% and 5% respectively, under the effect strong wind load, but there are considerable differences at stories

affected by temperature. Thus the drift ratio and displacement are affected by both post fire deformation and also their configuration along building (post fire scenario).

4. Bending stress, shear stress, bending moment and shear force from post-fire state Case F2 are large than before fire state by 33%, 70%, 30% and 0% respectively, under the effect strong wind load while due to moderate wind load 26%, 70%, 23% and 0% respectively, but there is large differences at first, second and third stories which affected by fire. Hence both velocities gave the approximately the same ratios, which yield that the increment in these quantities due to post fire state is less sensitive to wind speed value.
5. Bending stress, shear stress, bending moment and shear force from post-fire state Case F1 are large than before fire state by 15%, 64%, 12% and 0% respectively, under the effect strong wind load, but there is clear differences at fourth, fifth and sixth stories which affected by fire. Thus based on points 6 and 7 these quantities are affected by both post fire deformation and also their configuration along building (post fire scenario).
6. For a given fire deformation configurations, there is a similarity between CaseF0 and Case $0.25\Delta F1$, this means that if the maximum deflection in beams is not exceeding $L/160$ and the columns drift is not exceeding $L/240$, the fire deformations may be neglected.
7. For a given fire deformation configurations, there is a differences between CaseF0 and Case $0.5\Delta F1$ are for maximum drift ratio and maximum displacement the difference is 18%, for maximum bending moment is 6% , for base shear and base moment are 4% and 6% respectively, with clear

differences at fourth, fifth and sixth stories which affected by fire. This means that if the maximum deflection in beams is equal to $L/120$ and the columns drift is equal to $L/80$, the fire deformations may be critical and the structural decision for the building safety should be done structural analysis of the building taking into consideration different issues related to post fire effects.

8. The increasing of wind velocity increases base shear and base moment significantly due to wind pressure is a square function of wind velocity. This reflect the importance of accurate estimation of design wind speeds in Iraq taking into account the average along past 100 years in Iraq and the maximum 3-second gust and its number of occurrence in past 100 years.
9. Base shear, base moment, drift ratio and displacement due to strong dynamic wind for building before fire (Case F0) is larger than static wind load under the same conditions by 50% while for bending stress, shear stress, bending moment and shear force by 5% in the first three stories and approximately negligible difference in the last three stories. This conclusion reflects the importance of select the time-history records for wind and application duration.
10. Nonlinear solution techniques gave results more than linear solution techniques for the same geometry and loading states, in which the differences for drift ratio and displacement is 25%, for bending stress is 50%, for shear stress is 13%, for bending moment is 13%, for shear force is 51%, and base shear and base moment are 20% and 25% respectively. This reflects that post fire analyses of steel buildings are nonlinear problems and

the structural quantities are sensitive for nonlinear analysis aspects such as P-Delta effect.

6.2 Recommendations

The following studies may be recommended as future work:

1. Two types of scenarios were used in this study, so its recommended to investigate more fire scenarios in different locations of the building.
2. Examining the effect of changing the plan dimensions, number of bays in both x and y direction and complex plan conditions.
3. Investigating more stories where medium rise building was used in this study, so its recommended to study high rise buildings in south of Iraq.
4. Moment-resisting frame was used in this study, so its recommended investigate to others types of steel buildings resistance system with fire under the effect of wind.
5. Study the addition of bracing system and examining the effectiveness after the fire under the influence of the wind in south of Iraq.
6. Investigating the post-fire performance of buildings constructed from material other than steel such as concrete building.
7. Using other methods to analyze dynamic wind loads on the building like random dynamic analysis.

8. Using more specialized program to represent the residual stress and others imperfections due to fire, because SAP v2000 software unable to model this topics.
9. Post-fire investigating of connection regions.
10. Evaluating more accurate wind time-history for southern Iraq region in deterministic approach.
11. Obtain exact representation of wind time-history in Iraq.

A vertical scroll of aged, yellowish paper is shown, partially unrolled. The scroll is held by four dark, circular fasteners at the top and bottom. The word "References" is written in a bold, italicized, black serif font in the center of the unrolled section. To the right of the scroll, a quill pen with a dark nib and a light-colored, textured shaft is positioned diagonally, resting against the edge of the paper. The entire illustration is set against a plain white background.

References

REFERENCES

1. Kirby B.R., Lapwood D.G. And Thomson G. , 1986 “The Reinstatement of Fire Damaged Steel and Iron Framed Structures”, British Steel Corporation, Swindon Laboratories, UK.
2. Konstantinos Miamis., 2001 “A Study Of The Effects of High Temperature on Structural Steel Framing ” M.Sc. Thesis, Purdue University, Indiana.
3. Dan Pada., 2011"Steel Skeleton Behaviour in Decaying Fire” ,Thesis Tampere University of Technology April 17.
4. Bungale, S.Taranth., 2004 “ Wind and Earthquake Resistant Buildings Structural Analysis and Design”,1st Edition ,CRC Press.
5. Prhabra Guha, Anupam Rajnuni, 2015 “Analysis of Wind And Earthquake Load for Different Shapes of High Rise Building”, IJCIET, Volume 6, Issue 2, pp. 38-45.
6. Dowrick, D. J., “ Earthquake Risk Reduction, 2003”, ISBN: 0-471-49688-X (HB).
7. Hague, S. D., , 2013 “Eccentrically Braced Steel Frames As A Seismic Force Resisting System” M.Sc. Thesis, the College of Engineering of the University of Kansas State.
8. Iraqi Standards IQ.301, “Iraqi Code for Forces and Loadings, 2014 ”, Iraqi Ministry of Building and Construction.
9. Dill, F.H., “Structural Steel after A Restatement, 1960 ”, Proceedings of National Steel Construction Conference,Denver,5-6 May, C.O., American Institute of Steel Construction, Chicago.
10. Digges, T., Rosenberg, S. and Geil, G., 1966 “Heat Treatment and Properties of Iron and Steel”, National Bureau of Standards, Monograph 88.

References

11. Tide, R.H.R., 1998 “Integrity of Structural Steel After Exposure to Restatement”, Engineering Journal, Vol. 35 No. 1, pp. 26-38.
12. Kirby, B.R., Lapwood, D.G. and Thompson, G., 1986 “The Reinstatement of Fire Damaged Steel and Iron Framed Structures”, British Steel Corporation, Swindon Laboratories.
13. Smith, C.I., Kirby, B.R., Lapwood, D.G., Cole, K.J., Cunningham, A.P. and Preston, R.R., 1981 “The Reinstatement of Fire Damaged Steel Framed Structures”, Fire Safety Journal, Vol. 4 No. 1, pp. 21-62.
14. Lee, J., Engelhardt, M.D. and Taleff, E.M., 2012 “Mechanical Properties of ASTM A992 Steel after Reinstatement”, Engineering Journal, Vol. 49 No. 1, pp. 33-44.
15. Qiang, X., Bijlaard, F.S.K. and Kolstein, H., 2012 “Post-Reinstatement Mechanical Properties of High Strength Structural Steels S460 and S690”, Engineering Structures, Vol. 35, pp. 1-10.
16. Qiang, X., Bijlaard, F.S.K. and Kolstein, H., 2013 “Post-Reinstatement Performance of Very High Strength Structural Steel S960”, Journal of Constructional Steel Research, Vol. 80, pp. 235-242.
17. Tao, Z., Wang, X.Q. and Uy, B., 2013 “Stress-Strain Curves of Structural and Reinforcing Steel after Exposure to Elevated Temperatures”, Journal of Materials in Civil Engineering, Vol. 25, No. 9, pp. 1306-1316.
18. Chiew, S.P., Zhao, M.S. and Lee, C.K., 2014 “Mechanical Properties of Heat-Treated High Strength Steel Under Fire/Post-Fire Conditions”, Journal of Constructional Steel Research, Vol. 98, pp. 12-19.
19. Outinen, J. and Makelainen, P., 2004 “Mechanical Properties of Structural Steel at Elevated Temperatures and after Cooling Down”, Fire and Materials Journal, Vol. 28, pp. 237-251.

References

20. Gunalan, S. and Mahendran, M., 2014 "Experimental Investigation of Post-Reinstatement Mechanical Properties of Cold-Formed Steels", *Thin-Walled Structures*, Vol. 84, pp. 241-254.
21. Wang, X.Q., Tao, Z., Song, T.Y. and Han, L.H., 2014 "Stress-Strain Model of Austenitic Stainless Steel after Exposure to Elevated Temperatures", *Journal of Constructional Steel Research*, Vol. 99, pp. 129-139.
22. Smith, C.I., Kirby, B.R., Lapwood, D.G., Cole, K.J., Cunningham, A.P., and Preston, R.R. (1981), "The Reinstatement of Fire Damaged Steel Framed Structures", *Fire Safety Journal*, pp. 21-62, Elsevier.
23. Chi Kin Iua, Siu Lai Chanb, Xiao Xiong Zhaa., 2005 "Nonlinear Pre-Fire and Post-Fire Analysis of Steel Frames "Engineering Structures,, Elsevier. Volume 27, Issue 11 , Pages 1689-1702
24. Zhou, Y., Kijewski, T. and Kareem, A., 2002" Along-Wind Load Effects on Tall Buildings: Comparative Study of Major International Codes and Standards", ASCE, *Journal of Structural Engineering*, Vol. 128, No. 6.
25. Holmes, J. D., Tamura, Y., and Krishna, P., 2009 "Comparison of Wind Loads Calculated By Fifteen Different Codes and Standards, For Low, Medium and High-Rise Buildings", 11th Americas Conference on Wind Engineering, San Juan., Puerto Rico, June 22-26.
26. Shilu, N. G., and, Patel, H. S., 2011 " Computational Tool for Wind Pressure and Forces on A Multistory Commercial Complex", *JERS, Journal of Engineering Research and Studies*, Vol. 2, Issue 3, pp.84-87.
27. Suresh, P., Panduranga, R. B., Kalyana, R. J. S., 2012" Influence of Diagonal Braces in RCC Multi-Storied Frames Under Wind Loads : A Case Study", *International Journal of Civil and Structural Engineering*, Volume 3, Issue 1.
28. Srikanth, I., and, Krishna, B., V., 2014" Study on the Effect of Gust Loads on Tall Buildings", *IJSCER, International Journal of Structural and Civil Engineering Research*, Vol. 3, No. 3.

References

29. Weerasuriya, A. U., Jayasinghe M.T.R., 2014 "Wind Loads on High-Rise Buildings by Using Five Major International Wind Codes and Standards", Engineer: Journal of the Institution of Engineers-Sri Lanka, Vol. XLVII, No. 03, pp. 13-25.
30. Alireza Mohammadi., 2016 "Wind Performance Based Design for High-Rise Buildings", FIU Electronic Theses and Dissertations.
31. Yin Zhou, Ahsan Kareem, Member, ASCE, and Ming Gu, Member, ASCE. "Equivalent Static Buffeting Loads on Structures, 2000" Journal of Structural Engineering, Vol. 126, No. 8.
32. B. Dean Kuma, B.L.P. Swami., 2010 "Wind effects on Tall Building Frames- Influence of Dynamic Parameters," Indian Journal of Science and Technology, Vol. 3, No. 5.
33. Ali Bakhshi and Hamed Nikbakht, 2014 "Loading Pattern and Spatial Distribution of Dynamic Wind Load and Comparison of Wind and Earthquake Effects along the Height of Tall Buildings., 2011" ASCE, Sharif University of Technology, Tehran, Iran, 8th International Conference on Structural Dynamics, Eurodyn, Leuven, Belgium.
34. Syed Rehan, S.H. Mahure "Study of Seismic and Wind Effect on Multi Storey R.C.C., Steel and Composite Building, 2014". International Journal of Engineering and Innovative Technology (IJEIT) Volume 3, Issue 12.
35. Side Reran and S.H. Mahure "Study of Seismic and Wind Effect on Multi Storey R.C.C. Steel and Composite Building , 2014 " International Journal of Engineering and Innovative Technology (IJEIT), 78-83.
36. Swati D. Ambadkar and Vipul S. Bawner , 2012 "Behavior of Multi story Building under the Effect of Wind load" International Journal of Applied sciences and Engineering research (IJASER), 656-662.

References

37. Suresh P, Panduranga Rae B, Kalian Rama J.S.” Influence of diagonal braces in RCC multistoried frames under wind loads: A case study, 2012 ” International journal of Civil and Structural Engineering Volume 3, No 1.
38. Josef Machacek “Lecture five on Structural Imperfections, 2009 ” Technical University in Prague.
39. Kapil Mathur, "Effects of Residual Stresses and Initial Imperfections on Earthquake Response of Steel Moment Frames, 2011" University of Illinois at Urbana-Champaign.
40. Richard G. Gewain, Nestor R. Iwankiw and Farid Alfawakhiri, 2003 “Facts for Steel Buildings fire,” ASCE.
41. Kirby, B. R., "Evaluation of the Temperature Attained by Five Bolts during a Fire in the Broad gate Phase eight Development London, 1991" British Steel Corporation, Swinden Laboratories, Moorgate, Rotherham, United Kingdom.
42. Dill, F. H., "Structural Steel After a Fire, 1960 " Proceedings of National Steel Construction Conference, May 5–6, Denver, CO, American Institute of Steel Construction, Chicago, IL.
43. Wildt, R. H., "Repair of Steel Structures After a Fire, 1972" International Conference on Planning and Design of Tall Buildings, Volume 3, August 21–26, Lehigh University, Bethlehem, PA.
44. K.H. Lien , Y.J. Chiou , R.Z. Wangc, P.A. Hsiao, " Nonlinear Behavior of Steel Structures Considering The Cooling Phase of A Fire, 2009" Journal of Constructional Steel Research 65, No.1, University Road, Tainan City pp.84-87.
45. American Society for Civil Engineers, 1971 "Plastic Design in Steel A Guide and Commentary," ASCE Manual of Engineering Practice, No. 41, 2nd Ed., New York, NY.

References

46. Lehigh, "Plastic Design of Multi-Story Frames, 1965" Summer Conference, Report No. 273.20—Lecture Notes, Report No. 273.24—Design Aids, Fritz Engineering Laboratory, Lehigh University, Bethlehem, PA.
47. Saul, F. W., "Structural Steel Bounces Back, 1956" AISC Steel Construction Digest, Vol. 13, No. 3, 3rd Qtr., Chicago, IL.
48. Eyre, D. G., and Galambos, T. V., 1979 "Deflection Analysis for Shakedown," Journal of the Structural Division, ASCE, ST 7, New York, NY
49. Wright, W., and Cayes, L., Route, 1990 " Viaduct Over Waverly Yards Bridge Fire" Material Test of Damaged Girders, Federal Highway Administration, Turner-Fairbank Highway Research Center, McLean, VA.
50. Stitt, J. R., "Distortion Control During Welding of Large Structures, 1964" Paper 844B Air Transport and Space Meeting, April 1964, Society of Automotive Engineers, Inc. and American Society of Mechanical Engineers, New York, NY.
51. Pattee, H. E., Evans, R. M., and Monroe, R. E., "Flame Straightening and Its Effect on Base Metal Properties," Summary Report, Ship Structure Committee, Department of the Navy, Battelle Memorial Institute, Columbus, OH, 1969.
52. Holt, R. E., 1971 "Primary Concepts of Flame Bending," The Welding Journal, AWS, Miami, FL.
53. Stewart, J. P., 1981 "Flame Straightening Technology," John P. Stewart, LaSalle, Quebec.
54. Avent, R. R., 1992 "Designing Heat-Straightening Repairs," Proceedings of National Steel Construction Conference, June 3–5, Las Vegas, Nevada, American Institute of Steel Construction, Inc., Chicago, IL.
55. Dawood, A.O. , 2017 "Wind design load on high_rise reinforced concrete building in Mayan province southern Iraq ", IJIRSET, Vol. 6, Issue 7.

References

56. Sachs, P., "Wind Forces in Engineering, 1978" Pergamon Press, Second Edition.
57. Dowrick, D. J., "Earthquake Resistant Design," John Wiley and Sons, 1977.
58. Amol S. Rajas, Dr.N.L.Shelke, 2016 "Wind Analysis of High Rise Building with Different Bracing Systems," IJARSET, Vol. 3, Issue 4.
59. K.J. Mork, PSH. Kirkegaard and J.D. Sorensen, 2012 "Wind Loads on Dynamic Sensitive Structures," Computer and Structures, November ISSN 7953-8232 U9917.
60. Krauthammer, T., "A Numerical Study of Wind-Induced Tower Vibrations , 1987" Computers & Structures, Vol. 26, No. 1/2, pp. 233-241.
61. Houghton, E. L. and Carruthers, N. B., 1976 "Wind Forces on Buildings and Structures," Edward Arnold publishers, London.
62. Solari, G., "Along wind Response Estimation Closed Form Solution, 1982 " ASCE, Journal of Structural Division, Vol. 108, No. ST1, pp. 225-244.
63. Dowrick, D. J., "Earthquake Resistant Design," John Wiley and Sons, 1977.
64. Hideki Kikumoto, Ryoza Ooka, Hirofumi Sugawara, 2015 "Variations in the power-law index with stability and height for wind profiles in the urban boundary layer." ICUC9.
65. Simiu, E. and Scanlan, R. H., 1985 "Wind Effect on Structures," A Wiley-Interscience Publication, Second Edition.
66. Erlin B., Hime W. G. and Kuenning, 1972 "Fire Damage to Concrete Structures" Concrete Construction, Vol. 17, No. 4.
67. MacLeod, I. A., "New Rectangular Finite Element for Shear Wall Analysis, 1969" ASCE, Journal of Structural Division, Vol. 95, No. ST3, pp. 399-409.
68. Chi Kin Iua, Siu Lai Chanb, Xiao XiongZhaa., 2005 " Nonlinear pre-fire and post-fire analysis of steel frames "Engineering Structures, Elsevier.
69. Oral Buyukozturk, 2003" Calculation of Wind and Earthquake Loads on Structures According to ASCE 7 & IBC" Lectures Notes.

References

70. Tony Yang , 2004 "Lecture Notes on Wind Loads" University of California, Berkeley.
71. BS 8110-2:1985, 1985 "Structural use of concrete - Part 2: Code of practice for special Circumstances".
72. Al-Mosawi, Fareed H. M., 2014 "Finite Element Analysis of Seismically Isolated Reinforced Concrete Buildings". Ph.D. Thesis, the College of Engineering of the University of Al-Basrah.
73. Khalaf, M. A., 2014 "Simulation of Iraqi Earthquakes and Response of Framed Buildings Using Time and Frequency Domain Analyses". Ph.D. Thesis, the College of Engineering of the University of Al-Basrah.
74. Ohtori, Y. J.; Christenson, R. E.; Spencer, B. F. and Dyke, S. J., 2004 "Benchmark control problems for seismically excited nonlinear Buildings", ASCE Journal of Engineering Mechanics, 130(4), pp. 366-385.
75. Luco, N., 2002 "Probabilistic seismic demand analysis, SMRF connection fractures, and near source effects", Ph. D. Dissertation, Dept. of Civil and Environmental Engineering, Stanford University, Stanford, California.
76. Gupta, A. and Krawinkler, H., 1999 "Seismic demands for performance evaluation of steel moment resisting frame structures", (SAC Task 5.4.3), Report No. 132, John A. Blume Earthquake Engineering Center, Stanford University, Stanford, California, .
77. Rackauskaite, E. Kotsovinos, P, and Rein, G, 2017 "Structural response of a steel-frame building to horizontal and vertical travelling fires in multiple floors," Fire Safety Journal , Vol. 91, pp. 542-552. Elsevier.
78. Maraveas, Fasoulakis, Tsavdaridis, 2004 "Fire Damage Assessment and Reinstatement Of Steel Structures", Journal of Structural Fire Engineering, Vol. 28, pp. 237-251.
79. Chrysanthos Maraveas., 2014 "Post-Fire Mechanical Properties of Structural Steel," National Steel Structures Conference, Tripoli, Greece.

References

80. Fatma Nur Kudu, Senay Ucak Gokhan, Osmancikli Temel Turker, Alemdar Bayraktar, 2015 "Estimation of Damping Ratios of Steel Structures by Operational Modal Analysis method", Volume 112, Pages 61-68.

الملخص

تم دراسة بناية حديدية الهيكل مربعة الشكل ٦ طوابق بارتفاع ١٩ م كل مقاطع حديد هي من نوع W-shape و تحت تأثير تشوهات بعد الحريق وتحت تأثير أحمال الرياح حيث تم اخذ قيم لتشوهات بناية في درجة حرارة ٥٥٠ سيليزية وكانت هذه التشوهات هي هطول جسر بقيمة $(\Delta = \text{طول الجسر} / 60)$ وإزاحة العمود بقيمة $(\Delta = \text{طول العمود} / 40)$ وكانت هذه التشوهات تتناقص من مكان الحريق إلى الأعلى حيث تقل كلما صعدنا إلى الأعلى تدريجيا وتم اخذ نوعين من سيناريو لحدوث الحريق حيث سمي النوع الأول CaseF1 والثاني Case F2 , استخدم برنامج SAP v2000 16 لتحليل هذه البنايات واستخدم طريقة Time-history لتحليل الرياح بطريقه تحليل الخطي واللاخطي بطريقة Direct Integration بينما Geometric nonlinear parameters كانت تتضمن تأثير P-delta.

إما من ناحية الرياح فقد تم اخذ نوع الرياح Along المسلطة على طول البناية ودرست نوعين من الرياح ثابتة والحركية ، تم الاعتماد على سرعة الرياح تصميمية ٤٢ م/ثا التي تم أخذها من Iraqi Code IQS.30 لرياح القوية بينما سرعة الرياح معتدلة فقد اعتمد على نصف سرعة الرياح تصميمية ٢١ م/ثا لكون السرعة قليلة جدا.

تمت المقارنة في هذه الحالات من خلال عدة عوامل مثل إزاحة الطوابق، نسبة انحراف الطوابق، واجهادات (العمودية ، الانحناء والمماس)، وعزم الانحناء، القص القاعدي ،عزم القاعدة ،القص عمودي والمماس ، قوه عمودية والمماس ،ترددات الطبيعية وإشكال تشوهات البناية بعد حريق.

الهدف الرئيسي من هذه الدراسة هو تقييم سلوك البناية بعد الحريق من خلال دراسة التحليل الديناميكي لرياح في جنوب العراق لما بعد الحرائق لمبنى حديدي من نوع Moment-resisting frame system متعدد الطوابق معرض لأحمال الرياح وإظهار ما إذا كان بإمكاننا إعادة المبنى بعد تأثير النار ضمن حدود مسموح بها .حيث تم معرفة إن زيادة درجة الحرارة تؤثر على الخواص ميكانيكية التي هي (إجهاد خضوع ومعامل المرونة) التي تقل بنسبة ١٠% من قيمتها قبل الحريق وكان الحديد المستخدم في بناية من نوع Normal strength.

حيث تبين إن هنالك تشابه في الترددات الطبيعية وأنماط إشكال التشوهات في Free Vibrations بعد وقبل الحريق وكذلك مقارنتها مع تردد الرياح حيث لم يكن هنالك حالة رنين بسبب عدم تشابه ترددات الطبيعية للبناية ووتردد الرياح. ووجدنا إن الرياح القوية هي الأكثر تأثيرا على المباني في جنوب العراق بسبب قوتها العالية جدا.مقارنتنا مع سرعة الرياح (معتدلة والثابتة) وتم ملاحظة إن جهاد وعزم القاعدة ،

نسبة انحراف ،جهاد الانحناء والمماس، وعزم الانحناء وقوه المماس تزداد قيمتهما بعد الحريق في الطوابق التي حدث فيها الحريق وتم استنتاج عدم قابلية رجوع البناية بعد الحريق لمقاومة الرياح في جنوب العراق لهكذا نوع من بناية ونسبة تشوهات وفق الحدود المسموح بها من قبل الكود.



جمهورية العراق
وزارة التعليم العالي والبحث العلمي
جامعة ميسان / كلية الهندسة
قسم الهندسة المدنية



التحليل الحركي لما بعد الحريق للمباني الحديدية تحت تأثيراحمال رياح جنوب العراق

رسالة
مقدمة إلى قسم الهندسة المدنية في جامعة ميسان كجزء من متطلبات نيل
شهادة الماجستير في علوم الهندسة المدنية/انشاءات

من قبل

امين اسماعيل عطيه
(بكالوريوس هندسة مدنية ٢٠١٦)

باشراف

ا.م.د.عباس عودة داود

أذار ٢٠١٩

ربيع الاول 1440